



ISSN 2518-718X (Print)
ISSN 2663-4872 (Online)

BULLETIN

OF THE KARAGANDA UNIVERSITY

CHEMISTRY

Series

№ 4(100)/2020

ISSN 2663-4872 (Online)
ISSN-L 2518-718X (Print)
Индексі 74617
Индекс 74617

**ҚАРАҒАНДЫ
УНИВЕРСИТЕТІНІҢ
ХАБАРШЫСЫ**

ВЕСТНИК
КАРАГАНДИНСКОГО
УНИВЕРСИТЕТА

BULLETIN
OF THE KARAGANDA
UNIVERSITY

ХИМИЯ сериясы

Серия **ХИМИЯ**

CHEMISTRY Series

№ 4(100)/2020

Қазан–қараша–желтоқсан
30 желтоқсан 2020 ж.

Октябрь–ноябрь–декабрь
30 декабря 2020 г.

October–November–December
December, 30th, 2020

1996 жылдан бастап шығады
Издается с 1996 года
Founded in 1996

Жылына 4 рет шығады
Выходит 4 раза в год
Published 4 times a year

Қарағанды, 2020
Караганда, 2020
Karaganda, 2020

Main Editor

Doctor of Chemical sciences

M.I. Baikenov

Responsible secretary

Candidate of chem. sciences PhD

I.A. Pustolaikina

Editorial board

- Z.M. Muldakhmetov**, Academician of NAS RK, Doctor of chem. sciences, Institute of Organic Synthesis and Coal Chemistry of the Republic of Kazakhstan, Karaganda (Kazakhstan);
- S.M. Adekenov**, Academician of NAS RK, Doctor of chem. sciences, International Research and Production Holding «Phytochemistry», Karaganda (Kazakhstan);
- S.E. Kudaibergenov**, Doctor of chem. sciences, Institute of Polymer Materials and Technologies, Almaty (Kazakhstan);
- V. Khutoryanskiy**, Professor, University of Reading, Reading (United Kingdom);
- Fengyung Ma**, Professor, Xinjiang University, Urumqi (PRC);
- Xintai Su**, Professor, South China University of Technology, Guangzhou (PRC);
- R.R. Rakhimov**, Doctor of chem. sciences, Norfolk State University, Norfolk (USA);
- M.B. Batkibekova**, Academician of the Engineering Academy of the Kyrgyz Republic, Doctor of chem. sciences, Kyrgyz State Technical University named after I. Razzakov, Bishkek (Kyrgyzstan);
- S.A. Beznosyuk**, Doctor of phys.-math. sciences, Altai State University, Barnaul (Russia);
- B.F. Minaev**, Doctor of chem. sciences, Bohdan Khmelnytsky National University of Cherkasy, Cherkasy (Ukraine);
- N.U. Aliev**, Doctor of chem. sciences, Asfendiyarov Kazakh national medical University, Almaty (Kazakhstan);
- R.Sh. Erkasov**, Doctor of chem. sciences, L.N. Gumilyov Eurasian National University, Nur-Sultan (Kazakhstan);
- V.P. Malyshev**, Doctor of techn. sciences, Zh. Abishev Chemical-Metallurgical Institute, Karaganda (Kazakhstan);
- L.K. Salkeeva**, Doctor of chem. sciences, Karagandy University of the name of acad. E.A. Buketov (Kazakhstan);
- Ye.M. Tazhbaev**, Doctor of chem. sciences, Karagandy University of the name of acad. E.A. Buketov (Kazakhstan);
- A.K. Tashenov**, Doctor of chem. sciences, L.N. Gumilyov Eurasian National University, Nur-Sultan (Kazakhstan);
- Xian Li**, Associated Professor, Huazhong University of Science and Technology, Wuhan (PRC);

Postal address: 28, University Str., Karaganda, 100024, Kazakhstan

Tel./fax: (7212) 34-19-40.

E-mail: vestnikku@gmail.com; ipustolaikina@gmail.com

Web-site: <http://chemistry-vestnik.ksu.kz>

Editors

Zh.T. Nurmukhanova, S.S. Balkeyeva

Computer layout

V.V. Butyaikin

Bulletin of the Karaganda University. Chemistry series.

ISSN 2663-4872 (Online). ISSN-L 2518-718X (Print).

Proprietary: NLC «Karagandy University of the name of academician E.A. Buketov».

Registered by the Ministry of Information and Social Development of the Republic of Kazakhstan. Rediscout certificate No. KZ27VPY00027382 dated 30.09.2020.

Signed in print 29.12.2020. Format 60×84 1/8. Offset paper. Volume 18,75 p.sh. Circulation 200 copies. Price upon request. Order № 89.

Printed in the Publishing house of NLC «Karagandy University of the name of acad. E.A. Buketov».
28, University Str., Karaganda, 100024, Kazakhstan. Tel.: (7212) 35-63-16. E-mail: izd_kargu@mail.ru

© Karagandy University of the name of acad. E.A. Buketov, 2020

DEAR READER!



We present you the 100th anniversary edition of the "Bulletin of the Karaganda University". "Bulletin of the Karaganda University" is the scientific periodical is aimed at publishing in the open press the results of research in various fields of science by scientists from Kazakhstan and other countries. The purpose of the journal is to create an effective environment for the exchange of important scientific and educational information, to acquaint the international scientific community with new methods and ideas. The journal is included in the list of publications recommended by the Committee for Control in Science and Education of the Ministry of Education and Science of the Republic of Kazakhstan for publication of the main results of scientific activity.

The journal was first published in 1996 in two series ("Humanities" and "Natural Sciences"), since 2004 "Mathematics"; "Physics"; "Chemistry"; "Biology. Medicine. Geography."; "Economics"; "Pedagogy"; "Philology"; "History. Philosophy. Law" published materials in eight series, and in 2010 the ninth series was added.

Since 2015, the series "Chemistry", "Physics", "Mathematics" of the journal "Bulletin of the Karaganda University" are included in the platform "Emerging Sources Citation Index (ESCI)" of the international database Web of Science Core Collection. Currently, the Bulletin of the Karaganda University is a prestigious publication that publishes 9 series of research papers in the CIS and Germany, Poland, China, Egypt, Turkey, India and Pakistan, in addition to research on topical issues by domestic scientists. The journal's personal website in 3 languages, complying with international standards, contains the policy of the editorial board, the requirements for online submission of articles and online peer review. All articles published in the journal are assigned a digital object ID. The journal cooperates with leading Kazakhstan and foreign library systems and databases, which in turn provides quick and open access to published materials.

We have a clear signature in the development of science and education of our independent country. I believe that such a rise to the heights of prestige is the result of many years of hard work, constant search and tireless progress. I am convinced that the publication, which has made the solution of the most pressing problems facing humankind its eternal and noble goal, will continue to be the herald of scientific discoveries. We would like to express our gratitude to all the authors and researchers who have contributed to the growth of the scientific potential of the journal, and sincerely congratulate you on the publication of the 100th anniversary edition!

*Chairman of the Editorial Board
Corresponding member of NAS RK,
Doctor of Law,
Professor N.O. Dulatbekov*

CONTENTS

ORGANIC CHEMISTRY

| | |
|---|----|
| <i>Bakibaev A.A., Malkov V.S., Kurgachev D.A., Kotelnikov O.A.</i> Methods of analysis of glycoluril and its derivatives | 5 |
| <i>Jalmakhanbetova R.I., Suleimen Ye.M., Eissa I.H., Metwaly A.M., Iskakova Zh.B., Balpanov D.S., Sissengalieva G.G., Khannanov R.A., Seilkhanov T.M.</i> Isolation and biological evaluation of roseofungin and its cyclodextrin inclusion complexes | 35 |
| <i>Turdybekov K.M., Nurmaganbetov Zh.S., Turdybekov D.M., Mukusheva G.K., Gatilov Yu.V.</i> Synthesis, molecular and crystalline structure of 8-formylharmine | 45 |
| <i>Kishkentayeva A.S., Mantler S.N., Zhakanov M.M., Adekenov S.M.</i> Biologically active substances from <i>Achillea nobilis</i> L..... | 52 |

PHYSICAL AND ANALYTICAL CHEMISTRY

| | |
|---|----|
| <i>Bakibaev A.A., Sadvakassova M.Zh., Malkov V.S., Erkasov R.Sh., Sorvanov A.A., Kotelnikov O.A.</i> Study of the biologically active acyclic ureas by nuclear magnetic resonance | 60 |
| <i>Stas' I.E., Pavlova S.S.</i> Effect of ultrahigh-frequency electromagnetic field on the properties of associated liquids | 75 |
| <i>Shcherban' M.G., Solovyev A.D., Saliakhova A.O.</i> The correlation between the surface-active characteristics of SAFOL 23 – alcohol – water systems and the length of the alkyl radical of the alcohol..... | 85 |
| <i>Stas' I.E., Pavlova S.S.</i> Effect of pH and water irradiation with the electromagnetic field on the gelation of gelatin solutions | 96 |

INORGANIC CHEMISTRY

| | |
|--|-----|
| <i>Zhumabekova A.K., Tastanova L.K., Orynbassar R.O., Zakumbaeva G.D.</i> Effect of modifiers on Fe-Pt/Al ₂ O ₃ catalysts for alkanes hydrotreatment | 104 |
|--|-----|

CHEMICAL TECHNOLOGY

| | |
|---|-----|
| <i>Mukhametgazy N., Gussenov I.Sh., Shakhvorostov A.V., Kudaibergenov S.E.</i> Salt tolerant acrylamide-based quenched polyampholytes for polymer flooding | 119 |
| <i>Zhaparkulova K.A., Gani G.M., Sakipova Z.B., Karaubayeva A.A.</i> Development of the orodispersible films based on CO ₂ extract of <i>Ziziphora bungeana</i> with antimicrobial activity..... | 128 |
| <i>Khabarov I.A., Zhurov V.V., Zhabayeva A.N., Adekenov S.M.</i> Modeling the extraction process of medicinal raw materials..... | 135 |
| INFORMATION ABOUT AUTHORS..... | 145 |
| Index of articles published in “Bulletin of the Karaganda University. Chemistry Series” in 2020..... | 148 |

DOI 10.31489/2020Ch4/5-34

UDC 547.495.2

A.A. Bakibaev¹, V.S. Malkov^{2*}, D.A. Kurgachev¹, O.A. Kotelnikov²¹Institute for Problems of Chemical and Energetic Technologies SB RAS, Biysk, Russia;²National Research Tomsk State University, Tomsk, Russia

(Corresponding author's e-mail: malkov.vics@gmail.com)

Methods of analysis of glycoluril and its derivatives

The present work provides the literature data generalization concerning analysis of glycoluril, its derivatives and related compounds that allows obtaining information about the structure and properties of these compounds. Basic methods for analysis of glycoluril and substances on the basis thereof are considered, advantages and disadvantages of these methods are described. The generalized results of the methods of analysis of glycoluril and its derivatives show that the majority of carried studies are focused on the revealing of purity and identification of related impurities for compounds that found practical application (drugs, monomers and polymers on the basis thereof). Consistent trend to active search of new methods to analyze macrocyclic and supramolecular systems synthesized on the basis of glycoluril is observed. The aim of the present review is to take attention of chemists to the most advanced methods of analysis of glycoluril and its derivatives with reference to promotion of further research. The literature analysis will be useful for researchers dealing with designing of new molecules based on glycoluril with given properties where the methods of process control and analysis of target compounds has a decisive importance.

Keywords: glycoluril, N-substituted glycoluril, supramolecules, analysis, spectroscopy, HPLC, isomers.

Introduction

Bicyclic bisureas (glycolurils) belong to well-known azaheterocycles among which many valuable substances were founded and some of them are manufactured industrially. With that, there is no detailed information on the impurity profile in the glycoluril synthesis as well as on its assay procedures. Besides there is no literature data on the reliable methods of assay of glycoluril and its derivatives. Based on the aforesaid, this review aims to draw the attention of chemists and specialists in related fields to the methods of analysis of glycoluril and its derivatives.

1. General information about glycoluril

In the chemistry of nitrogen-containing heterocyclic compounds bicyclic bisureas occupy a special place, and 2,4,6,8-tetraazabicyclo[3.3.0]octane-3,7-dione (glycoluril) **1** and its derivatives (Fig. 1) are among the most interesting of them.

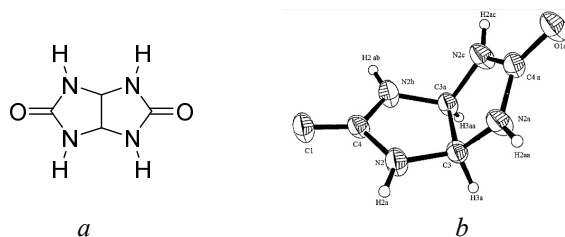


Figure 1. Structural formula of glycoluril **1** (1a) and its spatial configuration in the crystal (1b)

*Corresponding author.

The chemistry of glycolurils, primarily due to the multifunctionality of their structure, has undergone a rapid development reflected in the creation of valuable substances on the basis thereof for various fields of human activity: antitumor drugs [1–4], their derivatives are used as stabilizers and antipyretics in production of rubbers [5], crosslinking agents [6], fibre modifiers in the manufacturing of fabrics [7], preservatives and bactericidal agents [8, 9] and modifiers of wood properties [10]. Currently, glycoluril **1** is an essential component for the manufacturing of a number of macrocyclic compounds: molecular clips, bambus[n]urils, tiara[n]urils, and several classes of cucurbit[n]urils [11]. Some glycoluril derivatives have found application in genetic research [12, 13] for the rapid analysis of glycolipids [14] and biogenic amines [15]. N-methylol derivatives of glycoluril are used in the production of organic thin-film components of microelectronics [16]. Based on the supramolecular derivatives of glycoluril, new promising targeted antitumor [17], antibacterial [18] and other [19] drugs are being developed. Moreover, porous ungrafted [20] and grafted adsorbents [21], explosives [22–25], organic regioselective catalysts [26, 27] are made on the basis of glycoluril. Glycoluril is used as a catalyst for selective peroxidation in the fine organic synthesis of biologically active substances [28]. The undoubted advantage of glycoluril **1** is that it is nontoxic and not carcinogenic in the absence of impurities [29, 30].

Glycoluril **1** is a multifunctional compound having the urea fragment that indeed determines the properties of molecule **1** caused by the presence of two reactive centers in the molecule, namely, four electron donating (NH) groups and two electron withdrawing (C=O) groups. Direct methods for the analysis of glycoluril **1** are based on its properties of a highly active n-nucleophile and a substantially deactivated p-nucleophile. On the other hand, molecule **1** has two symmetry planes, namely, σ_1 and σ_2 (Fig. 2), that pass along the methine CH–CH bridge and two carbonyl oxygen atoms, respectively [31].

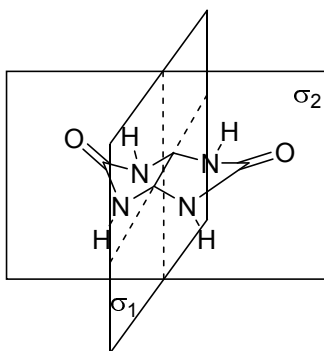


Figure 2. Symmetry planes σ_1 and σ_2 in glycoluril molecule

However, when studying the crystal structure of glycoluril **1** by X-ray structural analysis (Fig. 1b), it was found for the first time that, in addition to symmetry, the conformation of the bicyclic skeleton **1** due to the rigidity of the cis-coupling of annelated imidazolidinone rings has a folded structure in the form of a "half-opened book" [32], where the dihedral angle between the imidazolidinone rings in molecule **1** is 124.1°. Moreover, it was found that nitrogen atoms in the molecule **1** are equidistant from each other. Hydrogen atoms with methine carbon are cis-oriented, and imidazolidinone rings are characterized by an almost flat structure with a slight deviation of the carbonyl groups from the middle plane.

A significant limiting condition for the effective analytical determination of glycoluril is its low solubility in water and organic solvents, although most of its N-substituted derivatives are already free of this disadvantage (see Table 1 for the example of N,N,N,N-tetraacetylglycoluril).

In addition, due to the widespread use of glycoluril **1** and its derivatives, there is a need for analytical methods to determine glycoluril and its related impurities. It is reliably known that targeted glycoluril **1** may contain closely related substances, such as hydantoin [33] and other unidentified impurities that accompany them after synthesis [34]. Moreover, in the open literature, there is no complete information about the profile of impurities and methods for their quantitative determination. The publications do not also provide reliable methods for the quantitative determination of glycoluril. Manufacturers and suppliers of glycoluril normalize only the elemental composition (%C, %N) [35] that is insufficient since the related glycoluril impurities often have similar elemental composition, therefore, elemental analysis cannot serve to unambiguously assess the purity of the desired compound.

Table 1

Comparative physical-chemical properties of glycoluril **1** and N,N,N,N-tetraacetylglycoluril

| Compound | Glycoluril (1) | Tetraacetylglycoluril |
|---|--|--|
| Melting point | 360 °C (with decomposition) | 236–238 °C |
| Solubility | Insoluble in halocarbons, alcohols, ketones, esters, upon heating it is soluble in DMSO, DMF, HCOOH, AcOH, Ac ₂ O | Insoluble in H ₂ O, alcohols, soluble in CH ₂ Cl ₂ , CHCl ₃ , HCOOH, AcOH, Ac ₂ O, MeCN |
| IR spectrum, ν , cm ⁻¹ | (KBr): 3209 (NH), 1675 (C=O) | (Nujol): 1753, 1733 (C=O), 1695 (C=O) |
| NMR ¹ H (400 MHz, δ , DMSO-d ₆ , ppm) | 5.24 (c, 2H, CH), 7.16 (c, 4H, NH) | 6.38 (c, 2H, CH), 2.38 (c, 12H, CH ₃) |
| NMR ¹³ C (100 MHz, δ , DMSO-d ₆ , ppm) | 160.30 (C=O), 64.60 (CH) | 169.42 (C=O acetyl), 151.48 (C=O), 62.61 (CH), 25.11 (CH ₃) |

Currently, to analyze glycoluril **1**, its N- and C-derivatives and their related compounds, a number of analysis methods are used that allow obtaining a significant amount of information about the structure and properties of these substances. Below we present the main methods for the analysis of glycolurils and compounds synthesized on the basis thereof. We discuss and critically examine the advantages and disadvantages of the methods proposed.

2. Spectral analysis methods

Spectral analysis methods are widely used to investigate and analyse glycoluril **1** and its derivatives. To study the structure and properties of glycoluril, various spectral analysis methods are used: spectroscopy in the ultraviolet (UV), visible, and infrared (IR) regions, nuclear magnetic resonance spectroscopy (NMR), mass spectrometry (MS) and, less commonly, other methods of spectral analysis.

2.1. Infrared spectroscopy

One of the most widely used methods to analyze glycolurils is the IR spectroscopy method that is most often used in the middle spectral region, i.e. from 2,500 to 25,000 nm (400 to 4000 cm⁻¹). IR spectroscopy is used to identify and confirm the structure of glycoluril [36, 37], its oligomers [38, 39], polymers [40], macrocyclic derivatives cucurbiturils [41], N-alkyl derivatives [42], N-acyl derivatives [43], C-phenyl glycolurils [44], C-amino derivatives [45], organosilicon [46], phosphorylated [47] and mercapto derivatives [48] as well as multifunctional glycoluril derivatives of complex composition [49]. There are known examples of the analysis of the confirmation of various N nitro derivatives of glycoluril: mono-, di-, tri-, tetranitroglycolurils and nitrophenyl derivatives [50, 51] by IR spectroscopy in a disk of potassium bromide and by IR spectroscopy of diamond attenuated total reflectance (DATR FTIR).

The IR spectrum of glycoluril derivatives contains characteristic signals of vibrations of chemical bonds included in the structure of glycoluril (Table 2).

Table 2

Characteristic absorption bands in the IR spectra of glycolurils

| Wavenumber, cm ⁻¹ | Bond, type of vibrations | Comment |
|------------------------------|--------------------------|---|
| 3350–3200 | N–H, stretching | No signal in N-tetrasubstituted derivatives |
| 3000–2048 | C–H, stretching | |
| 1680 | C=O, stretching | Carbonyl group of N-unsubstituted fragment |
| 1640 | C=O, stretching | Carbonyl group of N-substituted fragment |
| 1500 | C–H, bending | |
| 1100 | C–N, stretching | |

As can be seen from the data (Table 2), the infrared spectroscopy method allows identifying and confirming the structure of glycoluril derivatives. The method allows obtaining the information about the presence of several types of bonds and functional groups in the structure of glycolurils shown in the table. Moreover, IR spectroscopy can be used to identify target compounds by the "fingerprints" principle, when the IR

spectra of the two glycoluril derivatives completely coincide, one can conclude that they are completely identical.

The disadvantages of this method are its comparative insufficient specificity, low resolution, and inability to analyse mixtures of substances with a similar structure. IR spectroscopy of glycolurils is practically unsuitable for quantitative analysis and features low sensitivity to the water content in the sample.

2.2. UV-Vis spectroscopy

The method of spectrophotometry in the visible region is limitedly used for the indirect quantitative determination of glycoluril [52]. Thus, a method is known based on the photometric determination of the reaction product of glycoluril, sodium arsenite and sodium nitroprusside in the presence of Trilon B. However, the reaction chemistry is not given in the work that significantly complicates the interpretation of the results. At the same time, the proposed method does not provide chemoselectivity of the ongoing processes and does not allow analysing the glycoluril content in the solution in the presence of its precursors, namely, urea and hydantoin.

In the structure of unsubstituted glycoluril **1** there are no chromophoric groups that provide an intense absorption in the UV spectrum with a wavelength above 200–220 nm. First of all, because of this, the UV spectroscopy is used to analyse the modified glycolurils, e.g., phenyl [53], pyridyl [54], and naphthyl derivatives [55], due to the presence of analytical signals in the spectra of the corresponding glycoluril derivatives caused by the interaction of aromatic fragments of the molecules with the irradiation.

The nature of the analytical signal in the direct spectrophotometric determination of aromatic derivatives of glycoluril is determined primarily by the spectral properties of aromatic substituents and, to a lesser extent, by the properties that arise from p- π conjugation of the fragments of substituted glycolurils. At the same time, the bicyclic glycoluril fragment has practically no effect on the absorption: the general view of the spectrum and the absorption maxima of 3-methyl-6-phenylglycoluril and the precursor, phenylurea, practically coincide (Table 3).

Table 3

Comparison of absorption maxima positions in the UV range for 3-methyl-6-phenylglycoluril and phenylurea

| Compound | Absorption maxima, nm |
|----------------------------------|-----------------------|
| Phenylurea [56] | 232 |
| | 274 |
| 3-Methyl-6-phenylglycoluril [53] | 217 |
| | 230 |
| | 274 |

Thus, it is obvious that the UV spectroscopy is not a specific method for derivatives and predecessors of glycoluril, namely, acyclic ureas since it does not allow selective assessment of the concentration and properties of the corresponding substances with their possible simultaneous presence in the mixture. The low specificity of the UV spectrophotometry makes it unsuitable for confirmation, identification, and quantification of glycoluril **1** and its derivatives without preliminary sample preparation, e.g., those associated with the separation of mixtures of closely related substances.

The method of fluorimetry differs from the absorption spectroscopy by significantly higher sensitivity and specificity that is used in the analysis of some glycoluril derivatives. Fluorimetry is widely used to analyze glycoluril derivatives capable of fluorescence or its quenching [57]. For instance, the fluorescence parameters of bis-tolane glycoluril derivatives were studied and the excitation and emission spectra were obtained [58]. The absorption region of the glycoluril derivatives under consideration is in the range from 200 nm to 350 nm, the absorption maximum is at 300 nm ($\pi \rightarrow \pi^*$ transition), the emission region is 400–600 nm, the emission maxima are 406 and 432 nm. In the course of the studies, a selective fluorescence quenching of bis-tolan glycoluril derivatives in the presence of nitrophenols was shown. The mechanism of the observed effect, as indicated in the work, can be presumably associated with the simultaneous occurrence of hydrogen bonds between the hydroxyl group of nitrophenol and the carbonyl group of glycoluril as well as the π - π -stacking interaction [59]. Interestingly, the phenols that do not contain nitro groups in the structure do not affect the changes in the fluorescence intensity.

The ability of dansyl glycoluril derivatives to fluorescence was studied in the presence of a wide range of metal ions: Ag^+ , Na^+ , Li^+ , Fe^{3+} , Cr^{3+} , Cu^{2+} , Pb^{2+} , Ni^{2+} , Zn^{2+} , Co^{2+} , Cd^{2+} , and Hg^{2+} [60]. The authors showed

that there is a dependence of the intensity of the light emitted by the complex on the metal nature. For instance, it was found that the addition of Cu^{2+} or Hg^{2+} ions leads to a decrease in the fluorescence intensity, while Pb^{2+} had practically no effect, and the remaining ions increase the fluorescence intensity of the dansyl glycoluril derivatives. Presumably, these properties are associated with the structure of the electron shell of metal atoms, their ionic radius, and the ability to complexation.

The opportunity for indirect fluorimetric determination of macrocyclic derivatives of glycoluril, namely, cucurbit[7]uril and cucurbit[8]uril, was demonstrated [61–64]. Cucurbit[n]urils specifically affect the fluorescence intensity of proflavin, pyronin, oxonin, Congo red, methylene blue, and other organic dyes. Thus, when interacting with the glycoluril-based macrocyclic compounds, the fluorescence intensity changes, e.g., at different pH, the acridine red fluorescence intensity increases naturally with the addition of cucurbit[7]uril.

A similar indirect method of fluorimetric determination was proposed to confirm the formation of a complex of cucurbit[n]urils with camptothecin [65]. Since the change in the fluorescence intensity of camptothecin with the addition of an equimolar amount of cucurbit[8]uril linearly decreases with the increasing concentration of the added cucurbit[8]uril until the point at which the molar ratio of the reagents is 1:1, the authors suggest the formation of a "guest-host" complex with the molar ratio of cucurbit[8]uril and camptothecin of 1:1 ratio.

The fluorimetric quantitative determination of cetylpyridinium in blood and urine with a limit of quantitation of $7 \mu\text{g/l}$ [66] is based on the differences in the emission spectra of complexes of cucurbit[7]uril-palmitin and free palmitin: the palmitin alkaloid is displaced by cetylpyridinium from the guest-host complex in this case, and a new emission maximum corresponding to free palmitin appears on the fluorescence spectrum. Due to the high selectivity of the fluorimetry method and the high affinity of the components of the "guest-host" complexes, high specificity of the method is achieved: the determination of cetylpyridinium does not interfere with the blood plasma components, anionic surfactants, amino acids, metal cations, many remedies, etc.

Using fluorimetric titration, a controlled transition was studied at different pH values of the rotaxane-like complex of cucurbit[6]uril with diaminobutane in various forms that differ in the position of the macrocyclic ring relative to the diaminobutane fragment of the molecule (Fig. 3) [67, 68].

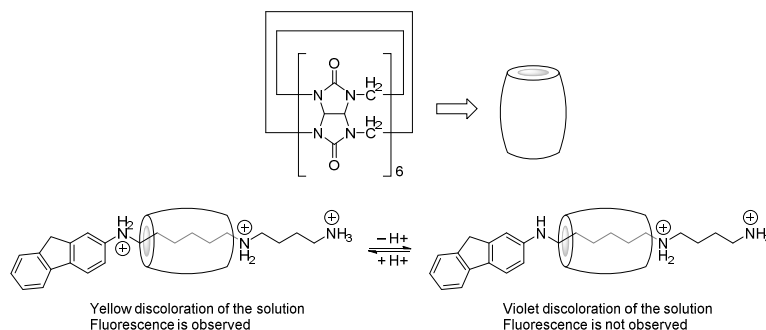


Figure 3. Dependence of the fluorescence of the "guest-host" complex on the relative position of the cucurbit[6]uril fragment in the structure

The authors found that with an increase in pH, the fluorescence intensity decreases, while at a pH value of 8.1, the fluorescence of the complex completely disappears indicating a quantitative transition of the complex to a non-fluorescent state.

The found fluorescence effects of such compounds can be used for the selective quantitative determination of "guest-host" complexes based on cucurbit[n]urils.

It is noteworthy that the fluorimetry is the most specific method for the direct determination of glycoluril derivatives containing conjugated aromatic fragments in the structure with the ability to fluorescence. The key advantages of the method are high sensitivity (the minimum detection limit is $\sim 10\text{--}17 \text{ g}$), the availability of equipment, the speed of analysis, and the safety of the structure of the substances being determined.

The main disadvantages of this method are the inability to obtain an analytical signal for non-fluorescent compounds, strict sample preparation requirements (the analytical signal is affected by the impurities in solvents, etc.) as well as the lack of flexibility of the method: the emission wavelength is an individual characteristic of the substance and cannot be changed. Thus, when two related compounds with close

emission wavelengths are in the sample, it is extremely difficult to achieve analysis selectivity without using preliminary separation of the sample components.

2.3. NMR spectroscopy

NMR spectroscopy is one of the most widely used methods in the analysis of glycoluril derivatives. An investigation of the NMR spectra of glycolurils makes it possible to determine accurately the spatial configurations of molecular symmetry when the hydrogen and carbon atoms of the bicyclic framework are expressed by equivalent signals. Using chemical shifts ^1H and ^{13}C in the NMR spectra of N-substituted glycolurils, it is possible to identify the type of substituent.

An analysis of chemical shifts in the ^1H and ^{13}C NMR spectra of glycoluril and its derivatives (library of 86 compounds) was carried out to determine the influence of the donor-acceptor nature of substituents on changes in the electron density in the bicyclic framework from the position of symmetry and asymmetry [69]. The range of changes in the chemical shifts of key atoms in the glycoluril series includes NH protons (7.49–9.96 ppm); CH–CH (5.14–6.63 ppm); carbon C=O (151.40–161.79 ppm); CH–CH (61.55–74.86 ppm). A general analysis of the ^1H and ^{13}C NMR spectra of the studied glycolurils allowed the authors to accurately identify the spatial symmetry configurations of the molecules, where the enantiotopic hydrogen and carbon atoms of the bicyclic framework (σ_1 and/or σ_2 , Fig. 2) appear as equivalent signals. It was established that according to the ^1H and ^{13}C chemical shifts in the NMR spectra of the N-substituted glycoluril framework, glycolurils with electron-withdrawing substituents for the screening of carbon atoms of C=O groups and electron-donating substituents for de-screening of CH–CH carbons can be distinguished. This is due to the redistribution of electron density and the occurrence of local paramagnetic contributions due to anisotropy.

In the course of a general analysis of the ^1H and ^{13}C NMR spectra of the studied glycolurils, it was concluded that screening of the carbonyl atom C=O in the imidazolidinone fragment of the molecule is observed for any type of N- or C-substitution. The generalizations made allow clearly distinguishing between symmetric and asymmetric molecules and distinguish impurity signals that can often accompany the synthesis of glycolurils and compounds on the basis thereof. According to the ^1H and ^{13}C NMR spectra, glycolurils can be clearly distinguished with electron-withdrawing N-substituents by screening the signals of the carbon atom of C=O groups, and electron-donating N-substituents by de-screening of CH–CH carbon.

In another review paper [70], a comprehensive systematic analysis of chemical shifts in the ^{31}P and ^{13}C NMR spectra of 89 phosphorus- and urea-containing heterocycles that differ in the valence state of the phosphorus atom, the size of the cycle, and the method of connection of the cycles was carried out. A comparative analysis of the chemical shifts of the phosphorus atom in phosphorus- and urea-containing heterocycles with five-coordinated phosphorus showed that they mainly undergo a negative shift, and their location mainly depends on the hybrid state of P in the cycle and the way the cycles are connected. An attempt of a comparative analysis of the chemical shifts of the –C=O carbonyl group in phosphorus- and urea-containing heterocycles did not reveal the significant differences due to their changes in a narrow range of values (151–156 ppm), regardless of the valence state of the phosphorus atom in the cycle and the way of connection of the cycles (e.g., in spiro- and bicyclic compounds). Of interest is only some screening of the C=O group in phosphorus- and urea-containing heterocycles compared to urea itself (159.5 ppm) and octane-bicyclic bisurea glycoluril **1** (161.9 ppm). This observed effect is apparently determined by an increase in steric stresses (compression) in phosphorus- and urea-containing heterocycles due to limitations in the flexibility of their skeleton, and, hence, an increase in the order of the amide bond. The informativity of analysis of the NMR spectra of phosphorus- and urea-containing heterocycles to some extent is reduced by the absence of chemical shifts of NH groups, but this circumstance is because almost all synthesized and identified phosphazacycles listed in the work contain substituents at nitrogen atoms.

Apparently, due to the low content of natural ^{15}N and ^{17}O isotopes and high complexity of the analysis, there is practically no information in the literature on the use of NMR on ^{17}O nuclei for several glycolurils, and to obtain the information on the position of chemical shifts of ^{15}N glycoluril **1** and its derivatives the 2D heterocorrelations of the ^1H – ^{15}N spectra [71] and the establishment of the direct coupling constant ^{15}N – ^1H are usually used [72].

Thus, NMR spectroscopy is a serious tool to identify and confirm the structure of glycoluril derivatives. This method is the most reliable way to study the structure of substituted glycolurils, i.e., the position, amount, and type of N-substituents. A particular advantage of NMR spectroscopy is that the method allows establishing the spatial configuration of the glycoluril symmetry with high accuracy. A number of studies

have demonstrated the opportunity to use NMR spectroscopy for the analysis of glycoluril-based supramolecular systems. Thus, a detailed analysis of ^{13}C NMR spectra was performed for the identification of a series of cucurbit[5–8]urils [73]. In Ref. [74] during the simulation of the binding process of the SF5 complex with cucurbit[6]uril, the NMR shifts of the formation of the inclusion system were calculated and compared with the experimental values. It was proposed to include the prochiral dimethyl sulfonic derivatives of biphenyls in the cucurbit[7,8]uril cavity that allows recording the proton chemical shifts due to the splitting of signals of a pair of methyl groups [75].

A key disadvantage of NMR spectroscopy as a method of analysis of glycoluril derivatives is its non-selectivity for related compounds when substances are present in the sample as a mixture. In addition, an important disadvantage is the relatively high cost of NMR spectrometers and the need to use deuterated solvents.

2.4. X-Ray structural analysis

The geometric features of glycolurils (Figs. 1 and 2) essentially determine the opportunity to synthesize and study supramolecular compounds on the basis thereof. In the course of such studies, it was found that glycolurils acted as building blocks of such polycyclic condensed systems as cucurbit[n]urils [76–78] and bambus[n]urils [79, 80] that have a number of unique physical & chemical properties.

A study of the spatial arrangement of molecules determined by intermolecular interaction and polarization of bonds in synthons often provides initial information on the organization of supramolecules on the basis thereof. The obtained information on the structure of molecular ensembles extracted from the crystal structures of synthons is used to judge on the structure of liquids and solutions, molecular clusters, and other supramolecular structures.

Taking into account the above, the analysis of the results of X-ray structural studies of glycoluril **1** and its derivatives (a library of 39 compounds) was carried out [81] and the structural features of these compounds were revealed, namely, the effect of substituents and their types on the geometry of molecules, and the formation of hydrogen bonds in crystals that ultimately determines the ability of glycolurils to form complexes, macro- and supramolecules. The result of the generalization of X-ray structural studies of a wide range of glycolurils made it possible to determine the centers of formation of hydrogen bonds and those participating in complexing since in these cases it is the elongation of precisely those bond lengths that are involved in intermolecular binding.

An analysis of the structural parameters of N-alkyl glycolurils and metal complexes showed the presence of conformational similarity of the molecular scaffolds of the compounds studied. It was shown that N-alkyl substituted glycolurils are potentially polydentate ligands (due to the contribution to the coordination of four nitrogen atoms and two oxygen atoms) and can fulfill both a monodentate and a bidentate bridging function with d-metals via binding of urea fragments through C=O groups depending on the coordination number of the metal atom.

For complexation, oxygen and nitrogen atoms are the most possible coordination centers in glycolurils, however, coordination through nitrogen atoms is usually sterically hindered due to its predominant pyramidal structure, especially since this center has a reduced electron density with respect to oxygen.

The basic geometric parameters of the bicyclic framework for N-arylalkyl glycolurils are similar to those for N-alkyl glycolurils. When a substituent with a strong electron-withdrawing property is introduced into the glycoluril skeleton, the bond lengths of the C–N amide fragment increase causing a decrease in the nature of doubling and an increase in the nature of the C=O double bond. This fact can be explained by more efficient hybridization of carbonyl carbon atoms to the sp^2 state and to the sp^3 state in the C–N fragment occurring for these compounds.

When considering the dihedral angles of the studied glycolurils together, it was concluded that for any type of substitution (C- or N-) in the glycoluril framework, the values of the dihedral angles change towards their reduction, i.e., the effect of "collapsing" of annelated imidazolidinone cycles is observed. However, when considering C1–C5 substituted glycolurils, a progressive decrease in the dihedral angle in these molecules occurs with an increase in the size of the hydrophobic substituent (H>Me>Ph compounds). The same pattern is observed in a series of compounds in the presence of an electron-withdrawing functional group (H>NH₂>CO₂Et) in C1–C5-substituted glycolurils.

The performed studies on the structure of glycolurils by X-ray structural analysis turned out to be useful for researchers involved in the designing of new molecules based on glycoluril **1** with predetermined properties in the synthesis of biologically active compounds, molecular clips, and supramolecular systems.

2.5. Mass-spectrometry

Mass spectrometry also finds its place in the study of glycoluril derivatives. The "direct input" mass spectrometry is most often used when a mixture of substances is introduced into the ionization source of the mass spectrometer without prior separation by chromatographic methods. A method of mass spectrometry with electrospray ionization (ESI-MS) of N-alkylated glycoluril dimers without their preliminary chromatographic separation was proposed [82]. In the given mass spectrum, three signals of molecular ions of a mixture of glycoluril dimers were observed (Fig. 4).

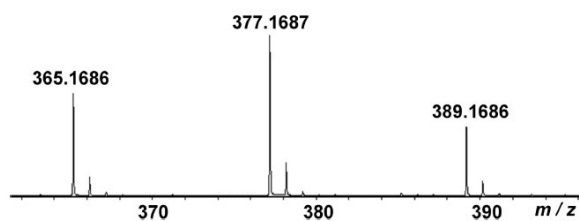


Figure 4. Mass spectrum of the mixture of glycoluril dimers without decomposition

The electron-ionization mass spectrometry (EI-MS) is widely used to confirm the structure of low molecular weight glycoluril derivatives [83]. Using this ionization method during mass spectrometric studies of synthesized samples, mass spectra of a large number of N-alkylated and N-acylated glycoluril derivatives are described. However, the EI-MS ionization mode used in mass spectrometers is de facto incompatible with liquid chromatography: modern EI-HPLC solutions do not provide sensitivity comparable to atmospheric pressure ionization modes (API). Thus, this method cannot be used to study and analyse mixtures of non-volatile compounds that is characteristic of many glycoluril derivatives.

Mass spectrometry was used to study the composition and decomposition paths of glycoluril nitro derivatives. It was shown that dinitroglycoluril, when introduced into the ion source of electronic ionization, is characterized by a number of ions $m/z=232, 231, 215, 183, 142$, etc., on the mass spectrum [23]. The key ionization pathways are related to the breaking of C–N and N–H bonds as well as OH group losses. A number of signals in the mass spectrum may not be associated with dinitroglycoluril, and their source may be connected with possible impurities formed during the synthesis of glycoluril. Dinitroglycoluril labeled with $2D$ and ^{15}N atoms was shown to undergo similar fragmentation without significant differences in the intensity of the fragment ions.

In Ref. [84], mass spectra were obtained from a study of the isolated samples for a number of isomeric dimethylglycolurils **3–5** by GC-MS (Fig. 5).

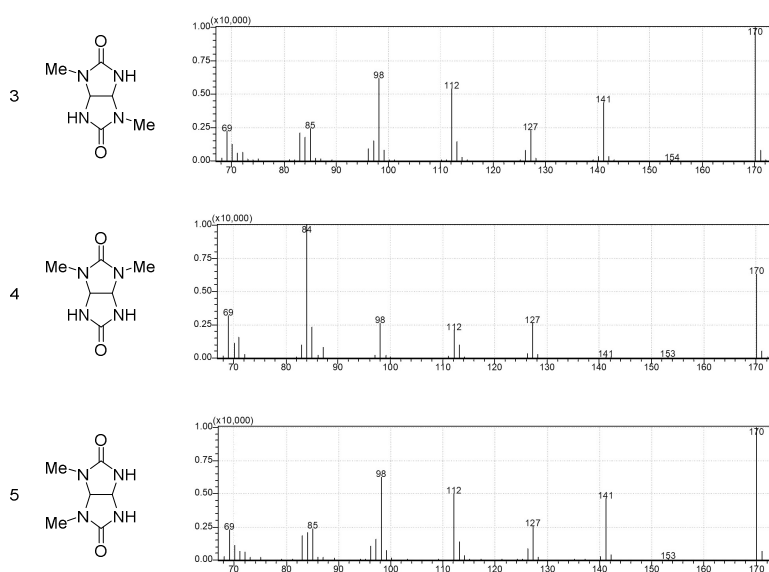


Figure 5 Structural formulas and mass spectra for isomers of N-dimethylglycolurils

As can be seen from the mass spectra of these compounds, the m/z values of the fragment ions of substances **3** and **5** are absolutely identical, therefore, gas chromatography-mass spectrometry can only be used to identify isomer **4**. The authors assumed that the absence of visible differences in fragmentation **3** and **5** are associated with similar trajectories of possible fragmentation paths **3** and **5** and the difference in the proposed mechanism of fragmentation of substance **4** (Fig. 6).

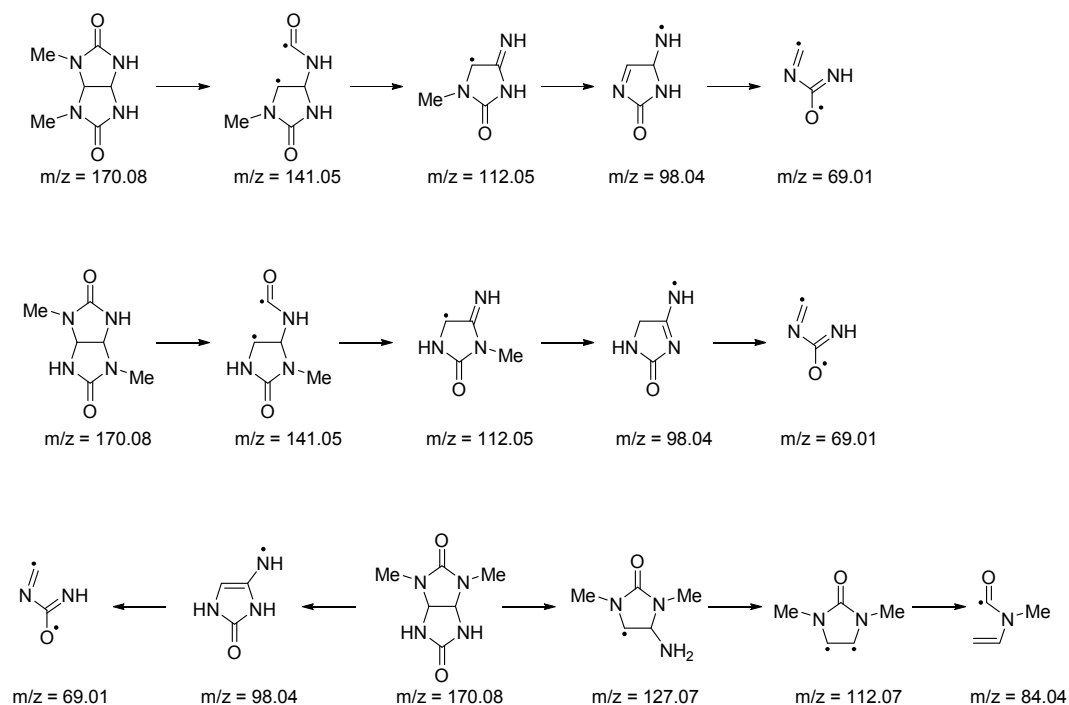


Figure 6. Tentative scheme of fragmentation of molecules **3**, **4**, and **5** during electron ionization

The proposed fragmentation scheme shows that substances **3** and **5**, when they are electronically ionized, form a series of successive ion radicals with similar m/z values. Contrary, during ionization, substance **4** forms two sequences of radical ions, and this mechanism excludes the possibility of the formation of a radical ion with a value of $m/z=141$. By the presence of this ion, it is possible to judge whether a particular N-dimethylglycoluril belongs to isomer **4** or one of isomers **3** or **5**. The results of the studies allow reliable identification of isomeric dimethylglycolurils **3–5**.

Refs. [85, 86] describe the use of the ESI-TOF-MS high-resolution mass spectrometry method to study the glycoluril derivatives. However, mass spectrometry was used without prior chromatographic separation to confirm the structure of oligomeric glycoluril derivatives. The authors of the work showed that the "Negative" ionization method can be used to obtain the analytical signal, while the formation of a number of adducts of the expected composition was observed, e.g., $[M^+Br]^-$, $[M^+Cl]^-$, $[M^+F]^-$, $[M^+H-3Na]^{2-}$.

The direct ionization mass spectrometry "Positive" is used to identify monomeric glycolurils, in particular, to identify phosphorylated derivatives of glycoluril [26], N,N'-diacetylglycolurils and N,N'-dibenzylglycoluril [87]. In both cases, molecular ions of the corresponding glycolurils with the composition $[M^+H]^+$ were detected; the fragmentation mechanism was not described by the authors.

To study the composition and quantitative determination of glycoluril derivatives by mass spectrometry, the method of matrix-associated laser desorption and ionization (MALDI-MS) was proposed [88]. The method is based on the soft ionization of molecules under the influence of laser radiation in the presence of acids or bases. The MALDI-MS allows the analysis of supramolecular glycoluril derivatives in matrices of complex composition, e.g., biological objects, without preliminary sample preparation and separation into components. Moreover, the advantages of the method are the high sensitivity (minimal detection limit is $\sim 10^{-15}$ g) and the ability to analyze compounds with high molecular weights (up to 150 kDa).

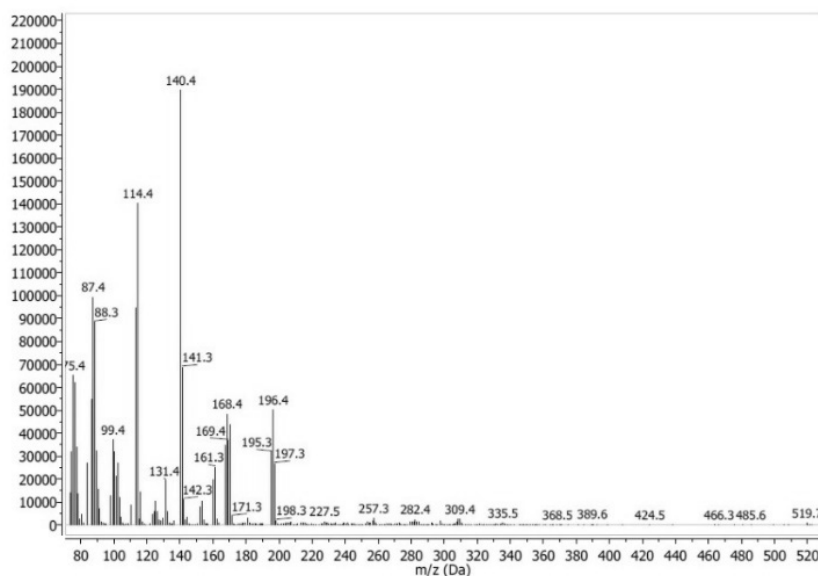


Figure 7. An example of mass spectrum of glycoluril derivative [26]

The widespread use of liquid mass spectrometry is largely hindered by the high cost of the equipment for the study as well as the complexity of the method and the requirements for the purity of the sample and the reagents and materials used.

2.6. Other spectroscopic methods

The method of nuclear gamma resonance spectroscopy (Mössbauer spectroscopy) is limitedly used to analyse glycoluril derivatives containing iron atoms in the structure: cucurbit[n]uril ferrocenes [89] and other glycoluril-based supramolecular complexes [90].

Raman spectroscopy is also used to a limited extent in the study of glycoluril derivatives, in particular, to control the course of reactions and study the structure of some glycoluril derivatives, namely, guest–host complexes. In particular, the difference between the signals on the spectra of new glycoluril-based complexes and those of their components was shown [91–93]. In particular, when using this type of spectroscopy, the spectrum cannot be deciphered in details, it is used only to monitor the synthesis and subsequently identify the compounds by the "fingerprints" principle.

EXAFS spectroscopy is a spectroscopic method based on the interpretation of the fine structure of X-ray absorption spectra. The Refs. [94–96] show examples of deciphering the 3D structure of cucurbit[n]uril complexes and metal compounds: Cu(II), U(VI), and Eu(III) (Fig. 8). The EXAFS spectroscopy method allows determining the interatomic distances, coordination numbers, valence states of atoms, and other parameters. The rarity of use of this method with respect to glycoluril derivatives is explained by the high cost of equipment and the inability to determine the spectral parameters of compounds that do not contain elements with a molecular weight below 20 in the structure.

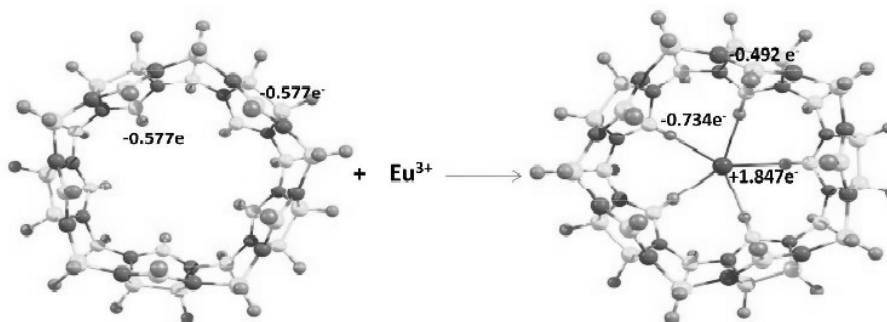


Figure 8. An example of visualization of EXAFS spectra of a complex of cucurbit[5]uril and Eu(III) [96]

3. Electrochemical methods of analysis

Electrochemical methods to analyze glycolurils are presented in very rare cases. Thus, the voltammetry method is limitedly used for the direct determination of glycoluril derivatives, e.g., for analysis of guest-host complexes based on cucurbit[7]uril and substituted metallocenes: ferrocene and cobaltocene [97, 98], and only due to the electrochemical activity of metals in these compounds.

Glycoluril derivatives are used as electrode modifiers. To analyze cholesterol in blood plasma and food products, the authors of Refs. [99,100] applied the electrode modification to a phosphorylated glycoluril derivative that does not have its own electrochemical activity.

The opportunity to study macrocyclic complexes of glycoluril with zinc, manganese, cobalt, nickel, and cadmium by polarography with a dropping mercury electrode was studied [101, 102]. The relationship between the analytical signal, the concentration of metal, cucurbit[n]uril, and the interaction constant of the components of the guest-host complex was shown.

Electrochemical methods of analysis are rarely used to study and analyse glycoluril derivatives. Obviously, this phenomenon is associated with their direct physical-chemical properties, namely, with low solubility and high chemical inertness.

4. Chemical methods of analysis

Currently, glycoluril derivatives are rarely analysed using "traditional" chemical methods of analysis. The study of the decomposition products of cucurbit[n]urils was carried out using a combination of instrumental physical-chemical and chemical analysis methods [103] in the latter case, using qualitative reactions. The evolution of ammonia and the formation of sodium carbonate during the boiling of glycoluril derivatives in a 30 % sodium hydroxide solution was confirmed by the colouring of the indicator paper.

The quantitative determination of N-alkylated glycoluril derivatives can be carried out using the Kjeldahl method [104]. To quantitatively determine the N,N,N,N-tetramethylglycoluril, the methods of cerimetric and iodometric titration can also be used [105]. These analysis methods are non-selective in nature and are suitable only for analysis of the mass fraction of the main substance provided that the impurities are identified and analysed by another method, e.g., chromatography.

5. Chromatographic methods of analysis

5.1. Gas chromatography (GC)

Several examples of the gas chromatographic analysis of glycoluril derivatives are known. For instance, it was proposed to separate fully alkylated glycoluril derivatives: N,N,N,N-tetramethylglycoluril, N,N,N,N-tetraethylglycoluril, N,N,N,N-dimethyldiethylglycoluril, and N,N,N,N-isopropyltrimethylglycoluril using a one-meter-long packed chromatographic column filled with stationary phase G3 OV-17 (50 % diphenyl-, 50 % dimethylpolysiloxane) [104].

A method to analyse the content of N,N,N,N-tetramethylglycoluril in biological fluids after extraction with chloroform was proposed [106]. The method consists in gas chromatographic separation of N,N,N,N-tetramethylglycoluril from the matrix components using a steel packed column filled with chromosorb-G, modified with 3 % diphenyldimethylpolysiloxane OV-17. The carrier gas is nitrogen, isothermal chromatography is carried out at 240 °C, the gas flow rate at the column outlet is 35 ml×min⁻¹. The injection volume of the solution is 2 µl.

The method of analysis of N,N,N,N-tetraethylglycoluril by gas chromatography using a capillary chromatographic column was recommended [107]. Analysis conditions: glass column 0.26 mm × 25 m, stationary phase was Xe-60 (cyanoethyl methylsiloxane), isothermal analysis, column temperature was 185 °C, carrier gas flow rate was 2 ml min⁻¹; stream division was 1/20. The internal standard was N,N-dimethyl-N,N-diethylglycoluril. Using this method, the retention times for N,N,N,N-tetraethylglycoluril and N-dimethyl-N-diethylglycoluril were 20 and 24 min, respectively.

5.2. Thin-layer chromatography

The chromatography method to separate and analyze glycoluril derivatives is used less frequently than spectral analysis methods. Most often, in the publications concerning glycoluril derivatives, the authors note that the reaction progress is monitored by TLC [36, 108–111]. However, a fairly common case is that the conditions for chromatographic analysis and typical chromatograms and photographs of TLC plates are not provided.

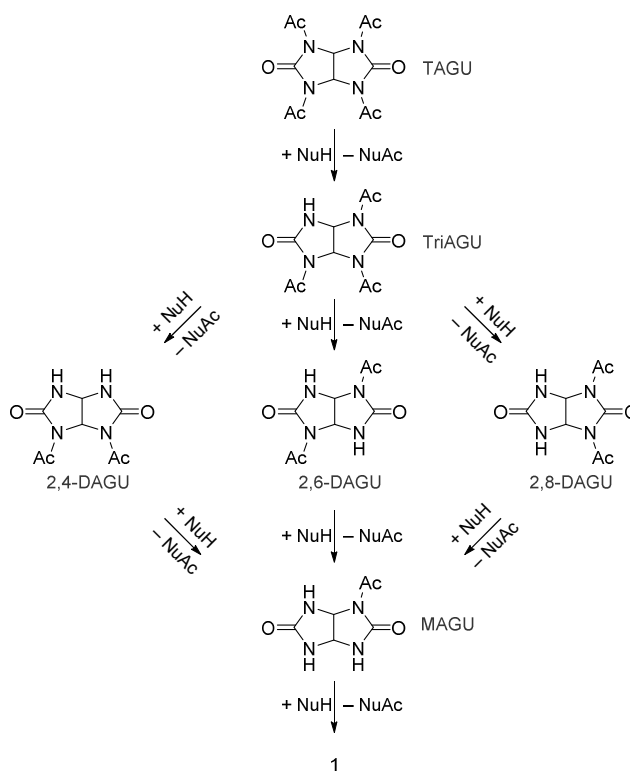
The hydrolysis of tetraacetylglycoluril under the action of various nucleophilic reagents at room temperature and pH=10 in an aqueous-alcoholic medium was studied in details (Fig. 9) [112].

The authors found that the hydrolysis of compound 2 occurs stepwise through the formation of a series of N-acetylglycolurils: triacetyl derivative; isomeric diacetylglycolurils; monoacetyl derivative and finally glycoluril **1**. The TLC is carried out on tetraacetylglycoluril hydrolyzate on kieselguhr plates, the eluent is chloroform-methanol-ethyl acetate (7:2:2) followed by the development with hydroxylamine and ferric chloride that allowed separating and establishing the R_f values for the acylated glycolurils (Table 4).

Table 4

The R_f values for products of tetraacetylglycoluril hydrolysis

| Substance | R _f |
|-----------|----------------|
| 1 | 0.04 |
| TAGU | 0.84 |
| TriAGU | 0.76 |
| 2,6-DAGU | 0.68 |
| 2,4-DAGU | 0.35 |
| 2,8-DAGU | 0.61 |
| MAGU | 0.21 |



TAGU = TetraAcetylGlycolUril, TriAGU = TriAcetylGlycolUril, DAGU = DiAcetylGlycolUril, MAGU = MonoAcetylGlycolUril

Figure 9. Scheme of tetraacetylglycoluril hydrolysis

Individual acetylglycolurils were characterized using NMR and mass spectrometry.

The TLC method was used to confirm the structure and content of impurities of N,N,N,N-tetramethyl glycoluril, the active substance of the remedy "Adaptol" (JSC "Olainfarm", Latvia) [113]. The identities of other alkylated glycoluril derivatives were also controlled by TLC [114]. The separation was carried out using "Silufol" plates as the stationary phase. The plates were chromatographed using supported samples with an ascending method with a solvent mixture of acetone-hexane in a volume ratio of 5:2. The plates were developed by keeping in the iodine chamber for 1–2 min. Under these conditions, the R_f values for N,N-dimethyl-N,N-diethylglycoluril and N,N,N,N-tetraethyl glycoluril were 0.41 and 0.49, respectively.

Similar chromatographic conditions for the analysis of N-dimethyl-N-diethylglycoluril and its impurities, N-monomethyl-N-diethylglycoluril, were proposed [105]. The stationary phase was "Silufol", the mobile phase was a mixture of chloroform and methanol in a ratio of 8:1 v/v. The development was carried out by spraying with a 10 % alcohol solution of the phosphoromolybdic acid followed by heating the plate to a temperature of 140 °C. When using this chromatographic system, the R_f values for N,N-dimethyl-N,N-diethylglycoluril and monomethyl-N,N-diethylglycoluril were 0.55 and 0.37, respectively.

In the vast majority of cases, TLC separation of glycoluril derivatives is realized using normal-phase mode on silica gel. The compositions of mobile phases for TLC were studied, and the separation of N,N,N,N-tetramethylglycoluril (Mebicar) from a number of drugs with similar pharmacological activity (chlorprothixene, imiprazine, clozapine, etc.) was carried out [115].

The normal-phase TLC mode was used for the separation and further preparative isolation of the "molecular clamps" based on glycoluril **1** [116], i.e., aromatic glycoluril derivatives with a complex composition. The authors proposed the use of silica gel as the stationary phase, and a mixture of methanol, ethyl acetate, and chloroform in various ratios as the mobile phase until optimal retention was achieved depending on the type of silica gel. Almost similar chromatographic conditions for C-substituted glycoluril derivatives were proposed [117, 118]. The stationary phase was unmodified silica gel with a particle size of 63–20 μm , the mobile phase was chloroform-ethyl acetate (8:2 v/v). The photograph given by the authors (Fig. 10) showed that when using this method, complete separation of the mixture was not achieved. Similar conditions were proposed to control the progress of the reaction of N, N, N, N-tetramethylolglycoluril with arylamines [119]. As a stationary phase, TLC plates based on silica gel-G Sorbfil-254 were used; the mobile phase was benzene-ethanol (8:2 v/v).

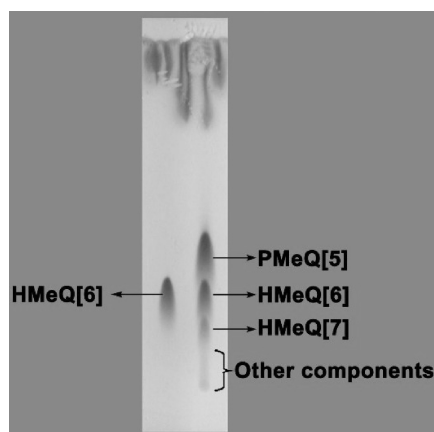


Figure 10. An image of TLC plate after separation of C-methylcucurbiturils [120]

The authors used a universal method to control the N,N,N,N-tetramethylolglycoluril derivatives by TLC using the mobile phase of chloroform-methanol (9:1 v/v) on aluminum plates coated with silica gel-G Silufol 254 [120, 121].

The authors of Ref. [122] described a method to identify and analyze the N,N,N,N-tetramethylglycoluril in blood plasma by TLC in an open unsaturated evaporation chamber. The stationary phase was silica gel-G produced by Sorbfil, the mobile phase was acetone.

Chromatography on paper is currently rarely used to separate the low molecular weight substances due to the high complexity. Ref. [123] describes a method for chromatographic separation of unsubstituted glycoluril **1** and its related concomitant substances, such as allantoin, hydantoin, and hydantoic acid. The mobile phase when the maximal separation of the components was achieved comprised n-butanol-acetic acid-water in a ratio of 100:22:5 v/v/v. After separation, the paper was dried, sprayed with a 0.25 % alcohol solution of mercury (II) acetate, redried, sprayed with a 0.05 % solution of diphenylcarbazone in ethanol and heated to a temperature of 90 °C. Glycoluril **1** and its related compounds were claimed to form light blue spots on the paper.

5.3. Column liquid chromatography (LC)

The column chromatography is used less frequently than the TLC to separate and analyze glycoluril derivatives. Ref. [124] presents an example of the separation by a method of low-pressure liquid chromatog-

raphy of a mixture of glycoluril derivatives. Thus, C, C'-diphenyl-N,N'-dibenzylglycoluril, the initial and by-products of the synthesis, were separated and isolated by normal-phase chromatography using spherical silica gel with a particle size of 50 μm as a stationary phase, and a mixture of chloroform-methanol (50:1 v/v) as a mobile phase.

The composition of the reaction products between formaldehyde and glycoluril **1** was studied by reverse phase chromatography with spectrometric detection in the UV region [125]. The best separation of the peaks of glycoluril **1** and the products of its interaction with formaldehyde was achieved using the stationary phase Hypersil MOS 5 μm 200 \times 4.6 mm and water as the mobile phase. However, according to the results of the study, the authors found various products of glycoluril methylation with formaldehyde. The compounds were not identified, moreover, a complete chromatographic separation of the components of the mixture was not achieved: the resolution between the peaks did not exceed the value $RS=1.2$ even with a retention time of the most retained component $t_R=34.3$ min.

The purity and yield of carboxylated glycoluril derivatives were evaluated by RP-HPLC using the stationary phase Kromasil C18 (spherical endcapped octadecylsilylated porous silica gel) [126]. The mobile phase was a water-methanol mixture (6:4 v/v). The isocratic elution was applied. The optical purity of glycoluril derivatives was evaluated by chiral chromatography using a stationary Astec Chirobiotic T phase based on the macrocyclic glycopeptide antibiotic teicoplanin grafted onto silica gel. A similar approach to the separation of enantiomers of glycoluril derivatives was described [127, 128]. The authors used similar sorbents as stationary phases to analyze the optical purity, i.e., silica gels modified with teicoplanin aglycon (Astec Chirobiotic TAG).

The diastereomers of the macrocyclic aromatic derivatives of glycoluril, xylenebambusurils, were separated using preparative reverse-phase gradient flash chromatography on a Grace C18 sorbent using a mixture of water and acetonitrile in volume ratios from 80:20 to 0:100 as a mobile phase [129]. The target diastereomers were found partially separated and eluted from the cartridge in 27–30 min.

According to Ref. [130], quantitative determination of N,N,N,N-tetramethylglycoluril (Mebicar) in the composition of drugs, in tablets, granules and capsules was carried out by HPLC, but the authors did not disclose the analysis conditions. In addition, some manufacturers of N,N,N,N-tetramethylglycoluril declared that the mass fraction of the main substance in their products was monitored by HPLC, however, the analysis methods were not publicly available.

Ref. [131] shows the opportunity for chromatographic determination of N,N,N,N-tetramethylglycoluril by the method of microcolumn HPLC using a chromatographic column filled with a ProntoSil 120-5-C18 Aq (Knauer) reversed phase spherical adsorbent (Knauer) was shown to be chromatographic. Mobile phase A was 200 mM lithium perchlorate solution, adjusted with a 5 mM perchloric acid solution to $\text{pH}=2.8$; mobile phase 2 was acetonitrile. Elution mode comprised a linear gradient from 5 % to 70 % acetonitrile. The retention time of N,N,N,N-tetramethylglycoluril was ~ 7 min; the total analysis time was 40 min.

Unlike unsubstituted glycoluril **1**, its N-methyl derivatives **2–6** are soluble in many polar organic solvents, including water. This circumstance served as the basis to study the chromatographic separation of N-methyl derivatives of glycoluril in several modes differing in the expected retention mechanism and selectivity: reverse phase chromatography and hydrophilic chromatography [84]. The development of chromatographic separation of N-methyl derivatives of glycoluril was carried out using the following samples of substances (Table 5).

Table 5

Model glycolurils used in Ref. [84]

| Number of compound | Name |
|--------------------|-------------------------------|
| 1 | Glycoluril |
| 2 | 2-Methylglycoluril |
| 3 | 2,6-Dimethylglycoluril |
| 4 | 2,8-Dimethylglycoluril |
| 5 | 2,4-Dimethylglycoluril |
| 6 | 2,4,6,8-Tetramethylglycoluril |

In the reverse phase mode, the retentions of N-methyl derivatives of glycoluril were found to increase with an increase in the number of alkyl substituents. Tetramethylglycoluril did not elute from the column

when a 1 % solution of acetonitrile in water was used as a mobile phase, and the L1 PerfectSil Target ODS-3 HD spherical porous silica gel with a particle size of 5 μm was used as a stationary phase (MZ-Analysentechnik GmbH). When 5 % acetonitrile was added to the composition of the mobile phase, substance 6 was eluted from the column, while in the reverse phase mode for substance 1, the minimal required retention was ensured to resolve the critical group of peaks (Fig. 11).

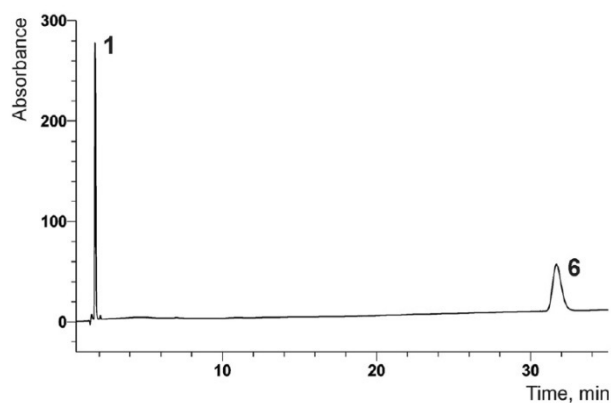


Figure 11. Chromatogram of a solution of mixture of glycoluril and tetramethylglycoluril

Since it is impossible to achieve sufficient chromatographic separation of weakly retained components 1–2 in the reverse phase chromatography under elution conditions of tetramethylglycoluril 6, it was assumed that the complete chromatographic resolution and elution of substances 1–6 in a short time was possible using the gradient elution mode comprising a continuous sequential increase in the eluting solvent strength. In order to verify this thesis, a series of experiments was carried out. For this, substances 1–6 were chromatographed under the following conditions: a column with the size of 150 \times 4.6 mm L100 Zorbax SB Aq, with a sorbent particle size of 5 μm (Agilent Technologies); mobile phase A was 5 % solution of acetonitrile in water; mobile phase B was 25 % solution of acetonitrile in water; gradient profile: 0.0 min — 0 % PF B, 1.5 min — 25 % PF B; volumetric flow rate $F=1.5 \text{ ml} \times \text{min}^{-1}$; column thermostat temperature was 30 $^{\circ}\text{C}$; injection volume was 5 μl .

Fig. 12 shows that the substances 3–6 are eluted from the column with the shortest time, and sufficient retention of substances 1–2 is observed; however, dimethyl glycoluril isomers 3–4 are not completely separated ($R_{S3/4}=1.35$) making up a critical pair of peaks due to insufficient chromatographic selectivity system.

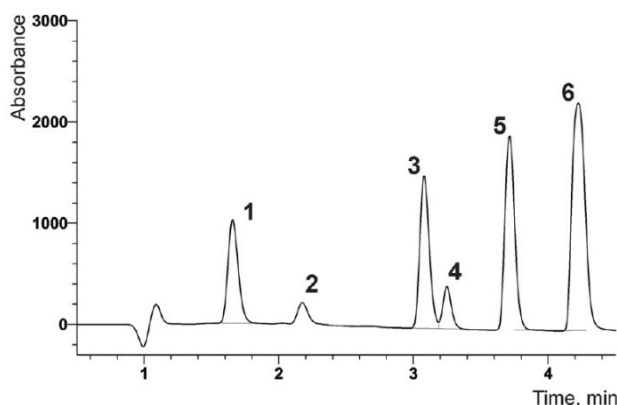


Figure 12. Chromatogram of a solution of a mixture of 1 and its derivatives 2–6 obtained using the stationary phase Zorbax SB-Aq. For this stationary phase, the separation conditions were practically not optimized

Thus, when optimizing the resolution using the approach of increasing N by extending the chromatographic column or by increasing the overall retention of the chromatographic system, the minimal resolution can be achieved by increasing the analysis time.

It has been suggested that the selectivity for structural isomers of dimethylglycoluril 3–4 can be increased by using the stationary phase with grafted "planar" polar fragments. Such stationary phases are char-

acterized by specificity with respect to structural isomers, i.e., "shape selectivity". In addition, a decrease in the selectivity of the chromatographic system with an increase in the retention coefficient in the reverse phase chromatography mechanism realized due to dispersion (hydrophobic) interactions is possible by combining gradient elution (linear increase in the eluting force of the mobile phase) and using a stationary phase containing a grafted linker layer short-chain fragment. Presumably, all of these requirements can be met using halogenated phenylalkylsilylated silica gels such as dimethyl(3-(pentafluorophenyl)propyl)silyl silica gel (F5, PFP, etc.) [85].

When using such stationary phases, according to the authors, a complex retention mechanism is realized by combining hydrophobic interactions between methyl and methine groups of glycolurils, dipole-dipole interactions, hydrogen bonds, and steric shape selectivity due to "flat" grafted selectors that are fragmentarily shown in Fig. 13.

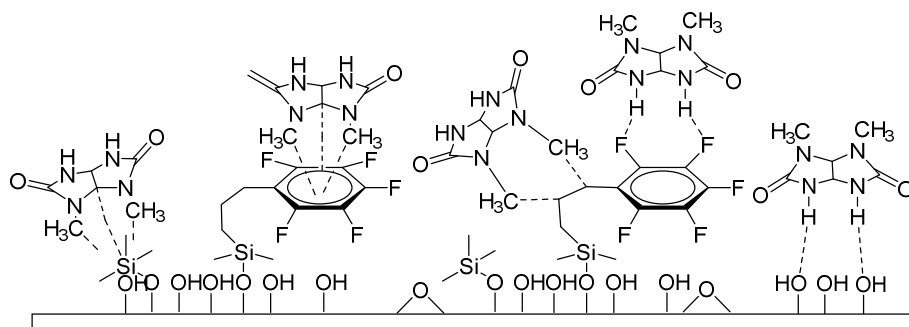


Figure 13. Simplified proposed multiple interactions between N-methyl derivatives of glycoluril (using 2,4-dimethylglycoluril as an example) and the stationary phase with a "flat" selector PFP; the dotted line indicates the intermolecular interactions

To verify the possibility of complete separation of methylglycolurils, a prefilled column with the size 150×4.6 mm filled with spherical endcapped pentafluorophenylpropylsilyl silica gel L43 — Luna 5u PFP (2) 100 Å with a particle size of 5 μm (Phenomenex) was used. Chromatographic conditions: mobile phase A was 5 % solution of acetonitrile in water; mobile phase B was 25 % solution of acetonitrile in water; gradient profile: 0.0 min — 0 % PF B, 1.5 min — 25 % PF B; volumetric flow rate $F=1.5 \text{ ml} \times \text{min}^{-1}$; column thermostat temperature was 30 °C; 5 μl injection volume was used.

When using this stationary phase in the gradient elution mode, complete chromatographic separation of substances 1–6 was achieved in less than 4 min (Fig. 16) with a minimum resolution of $R_S=1.6$.

Thus, the approach allowed achieving effective chromatographic separation of glycoluril 1 and its methyl derivatives 2–6, including isomeric dimethylglycolurils 3–5.

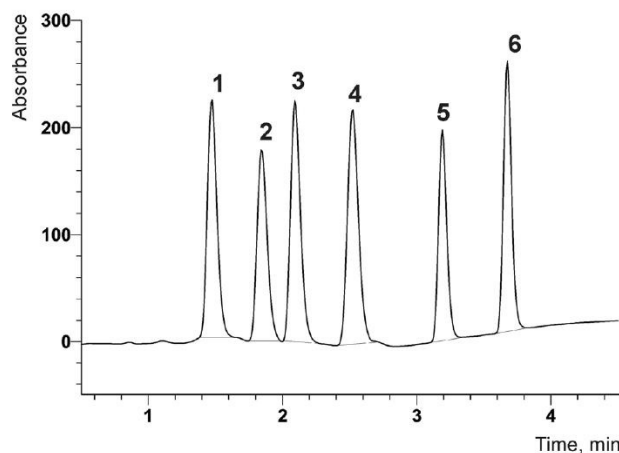


Figure 14. Chromatogram of a solution of a mixture of glycoluril 1 and its N-methyl derivatives 2–6 under optimized conditions using stationary phase Luna PFP(2) 5u

Aromatic derivatives of glycoluril (1,6-bis(*p*-methoxybenzyl)-7,8-di-*p*-tolyl glycoluril, 1,6-dibenzyl glycoluril) were isolated from the reaction mass by flash chromatography [132]. Dry unmodified silica gels were used as the stationary phase, mixtures of ethyl acetate with *n*-hexane with an ethyl acetate content of 30 % to 50 %, and methanol with methylene chloride in a ratio of 1:10 v/v were used as the mobile phase.

Ion exchange and ligand exchange chromatography methods are used to a limited extent to isolate glycoluril derivatives. For instance, the sodium complexes of glycoluril oligomers (decamers) were isolated from the reaction mass by ligand exchange preparative chromatography [133].

Size exclusion chromatography is used to analyze the molecular weight of glycoluril-based polymers. The gel permeation chromatography (GPC) mode was used to determine the molecular weight of water-insoluble glycoluril-based polymers [134, 135]. The stationary phase in this mode was a porous, hyper-crosslinked polystyrene polymer; the mobile phase was most often chloroform or dimethylformamide.

The molecular weight of water-soluble glycoluril-based polymers is most often analyzed using size exclusion chromatography (SEC). For instance, water-soluble polymers based on glycoluril, epichlorohydrin, and formaldehyde were studied by the SEC method [136].

Ref. [137] showed the use of HPLC method to confirm the hypothesis of the formation of a guest-host supramolecular complex (Fig. 15). As the authors suggested, when cucurbit[*n*]urils were added to the lipophilic compounds, the retention time of the compound in the reverse phase mode was reduced. The analysis was performed under the following conditions: column was Agilent XDB-C18 (4.6 mm × 150 mm, 5 μm), elution was gradient water → acetonitrile in a v/v ratio of 95:5 to 5:95 in 18 min, flow rate was 1 ml×min⁻¹. The mobile phase was acidified with 0.1 % trifluoroacetic acid to suppress secondary interactions in the column.

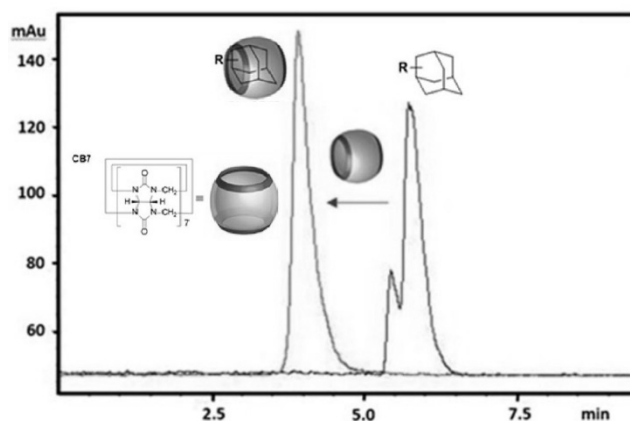


Figure 15. Chromatogram of the starting compound (blue curve) and its guest-host complex with cucurbit[7]uril (red curve)

Using preparative chromatography with the stationary C18 phase, it was proposed to isolate substituted macrocyclic glycoluril derivatives from the reaction mass, but the authors did not present the separation conditions and chromatograms [138].

N,N-Diglycidyl derivatives of glycoluril used as crosslinking agents for the production of high-purity polymeric materials were purified from the related impurities by preparative chromatography [139]. Unmodified silica gel was used as a sorbent; eluent was a mixture of chloroform and methanol 10:1 v/v.

The authors of Refs. [140–143] indicated that the analysis of glycolurils was carried out by HPLC, but the conditions of analysis and chromatograms were not provided.

Conclusions

Thus, chromatographic methods are the most promising and informative for the analysis of glycoluril 1 and its related compounds, since they allow rapid separation of complex mixtures of organic substances simultaneously with a quantitative determination. In addition, chromatographic separation can be adapted for preparative isolation of individual glycoluril derivatives in pure form as well as for combination with other analysis methods: UV and mass spectroscopy, fluorimetry, electrochemical analysis methods, etc.

However, chromatography-based separation and analysis methods are applied to glycoluril derivatives to a limited extent: for instance, the open literature does not show the fundamental opportunity to analyze

glycoluril by chromatography. In most studies, the chromatographic analyses of glycoluril derivatives are limited to the determination of its supramolecular guest-host compounds, while the purity of the starting compounds is not controlled. However, since the content of related glycoluril compounds in the synthesis of supramolecular compounds on the basis thereof is undesirable due to the possible formation of macromolecules that differ in properties from the given ones, it is necessary to control the purity of low molecular weight glycoluril derivatives, especially with respect to specific impurities, i.e. spatial isomers.

Summarizing the generalized results of the methods of analysis of glycoluril and its derivatives, we can point out that most of the studies conducted aimed at establishing the purity of the sample and identification of the related impurities for substances that have found practical use (drugs, monomers, and polymers on the basis thereof). The search for new methods to analyze macrocyclic and supramolecular systems synthesized based on glycolurils is carried out most intensively due to the unique properties found for such molecules.

Acknowledgement

This work was financially supported by the Ministry of Science and Higher Education of the Russian Federation in the framework of the Federal Target Program "Investigation and Developments on Priority Directions of Development of the Scientific Technological Complex of Russia for 2014–2020", Agreement No. 05.604.21.0251, unique identifier of project RFMEFI60419X0251.

References

- 1 Wheate N.J. Improving platinum(II)-based anticancer drug delivery using cucurbit[n]urils / N.J. Wheate // *Journal of Inorganic Biochemistry*. — 2008. — Vol. 102(12). — P. 2060–2066.
- 2 Wheate N.J. Multi-nuclear platinum complexes encapsulated in cucurbit[n]uril as an approach to reduce toxicity in cancer treatment / N.J. Wheate, A.I. Day, R.J. Blanch, A.P. Arnold, C. Cullinane, J.G. Collins // *Chemical Communications*. — 2004. — Vol. 12. — P. 1424–1425.
- 3 Zhao Y. Synthesis, cytotoxicity and cucurbituril binding of triamine linked dinuclear platinum complexes / Y. Zhao, M.S. Bali, C. Cullinane, A.I. Day, J.G. Collins // *Dalton Transactions*. — 2009. — Vol. 26. — P. 5190–5198.
- 4 Buczkowski A. Calorimetric and spectroscopic investigations of interactions between cucurbituril Q7 and gemcitabine in aqueous solutions / A. Buczkowski, A. Stepniak, P. Urbaniak, B. Palecz // *Journal of Thermal Analysis and Calorimetry*. — 2018. — Vol. 134. — P. 595–607.
- 5 Sal'keeva L.K. Effect of glycoluril and its derivatives on the flame resistance and physico-mechanical properties of rubber / L.K. Sal'keeva, A.A. Bakibaev, G.T. Khasenova, Y.K. Taishibekova, L.M. Sugralina, Y.V. Minaeva et al. // *Russian Journal of Applied Chemistry*. — 2016. — Vol. 89. — P. 132–139.
- 6 Jacobs W. Durable glossy, matte and wrinkle finish powder coatings crosslinked with tetramethoxymethyl glycoluril / W. Jacobs, D. Foster, S. Sansur, R.G. Lees // *Progress in Organic Coatings*. — 1996. — Vol. 29. — P. 127–138.
- 7 Ambrose R.R. U.S. Patent No. 6451928 / R.R. Ambrose, A.M. Chasser, S. Hu. — Washington, DC: U.S. Patent and Trademark Office, 2002.
- 8 Bockmuehl D. U.S. Patent No. 2013237470 / D. Bockmuehl, M. Hutmacher, S. Schuemann, T. Ott, U. Pegelow. — Washington, DC: U.S. Patent and Trademark Office, 2012.
- 9 The European Chemical Agency. Tetrahydro-1,3,4,6-tetrakis(hydroxymethyl)imidazo[4,5-d]imidazole-2,5(1H,3H)-dione. — URL: <https://echa.europa.eu/substance-information/-/substanceinfo/100.024.007>
- 10 Iacovello J. U.S. Patent No. 5182328 / J. Iacovello, D.W. Horwat. — Washington, DC: U.S. Patent and Trademark Office, 1993.
- 11 Dhiman R. Glycoluril derived cucurbituril analogues and the emergence of the most recent example: tiarauril / R. Dhiman, S. Pen, P.K. Chandrakumar, T.J. Frankcombe, A.I. Day // *Chemical Communications*. — 2020. — Vol. 56. — P. 2529–2537.
- 12 Lim Y. Self-Assembled Ternary Complex of Cationic Dendrimer, Cucurbituril, and DNA: Noncovalent Strategy in Developing a Gene Delivery Carrier / Y. Lim, T. Kim, J.W. Lee, S. Kim, H.-J. Kim, K. Kim, et al. // *Bioconjugate Chemistry*. — 2002. — Vol. 13(6). — P. 1181–1185.
- 13 Isobe H. Ternary Complexes Between DNA, Polyamine, and Cucurbituril: A Modular Approach to DNA-Binding Molecules / H. Isobe, N. Tomita, J.W. Lee, H.-J. Kim, K. Kim, E. Nakamura // *Angewandte Chemie*. — 2000. — Vol. 39(23). — P. 4257–4260.
- 14 Xu M. A Multi-Component Sensor System for Detection of Amphiphilic Compounds / M. Xu, S. Kelley, T.E. Glass // *Angewandte Chemie International Edition*. — 2018. — Vol. 130. — P. 12923–12926.
- 15 Park K.M. Dye-Cucurbit[n]uril Complexes as Sensor Elements for Reliable Pattern Recognition of Biogenic Polyamines / K.M. Park, J. Kim, Y.H. Ko, Y. Ahn, J. Murray, M. et al. // *Bulletin of the Chemical Society of Japan*. — 2018. — Vol. 91(1). — P. 95–99.

- 16 Fengyu Y. China Patent No. 101399316 / Y. Fengyu, X. Meiyu. — Beijing, China: State Intellectual Property Office of P.R.C., 2009.
- 17 Cao, L. Cucurbit[7]uril Containers for Targeted Delivery of Oxaliplatin to Cancer Cells / L. Cao, G. Hettiarachchi, V. Briken, L. Isaacs // *Angewandte Chemie International Edition*. — 2013. — Vol. 52(46). — P. 12033–12037.
- 18 Ozkan M. Rotaxane-Based Photosensitizer for Photodynamic Therapy / M. Ozkan, Y. Keser, S.E. Hadi, D. Tuncel // *European Journal of Organic Chemistry*. — 2019. — Vol. 21. — P. 3534–3541.
- 19 Das D. Applications of Cucurbiturils in Medicinal Chemistry and Chemical Biology / D. Das, K.I. Assaf, W.M. Nau // *Front Chemistry*. — 2019. — Vol. 7. — P. 619–685.
- 20 Zou L. Facile one-pot synthesis of porphyrin based porous polymer networks (PPNs) as biomimetic catalysts / L. Zou, D. Feng, T.-F. Liu, Y.-P. Chen, S. Fordham, S. Yuan et al. // *Chemical Communications*. — 2015. — Vol. 51(19). — P. 4005–4008.
- 21 Kim K. U.S. Patent No. 8002987 / K. Kim, K.-M. Park, Y.-H. Ko, H. Selvapalam, E.R. Nagarajan. — Washington, DC: U.S. Patent and Trademark Office, 2011.
- 22 Rongzu H. Kinetics and mechanism of the exothermic first-stage decomposition reaction for 1,4-dinitro-3,6-bis(trinitroethyl)-glycoluril / H. Rongzu, Y. Desuo, Z. Hongan, G. Shengli, S. Qizhen // *Thermochimica Acta*. — 2002. — Vol. 389(1–2). — P. 65–69.
- 23 Yinon J. Mass spectral fragmentation pathways in some glycoluril-type explosives. A study by collision-induced dissociation and isotope labeling / J. Yinon, S. Bulusu, T. Axenrod, H. Yazdekhasi // *Organic Mass Spectrometry*. — 1994. — Vol. 29(11). — P. 625–631.
- 24 Boileau J. U.S. Patent No. 4487938 / J. Boileau, J.-M. Emeury, J.-P. Kehren. — Washington, DC: U.S. Patent and Trademark Office, 1984.
- 25 Boileau J. Dérivés nitrés acétylés du glycoluril / J. Boileau, M. Carail, E. Wimmer, R. Gallo, M. Pierrot // *Propellants, Explosives, Pyrotechnics*. — 1985. — Vol. 10(4). — P. 118–120.
- 26 Moradi S. Synthesis of a Biological-Based Glycoluril with Phosphorous Acid Tags as a New Nanostructured Catalyst: Application for the Synthesis of Novel Natural Henna-Based Compounds / S. Moradi, M.A. Zolfigol, M. Zarei, D.A. Alonso, A. Khoshnood // *ChemistrySelect*. — 2018. — Vol. 3(11). — P. 3042–3047.
- 27 Funk S. Cucurbiturils in supramolecular catalysis / S. Funk, J. Schatz // *Journal of Inclusion Phenomena and Macrocyclic Chemistry*. — 2019. — Vol. 96. — P. 1–27.
- 28 Patel P. Glycoluril: A heterogeneous organocatalyst for oxidation of alcohols and benzylic sp³ carbons / P. Patel, S. Nandi, T. Menapara, A.V. Biradar, R.K. Nagarale, N.H. Khan et al. // *Applied Catalysis A: General*. — 2018. — Vol. 565. — P. 127–134.
- 29 The National Toxicology Program (1997). Glycoluril. — [Электронный ресурс]. — Режим доступа: https://ntp.niehs.nih.gov/ntp/htdocs/chem_background/exsumpdf/glycoluril_508.pdf
- 30 United States Environmental Protection Agency (1998). Forty-Second Report of the TSCA Interagency Testing Committee; Notice. — [Электронный ресурс]. — Режим доступа: <https://www.epa.gov/sites/production/files/2015-08/documents/42nd.pdf>
- 31 Kravchenko A.N. Synthesis of 2-Monofunctionalized 2,4,6,8-Tetraazabicyclo[3.3.0]octane-3,7-diones / A.N. Kravchenko, E.Y. Maksareva, P.A. Belyakov, A.S. Sigachev, K.Y. Chegaev, K.A. Lyssenko et al. // *Russian Chemical Bulletin*. — 2003. — Vol. 52. — P. 192–197.
- 32 Xu S. Glycoluril / S. Xu, P.K. Gantzel, L.B. Clark // *Acta Crystallographica Section C Crystal Structure Communications*. — 1994. — Vol. 50. — P. 1988–1989.
- 33 Baeyer A. *Gesammelte Werke* / A. Baeyer. — Frankfurt: Salzwasser-Verlag GmbH, 1905. — 1126 p.
- 34 Behrend R. Ueber Condensationsproducte aus Glycoluril und Formaldehyd / R. Behrend, E. Meyer, F. Rusche // *Justus Liebig's Annalen Der Chemie*. — 1905. — Vol. 339. — P. 1–37.
- 35 Fischer Chemicals AG. Glycoluril. Certificate of Analysis. — URL: <https://www.fishersci.com/shop/products/glycoluril-97-acros-organics-3/AC120130250>
- 36 Vessally E. Synthesis of the glycoluril derivatives by the HZSM-5 nanozeolite as a catalyst / E. Vessally, M.D. Esrafil, Z. Alimadadi, M. Rouhani // *Green Chemistry Letters and Reviews*. — 2014. — Vol. 7(2). — P. 119–125.
- 37 Saghanezhad S.J. Cucurbit[6]uril-OSO₃H: a novel acidic nanocatalyst for the one-pot preparation of 14-aryl-14H-dibenzo[a,j]xanthenes and 1,8-dioxo-octahydro-xanthenes / S.J. Saghanezhad, Y. Nazari, F. Davod // *RSC Advances*. — 2016. — Vol. 6(30). — P. 25525–25530.
- 38 Liu W. A Glycoluril Dimer-Triptycene Hybrid Receptor: Synthesis and Molecular Recognition Properties / W. Liu, X. Lu, Z. Meng, L. Isaacs // *Organic & Biomolecular Chemistry*. — 2018. — Vol. 16. — P. 6499–6505.
- 39 Stancl M. Synthesis and supramolecular properties of glycoluril tetramer / M. Stancl, L. Gilberg, L. Ustrnul, M. Necas, V. Sindelar // *Supramolecular Chemistry*. — 2013. — Vol. 26. — P. 168–172.
- 40 Wang T. Facile one-pot synthesis of glycoluril-based porous organic polymers / T. Wang, Y.-C. Zhao, M. Luo, L.-M. Zhang, Y. Cui, C.-S. Zhang et al. // *Polymer*. — 2015. — Vol. 60. — P. 26–31.
- 41 Benyettou F. Toward theranostic nanoparticles: CB[7]-functionalized iron oxide for drug delivery and MRI / F. Benyettou, I. Milosevic, Y. Lalatonne, F. Warmont, R. Assah, J.-C. Olsen et al. // *Journal of Materials Chemistry B*. — 2013. — Vol. 1(38). — P. 5076–5082.
- 42 Sinitsyna A.A. N-Alkylation Reaction in the Synthesis of Tetra-Substituted Glycolurils / A.A. Sinitsyna, S.G. Il'asov // *Journal of Siberian Federal University. Chemistry*. — 2020. — Vol. 13. — P. 40–45.

- 43 Boudebouz I. Tetra Acetoxymethyl Glycoluril as an Efficient and Novel Reagent for Acylation of Amines / I. Boudebouz, S. Arrous, A. Bakibaev, P. Hoang, V. Malkov // *International Journal of ChemTech Research*. — 2018. — Vol. 11. — P. 301–315.
- 44 Rebek R.R. U.S. Patent No. 7126006 / R.R. Rebek, K.E. Pryor. Washington, DC: U.S. Patent and Trademark Office, 2005.
- 45 Sinitsyna A.A. A search for synthetic routes to tetrabenzylglycoluril / A.A. Sinitsyna, S.G. Il'yasov, M.V. Chikina, I.V. El'tsov, A.A. Nefedov // *Chemical Papers*. — 2019. — Vol. 74. — P. 1019–1025.
- 46 Nyuugaku T. U.S. Patent No. 10683312 / T. Nyuugaku, A. Kiyomori. — Washington, DC: U.S. Patent and Trademark Office, 2019.
- 47 Sal'keeva L.K. New phosphorylated glycoluril derivatives / L.K. Sal'keeva, E.K. Taishibekova, A.A. Bakibaev, E.V. Minaeva, B.K. Makin, L.M. Sugralina et al. // *Russian Journal of General Chemistry*. — 2017. — Vol. 87(3). — P. 442–446.
- 48 Matsuda A. U.S. Patent No. 10550131 / A. Matsuda, N. Okumura, T. Kumano. — Washington, DC: U.S. Patent and Trademark Office, 2020.
- 49 Gazieva G.A. Crystal structure, IR and ¹H NMR spectra of tetranitratobis μ-(2,4,6,8-tetraethyl-2,4,6,8-tetraaza-bicyclo[3.3.0]octane-3,7-dione-O,O')diethanolodicadmium / G.A. Gazieva, D.G. Golovanov, P.V. Lozhkin, K.A. Lysenko, A.N. Kravchenko // *Russian Journal of Inorganic Chemistry*. — 2007. — Vol. 52(9). — P. 1441–1445.
- 50 Sherrill W.M. U.S. Patent No. 9695177 / W.M. Sherrill, E.C. Johnson. — Washington, DC: U.S. Patent and Trademark Office, 2016.
- 51 Il'yasov S.G. A novel approach for the synthesis of hexaazaisowurtzitane derivatives / S.G. Il'yasov, M.V. Chikina // *Tetrahedron Letters*. — 2013. — Vol. 54(15). — P. 1931–1932.
- 52 DePablo R.S. Determination of Total Glycoluril in Swimming Pool Water / R.S. DePablo // *Journal — American Water Works Association*. — 1966. — Vol. 58(3). — P. 379–382.
- 53 Patel C. Investigation of reaction intermediates of the urea-diacetylmonoxime reaction / C. Patel, R.J. Thibert, B. Zak // *Clinical Biochemistry*. — 1979. — Vol. 12(4). — P. 126–129.
- 54 Deshpande M.S. Ruthenium(II) Complexes of Bipyridine–Glycoluril and their Interactions with DNA / M.S. Deshpande, A.A. Kumbhar, A.S. Kumbhar, M. Kumbhakar, H. Pal, U.B. Sonawane et al. // *Bioconjugate Chemistry*. — 2009. — Vol. 20(3). — P. 447–459.
- 55 She N. Glycoluril-Derived Molecular Clips are Potent and Selective Receptors for Cationic Dyes in Water / N. She, D. Moncelet, L. Gilberg, X. Lu, V. Sindelar, V. Briken, L. Isaacs // *Chemistry — A European Journal*. — 2016. — Vol. 22(43). — P. 15270–15279.
- 56 National Institute of Standards and Technology. Urea, -phenyl. — URL: <https://webbook.nist.gov/cgi/cbook.cgi?Source=1953GRA86>
- 57 Yan, Q. A New Fluorescent Sensor for Fe³⁺ Based on Glycoluril Molecular Clip / Q. Yan, W. Liu, H. Wen, X. Zhibin, Z. Meng // *ChemistrySelect*. — 2020. — Vol. 5(6). — P. 1878–1883.
- 58 Li L. New fluorescent probes based on supramolecular diastereomers for the detection of 2-nitrophenol / L. Li, Y. Sun, S. Wang, M. Qiu, A. Wu // *Talanta*. — 2010. — Vol. 81(4–5). — P. 1643–1649.
- 59 Martinez C.R. Rethinking the term "pi-stacking" / C.R. Martinez, B.L. Iverson // *Chemical Science*. — 2012. — Vol. 3(7). — P. 2191–2201.
- 60 Azam A. A novel dansyl-appended glycoluril-based fluorescence sensor for silver ions / A. Azam, H.M. Chawla, S. Pandey // *Tetrahedron Letters*. — 2010. — Vol. 51(36). — P. 4710–4711.
- 61 Montes-Navajas P. Complexation and Fluorescence of Tricyclic Basic Dyes Encapsulated in Cucurbiturils / P. Montes-Navajas, A. Corma, H. Garcia // *ChemPhysChem*. — 2008. — Vol. 9(5). — P. 713–720.
- 62 Wagner B.D. A Cucurbit[6]uril Analogue: Host Properties Monitored by Fluorescence Spectroscopy / B.D. Wagner, P.G. Boland, J. Lagona, L. Isaacs // *The Journal of Physical Chemistry B*. — 2005. — Vol. 109(16). — P. 7686–7691.
- 63 Costa A.L. Evaluation of the supramolecular interaction of Congo red with cucurbiturils using mass spectrometry and spectroscopic methods / A.L. Costa, A.C. Gomes, A.D. Lopes, J.P. Da Silva, M. Pillinger, I.S. Gonçalves et al. // *New Journal of Chemistry*. — 2020. — Vol. 44. — P. 2587–2596.
- 64 Koner A.L. Cucurbituril Encapsulation of Fluorescent Dyes / A.L. Koner, W.M. Nau // *Supramolecular Chemistry*. — 2007. — Vol. 19(1–2). — P. 55–66.
- 65 Dong N. Preparation and characterization of inclusion complexes of antitumor camptothecin with cucurbit[n = 7, 8]urils / N. Dong, M. Dong, A. Zhao, Q. Zhu, Z. Tao, Y. Zhao // *Science China Chemistry*. — 2010. — Vol. 53(11). — P. 2304–2310.
- 66 Lisbjerg M. Biotin[6]uril Esters: Chloride-Selective Transmembrane Anion Carriers Employing C—H···Anion Interactions / M. Lisbjerg, H. Valkenier, B.M. Jessen, H. Al-Kerdi, A.P. Davis, M. Pittelkow // *Journal of the American Chemical Society*. — 2015. — Vol. 137(15). — P. 4948–4951.
- 67 Balzani V. Molecular Devices and Machines: Concepts and Perspectives for the Nanoworld / V. Balzani, A. Credi, M. Venturi. — Wiley-VCH Verlag GmbH & Co. KGaA, 2008. — 588 p.
- 68 Jun S.I. Rotaxane-based molecular switch with fluorescence signaling / S.I. Jun, J.L. Wook, S. Sakamoto, K. Yamaguchi, K. Kim // *Tetrahedron Letters*. — 2000. — Vol. 41(4). — P. 471–475.
- 69 Panshina S.Yu. Study of glycoluril and its derivatives by ¹H and ¹³C NMR spectroscopy / S.Yu. Panshina, O.V. Ponomarenko, A.A. Bakibaev, V.S. Malkov // *Bulletin of the University of Karaganda — Chemistry*. — 2020. — Vol. 99(3). — P. 21–37.

- 70 Bakibaev A.A. NMR Spectra of phosphorylated carbamide-containing heterocycles: peculiarities of chemical shifts from the valence state of the phosphorus and the size of the cycle / A.A. Bakibaev, K.B. Zhumanov, S. Yu. Panshina, S.I. Gorbin, V.S. Malkov, D.V. Khrebtova et al. // *News of the Academy of sciences of the Republic of Kazakhstan*. — 2019. — Vol. 5. — P. 100–107.
- 71 Mason J. Nitrogen NMR Spectroscopy of Metal Nitrosyls and Related Compounds / J. Mason, L.F. Larkworthy, E.A. Moore // *Chemical Reviews*. — 2002. — Vol. 102(4). — P. 913–934.
- 72 Chegaev K.Y. New functional glycoluril derivatives / K.Y. Chegaev, A.N. Kravchenko, O.V. Lebedev, Y.A. Strelenko // *Mendeleev Communications*. — 2001. — Vol. 11(1). — P. 32–33.
- 73 Bardelang D. High field solid state ^{13}C NMR spectroscopy of cucurbituril materials / D. Bardelang, A. Brinkmann, C.I. Ratcliffe, J.A. Ripmeester, V.V. Terskikh, K.A. Udachin // *CrystEngComm*. — 2014. — Vol. 16(18). — P. 3788–3795.
- 74 Gobre V.V. Density Functional Investigations on the Charge Distribution, Vibrational Spectra, and NMR Chemical Shifts in Cucurbit[n]uril ($n= 5-12$) Hosts / V.V. Gobre, R.V. Pinjari, S.P. Gejji // *The Journal of Physical Chemistry A*. — 2010. — Vol. 114(12). — P. 4464–4470.
- 75 Joseph R. Atropisomerization in Confined Space; Cucurbiturils as Tools to Determine the Torsional Barrier of Substituted Biphenyls / R. Joseph, E. Masson // *European Journal of Organic Chemistry*. — 2013. — Vol. 1. — P. 105–110.
- 76 Assaf K.I. Cucurbiturils: from synthesis to high-affinity binding and catalysis / K.I. Assaf, W.M. Nau // *Chemical Society Reviews*. — 2015. — Vol. 44(2). — P. 394–418.
- 77 Barrow S.J. Cucurbituril-Based Molecular Recognition / S.J. Barrow, S. Kasera, M.J. Rowland, J. del Barrio, O.A. Schermann // *Chemical Reviews*. — 2015. — Vol. 115(22). — P. 12320–12406.
- 78 Lagona J. The Cucurbit[n]uril Family / J. Lagona, P. Mukhopadhyay, S. Chakrabarti, L. Isaacs // *Angewandte Chemie International Edition*. — 2005. — Vol. 44(31). — P. 4844–4870.
- 79 Havel V. Modulation of Bambusuril Anion Affinity in Water / V. Havel, M. Babiak, V. Sindelar // *Chemistry — A European Journal*. — 2017. — Vol. 23(37). — P. 8963–8968.
- 80 Svec J. Bambus[6]uril / J. Svec, M. Necas, V. Sindelar // *Angewandte Chemie International Edition*. — 2010. — Vol. 49(13). — P. 2378–2381.
- 81 Panshina S.Yu. Analysis of XRD structural parameters of glycoluril and its derivatives / S.Yu. Panshina, O.V. Ponomarenko, A.A. Bakibaev, V.S. Malkov // *Journal of Structural Chemistry*. — 2020. — Vol. 61(9). — C. 1315–1355.
- 82 Stancl M. Glycoluril Dimer Isomerization under Aqueous Acidic Conditions Related to Cucurbituril Formation / M. Stancl, Z. Gargulakova, V. Sindelar // *Journal of Organic Chemistry*. — 2012. — Vol. 77(23). — P. 10945–10948.
- 83 Burnett C.A. Preparation of glycoluril monomers for expanded cucurbit[n]uril synthesis / C.A. Burnett, J. Lagona, A. Wu, J.A. Shaw, D. Coady, J. Fettinger et al. // *Tetrahedron*. — 2003. — Vol. 59(11). — P. 1961–1970.
- 84 Kurgachev D.A. Isolation, Identification, and Chromatographic Separation of N-Methyl Derivatives of Glycoluril / D.A. Kurgachev, O.A. Kotelnikov, D.V. Novikov, V.R. Kusherbaeva, S.I. Gorbin, E.V. Tomilova et al. // *Chromatographia*. — 2018. — Vol. 81. — P. 1431–1437.
- 85 Ndjendjio S.Z. Triptycene Walled Glycoluril Trimer: Synthesis and Recognition Properties / S.Z. Ndjendjio, W. Liu, N. Yvanez, Z. Meng, P.Y. Zavaliy, L.D. Isaacs // *New Journal of Chemistry*. — 2020. — Vol. 44. — P. 338–345.
- 86 Rodrigues M.A.A. ESI-MS of Cucurbituril Complexes Under Negative Polarity / M.A.A. Rodrigues, D.C. Mendes, V. Ramamurthy, J.P. Da Silva // *Journal of The American Society for Mass Spectrometry*. — 2017. — Vol. 28(11). — P. 2508–2514.
- 87 Stancl M. 1,6-Dibenzylglycoluril for synthesis of deprotected glycoluril dimer / M. Stancl, M.S. Khan, V. Sindelar // *Tetrahedron*. — 2011. — Vol. 67(46). — P. 8937–8941.
- 88 Ding J. Matrix-assisted laser desorption/ionization mass spectrometry for the analysis of polyamines in plant micro-tissues using cucurbituril as a host molecule / J. Ding, S. Liu, H.-M. Xiao, T. Ye, P. Zhou, Y.-Q. Feng // *Analytica Chimica Acta*. — 2017. — Vol. 987. — P. 56–63.
- 89 Magalhães C.I.R. Ferrocene and ferrocenium inclusion compounds with cucurbiturils: a study of metal atom dynamics probed by Mössbauer spectroscopy / C.I.R. Magalhães, A.C. Gomes, A.D. Lopes, I.S. Gonçalves, M. Pillinger, E. Jin et al. // *Physical Chemistry Chemical Physics*. — 2017. — Vol. 19(32). — P. 21548–21555.
- 90 Day, A. I. A Cucurbituril-Based Gyroscane: A New Supramolecular Form / A.I. Day, R.J. Blanch, A.P. Arnold, S. Lorenzo, G.R. Lewis, I. Dance // *Angewandte Chemie International Edition*. — 2002. — Vol. 41(2). — P. 275–277.
- 91 Chen Y. Structural interrogation of a cucurbit[7]uril-ferrocene host–guest complex in the solid state: a Raman spectroscopy study / Y. Chen, A. Klimczak, E. Galoppini, J.V. Lockard // *RSC Adv*. — 2013. — Vol. 3(5). — P. 1354–1358.
- 92 Gürbüz S. Cucurbituril-based supramolecular engineered nanostructured materials / S. Gürbüz, M. Idris, D. Tuncel // *Organic & Biomolecular Chemistry*. — 2015. — Vol. 13(2). — P. 330–347.
- 93 Cicolani R.S. Formation of the non-classical interhalide anion $[\text{I}_2\text{Cl}]^-$ in methyl-bambus[6]uril cavity / R.S. Cicolani, A.G. Sampaio de Oliveira Filho, A.P. de Lima Batista, G.J.-F. Demets // *New Journal of Chemistry*. — 2020. — Vol. 44. — P. 2697–2700.
- 94 Trubina S. EXAFS spectroscopy investigation Cu(II) complexes encapsulated in cucurbit[8]uril / S. Trubina, S. Erenburg, N. Bausk, V. Nadolinny, V. Bakovets, I. Dolgovesova et al. // *Journal of Physics: Conference Series*. — 2009. — Vol. 190. — P. 012128.

- 120 Gazieva G.A. Synthesis and structure of 2,4,6,8-tetramethyl-3,7-dithia-2,4,6,8-tetraazabicyclo[3.3.0]octane 3,3,7,7-tetraoxide / G.A. Gazieva, K.A. Lysenko, A.N. Kravchenko, O.V. Lebedev // *Russian Journal of Organic Chemistry*. — 2007. — Vol. 43(11). — P. 1715–1718.
- 121 Kravchenko A.N. Reaction of N-alkylglycolurils with electrophilic reagents / A.N. Kravchenko, A.S. Sigachev, G.A. Gazieva, E.Y. Maksareva, N.S. Trunova, K.A. Chegaev et al. // *Chemistry of Heterocyclic Compounds*. — 2006. — Vol. 42(3). — P. 365–376.
- 122 Карташов В.А. ТСХ-скрининг и индексы удерживания токсических веществ / В.А. Карташов // *Вестн. КазНМУ*. — 2012. — № 1. — С. 430.
- 123 Ammann E.C. Purine metabolism of unicellular algae / E.C. Ammann, V.H. Lynch // *Analytical Biochemistry*. — 1964. — Vol. 7(4). — P. 387–392.
- 124 Wu A. Glycoluril derivatives form hydrogen bonded tapes rather than cucurbit[n]uril congeners / A. Wu, J.C. Fettinger, L. Isaacs // *Tetrahedron*. — 2002. — Vol. 58(49). — P. 9769–9777.
- 125 Poskrobko M. HPLC Analysis of the Products of the Reaction Between Glycoluril and Formaldehyde / M. Poskrobko, M. Dejnega // *Journal of Liquid Chromatography & Related Technologies*. — 1998. — Vol. 21(17). — P. 2725–2731.
- 126 Hidalgo-Fernández P. Avidin and streptavidin ligands based on the glycoluril bicyclic system / P. Hidalgo-Fernández, E. Ayet, I. Canal, J.-A. Farrera // *Organic and Biomolecular Chemistry*. — 2006. — Vol. 4(16). — P. 3147–3154.
- 127 Kravchenko A.N. Synthesis of new chiral mono-, di-, tri-, and tetraalkylglycolurils / A.N. Kravchenko, A.S. Sigachev, E.Y. Maksareva, G.A. Gazieva, N.S. Trunova, B.V. Lozhkin et al. // *Russian Chemical Bulletin*. — 2005. — Vol. 54(3). — P. 691–704.
- 128 Kravchenko A.N. 4,5-Dihydroxyimidazolidin-2-ones in α -ureidoalkylation of N-carboxy-, N-hydroxy-, and N-amino-alkylureas 2. α -Ureidoalkylation of N-(hydroxyalkyl)ureas / A.N. Kravchenko, A.S. Sigachev, P.A. Belyakov, M.M. Ilyin, K.A. Lyssenko, V.A. Davankov et al. // *Russian Chemical Bulletin*. — 2009. — Vol. 58(6). — P. 1264–1269.
- 129 Lízal T. Bambusuril analogs based on alternating glycoluril and xylylene units / T. Lízal, V. Šindelář // *Beilstein Journal of Organic Chemistry*. — 2019. — Vol. 15. — P. 1268–1274.
- 130 Патент 2576240. Российская Федерация, МПК А 61 К 31/4188, А 61 К 31/198, А 61 К 47/00, А 61 К 9/20, А 61 Р 25/22. Фармацевтическая композиция, содержащая комбинацию глицина и тетраметилтетраазабициклооктандиона (варианты) [Текст] / Ханнанов Т.Ш., Анисимов А.Н., Камаева С.С., Кашапова К.И., Лефтерова М.И., Хамидуллин Р.Т.; заявитель и патентообладатель Открытое акционерное общество «Татхимфармпрепараты». — № 2015104695/15; заявл. 11.02.2015; опубл. 27.02.2016. Бюл. № 6. — 13 с.
- 131 FisherScientific. N,N',N'',N'''-Tetraacetylglycoluril. — URL: <https://www.fishersci.ca/shop/products/n-n-n-n-tetraacetyl-glycoluril-tci-america-2/p-7136535>
- 132 Johnson D.W. Glycoluril ribbons tethered by complementary hydrogen bonds / D.W. Johnson, F. Hof, L.C. Palmer, T. Martín, U. Obst, J. Rebek // *Chemical Communications*. — 2003. — Vol. 14. — P. 1638–1639.
- 133 Huang W.-H. Metal-Ion-Induced Folding and Dimerization of a Glycoluril Decamer in Water / W.-H. Huang, P.Y. Zavalij, L. Isaacs // *Organic Letters*. — 2009. — Vol. 11(17). — P. 3918–3921.
- 134 Gosecki M. A Glycoluril Clips for the Construction of Chemoresponsive Supramolecular Polymer Network through Homodimer Cross-Links / M. Gosecki, M. Urbaniak, M. Gosecka, // *ChemPlusChem*. — 2019. — Vol. 84. — P. 981–988.
- 135 Takei S. High-resolution nanopatterning of biodegradable polylactide by thermal nanoimprint lithography using gas permeable mold / S. Takei, M. Hanabata // *AIP Advances*. — 2017. — Vol. 7(3). — P. 035110.
- 136 Сорванов А.А. Синтез новых водорастворимых полимеров на основе гидроксиметильных производных гликолури-ла / А.А. Сорванов, К.В. Рубцов // *Перспективы развития фундаментальных наук: сб. науч. тр. XVI Междунар. конф. студ., аспирантов и молодых учёных (23–26 апреля 2019 г.)*. — Томск, 2019. — С. 204–206.
- 137 Strelb M.G. Adamantane/Cucurbituril: A Potential Pretargeted Imaging Strategy in Immuno-PET / M.G. Strelb, J. Yang, L. Isaacs, J.M. Hooker // *Molecular Imaging*. — 2018. — Vol. 17. — P. 1–7.
- 138 Day A. A Method for Synthesizing Partially Substituted Cucurbit[n]uril / A. Day, A. Arnold, R. Blanch // *Molecules*. — 2003. — Vol. 8(1). — P. 74–84.
- 139 Kumano T. U.S. Patent No. 10000622 / T. Kumano, T. Takeda, S. Miura, T. Kashiwabara, N. Mizobe. — Washington, DC: U.S. Patent and Trademark Office, 2018.
- 140 Ivanov E.V. Equimolecular cocrystal of cis- and trans-coordinated N,N'-dimethylglycolurils: Some standard thermodynamic properties in the aqueous solution between 278.15 K and 318.15 K / E.V. Ivanov, E.Y. Lebedeva, D.V. Batov, V.V. Baranov, A.N. Kravchenko // *Journal of Molecular Liquids*. — 2019. — Vol. 297. — P. 111891–111899.
- 141 Zheng Z.-H. Study on promoting the synthesis of glycoluril by microwave technology / Z.-H. Zheng, J.-L. Wang, Y.-X. Li, Y.-H. Wang // *Journal of North University of China*. — 2015. — Vol. 36. — P. 202–207.
- 142 Ivanov E.V. Enthalpy-related parameters of interaction of simplest α -amino acids with the pharmaceutical mebicar (N-tetramethylglycoluril) in water at 298.15 K / E.V. Ivanov, D.V. Batov // *The Journal of Chemical Thermodynamics*. — 2019. — Vol. 128. — P. 159–163.
- 143 Ivanov E.V. Effect of the H/D solvent isotope substitution on enthalpy-related interaction parameters in aqueous solutions of the racemic Albicar at T = 298.15 K and ambient pressure / E.V. Ivanov, D.V. Batov // *The Journal of Chemical Thermodynamics*. — 2016. — Vol. 102. — P. 9–11.

А.А. Бакибаев, В.С. Мальков, Д.А. Кургачёв, О.А. Котельников

Гликолурил және оның туындыларын талдау әдістері

Мақалада гликолурилді, оның туындыларын және олардың байланысты қосылыстарын талдау әдістерінің әдеби мәліметтерін жалпылау жүргізілді, бұл осы заттардың құрылымы мен қасиеттері туралы ақпаратты біріктірілген түрде алуға мүмкіндік береді. Гликолурилдер мен олардың негізінде синтезделген қосылыстарды талдаудың негізгі әдістері зерттелген, оларды ұсыну барысында ұсынылған әдістердің артықшылықтары мен кемшіліктері сыни қарастырылған. Гликолурил мен оның туындыларын талдау әдістерінің жалпыланған нәтижелері көрсеткендей, жүргізілген зерттеулердің көпшілігі үлгінің тазалығын анықтауға және практикалық қолданысқа ие заттарға (дәрі-дәрмектер, мономерлер және олардың негізіндегі полимерлер) байланысты қоспаларды анықтауға бағытталған. Гликолурилдер негізінде синтезделген макроциклді және супрамолекулалық жүйелерді талдаудың жаңа әдістерін қарқынды іздеудің тұрақты үрдісі байқалады. Осы шолудың мақсаты — химия саласындағы мамандардың назарын гликолурил мен оның туындыларын талдаудың қолданыстағы әдістеріне аудару және одан әрі осындай зерттеулерді ынталандыру. Жүргізілген әдеби талдау алдына анықталған қасиеттері бар гликолурил негізіндегі жаңа молекулаларды жасаумен айналысатын зерттеушілер үшін пайдалы, оның барысында процестерді бақылау және мақсатты қосылыстарды талдау әдістері өте маңызды.

Кілт сөздер: гликолурил, N-алмастырылған гликолурилдер, супрамолекулалар, талдау, спектроскопия, тиімділігі жоғары сұйық хроматография, изомерлер.

А.А. Бакибаев, В.С. Мальков, Д.А. Кургачёв, О.А. Котельников

Методы анализа гликолурила и его производных

В статье проведено обобщение литературных сведений о методах анализа гликолурила, его производных и их родственных соединениях, позволяющих получить информацию о структуре и свойствах этих веществ в интегрированном виде. Рассмотрены основные методы анализа гликолурилов и соединений, синтезируемых на их основе, в ходе изложения которых критически рассмотрены достоинства и недостатки предлагаемых методов. Обобщенные результаты методов анализа гликолурила и его производных говорят о том, что большинство проведенных исследований направлено в сторону установления чистоты образца и идентификации родственных примесей для веществ, нашедших практическое применение (лекарственные препараты, мономеры и полимеры на их основе). Наблюдается устойчивая тенденция к интенсивному поиску новых методов анализа макроциклических и супрамолекулярных систем, синтезируемых на основе гликолурилов. Цель настоящего обзора — привлечение внимания химиков к существующим методам анализа гликолурила и его производных и дальнейшее стимулирование подобных исследований. Проведенный авторами литературный анализ будет полезным для исследователей, занимающихся конструированием новых молекул на основе гликолурила с заранее заданными свойствами, в ходе которых методы контроля процессов и анализа целевых соединений имеют решающее значение.

Ключевые слова: гликолурил, N-замещённые гликолурилы, супрамолекулы, анализ, спектроскопия, высокоэффективная жидкостная хроматография, изомеры.

References

- 1 Wheate, N.J. (2008). Improving platinum(II)-based anticancer drug delivery using cucurbit[n]urils. *Journal of Inorganic Biochemistry*, 102(12), 2060–2066. DOI: 10.1016/j.jinorgbio.2008.06.005
- 2 Wheate, N.J., Day, A.I., Blanch, R.J., Arnold, A.P., Cullinane, C., & Grant Collins, J. (2004). Multi-nuclear platinum complexes encapsulated in cucurbit[n]uril as an approach to reduce toxicity in cancer treatment. *Chemical Communications*, 12, 1424–1425. DOI: 10.1039/b404358h
- 3 Zhao, Y., Bali, M. S., Cullinane, C., Day, A. I., & Collins, J. G. (2009). Synthesis, cytotoxicity and cucurbituril binding of triamine linked dinuclear platinum complexes. *Dalton Transactions*, 26, 5190–5198. DOI: 10.1039/b905112k
- 4 Buczkowski, A., Stepniak, A., Urbaniak, P., & Palecz, B. (2018). Calorimetric and spectroscopic investigations of interactions between cucurbituril Q7 and gemcitabine in aqueous solutions. *Journal of Thermal Analysis and Calorimetry*, 134, 595–607. DOI: 10.1007/s10973-018-7295-7.
- 5 Sal'keeva, L.K., Bakibaev, A.A., Khasenova, G.T., Taishibekova, Y.K., Sugralina, L.M., Minaeva, Y.V., & Sal'keeva, A.K. (2016). Effect of glycoluril and its derivatives on the flame resistance and physico-mechanical properties of rubber. *Russian Journal of Applied Chemistry*, 89, 132–139. DOI: 10.1134/s1070427216010213

- 6 Jacobs, W., Foster, D., Sansur, S., & Lees, R.G. (1996). Durable glossy, matte and wrinkle finish powder coatings crosslinked with tetramethoxymethyl glycoluril. *Progress in Organic Coatings*, 29(1–4), 127–138. DOI: 10.1016/s0300-9440(96)00643-1
- 7 Ambrose, R.R., Chasser, A.M., & Hu, S. (2002). *U.S. Patent No. 6451928*. Washington, DC: U.S. Patent and Trademark Office.
- 8 Bockmuehl, D., Hutmacher, M., Schuemann, S., Ott, T., & Pegelow, U. (2012). *U.S. Patent No 2013237470*. Washington, DC: U.S. Patent and Trademark Office.
- 9 The European Chemical Agency. (2020, May 12). *Tetrahydro-1,3,4,6-tetrakis(hydroxymethyl)imidazo[4,5-d]imidazole-2,5(1H,3H)-dione*. <https://echa.europa.eu/substance-information/-/substanceinfo/100.024.007>
- 10 Iacovello, J., & Horwat, D.W. (1993). *U.S. Patent No. 5182328*. Washington, DC: U.S. Patent and Trademark Office.
- 11 Dhiman, R., Pen, S., Chandrakumar, P.K., Frankcombe, T.J., & Day, A.I. (2020). Glycoluril derived cucurbituril analogues and the emergence of the most recent example: tiarauril. *Chemical Communications*, 56, 2529–2537. DOI: 10.1039/c9cc07233k
- 12 Lim, Y., Kim, T., Lee, J. W., Kim, S., Kim, H.-J., Kim, K., & Park, J. (2002). Self-Assembled Ternary Complex of Cationic Dendrimer, Cucurbituril, and DNA: Noncovalent Strategy in Developing a Gene Delivery Carrier. *Bioconjugate Chemistry*, 13(6), 1181–1185. DOI: 10.1021/bc025581r
- 13 Isobe, H., Tomita, N., Lee, J. W., Kim, H.-J., Kim, K., & Nakamura, E. (2000). Ternary Complexes Between DNA, Polyamine, and Cucurbituril: A Modular Approach to DNA-Binding Molecules. *Angewandte Chemie*, 39(23), 4257–4260. DOI: 10.1002/1521-3773(20001201)39:23<4257::aid-anie4257>3.0.co;2-6
- 14 Xu, M., Kelley, S., & Glass, T.E. (2018). A Multi-Component Sensor System for Detection of Amphiphilic Compounds. *Angewandte Chemie International Edition*, 130 DOI: 10.1002/anie.201807221
- 15 Park, K.M., Kim, J., Ko, Y.H., Ahn, Y., Murray, J., Li, M., Shrinidhi, A., & Kim, K. (2018). Dye-Cucurbit[n]uril Complexes as Sensor Elements for Reliable Pattern Recognition of Biogenic Polyamines. *Bulletin of the Chemical Society of Japan*, 91(1), 95–99. DOI: 10.1246/bcsj.20170302
- 16 Fengyu, Y., & Meiyu, X. (2009). *China Patent No. 101399316*. Beijing, China: State Intellectual Property Office of P.R.C.
- 17 Cao, L., Hettiarachchi, G., Briken, V., & Isaacs, L. (2013). Cucurbit[7]uril Containers for Targeted Delivery of Oxaliplatin to Cancer Cells. *Angewandte Chemie International Edition*, 52(46), 12033–12037. DOI: 10.1002/anie.201305061
- 18 Ozkan, M., Keser, Y., Hadi, S.E., & Tuncel, D. (2019). Rotaxane-Based Photosensitizer for Photodynamic Therapy. *European Journal of Organic Chemistry*, 21, 3534–3541. DOI: 10.1002/ejoc.201900278
- 19 Das, D., Assaf, K.I., & Nau, W.M. (2019). Applications of Cucurbiturils in Medicinal Chemistry and Chemical Biology. *Front Chemistry*, 7, 619–685. DOI: 10.3389/fchem.2019.00619
- 20 Zou, L., Feng, D., Liu, T.-F., Chen, Y.-P., Fordham, S., & Yuan, S., et al. (2015). Facile one-pot synthesis of porphyrin based porous polymer networks (PPNs) as biomimetic catalysts. *Chemical Communications*, 51(19), 4005–4008. DOI: 10.1039/c4cc09479d
- 21 Kim, K., Park, K.-M., Ko, Y.-H., Selvapalam, H., & Nagarajan, E.R. (2011). *U.S. Patent No. 8002987*. Washington, DC: U.S. Patent and Trademark Office.
- 22 Rongzu, H., Desuo, Y., Hongan, Z., Shengli, G., & Qizhen, S. (2002). Kinetics and mechanism of the exothermic first-stage decomposition reaction for 1,4-dinitro-3,6-bis(trinitroethyl) glycoluril. *Thermochimica Acta*, 389(1–2), 65–69. DOI: 10.1016/s0040-6031(02)00005-9
- 23 Yinon, J., Bulusu, S., Axenrod, T., & Yazdekhashti, H. (1994). Mass spectral fragmentation pathways in some glycoluril-type explosives. A study by collision-induced dissociation and isotope labeling. *Organic Mass Spectrometry*, 29(11), 625–631. DOI: 10.1002/oms.1210291109
- 24 Boileau, J., Emeury, J.-M., & Kehren, J.-P. (1984). *U.S. Patent No. 4487938*. Washington, DC: U.S. Patent and Trademark Office.
- 25 Boileau, J., Carail, M., Wimmer, E., Gallo, R., & Pierrot, M. (1985). Dérivés nitrés acétylés du glycoluril. *Propellants, Explosives, Pyrotechnics*, 10(4), 118–120. DOI: 10.1002/prep.19850100407
- 26 Moradi, S., Zolfigol, M.A., Zarei, M., Alonso, D.A., & Khoshnood, A. (2018). Synthesis of a Biological-Based Glycoluril with Phosphorous Acid Tags as a New Nanostructured Catalyst: Application for the Synthesis of Novel Natural Henna-Based Compounds. *ChemistrySelect*, 3(11), 3042–3047. DOI: 10.1002/slct.201702544
- 27 Funk, S., & Schatz, J. (2019). Cucurbiturils in supramolecular catalysis. *Journal of Inclusion Phenomena and Macrocyclic Chemistry*, 96, 1–27. DOI: 10.1007/s10847-019-00956-0
- 28 Patel, P., Nandi, S., Menapara, T., Biradar, A.V., Nagarale, R.K., Khan, N. H., & Kureshy, R.I. (2018). Glycoluril: A heterogeneous organocatalyst for oxidation of alcohols and benzylic sp³ carbons. *Applied Catalysis A: General*, 565, 127–134. DOI: 10.1016/j.apcata.2018.08.005
- 29 The National Toxicology Program. (2020, May 14). *Glycoluril*. https://ntp.niehs.nih.gov/ntp/htdocs/chem_background/exsumpdf/glycoluril_508.pdf
- 30 United States Environmental Protection Agency. (2020, May 14). *Forty-Second Report of the TSCA Interagency Testing Committee; Notice*. <https://www.epa.gov/sites/production/files/2015-08/documents/42nd.pdf>
- 31 Kravchenko, A.N., Maksareva, E.Y., Belyakov, P.A., Sigachev, A.S., Chegaev, K.Y., & Lyssenko, K.A., et al. (2003). Synthesis of 2-Monofunctionalized 2,4,6,8-Tetraazabicyclo[3.3.0]octane-3,7-diones. *Russian Chemical Bulletin*, 52, 192–197. DOI: 10.1002/chin.200326137

- 32 Xu, S., Gantzel, P.K., & Clark, L.B. (1994). Glycoluril. *Acta Crystallographica Section C Crystal Structure Communications*, 50(12), 1988–1989. DOI: 10.1107/s0108270194006955
- 33 Baeyer, A. (1905). *Gesammelte Werke*. Frankfurt: Salzwasser-Verlag GmbH.
- 34 Behrend, R., Meyer, E., & Rusche, F. (1905). I. Ueber Condensationsproducte aus Glycoluril und Formaldehyd. *Justus Liebig's Annalen Der Chemie*, 339(1), 1–37. DOI: 10.1002/jlac.19053390102
- 35 Fischer Chemicals AG. (2020, June 01). *Glycoluril. Certificate of Analysis*. <https://www.fishersci.com/shop/products/glycoluril-97-acros-organics-3/AC120130250>
- 36 Vessally, E., Esrafil, M.D., Alimadadi, Z., & Rouhani, M. (2014). Synthesis of the glycoluril derivatives by the HZSM-5 nanozeolite as a catalyst. *Green Chemistry Letters and Reviews*, 7(2), 119–125. DOI: 10.1080/17518253.2014.895865
- 37 Saghanezhad, S.J., Nazari, Y., & Davod, F. (2016). Cucurbit[6]uril-OSO₃H: a novel acidic nanocatalyst for the one-pot preparation of 14-aryl-14H-dibenzo[a,j]xanthenes and 1,8-dioxo-octahydro-xanthenes. *RSC Advances*, 6(30), 25525–25530. DOI: 10.1039/c6ra02255c
- 38 Liu, W., Lu, X., Meng, Z., & Isaacs, L.D. (2018). A Glycoluril Dimer–Triptycene Hybrid Receptor: Synthesis and Molecular Recognition Properties. *Organic & Biomolecular Chemistry*, 16, 6499–6505. DOI: 10.1039/c8ob01575a
- 39 Stancl, M., Gilberg, L., Ustrnul, L., Necas, M., & Sindelar, V. (2013). Synthesis and supramolecular properties of glycoluril tetramer. *Supramolecular Chemistry*, 26(3–4), 168–172. DOI: 10.1080/10610278.2013.842643
- 40 Wang, T., Zhao, Y.-C., Luo, M., Zhang, L.-M., Cui, Y., Zhang, C.-S., & Han, B.-H. (2015). Facile one-pot synthesis of glycoluril-based porous organic polymers. *Polymer*, 60, 26–31. DOI: 10.1016/j.polymer.2014.12.072
- 41 Benyettou, F., Milosevic, I., Lalatonne, Y., Warmont, F., Assah, R., & Olsen, J.-C., et al. (2013). Toward theranostic nanoparticles: CB[7]-functionalized iron oxide for drug delivery and MRI. *Journal of Materials Chemistry B*, 1(38), 5076–5082. DOI: 10.1039/c3tb20852d
- 42 Sinitsyna, A.A., & Il'asov, S.G. (2020). N-Alkylation Reaction in the Synthesis of Tetra-Substituted Glycolurils. *Journal of Siberian Federal University. Chemistry*, 13, 40–45. DOI: 10.17516/1998–2836–0164
- 43 Boudebouz, I., Arrous, S., Bakibaev, A., Hoang, P., & Malkov, V. (2018). Tetra Acetoxymethyl Glycoluril as an Efficient and Novel Reagent for Acylation of Amines. *International Journal of ChemTech Research*, 11, 301–315. DOI: 10.20902/IJCTR.2018.110533
- 44 Rebek, R.R., & Pryor, K.E. (2005). *U.S. Patent No. 7126006*. Washington, DC: U.S. Patent and Trademark Office.
- 45 Sinitsyna, A.A., Il'asov, S.G., Chikina, M.V., El'tsov, I.V., & Nefedov, A.A. (2019). A search for synthetic routes to tetrabenzylglycoluril. *Chemical Papers*, 74, 1019–1025. DOI: 10.1007/s11696–019–00941–4
- 46 Nyuugaku, T., & Kiyomori, A. (2019). *U.S. Patent No. 10683312*. Washington, DC: U.S. Patent and Trademark Office.
- 47 Sal'keeva, L.K., Taishibekova, E.K., Bakibaev, A.A., Minaeva, E.V., Makin, B.K., Sugralina, L.M., & Sal'keeva, A.K. (2017). New phosphorylated glycoluril derivatives. *Russian Journal of General Chemistry*, 87(3), 442–446. DOI: 10.1134/s1070363217030124
- 48 Matsuda, A., Okumura, N., & Kumano, T. (2020). *U.S. Patent No. 10550131*. Washington, DC: U.S. Patent and Trademark Office.
- 49 Gazieva, G.A., Golovanov, D.G., Lozhkin, P.V., Lysenko, K.A., & Kravchenko, A.N. (2007). Crystal structure, IR and ¹H NMR spectra of tetranitratobis μ-(2,4,6,8-tetraethyl-2,4,6,8-tetraazabicyclo[3.3.0]octane-3,7-dione-O,O')diethanolodcadmium. *Russian Journal of Inorganic Chemistry*, 52(9), 1441–1445. DOI: 10.1134/s0036023607090215
- 50 Sherrill, W.M., & Johnson, E.C. (2016). *U.S. Patent No. 9695177*. Washington, DC: U.S. Patent and Trademark Office.
- 51 Il'asov, S.G., & Chikina, M.V. (2013). A novel approach for the synthesis of hexaazaisowurtzitane derivatives. *Tetrahedron Letters*, 54(15), 1931–1932. DOI: 10.1016/j.tetlet.2013.01.102
- 52 DePablo, R.S. (1966). Determination of Total Glycoluril in Swimming Pool Water. *Journal — American Water Works Association*, 58(3), 379–382. DOI: 10.1002/j.1551–8833.1966.tb01592.x
- 53 Patel, C., Thibert, R.J., & Zak, B. (1979). Investigation of reaction intermediates of the urea-diacetylmonoxime reaction. *Clinical Biochemistry*, 12(4), 126–129. DOI: 10.1016/s0009–9120(79)80138–1
- 54 Deshpande, M.S., Kumbhar, A.A., Kumbhar, A.S., Kumbhakar, M., Pal, H., Sonawane, U.B., & Joshi, R.R. (2009). Ruthenium(II) Complexes of Bipyridine–Glycoluril and their Interactions with DNA. *Bioconjugate Chemistry*, 20(3), 447–459. DOI: 10.1021/bc800298t
- 55 She, N., Moncelet, D., Gilberg, L., Lu, X., Sindelar, V., Briken, V., & Isaacs, L. (2016). Glycoluril-Derived Molecular Clips are Potent and Selective Receptors for Cationic Dyes in Water. *Chemistry — A European Journal*, 22(43), 15270–15279. DOI: 10.1002/chem.201601796
- 56 National Institute of Standards and Technology. (2020, May 14). *Urea, -phenyl*. <https://webbook.nist.gov/cgi/cbook.cgi?Source=1953GRA86>
- 57 Yan, Q., Liu, W., Wen, H., Zhibin, X., & Meng, Z. (2020). A New Fluorescent Sensor for Fe³⁺ Based on Glycoluril Molecular Clip. *ChemistrySelect*, 5(6), 1878–1883. DOI: 10.1002/slct.201904902
- 58 Li, L., Sun, Y., Wang, S., Qiu, M., & Wu, A. (2010). New fluorescent probes based on supramolecular diastereomers for the detection of 2-nitrophenol. *Talanta*, 81(4–5), 1643–1649. DOI: 10.1016/j.talanta.2010.03.018
- 59 Martinez, C.R., & Iverson, B.L. (2012). Rethinking the term "pi-stacking." *Chemical Science*, 3(7), 2191–2201. DOI: 10.1039/c2sc20045g

- 60 Azam, A., Chawla, H.M., & Pandey, S. (2010). A novel dansyl-appended glycoluril-based fluorescence sensor for silver ions. *Tetrahedron Letters*, 51(36), 4710–4711. DOI: 10.1016/j.tetlet.2010.07.005
- 61 Montes-Navajas, P., Corma, A., & Garcia, H. (2008). Complexation and Fluorescence of Tricyclic Basic Dyes Encapsulated in Cucurbiturils. *ChemPhysChem*, 9(5), 713–720. DOI: 10.1002/cphc.200700735
- 62 Wagner, B.D., Boland, P.G., Lagona, J., & Isaacs, L. (2005). A Cucurbit[6]uril Analogue: Host Properties Monitored by Fluorescence Spectroscopy. *The Journal of Physical Chemistry B*, 109(16), 7686–7691. DOI: 10.1021/jp044369c
- 63 Costa, A.L., Gomes, A.C., Lopes, A.D., Da Silva, J.P., Pillinger, M., Gonçalves, I.S., & Seixas de Melo, J.S. (2020). Evaluation of the supramolecular interaction of Congo red with cucurbiturils using mass spectrometry and spectroscopic methods. *New Journal of Chemistry*, 44, 2587–2596. DOI: 10.1039/c9nj05706d
- 64 Koner, A.L., & Nau, W.M. (2007). Cucurbituril Encapsulation of Fluorescent Dyes. *Supramolecular Chemistry*, 19(1–2), 55–66. DOI: 10.1080/10610270600910749
- 65 Dong, N., Dong, M., Zhao, A., Zhu, Q., Tao, Z., & Zhao, Y. (2010). Preparation and characterization of inclusion complexes of antitumor camptothecin with cucurbit[n = 7, 8]urils. *Science China Chemistry*, 53(11), 2304–2310. DOI: 10.1007/s11426-010-4067-z
- 66 Lisbjerg, M., Valkenier, H., Jessen, B.M., Al-Kerdi, H., Davis, A.P., & Pittelkow, M. (2015). Biotin[6]uril Esters: Chloride-Selective Transmembrane Anion Carriers Employing C—H···Anion Interactions. *Journal of the American Chemical Society*, 137(15), 4948–4951. DOI: 10.1021/jacs.5b02306
- 67 Balzani, V., Credi, A., & Venturi, M. (2008). *Molecular Devices and Machines: Concepts and Perspectives for the Nanoworld*, Wiley-VCH Verlag GmbH & Co. KGaA.
- 68 Jun, S.I., Wook J.L., Sakamoto, S., Yamaguchi, K., & Kim, K. (2000). Rotaxane-based molecular switch with fluorescence signaling. *Tetrahedron Letters*, 41(4), 471–475. DOI: 10.1016/s0040-4039(99)02094-8
- 69 Panshina, S.Yu., Ponomarenko, O.V., Bakibaev, A.A., & Malkov, V.S. (2020). Study of glycoluril and its derivatives by ¹H and ¹³C NMR spectroscopy. *Bulletin of the University of Karaganda — Chemistry*, 99(3), 21–37. DOI: 10.31489/2020Ch3/21-37
- 70 Bakibaev, A.A., Zhumanov, K.B., Panshina, S.Yu., Gorbin, S.I., Malkov V.S., & Khrebtova, D.V., et al. (2019). NMR Spectra of phosphorylated carbamide-containing heterocycles: peculiarities of chemical shifts from the valence state of the phosphorus and the size of the cycle. *News of the Academy of sciences of the Republic of Kazakhstan*, 5, 100–107. DOI: 10.32014/2019.2518-1491.60
- 71 Mason, J., Larkworthy, L.F., & Moore, E.A. (2002). Nitrogen NMR Spectroscopy of Metal Nitrosyls and Related Compounds. *Chemical Reviews*, 102(4), 913–934. DOI: 10.1021/cr0000751
- 72 Chegaev, K.Y., Kravchenko, A.N., Lebedev, O.V., & Strelenko, Y.A. (2001). New functional glycoluril derivatives. *Mendeleev Communications*, 11(1), 32–33. DOI: 10.1070/mc2001v011n01abeh001357
- 73 Bardelang, D., Brinkmann, A., Ratcliffe, C.I., Ripmeester, J.A., Tersikh, V.V., & Udachin, K.A. (2014). High field solid state ¹³C NMR spectroscopy of cucurbituril materials. *CrystEngComm*, 16(18), 3788–3795. DOI: 10.1039/c3ce42467g
- 74 Gobre, V.V., Pinjari, R.V., & Gejji, S.P. (2010). Density Functional Investigations on the Charge Distribution, Vibrational Spectra, and NMR Chemical Shifts in Cucurbit[n]uril (n= 5–12) Hosts. *The Journal of Physical Chemistry A*, 114(12), 4464–4470. DOI: 10.1021/jp100904c
- 75 Joseph, R., & Masson, E. (2013). Atropisomerization in Confined Space; Cucurbiturils as Tools to Determine the Torsional Barrier of Substituted Biphenyls. *European Journal of Organic Chemistry*, 2014(1), 105–110. DOI: 10.1002/ejoc.201301460
- 76 Assaf, K.I., & Nau, W.M. (2015). Cucurbiturils: from synthesis to high-affinity binding and catalysis. *Chemical Society Reviews*, 44(2), 394–418. DOI: 10.1039/c4cs00273c
- 77 Barrow, S.J., Kaser, S., Rowland, M.J., del Barrio, J., & Scherman, O.A. (2015). Cucurbituril-Based Molecular Recognition. *Chemical Reviews*, 115(22), 12320–12406. DOI: 10.1021/acs.chemrev.5b00341
- 78 Lagona, J., Mukhopadhyay, P., Chakrabarti, S., & Isaacs, L. (2005). The Cucurbit[n]uril Family. *Angewandte Chemie International Edition*, 44(31), 4844–4870. DOI: 10.1002/anie.200460675
- 79 Havel, V., Babiak, M., & Sindelar, V. (2017). Modulation of Bambusuril Anion Affinity in Water. *Chemistry — A European Journal*, 23(37), 8963–8968. DOI: 10.1002/chem.201701316
- 80 Svec, J., Necas, M., & Sindelar, V. (2010). Bambus[6]uril. *Angewandte Chemie International Edition*, 49(13), 2378–2381. DOI: 10.1002/anie.201000420
- 81 Panshina, S. Yu., Ponomarenko, O.V., Bakibaev, A.A., & Malkov, V.S. (2020). Analysis of XRD structural parameters of glycoluril and its derivatives. *Journal of Structural Chemistry*, 61, 1315–1355. DOI: 10.1134/S0022476620090012.
- 82 Stancl, M., Gargulakova, Z., & Sindelar, V. (2012). Glycoluril Dimer Isomerization under Aqueous Acidic Conditions Related to Cucurbituril Formation. *The Journal of Organic Chemistry*, 77(23), 10945–10948. DOI: 10.1021/jo302063j
- 83 Burnett, C.A., Lagona, J., Wu, A., Shaw, J.A., Coady, D., Fettinger, J.C., Day, A.I., & Isaacs, L. (2003). Preparation of glycoluril monomers for expanded cucurbit[n]uril synthesis. *Tetrahedron*, 59(11), 1961–1970. DOI: 10.1016/s0040-4020(03)00150-9
- 84 Kurgachev, D.A., Kotelnikov, O.A., Novikov, D.V., Kuserbaeva, V.R., Gorbin, S.I., & Tomilova, E.V., et al. (2018). Isolation, Identification, and Chromatographic Separation of N-Methyl Derivatives of Glycoluril. *Chromatographia*, 81, 1431–1437. DOI: 10.1007/s10337-018-3599-9
- 85 Ndendjio, S.Z., Liu, W., Yvanez, N., Meng, Z., Zavalij, P.Y., & Isaacs, L.D. (2020). Triptycene Walled Glycoluril Trimer: Synthesis and Recognition Properties. *New Journal of Chemistry*, 44, 338–345. DOI: 10.1039/c9nj05336k

- 86 Rodrigues, M.A.A., Mendes, D.C., Ramamurthy, V., & Da Silva, J.P. (2017). ESI-MS of Cucurbituril Complexes Under Negative Polarity. *Journal of The American Society for Mass Spectrometry*, 28(11), 2508–2514. DOI: 10.1007/s13361-017-1758-0
- 87 Stancl, M., Khan, M. S. A., & Sindelar, V. (2011). 1,6-Dibenzylglycoluril for synthesis of deprotected glycoluril dimer. *Tetrahedron*, 67(46), 8937–8941. DOI: 10.1016/j.tet.2011.08.097
- 88 Ding, J., Liu, S., Xiao, H.-M., Ye, T., Zhou, P., & Feng, Y.-Q. (2017). Matrix-assisted laser desorption/ionization mass spectrometry for the analysis of polyamines in plant micro-tissues using cucurbituril as a host molecule. *Analytica Chimica Acta*, 987, 56–63. DOI: 10.1016/j.aca.2017.08.027
- 89 Magalhães, C.I.R., Gomes, A.C., Lopes, A.D., Gonçalves, I.S., Pillinger, M., Jin, E., & Herber, R.H. (2017). Ferrocene and ferrocenium inclusion compounds with cucurbiturils: a study of metal atom dynamics probed by Mössbauer spectroscopy. *Physical Chemistry Chemical Physics*, 19(32), 21548–21555. DOI: 10.1039/c7cp04416j
- 90 Day, A.I., Blanch, R.J., Arnold, A.P., Lorenzo, S., Lewis, G.R., & Dance, I. (2002). A Cucurbituril-Based Gyroscane: A New Supramolecular Form. *Angewandte Chemie International Edition*, 41(2), 275–277. DOI: 10.1002/1521-3773(20020118)41:2<275::aid-anie275>3.0.co;2-m
- 91 Chen, Y., Klimczak, A., Galoppini, E., & Lockard, J.V. (2013). Structural interrogation of a cucurbit[7]uril-ferrocene host-guest complex in the solid state: a Raman spectroscopy study. *RSC Adv.*, 3(5), 1354–1358. DOI: 10.1039/c2ra21584e
- 92 Gürbüz, S., Idris, M., & Tuncel, D. (2015). Cucurbituril-based supramolecular engineered nanostructured materials. *Organic & Biomolecular Chemistry*, 13(2), 330–347. DOI: 10.1039/c4ob02065k
- 93 Cicolani, R.S., Sampaio de Oliveira Filho, A.G., de Lima Batista, A.P., & Demets, G.J.-F. (2020). Formation of the non-classical interhalide anion [I₂Cl]⁻ in methyl-bambus[6]uril cavity. *New Journal of Chemistry*, 44, 2697–2700. DOI: 10.1039/c9nj05352b
- 94 Trubina, S., Erenburg, S., Bausk, N., Nadolinny, V., Bakovets, V., Dolgovesova, I., & Mitkina, T. (2009). EXAFS spectroscopy investigation Cu(II) complexes encapsulated in cucurbit[8]uril. *Journal of Physics: Conference Series*, 190, 012128. DOI: 10.1088/1742-6596/190/1/012128
- 95 Rawat, N., Kar, A., Bhattacharyya, A., Rao, A., Nayak, S.K., Nayak, C., Jha, S.N., Bhattacharyya, D., & Tomar, B.S. (2015). Complexation of Eu(III) with Cucurbit[n]uril, n = 5 and 7: A Thermodynamic and Structural Study. *Dalton Transactions*, 44(9), 4246–4258. DOI: 10.1039/c4dt03623a
- 96 Rawat, N., Kar, A., Bhattacharyya, A., Yadav, A.K., Bhattacharyya, D., Jha, S.N., & Tomar, B.S. (2019). Complexation of U(VI) with Cucurbit[5]uril: Thermodynamic and Structural investigation in aqueous medium. *Spectrochimica Acta Part A: Molecular and Biomolecular Spectroscopy*, 207, 354–362. DOI: 10.1016/j.saa.2018.09.037
- 97 Ong, W., & Kaifer, A.E. (2003). Unusual Electrochemical Properties of the Inclusion Complexes of Ferrocenium and Cobaltocenium with Cucurbit[7]uril. *Organometallics*, 22(21), 4181–4183. DOI: 10.1021/om030305x
- 98 Kaifer, A.E. (2014). Toward Reversible Control of Cucurbit[n]uril Complexes. *Accounts of Chemical Research*, 47(7), 2160–2167. DOI: 10.1021/ar5001204
- 99 Sal'keeva, L.K., Korotkova, E.I., Dyorina, K.V., Taishibekova, E.K., Minaeva, E.V., Muratbekova, A.A., & Sal'keeva, A.K. (2019). Electrochemical Study of the Complex-Forming Properties of Phosphorylated Glucoluril. *Russian Journal of General Chemistry*, 89(3), 466–469. DOI: 10.1134/s1070363219030162
- 100 Derina, K.V., Korotkova, E.I., Dorozhko, E.V., Voronova, O.A., & Chulkova, I.V. (2016). Opredelenie kholesterina v pishchevykh produktakh voltamperometricheskim metodom [Voltammetric Determination of Cholesterol in Food]. *Zavodskaya laboratoriya. Diagnostika materialov — Industrial laboratory. Diagnostics of materials*, 82(11), 11–16 [in Russian].
- 101 Blanco, E., Quintana, C., Hernández, P., & Hernández, L. (2010). A Voltammetric Study of the Interaction Between Cucurbit[6]uril and Divalent Metal Ions. *Electroanalysis*, 22(17–18), 2123–2130. DOI: 10.1002/elan.201000066
- 102 Blanco, E., Quintana, C., & Hernández, P. (2014). An Electrochemical Study of Cucurbit[6]uril–Cadmium(II) Interactions and the Effect of Electrolyte Cations and Guest Molecules. *Analytical Letters*, 48(5), 783–795. DOI: 10.1080/00032719.2014.961604
- 103 Zhu, C., Meng, Z., Liu, W., Ma, H., Li, J., & Yang, T., et al. (2018). Investigation on the hydrolytic mechanism of cucurbit[6]uril in alkaline solution. *Royal Society Open Science*, 5(5), 180038. DOI: 10.1098/rsos.180038
- 104 Berlyand, A.S., Lebedev, O.V., & Prokopov, A.A. (2013). Khimiko-farmatsevticheskii analiz biolohicheskii aktivnoho veshchestva Albikar [Chemical-pharmaceutical analysis of biologically active substance Albikar]. *Khimiko-farmatsevticheskii zhurnal — Pharmaceutical Chemical Journal*, 47, 52–54. DOI: 10.30906/0023-1134-2013-47-3-52-54 [in Russian].
- 105 Berlyand, A.S., & Prokopov, A.A. (2012). Analiz biolohicheskii aktivnykh bitsiklicheskiikh bismochevin metodom hazozhidkostnoi khromatografii [Analysis of biologically active bicyclic bismocetins by the gas-liquid chromatography]. *Zhurnal nauchnykh statei «Zdorovie i obrazovanie v XXI veke» — The journal of scientific articles "Health & education millennium"*, 14, 35 [in Russian].
- 106 Serov, N.V., Berlyand, A.S., Knizhnik, A.Z., & Volkenstein, Yu.B. (1982). Sposob kolichestvennoho opredeleniia Mebikara v biolohicheskikh zhidkostiakh [Method of quantitative determination of mebikar in biological liquids]. *Avtorskoe svidetelstvo 943571 SSSR — USSR Patent No. 943571*. Moscow, Russian Federation: Federal Service for Intellectual Property, Patents and Trademarks [in Russian].
- 107 Berlyand, A.S., & Prokopov, A.A. (2014). Issledovanie hidroliticheskoi stabilnosti biolohicheskii aktivnoho veshchestva Bikaret [Investigation of hydrolytic stability of biologically active substance Bikaret]. *Khimiko-farmatsevticheskii zhurnal — Pharmaceutical Chemical Journal*, 48, 347–349. DOI: 10.30906/0023-1134-2014-48-5-47-49 [in Russian].
- 108 Rezaei-Seresht, E., & Tayeb, R. (2011). Synthesis of Glycoluril Derivatives Catalyzed by Some Heteropolyoxometalates. *Journal of Chemical and Pharmaceutical Research*, 3, 103–107.

- 109 Wu, A., She, N., Gao, M., Cao, L., & Yin, G. (2007). Synthesis and Spectral Properties of Novel Fluorescent Diethoxycarbonyl Glycoluril Derivatives. *Synlett*, 2007(16), 2533–2536. DOI: 10.1055/s-2007-986671
- 110 Qin, S.-Q., Pang, T., & Li, Y.-T. (2008). 4,4'-[8b,8c-Bis(ethoxycarbonyl)-4,8-dioxo-2,3,5,6-tetrahydro-1H,4H-2,3a,4a,6,7a,8a-hexaazacyclopenta[de]fluorene-2,6-diyl]dipyridinium bis(tetrafluoridoborate). *Acta Crystallographica E*, 64, o1689. DOI: 10.1107/S1600536808023635
- 111 Lu, L.-B., Zhang, Y.-Q., Zhu, Q.-J., Xue, S.-F., & Tao, Z. (2007). Synthesis and X-ray Structure of the Inclusion Complex of Dodecamethylcucurbit[6]uril with 1,4-Dihydroxybenzene. *Molecules*, 12(4), 716–722. DOI: 10.3390/12040716
- 112 Hase, C., & Kühling, D. (1975). Umsetzung von Tetraacetylglykoluril mit Nucleophilen. *Justus Liebigs Annalen Der Chemie*, 1975(1), 95–102. DOI: 10.1002/jlac.197519750111
- 113 OlainFarm (2020, May 15). "Adaptol" Sertificate. <https://gorzdrav.org/medias/24739-01307342-1.jpg?context=bWFzdGVyfHByb2R1Y3QtY2VydGlmaWNhdGVzZDM2NzYzMHxpbWFnZS9qcGVnfHB2R1Y3QtY2VydGlmaWNhdGVzL2g4Yi9oYjEvOTA3ODU5NzA5MTM1OC5qcGd8NGM2YTI4NGM1YWZiMjdlMTZlOGJmNzg5MzJhYTlywYjBINzEwYTU0NmVjMDVhNmI0OGE2NzcxZWFnNDlkZGJmMg>
- 114 Berlyand, A.S., Kostebelov, N.V., & Prokopov, A.A. (2015). Issledovanie hidroliticheskoi stabilnosti Albikara [Investigation of hydrolytic stability of albikar]. *Khimiko-farmatsevticheskii zhurnal — Pharmaceutical Chemical Journal*, 49, 55–56. DOI: 10.30906/0023-1134-2015-49-8-55-56 [in Russian].
- 115 Gonchikova, Yu.A., Chmelevskaya, N.V., & Illarionova, E.A. (2018). Analiz kombinirovannykh sochetanii lekarstvennykh sredstv na osnove Abakavira, Lamivudina, Zidovudina metodom vysokoeffektivnoi zhidkostnoi khromatografii [Analysis of mixed combinations of medicinal products based on abacavir, lamivudin, zidovudin using the method of microcolonies liquid chromatography]. *Kubanskii nauchnyi meditsinskii vestnik — Kuban Scientific Medical Bulletin*, 25, 46–50 [in Russian].
- 116 Urbaniak, M., Gosecki, M., Gostynski, B., & Gosecka, M. (2020). Synthesis of a monofunctional glycoluril molecular clip via cyclic imide formation on the convex site. *New Journal of Chemistry*, 44, 596–604. DOI: 10.1039/c9nj04357h
- 117 Saloutina, L.V., Zapevalov, A.Y., Slepukhin, P.A., Kodess, M.I., Saloutin, V.I., & Chupakhin, O.N. (2014). Synthesis of Fluorine-Containing Imidazolidin-2-Ones, Glycolurils, and Hydantoins Based on Perfluorodiacetyl and Ureas. *Chemistry of Heterocyclic Compounds*, 50(7), 958–966. DOI: 10.1007/s10593-014-1550-z
- 118 Zhao, W.-X., Wang, C.-Z., Chen, L.-X., Cong, H., Xiao, X., Zhang, Y.-Q., & Xue, S.-F., et al. (2015). A Hemimethyl-Substituted Cucurbit[7]uril Derived from 3 α -Methyl-glycoluril. *Organic Letters*, 17(20), 5072–5075. DOI: 10.1021/acs.orglett.5b02588
- 119 Panshina, S.Y., Ponomarenko, O.V., Bakibayev, A.A., & Malkov, V.S. (2020). Tetrakis(hydroxymethyl)glycoluril in N-methylenation reactions with arylamines. *Chemistry of Heterocyclic Compounds*. DOI: 10.1007/s10593-020-02633-4
- 120 Gazieva, G.A., Lysenko, K.A., Kravchenko, A.N., & Lebedev, O.V. (2007). Synthesis and structure of 2,4,6,8-tetramethyl-3,7-dithia-2,4,6,8-tetraazabicyclo[3.3.0]octane 3,3,7,7-tetraoxide. *Russian Journal of Organic Chemistry*, 43(11), 1715–1718. DOI: 10.1134/s107042800711022x
- 121 Kravchenko, A.N., Sigachev, A.S., Gazieva, G.A., Maksareva, E.Y., Trunova, N.S., & Chegaev, K.A., et al. (2006). Reaction of N-alkylglycolurils with electrophilic reagents. *Chemistry of Heterocyclic Compounds*, 42(3), 365–376. DOI: 10.1007/s10593-006-0094-2
- 122 Kartashov, V.A. (2012). TSKH-skrininih i indeksy uderzhivaniia toksicheskikh veshchestv [TLC-screening and retention indexes of toxic substances]. *Vestnik Kazakhskoho natsionalnoho meditsinskoho universiteta — Kazakh national medical university bulletin*, 25, 39–41 [in Russian].
- 123 Ammann, E.C.B., & Lynch, V.H. (1964). Purine metabolism of unicellular algae. *Analytical Biochemistry*, 7(4), 387–392. DOI: 10.1016/0003-2697(64)90150-2
- 124 Wu, A., Fetting, J.C., & Isaacs, L. (2002). Glycoluril derivatives form hydrogen bonded tapes rather than cucurbit[n]uril congeners. *Tetrahedron*, 58(49), 9769–9777. DOI: 10.1016/s0040-4020(02)01307-8
- 125 Poskrobko, M., & Dejnega, M. (1998). HPLC Analysis of the Products of the Reaction Between Glycoluril and Formaldehyde. *Journal of Liquid Chromatography & Related Technologies*, 21(17), 2725–2731. DOI: 10.1080/10826079808003419
- 126 Hidalgo-Fernández, P., Ayet, E., Canal, I., & Farrera, J.-A. (2006). Avidin and streptavidin ligands based on the glycoluril bicyclic system. *Organic and Biomolecular Chemistry*, 4(16), 3147–3154. DOI: 10.1039/b605081f
- 127 Kravchenko, A.N., Sigachev, A.S., Maksareva, E.Y., Gazieva, G.A., Trunova, N.S., & Lozhkin, B.V., et al. (2005). Synthesis of new chiral mono-, di-, tri-, and tetraalkylglycolurils. *Russian Chemical Bulletin*, 54(3), 691–704. DOI: 10.1007/s11172-005-0307-3
- 128 Kravchenko, A.N., Sigachev, A.S., Belyakov, P.A., Ilyin, M.M., Lyssenko, K.A., & Davankov, V.A., et al. (2009). 4,5-Dihydroxyimidazolidin-2-ones in α -ureidoalkylation of N-carboxy-, N-hydroxy-, and N-aminoalkylureas. 2. α -Ureidoalkylation of N-(hydroxyalkyl)ureas. *Russian Chemical Bulletin*, 58(6), 1264–1269. DOI: 10.1007/s11172-009-0165-5
- 129 Lízal, T., & Šindelář, V. (2019). Bambusuril analogs based on alternating glycoluril and xylylene units. *Beilstein Journal of Organic Chemistry*, 15, 1268–1274. DOI: 10.3762/bjoc.15.124
- 130 Khannanov, T.Sh., Anisimov, A.N., Kamaeva, S.S., Kashapova, K.I., Lefterova, M.I., & Khamidullin, R.T., et al. (2016). Farmatsevticheskaja kompozitsiia, sodержashchaya kombinatsiiu hlitsina i tetramethyltetraazabitsikloktandiona (varianty) [Pharmaceutical composition comprising combination of glycine and tetramethyltetraazabicyclooctandione (version)]. *Patent 2576240. Rossiiskaia Federatsiia — Russian Patent No. 2576240*. Moscow, Russian Federation: Federal Service for Intellectual Property, Patents and Trademarks [in Russian].

- 131 FisherScientific. (2020, May 15) *N,N',N'',N'''-Tetraacetylglucosyluril*. <https://www.fishersci.ca/shop/products/n-n-n-n-tetraacetylglucosyluril-tci-america-2/p-7136535>
- 132 Johnson, D.W., Hof, F., Palmer, L.C., Martín, T., Obst, U., & Rebek, Jr., J. (2003). Glycoluril ribbons tethered by complementary hydrogen bonds. *Chemical Communications*, *14*, 1638–1639. DOI: 10.1039/b303508e
- 133 Huang, W.-H., Zavalij, P.Y., & Isaacs, L. (2009). Metal-Ion-Induced Folding and Dimerization of a Glycoluril Decamer in Water. *Organic Letters*, *11*(17), 3918–3921. DOI: 10.1021/ol901539q
- 134 Gosecki, M., Urbaniak, M., & Gosecka, M. (2019). A Glycoluril Clips for the Construction of Chemoresponsive Supramolecular Polymer Network through Homodimer Cross-Links. *ChemPlusChem*, *84*, 981–988. DOI: 10.1002/cplu.201900367
- 135 Takei, S., & Hanabata, M. (2017). High-resolution nanopatterning of biodegradable polylactide by thermal nanoimprint lithography using gas permeable mold. *AIP Advances*, *7*(3), 035110. DOI: 10.1063/1.4978448
- 136 Sorvanov, A.A., & Rubtsov, K.V. (2019). Sintez novykh vodorastvorimyykh polimerov na osnove hidroksimetilnykh proizvodnykh hlikolurila [Development of new water-soluble polymers based on hydroxymethyl derivatives of glycoluril]. Proceedings from Prospects for the development of fundamental sciences: XVI Mezhdunarodnaia konferentsiia studentov, aspirantov i molodykh uchenykh — XVI International Conference of students, graduate students and young scientists. (p. 204–206). Tomsk, Russia, April, 2019 [in Russian].
- 137 Strebl, M.G., Yang, J., Isaacs, L., & Hooker, J.M. (2018). Adamantane/Cucurbituril: A Potential Pretargeted Imaging Strategy in Immuno-PET. *Molecular Imaging*, *17*, 1–7. DOI: 10.1177/1536012118799838
- 138 Day, A., Arnold, A., & Blanch, R. (2003). A Method for Synthesizing Partially Substituted Cucurbit[n]uril. *Molecules*, *8*(1), 74–84. DOI: 10.3390/80100074
- 139 Kumano, T., Takeda, T., Miura, S., Kashiwabara, T., & Mizobe, N. (2018). *U.S. Patent No 10000622*. Washington, DC: U.S. Patent and Trademark Office.
- 140 Ivanov, E.V., Lebedeva, E.Y., Batov, D.V., Baranov, V.V., & Kravchenko, A.N. (2019). Equimolecular cocrystal of cis- and trans-coordinated N,N'-dimethylglycolurils: Some standard thermodynamic properties in the aqueous solution between 278.15 K and 318.15 K. *Journal of Molecular Liquids*, *297*, 111891–111899. DOI: 10.1016/j.molliq.2019.111891
- 141 Zheng, Z.-H., Wang, J.-L., Li, Y.-X., & Wang, Y.-H. (2015). Study on promoting the synthesis of glycoluril by microwave technology. *Journal of North University of China*, *36*, 202–207. DOI: 10.3969/j.issn.1673-3193.2015.02.022
- 142 Ivanov, E.V., & Batov, D.V. (2019). Enthalpy-related parameters of interaction of simplest α -amino acids with the pharmaceutical mebicar (N-tetramethylglycoluril) in water at 298.15 K. *The Journal of Chemical Thermodynamics*, *128*, 159–163. DOI: 10.1016/j.jct.2018.08.022
- 143 Ivanov, E.V., & Batov, D.V. (2016). Effect of the H/D solvent isotope substitution on enthalpy-related interaction parameters in aqueous solutions of the racemic Albicar at T = 298.15 K and ambient pressure. *The Journal of Chemical Thermodynamics*, *102*, 9–11. DOI: 10.1016/j.jct.2016.06.020

Information about authors

Bakibaev, Abdigali Abdimanapovich — Doctor of Chemical sciences, Engineer, Institute for Problems of Chemical and Energetic Technologies SB RAS, Socialisticheskaya street, 1, 659322, Biysk, Russia; e-mail: bakibaev@mail.ru; <https://orcid.org/0000-0002-3335-3166>.

Malkov, Victor Sergeevich — Candidate of Chemical sciences, Head of laboratory of organic synthesis, National Research Tomsk State University, Lenin avenue, 36, 634050, Tomsk, Russia; e-mail: malkov.vics@gmail.com; <https://orcid.org/0000-0003-4532-2882>

Kurgachev, Dmitriy Andreevich — Engineer, Institute for Problems of Chemical and Energetic Technologies SB RAS, Socialisticheskaya street, 1, 659322, Biysk, Russia; e-mail: daemond91@mail.ru; <https://orcid.org/0000-0003-2471-7287>.

Kotelnikov, Oleg Alexeevich — Junior researcher, National Research Tomsk State University, Lenin avenue, 36, 634050, Tomsk, Russia; e-mail: kot_o_a@mail.ru; <https://orcid.org/0000-0002-1241-1312>.

R.I. Jalmakhanbetova¹, Ye.M. Suleimen^{2,3*}, I.H. Eissa⁴, A.M. Metwaly⁵, Zh.B. Iskakova¹,
D.S. Balpanov⁶, G.G. Sissengaliyeva⁷, R.A. Khannanov⁶, T.M. Seilkhanov²

¹Kazakh University of Technology and Business, Nur-Sultan, Kazakhstan;

²Sh. Ualikhanov Kokshetau University, Kokshetau, Kazakhstan;

³Republican collection of microorganisms, Nur-Sultan, Kazakhstan;

⁴Pharmaceutical Medicinal Chemistry Department, Faculty of Pharmacy, Al-Azhar University, Cairo, Egypt;

⁵Pharmacognosy Department, Faculty of Pharmacy, Al-Azhar University, Cairo, Egypt;

⁶"Biolife" Ltd, Stepnogorsk, Kazakhstan;

⁷L.N. Gumilyov Eurasian National University, Nur-Sultan, Kazakhstan

(Corresponding author's e-mail: syerlan75@yandex.kz)

Isolation and biological evaluation of roseofungin and its cyclodextrin inclusion complexes

Roseofungin belongs to polyene antibiotics which is more active and less toxic comparing other polyenes of this group. Roseofungin was isolated from *Actinomyces roseoflavus* var. *Roseofungini* using different chromatographic techniques and for the first time, the complexation of roseofungin with α -, β - and γ -cyclodextrin derivatives was performed. The binding patterns of the resulted complexes were studied *in silico* using molecular docking techniques. The best binding mode was for roseofungin against γ -CD with an affinity value of -42.98 kcal/mol. The proposed binding mode of roseofungin against α -CD showed unusual interaction with an affinity value of -41.80 kcal/mol. Also, roseofungin bonded to β -CD with a binding affinity value of -35.03 kcal/mol. The antiradical and cytotoxic activities of roseofungin and its obtained α -, β - and γ -cyclodextrin complexes were determined. The antiradical activity was performed using butylhydroxyanisole as a reference, while the cytotoxic activity was determined using *Artemia salina* crustaceans. As a result of the biological activity study, it was found that roseofungin and some of its complexes have weak antiradical activities.

Keywords: roseofungin, cyclodextrin, *in silico*, molecular docking, complexation, antiradical activity, cytotoxicity.

Introduction

The development of modern industries and the rapid growth of the population in the past 50 years set the task of searching for new renewable resources: food sources, biofuels, medicines, cosmetics and hygiene products, which will undoubtedly lead to increased interest in natural renewable resources.

At the present time, the Republic of Kazakhstan does not have any its own drug that has antibacterial and anti-infective effect. The pharmaceutical industry of the Republic of Kazakhstan mainly produces galena preparations, as well as consumable medical devices such as masks, gloves, syringes, etc. The pharmaceutical and medical industry of the Republic of Kazakhstan has a big task to increase the share of domestic manufacturers in the market to 50 % in the next 20 years. It is planned to modernize existing and build new pharmaceutical enterprises in the framework of the investment projects, to ensure the implementation of quality production standards in the pharmaceutical enterprises and to provide this industry with highly qualified staff.

In Kazakhstan, specialists of the Institute of Microbiology and Virology, al-Farabi Kazakh National University and South Kazakhstan state University named after M. Auezov are engaged in the search and study of new antibiotics, increasing the activity of produced known antibiotics. Thus, the broad-spectrum antifungal polyene antibiotic roseofungin was obtained for the treatment of deep and superficial mycoses. The spectrum of action of this antibiotic was found to be much broader than other known antifungal drugs [1, 2].

The antifungal ointment rosentin[®] is a roseofungin 2 % ointment which was developed by the Institute of pharmaceutical biotechnology of the National Center of Biotechnology of the Republic of Kazakhstan [3]. The strong antiviral activity of roseofungin against influenza and parainfluenza viruses was proven before [4, 5].

From a chemical point of view, the roseofungin molecule is of great interest, since there are several reaction centers in the molecule that make it possible to obtain various derivatives.

The relevance of this work lies in the lack of research and sufficient production of domestic antibiotics.

The purpose of the work was to obtain new derivatives of the antibiotic roseofungin and to study their physical, chemical and biological properties.

Experimental

1. Isolation of roseofungin (1)

An aqueous micelle (56.52 g) (the micelle was obtained from the culture fluid *Actinomyces roseoflavus* var. *Roseofungini*, Stepnogorsk, Kazakhstan) was treated twice with acetone. After that, the solution was filtered out using a vacuum pump. The resulting filtrate (acetone layer) was evaporated at 30–35 °C on a rotary evaporator. The remaining concentrate (orange color) was extracted with *n*-butanol. Then the butanol layer was washed three times with 100, 50, 50 ml of 1 % aqueous solution of sodium hydroxide, and then twice with 100 ml of water. After separation, the butanol layer was evaporated at 42 °C on a rotary evaporator. A precipitate was formed when 200 ml of diethyl ether was added. The precipitate was filtered out in a vacuum. 0.71 g of raw roseofungin was obtained as a result. The mass was 0.69 g after drying in a vacuum concentrate. The roseofungin raw material was purified by gel filtration on Sephadex LH-20.

2. Obtaining roseofungin / cyclodextrin complexes

2.1. Obtaining roseofungin complex with α -cyclodextrin (2)

0.05 g of α -cyclodextrin was placed in the crucible, a mixture of solvents (C₂H₅OH: H₂O, 1: 1) was added, and 0.05 g of roseofungin (1) was added. The reaction was performed for 2 hours. Then the suspension was left inside the desiccator overnight. After the obtained complex (2) was dried in vacuum to constant mass. The mass of the compound (2) was 0.07 g, and the melting point was 210 °C (decomp.).

The peaks of IR spectra were fixed at 696, 777, 1015, 1148, 1559, 1653, 2025, 2159, 2925, 3351 (neat, ν , cm⁻¹).

2.2. Obtaining roseofungin complex with β -cyclodextrin (3)

0.05 g of β -cyclodextrin was placed in the crucible, a mixture of solvents (C₂H₅OH: H₂O, 1: 1) was added, and 0.05 g of roseofungin (1) was added. The reaction was performed for 2 hours. Then the suspension was left inside the desiccator overnight. After the obtained complex (3) was dried in vacuum to constant mass. The mass of the compound (3) was 0.098 g, and the melting point was 179 °C (decomp.).

The peaks of IR spectra were fixed at 668, 695, 777, 795, 1026, 1419, 1436, 1457, 1472, 1507, 1521, 1540, 1559, 1636, 1653, 1684, 1717, 1734, 2024, 2158, 2360, 2922, 3629, 3649, 3675, 3744, 3735, 3853 (neat, ν , cm⁻¹).

2.3. Obtaining roseofungin complex with γ -cyclodextrin (4)

0.05 g of α -cyclodextrin was placed in the crucible, a mixture of solvents (C₂H₅OH: H₂O, 1: 1) was added, and 0.05 g of roseofungin (1) was added. The reaction was performed for 2 hours. The suspension was then left inside the desiccator overnight. After the obtained complex (4) was dried in vacuum to constant mass. The mass of the compound (4) was 0.13 g, and the melting point was 200 °C (decomp.).

The peaks of IR spectra were fixed at 695, 777, 795, 940, 1023, 1419, 1457, 1507, 1521, 1540, 1559, 1636, 1653, 1684, 1700, 1717, 1734, 2023, 2159, 2360, 2925, 3335, 3629, 3649, 3675, 3735, 3744, 3853 (neat, ν , cm⁻¹).

3. Determination of antiradical activity

3 ml of 6*10⁻⁵ M radical solution was added to 0.1 ml of the studied alcohol solutions in the concentration range of 0.1; 0.25; 0.5; 0.75 and 1.0 mg ml⁻¹ to determine the inhibition of 2,2-diphenyl-1-picrylhydrazyl radical (DPPH). The test tubes were in a tripod wrapped in black plastic. After intensive mixing, the solutions were left in the dark for 30 minutes, then the optical densities were measured at 520 nm wavelength. The antiradical activity (ARA) value of the studied objects were determined by the formula (1):

$$\text{APA (\%)} = A_0 - A_t / A_0 * 100, \quad (1)$$

where A₀ — is the optical density of the control sample; A_t — is the optical density of the working sample.

The optical density of the studied compounds was measured at 520 nm using the Cary 60 UV-Vis device. The obtained antiradical activity was compared with the antiradical activity of butylhydroxyanisole (BHA) [6]. The optical density of the studied solutions, calculated by the formula 1, are shown in Table 1.

4. Determination of cytotoxicity

The cytotoxic activity was determined by a well-known method using *Artemia salina* crustaceans. *Artemia* is one of the standard organisms for testing the toxicity of chemical substances.

The flask was filled with artificial seawater and 200 mg of *Artemia salina* eggs were added. It was kept for 3 days with a soft supply of air, until the crustaceans were hatched from the eggs. One side of the tube was covered with aluminum foil, and 5 minutes later, the larvae that gather on the bright side of the flask were removed with a Pasteur pipette.

20–40 larvae were placed in 990 ml of seawater in each of 30 test tubes. The number of dead larvae was counted under a microscope. 10 ml of dimethylsulfoxide solution (DMSO) was added to 10 mg ml⁻¹ of the sample. The test substance was used as a comparison drug. Only 10 ml of DMSO was added for negative control. The number of dead larvae were counted under a microscope after 24 hours of incubation [7].

Mortality P was determined by the following formula (2):

$$P = (A - N - B)/Z * 100, \quad (2)$$

where A — is the number of dead larvae after 24 h; N — is the number of dead larvae before the test; B — is the average number of dead larvae in negative control; Z — is the total number of larvae.

3 solutions were prepared with different concentrations of each substance.

5. Docking studies

5.1. Preparation of the α -, β -, and γ -cyclodextrin (CD) structure

The 3D crystal structures of the α -, β -, and γ -CD were extracted from the cyclo/maltodextrin/alpha-cyclodextrin complex, beta-amylase/ beta-cyclodextrin complex, and glycogen phosphorylase B/gamma-cyclodextrin complex, respectively. These complexes were retrieved from RCSB Protein Data Bank with PDB IDs of 2ZYM (resolution 1.80 Å), 1BFN (resolution 2.07 Å), and 1p2g (resolution 2.30 Å), respectively. The docking analyses were performed using Discovery Studio 4.0 software to evaluate the free energies and binding mode of roseofungin molecule with the core site of α -, β -, and γ -CD. The most promising poses were selected depending the increased binding free energy (ΔG) [8–10].

The 3D crystal structures of α -, β -, and γ -CD were prepared by selecting α , β , and γ CD subunits and removing protein and all water molecules, heteroatoms and co-factors. Moreover, the correction of uncorrected valence atoms and crystallographic disorders were performed using alternate conformations and valence monitor options. Then, the α -, β -, and γ -CD were protonated and its inflexibility was obtained by creating fixed atom constraint. Next, the energy was minimized by applying CHARMM (Chemistry at HARvard Macromolecular Mechanics) force fields, and MMFF94 (Merck Molecular force field) force field for charge and partial charge, respectively [11]. The binding sites of the α -, β -, and γ -CD were defined as receptor molecules and prepared for docking.

5.2. Preparation of ligand

The 2D structure of roseofungin molecule was sketched using ChemBioDraw Ultra 14.0 and saved in MDL-SD file format. Then, the SD file was opened (by Discovery studio 4.0 software) and protonated. Force fields were applied on the molecule to get lowest energy minimum structure via CHARMM and MMFF94 force fields for charge and partial charge, respectively. Then, each of them was prepared for docking by applying ligand preparation protocol.

5.3. Docking simulation

The docking is a technique that can reliably predict the preferred configuration of one molecule relative to another molecule when they are bound to each other to form a stable complex. The evaluation of generated poses was mainly based on the number of interactions they formed with the residues of active site upon binding [12–15].

The molecular docking of roseofungin was performed using CDOCKER protocol which is an implementation of the CDOCKER algorithm [16]. CDOCKER is a grid-based molecular docking method that employs CHARMM-based molecular dynamics (MD) scheme to dock ligands into a receptor binding site [17]. The default values were selected for the CDOCKER protocol. The CDOCKER energy (receptor-ligand interaction energy) of best docked poses was calculated [18, 19].

Results and Discussion

We worked out extracts of culture fluid and prepared a condensed extract. The antibiotic roseofungin was extracted twice from the wet mycelium with acetone under neutral reaction. The extracts were separated from the mycelium, combined, and the solvent was distilled in a vacuum. From the aqueous residue the antibiotic roseofungin was extracted with butanol.

Butanol extract was separated, washed several times first with sodium hydroxide, then with water. The extract was evaporated in vacuum and the antibiotic roseofungin was precipitated by diethyl ether. The sediment was filtered, washed with ether and dried in a vacuum.

Subsequently, the roseofungin raw material was purified by gel filtration on Sephadex LH-20. Spirit eluates corresponding to the lemon-yellow zone were combined and stored in a vacuum. The sediment was filtered out, washed several times with ether, and dried. Amorphous lemon-yellow powder was obtained [20].

At the next stage of separation of the antibiotic roseofungin mixture, column chromatography was used, and the isolated fractions were once again purified by chromatography. The mixture of separated antibiotics was stored in an inert medium (argon) due to instability in light and air.

In order to obtain new derivatives, we carried out the complexation of roseofungin (1) with cyclodextrins. Cyclodextrins are macrocyclic compounds with a natural carbohydrate structure. Cyclodextrins contain molecules including a cylindrical plane.

It contains glucose residues connected by β -1,4-glycosidic bonds. Cyclodextrins differ depending on the number of monomers α -, β -, γ - and others. All the hydroxyl groups in the molecule are located on the outer surface of the molecule. Therefore, the inner cavity of cyclodextrins is hydrophobic.

Roseofungin (1) interacted with α -cyclodextrin by the friction method. This is how the molecule (2) was formed. The compound (2) was powdery, with m.p. 210 °C (decomp.).

Next, the roseofungin molecule (1) interacted with β -cyclodextrin. Compound (3) was obtained, it was powdery, with m.p. 179 °C (decomp.).

Compound (4) was obtained as a result of the interaction of roseofungin with γ -cyclodextrin. The synthesized compound (4) was powdery, with m.p. 200 °C (decomp.).

The optical density of the studied solutions, depending on the concentration, was measured on a spectrophotometer at the 520 nm wavelength. The optical density of the studied solutions, calculated by formula 1, are shown in Table 1.

Table 1

Changes in the optical density of the studied solutions with changes in concentration

| No. | Studied substances | Optical density values by concentration (mg ml ⁻¹) | | | | |
|-----|----------------------------|--|---------------|---------------|---------------|---------------|
| | | 0.1 | 0.25 | 0.5 | 0.75 | 1.0 |
| 1 | Butylhydroxyanisole (BHA) | 0.1362±0.0000 | 0.1333±0.0000 | 0.1257±0.0000 | 0.1202±0.0000 | 0.1145±0.0000 |
| 2 | R-ACD (2) | 0.6485±0.0100 | 0.6415±0.0000 | 0.6481±0.0000 | 0.6849±0.0000 | 0.6849±0.0000 |
| 3 | R-BCD (3) | 0.7358±0.0000 | 0.7550±0.0320 | 0.7583±0.0000 | 0.7601±0.0000 | 0.7604±0.0000 |
| 4 | R-GCD (4) | 0.7335±0.0141 | 0.7428±0.0000 | 0.7577±0.0000 | 0.7666±0.0000 | 0.7665±0.0000 |
| 5 | Roseofungin (Roseof-1) (1) | 0.6364±0.0000 | 0.6062±0.0000 | 0.5781±0.0000 | 0.5764±0.0223 | 0.5631±0.0264 |

The antiradical activity of the studied solutions was compared with the antiradical activity of butylhydroxyanisole (BHA). The antiradical effect values of the studied extracts, calculated by the formula 1, are shown in Table 2.

Table 2

Antiradical activity (%) at different concentrations

| No. | Studied substances | Concentration (mg ml ⁻¹) | | | | |
|-----|----------------------------|--------------------------------------|-------|-------|-------|-------|
| | | 0.1 | 0.25 | 0.5 | 0.75 | 1.0 |
| 1 | Butylhydroxyanisole (BHA) | 80.82 | 81.23 | 82.30 | 83.08 | 83.88 |
| 2 | R-ACD (2) | 12.03 | 12.98 | 12.09 | 7.09 | 7.09 |
| 3 | R-BCD (3) | 8.97 | 6.59 | 6.19 | 5.96 | 5.93 |
| 4 | R-GCD (4) | 9.26 | 8.10 | 6.26 | 5.16 | 5.17 |
| 5 | Roseofungin (Roseof-1) (1) | 12.94 | 17.07 | 20.92 | 21.15 | 22.97 |

The graphical dependence of the change in the studied substances antiradical activity on the change in concentration is shown in the Figure 1.

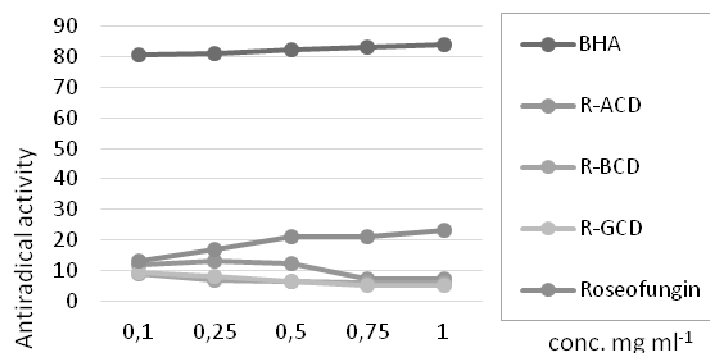


Figure 1. Dynamics of antiradical activity when the concentration of substances changes

Based on the analysis of data from tables and graphs, it can be seen that the substances R-ACD (2), R-BCD (3), R-GCD (4) and roseofungin (1) have very low antiradical activity compared to HPA.

The cytotoxic activity of the obtained complexes roseofungin (2–4) was studied. The results of cytotoxic activity of roseofungin derivatives are presented in Table 3.

Table 3

Results of cytotoxic activity of roseofungin derivatives

| Test substances | Concentration, mg ml ⁻¹ | Number of larvae in control | | Number of larvae in the sample | | | % of surviving larvae in control | % of surviving larvae in the sample | Mortality, A, % | The presence of neurotoxicity, % |
|-----------------|------------------------------------|-----------------------------|-------|--------------------------------|-------|-------|----------------------------------|-------------------------------------|-----------------|----------------------------------|
| | | surv. | dead | surv. | dead | par. | | | | |
| R-ACD (2) | 10 | 22±2.1 | 1±0.0 | 25±2.6 | 1±0.7 | 0±0.0 | 96 | 96 | 0 | 0 |
| | 5 | 22±2.1 | 1±0.0 | 23±1.6 | 1±0.7 | 0±0.0 | 96 | 96 | 0 | 0 |
| | 1 | 22±2.1 | 1±0.0 | 22±2.5 | 0±0.0 | 0±0.0 | 96 | 96 | 0 | 0 |
| R-BCD (3) | 10 | 22±2.1 | 1±0.0 | 23±2.5 | 1±1.0 | 0±0.0 | 96 | 96 | 0 | 0 |
| | 5 | 22±2.1 | 1±0.0 | 25±2.1 | 1±1.0 | 0±0.0 | 96 | 96 | 0 | 0 |
| | 1 | 22±2.1 | 1±0.0 | 26±2.1 | 1±0.7 | 0±0.0 | 96 | 96 | 0 | 0 |
| R-GCD (4) | 10 | 22±2.1 | 1±0.0 | 26±2.5 | 3±1.6 | 0±0.0 | 96 | 89 | 7 | 0 |
| | 5 | 22±2.1 | 1±0.0 | 21±1.7 | 3±1.6 | 0±0.0 | 96 | 88 | 8 | 0 |
| | 1 | 22±2.1 | 1±0.0 | 26±3.0 | 2±2.1 | 0±0.0 | 96 | 93 | 3 | 0 |

It can be assumed on the basis of conducted experiment, that complexes of cyclodextrins with roseofungin at all concentrations did not show cytotoxicity.

Docking technique was used to investigate the binding pattern of roseofungin with the α -, β -, and γ -cyclodextrin. The α -, β -, and γ -CD cavities are O-shaped structures consisting of 6, 7, and 8 glucose unites, respectively.

Firstly, roseofungin exhibited ideal binding mode with β - and γ -CD, where roseofungin was buried inside the β - and γ -CD. These roseofungin involved in hydrogen bond network with glucose unites of β , and γ -CD. On the other hand, the binding mode of roseofungin against α CD was unusual, where the α -CD consists from 6 glucose subunits forming too small cavity to receive the bulk structure of roseofungin. While the cavities of both β - and γ -CD were large enough to ingest roseofungin.

The proposed binding mode of roseofungin against α -CD revealed an affinity value of -41.80 kcal/mol. Although the good binding affinity, the binding mode was not good at all. The α -CD was impeded inside the cavity of roseofungin, forming many interactions. Roseofungin has different hydroxyl and carbonyl groups which made eight hydrogen bonds with the different hydroxy groups of glucose subunits (Figures 2–8).

Contrastively, roseofungin bonded to β -CD with a binding affinity value of -35.03 kcal/mol. The roseofungin was impeded inside the cavity of β -CD and made several important interactions. The different hydroxyls and carbonyls of roseofungin made five hydrogen bonds with the hydroxyls of glucose subunits (Figures 9–15).

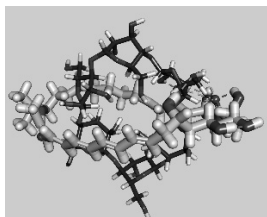


Figure 2. Docked pose of best ranked docking score of roseofungin (sticks) with α -CD (sticks) (front view)

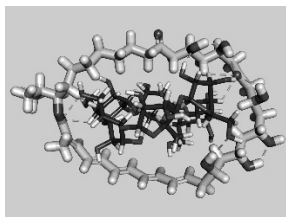


Figure 3. Docked pose of best ranked docking score of roseofungin (sticks) with α -CD (sticks) (top view)

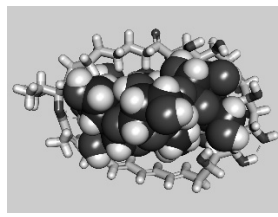


Figure 4. Docked pose of best ranked docking score of roseofungin (sticks) with α -CD (CPK) (top view)

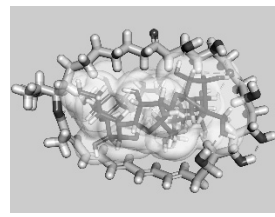


Figure 5. Surface view of α -CD inside the cavity of roseofungin (top view)

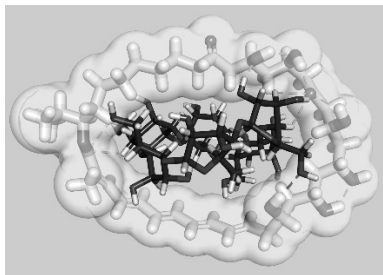


Figure 6. Surface view of α -CD inside the cavity of roseofungin (top view)

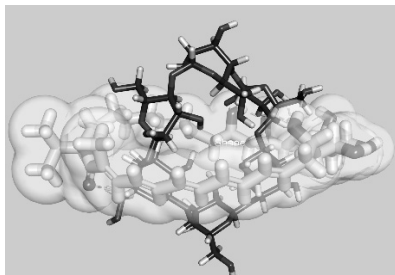


Figure 7. Surface view of α -CD inside the cavity of roseofungin (front view)

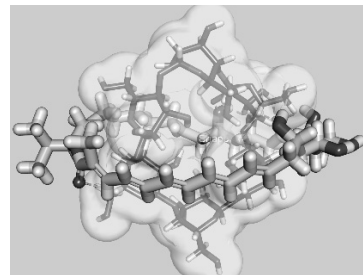


Figure 8. Surface view of α -CD inside the cavity of roseofungin (front view)

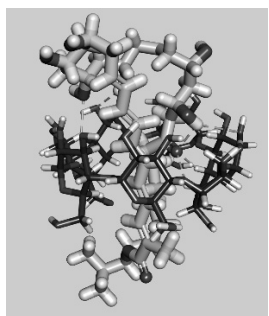


Figure 9. Docked pose of best ranked docking score of roseofungin (sticks) in the inner cavity of β -CD (sticks) (front view)



Figure 10. Docked pose of best ranked docking score of roseofungin (sticks) in the inner cavity of β -CD (sticks) (top view)

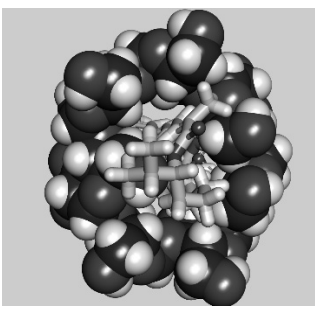


Figure 11. Docked pose of best ranked docking score of roseofungin (sticks) in the inner cavity of β -CD (CPK) (top view)

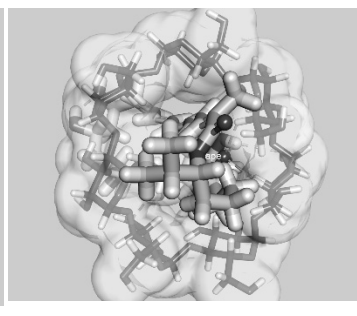


Figure 12. Surface view of roseofungin inside the cavity of β -CD (top view)



Figure 13. Surface view of roseofungin inside the cavity of β -CD (top view)

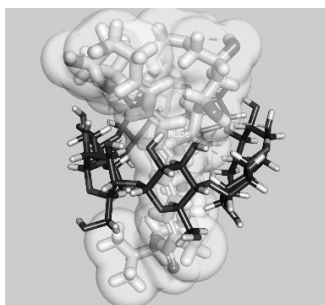


Figure 14. Surface view of roseofungin inside the cavity of β -CD (front view)

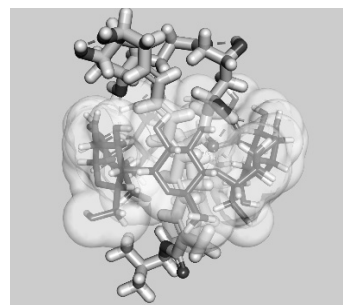


Figure 15. Surface view of roseofungin inside the cavity of β -CD (front view)

Fortunately, the expected binding mode of roseofungin against γ -CD was the best with an affinity value of -42.98 kcal/mol. The roseofungin was impeded perfectly inside the cavity of γ -CD, forming many essential interactions. Roseofungin's hydroxyls and carbonyls could form ten hydrogen bonds with the hydroxyls of glucose subunits (Figures 16–22).

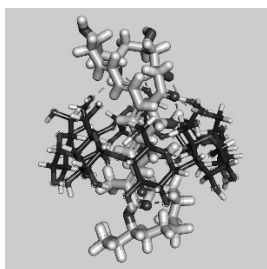


Figure 16. Docked pose of best ranked docking score of roseofungin (sticks) in the inner cavity of γ -CD (sticks) (front view)

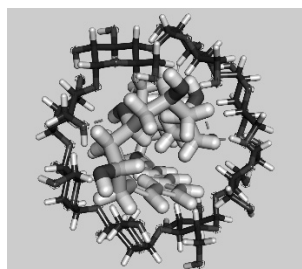


Figure 17. Docked pose of best ranked docking score of roseofungin (sticks) in the inner cavity of γ -CD (sticks) (top view)

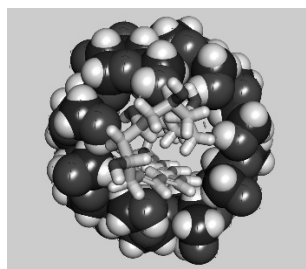


Figure 18. Docked pose of best ranked docking score of roseofungin (sticks) in the inner cavity of γ -CD (CPK) (top view)

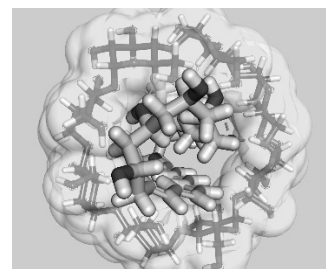


Figure 19. Surface view of roseofungin inside the cavity of γ -CD (top view)

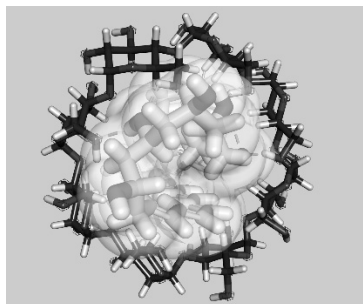


Figure 20. Surface view of roseofungin inside the cavity of γ -CD (top view)

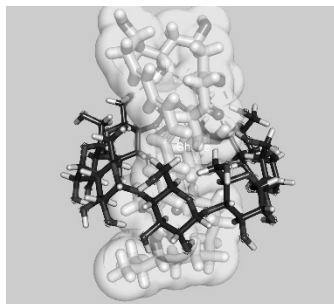


Figure 21. Surface view of roseofungin inside the cavity of γ -CD (front view)

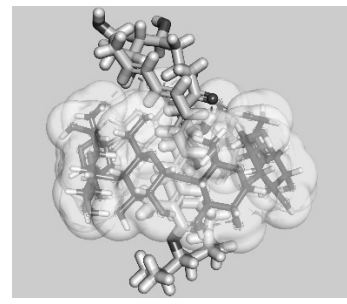


Figure 22. Surface view of roseofungin inside the cavity of γ -CD (front view)

This finding indicated that the binding of roseofungin with γ -CD is more advantageous.

Conclusions

Thus, roseofungin was isolated by chromatographic methods, also, its α -, β -, and γ -cyclodextrin inclusion complexes were obtained. The results of the docking studies indicate that the complex of roseofungin with γ -CD is more advantageous. As a result of studying the biological activity, it was found that roseofungin and its cyclodextrin complexes have weak antiradical activity and not toxic.

Acknowledgments

This research has been funded by the Science Committee of the Ministry of Education and Science of the Republic of Kazakhstan (Grant No. AP 05130941).

References

- 1 Осипова Н.И. Ветеринарно-санитарная оценка продуктов животного происхождения, содержащих антибиотики / Н.И. Осипова // Ветеринария. Реф. журн. — 2010. — № 3. — С. 503.
- 2 Саубенова М.Г. Достижения Института микробиологии и вирусологии КН МОН РК / М.Г. Саубенова // Вестн. КазНУ. Сер. биол. — 2012. — № 4. — С. 6–8.
- 3 Waksman S.A. The species concept in relation to the Actinomycetes / S.A. Waksman // The Actinomycetes. Classification, Identification, and Description of Genera and Species, Waverly Press, Inc., Baltimore. — 1961. — Vol. 2. — P. 15–18.

- 4 Шнейдер М.А. Вирусингибирующие свойства карбонил-конъюгированного пентаена розеофунгина / М.А. Шнейдер, Е.Б. Штильбанс, Л.А. Рачковская, Л.А. Ветлугина, Е.Т. Никитина // Антибиотики. — 2012. — Т. 29, № 5. — С. 344–349.
- 5 Ермакова О.С. Антивирусные свойства пентаенового антибиотика розеофунгина / О.С. Ермакова, В.П. Толмачева, С.В. Левандовская, С.С. Худякова, А.П. Богоявленский, Н.Р. Махмудова и др. // Клиническая микробиология и антимикробная химиотерапия. — 2001. — № 3. — С. 13.
- 6 Suleimenov Ye.M. Components of *Peusedanum morisonii* and their antimicrobial and cytotoxic activity / Ye.M. Suleimenov // Chemistry of Natural Compounds. — 2009. — Vol. 45, No. 5. — P. 710–711.
- 7 Sawant O. *In vitro* free radical scavenging activity of *Adiantum lunulatum* / O. Sawant, V.J. Kadam, R. Ghosh // Journal of Herbal Medicine and Toxicology. — 2009. — Vol. 3, No. 2. — P. 39–44.
- 8 Ibrahim M.K. Design, synthesis, molecular modeling and anti-hyperglycemic evaluation of novel quinoxaline derivatives as potential PPAR γ and SUR agonists / M.K. Ibrahim, et al. // Bioorganic & medicinal chemistry. — 2017. — Vol. 25, No. 4. — P. 1496–1513.
- 9 Eissa I.H. Design and discovery of novel quinoxaline derivatives as dual DNA intercalators and topoisomerase II inhibitors / I.H. Eissa, et al. // Anti-Cancer Agents in Medicinal Chemistry (Formerly Current Medicinal Chemistry-Anti-Cancer Agents). — 2018. — Vol. 18, No. 2. — P. 195–209.
- 10 Ibrahim M.K. Design, synthesis, molecular modeling and anti-hyperglycemic evaluation of quinazolin-4 (3H)-one derivatives as potential PPAR γ and SUR agonists / M.K. Ibrahim, et al. // Bioorganic & medicinal chemistry. — 2017. — Vol. 25, No. 17. — P. 4723–4744.
- 11 Roux B. CHARMM: the biomolecular simulation program / B. Roux, et al. // J Comput Chem. — 2009. — Vol. 30, No. 10. — P. 1545614 Capriotti.
- 12 Elmetwally S.A. Design, synthesis and anticancer evaluation of thieno[2,3-d]pyrimidine derivatives as dual EGFR/HER2 inhibitors and apoptosis inducers / S.A. Elmetwally, et al. // Bioorganic chemistry. — 2019. — Vol. 88. — P. 102944.
- 13 Mahdy H.A. Design, synthesis, molecular modeling, in vivo studies and anticancer evaluation of quinazolin-4(3H)-one derivatives as potential VEGFR-2 inhibitors and apoptosis inducers / H.A. Mahdy, et al. // Bioorganic Chemistry. — 2020. — Vol. 94. — P. 103422.
- 14 El-Naggar A.M. Design, eco-friendly synthesis, molecular modeling and anticancer evaluation of thiazol-5(4H)-ones as potential tubulin polymerization inhibitors targeting the colchicine binding site / A.M. El-Naggar, et al. // RSC Advances. — 2020. — Vol. 10, No. 5. — P. 2791–2811.
- 15 Li N. Screening of Some Sulfonamide and Sulfonylurea Derivatives as Anti-Alzheimer's Agents Targeting BACE1 and PPAR γ / N. Li, et al. // Journal of Chemistry. — 2020. — P. 19.
- 16 Li D.-D. Discovery of 6-substituted 4-anilinoquinazolines with dioxxygenated rings as novel EGFR tyrosine kinase inhibitors / D.-D. Li, et al. // Bioorganic & medicinal chemistry letters. — 2012. — Vol. 22, No. 18. — P. 5870–5875.
- 17 Sun J. Design, synthesis, biological evaluation, and molecular modeling study of 4-alkoxyquinazoline derivatives as potential VEGFR2 kinase inhibitors / J. Sun, et al. // Organic & biomolecular chemistry. — 2013. — Vol. 11, No. 44. — P. 7676–7686.
- 18 El-Gamal K.M. Synthesis, docking, QSAR, ADMET and antimicrobial evaluation of new quinoline-3-carbonitrile derivatives as potential DNA-gyrase inhibitors / K.M. El-Gamal, et al. // Journal of Molecular Structure. — 2018. — Vol. 1166. — P. 15–33.
- 19 Ibrahim, M., et al. (2018). Design, synthesis, molecular modeling and anti-proliferative evaluation of novel quinoxaline derivatives as potential DNA intercalators and topoisomerase II inhibitors / M. Ibrahim, et al. // European journal of medicinal chemistry. — Vol. 155. — P. 117–134.
- 20 Sadanov A.K. Isolation and characterization of "brown impurity" accompanying the antibiotic rozeofungin / A.K. Sadanov, A.S. Balgimbaeva, L.P. Trenzchnikova, V.E. Berezin // News of the national academy of sciences of the Republic of Kazakhstan. Series: biological and medical. — 2015. — No. 2. — С. 97–100.

Р.И. Жалмаханбетова, Е.М. Сүлеймен, И.Х. Әйса, А.М. Метуали, Ж.Б. Исакова,
Д.С. Балпанов, Г.Ғ. Сисенғалиева, Р.А. Ханнанов, Т.М. Сейлханов

Розеофунгинді оқшаулау және биологиялық бағалау және оның циклодекстринді енгізу кешендері

Розеофунгин полиен антибиотиктеріне жатады, ол осы топтың басқа полиендерімен салыстырғанда белсенді және аз уытты. Розеофунгин әр түрлі хроматографиялық әдістерді қолдана отырып *Actinomyces roseoflavus* var *Roseofungini*-ден оқшауланған және алғаш рет α -, β - және γ -циклодекстрин туындыларымен розеофунгиннің кешенді түзілуі жүргізілді. Алынған кешендердің байланыстыру заңдылықтары *in silico* молекулалық докинг әдістерін қолдана отырып зерттелді. Ең жақсы байланыстыру режимі $-42,98$ ккал/моль жақындық мәні бар γ -CD-ге қарсы розеофунгин үшін болды. Розеофунгинді α -CD-мен байланыстырудың ұсынылған әдісі жақындық мәні $-41,80$ ккал/моль болатын ерекше әрекеттесуді көрсетті. Сонымен қатар, розеофунгин β -CD-мен байланыстың жақындық мәні $-35,03$ ккал/моль арқылы байланысады. Розеофунгиннің және оның алынған α -, β -

және γ -циклодекстринді кешендерінің радикалға қарсы және цитоуыттылық белсенділігі анықталды. Радикалға қарсы белсенділік эталон ретінде бутилгидроксианизолды қолдану арқылы жүргізілді, ал цитоуыттылық белсенділік *Artemia salina* шаян тәрізділерді қолдану арқылы табылды. Биологиялық белсенділікті зерттеу нәтижесінде розеофунгиннің және оның кейбір кешендерінің әлсіз антирадикалды белсенділігі бар екендігі анықталды.

Кілт сөздер: розеофунгин, циклодекстрин, *in silico*, молекулалық докинг, комплекс түзілу, антирадикалды белсенділік, цитоуыттылық.

Р.И. Джалмаханбетова, Е.М. Сулеймен, И.Х. Эйса, А.М. Метуали, Ж.Б. Искакова,
Д.С. Балпанов, Г.Г. Сисенгалиева, Р.А. Ханнанов, Т.М. Сейлханов

Выделение и биологическая оценка розеофунгина и его циклодекстриновые комплексы включения

Розеофунгин относится к полиеновым антибиотикам и является более активным и менее токсичным по сравнению с другими полиенами этой группы. Розеофунгин был выделен из *Actinomyces roseoflavus* var. *Roseofungini* с использованием различных хроматографических методов. Авторами впервые было проведено комплексобразование розеофунгина с производными α -, β - и γ -циклодекстрина. Паттерны связывания полученных комплексов были изучены *in silico* с использованием методов молекулярного докинга. Наилучший режим связывания был для розеофунгина против γ -CD со значением аффинности $-42,98$ ккал/моль. Предложенный способ связывания розеофунгина с α -CD показал необычное взаимодействие со значением аффинности $-41,80$ ккал/моль. Кроме того, розеофунгин связывается с β CD со значением аффинности связывания $-35,03$ ккал/моль. Определена антирадикальная и цитотоксическая активность розеофунгина и полученных его α -, β - и γ -циклодекстриновых комплексов. Антирадикальную активность определяли используя в качестве эталона бутилгидроксианизол, а цитотоксическую активность — на ракообразных *Artemia salina*. В результате исследования биологической активности было установлено, что розеофунгин и некоторые его комплексы обладают слабой антирадикальной активностью.

Ключевые слова: розеофунгин, циклодекстрин, *in silico*, молекулярный докинг, комплексобразование, антирадикальная активность, цитотоксичность.

References

- Osipova, N.I. (2010). Veterinarno-sanitarnaia otsenka produktov zhivotnoho proiskhozhdeniia, sodержashchikh antibiotiki [Veterinary and sanitary assessment of animal products containing antibiotics]. *Veterinariia. Referativnyi zhurnal — Veterinary. Abstract journal*, 3, 503 [in Russian].
- Saubenova, M.G. (2012). Dostizheniia Instituta mikrobiologii i virusologii KN MON RK [Achievements of the Institute of Microbiology and Virology SC MES RK]. *Vestnik Kazakhskogo natsionalnogo universiteta. Seriya biologicheskaya — Bulletin of Kazakh National University. Biological series*, 4, 6–8 [in Russian].
- Waksman, S.A. (1961). The species concept in relation to the Actinomycetes. *The Actinomycetes. Classification, Identification, and Description of Genera and Species*, (Vol. 2). Waverly Press, Inc., Baltimore.
- Shneider, M.A. (2012). Virusinhibiruiushchie svoistva karbonil-koniuhirovannogo pentaena rozeofunhina [Verosimilitudes properties of the carbonyl-conjugated pentaen of roseofungin]. *Antibiotiki — Antibiotics*, 29(5), 344–349 [in Russian].
- Ermakova, O.S., Tolmacheva, V.P., Levandovskaya, S.V., Hudyakova, S.S., Bogoyavlenskij, A.P., & Mahmudova, N.R., et al. (2001). Antivirusnye svoistva pentaenovogo antibiotika rozeofunhina [Antiviral properties of the pentaenotic roseofungin]. *Klinicheskaya mikrobiologiya i antimikrobnaya khimioterapiya — Clinical Microbiology and antimicrobial chemotherapy*, 3, 13 [in Russian].
- Suleimenov, Ye.M. (2009). Components of *Peusedanum morisonii* and their antimicrobial and cytotoxic activity. *Chemistry of Natural Compounds*, 45(5), 710–711.
- Sawant, O., Kadam, V.J., & Ghosh, R. (2009). *In vitro* free radical scavenging activity of *Adiantum lunulatum*. *Journal of Herbal Medicine and Toxicology*, 3(2), 39–44.
- Ibrahim, M.K., et al. (2017). Design, synthesis, molecular modeling and anti-hyperglycemic evaluation of novel quinoxaline derivatives as potential PPAR γ and SUR agonists. *Bioorganic & medicinal chemistry*, 25(4), 1496–1513.
- Eissa, I.H., et al. (2018). Design and discovery of novel quinoxaline derivatives as dual DNA intercalators and topoisomerase II inhibitors. *Anti-Cancer Agents in Medicinal Chemistry (Formerly Current Medicinal Chemistry-Anti-Cancer Agents)*, 18(2), 195–209.
- Ibrahim, M.K., et al. (2017). Design, synthesis, molecular modeling and anti-hyperglycemic evaluation of quinazolin-4(3H)-one derivatives as potential PPAR γ and SUR agonists. *Bioorganic & medicinal chemistry*, 25(17), 4723–4744.

- 11 Roux, B., et al. (2009). CHARMM: the biomolecular simulation program. *J Comput Chem*, 30(10), 1545614 Capriotti.
- 12 Elmetwally, S.A., et al. (2019). Design, synthesis and anticancer evaluation of thieno[2,3-d]pyrimidine derivatives as dual EGFR/HER2 inhibitors and apoptosis inducers. *Bioorganic chemistry*, 88, 102944.
- 13 Mahdy, H.A., et al. (2020). Design, synthesis, molecular modeling, in vivo studies and anticancer evaluation of quinazolin-4(3H)-one derivatives as potential VEGFR-2 inhibitors and apoptosis inducers. *Bioorganic Chemistry*, 94, 103422.
- 14 El-Naggar, A.M., et al. (2020). Design, eco-friendly synthesis, molecular modeling and anticancer evaluation of thiazol-5(4H)-ones as potential tubulin polymerization inhibitors targeting the colchicine binding site. *RSC Advances*, 10(5), 2791–2811.
- 15 Li, N., et al. (2020). Screening of Some Sulfonamide and Sulfonylurea Derivatives as Anti-Alzheimer's Agents Targeting BACE1 and PPAR γ . *Journal of Chemistry*, 19.
- 16 Li, D.-D., et al. (2012). Discovery of 6-substituted 4-anilinoquinazolines with dioxxygenated rings as novel EGFR tyrosine kinase inhibitors. *Bioorganic & medicinal chemistry letters*, 22(18), 5870–5875.
- 17 Sun, J., et al. (2013). Design, synthesis, biological evaluation, and molecular modeling study of 4-alkoxyquinazoline derivatives as potential VEGFR2 kinase inhibitors. *Organic & biomolecular chemistry*, 11(44), 7676–7686.
- 18 El-Gamal, K.M., et al. (2018). Synthesis, docking, QSAR, ADMET and antimicrobial evaluation of new quinoline-3-carbonitrile derivatives as potential DNA-gyrase inhibitors. *Journal of Molecular Structure*, 1166, 15–33.
- 19 Ibrahim, M., et al. (2018). Design, synthesis, molecular modeling and anti-proliferative evaluation of novel quinoxaline derivatives as potential DNA intercalators and topoisomerase II inhibitors. *European journal of medicinal chemistry*, 155, 117–134.
- 20 Sadanov, A.K., Balgimbaeva, A.S., Trenozhnikova, L.P., & Berezin, V.E. (2015). Isolation and characterization of "brown impurity" accompanying the antibiotic rozeofungin. *News of the national academy of sciences of the Republic of Kazakhstan. Series: biological and medical*, 2, 97–100.

Information about authors

Jalmakhanbetova, Roza Ilemisovna — Doctor of chemical sciences, Kazakh University of Technology and Business, Nur-Sultan, K. Mukhamedkhanov Str., 37A, Kazakhstan; e-mail: rozadichem@mail.ru, ORCID: 0000-0001-9937-275X.

Suleimen, Yerlan Melsuly — Candidate of chemical sciences, PhD, 1) Senior researcher of the laboratory of Engineering Profile of NMR Spectroscopy, Sh. Ualikhanov Kokshetau university, Kokshetau, Abay street, 76, 020000, Kazakhstan; 2) Main Scientific Secretary of Republican collection of microorganisms, Nur-Sultan, Sh. Ualikhanov 13/1, 010000, Kazakhstan; e-mail: syerlan75@yandex.kz, ORCID 0000-0002-5959-4013.

Eissa, Ibrahim Hasan — Associate professor, Pharmaceutical Medicinal Chemistry & Drug Design Department, Faculty of Pharmacy (Boys), Al-Azhar University, Cairo11884, Egypt; e-mail: ibrahimeissa@azhar.edu.eg, ORCID 0000-0002-6955-2263.

Metwaly, Ahmed Mohamed — Associate professor, Pharmacognosy Department, Faculty of Pharmacy (Boys), Al-Azhar University, Cairo11884, Egypt; e-mail: ametwaly@azhar.edu.eg, ORCID 0000-0001-8566-1980.

Iskakova, Zhanar Baktybaevna — Candidate of chemical sciences, Kazakh University of Technology and Business, Nur-Sultan, K. Mukhamedkhanov Str., 37A, Kazakhstan; e-mail: zhanariskakova@mail.ru; <https://orcid.org/0000-0002-3540-8263>.

Balpanov, Darhan Serikovich — Candidate of chemical sciences, research associate of "Biolife" Ltd, Stepnogorsk, 5 district, 8–80, Kazakhstan; e-mail: balpan@mail.ru.

Sissengaliyeva, Gulsana Galimzhankyzy — L.N. Gumilyov Eurasian National University, Satpaev street, 2, 010000, Nur-Sultan, Kazakhstan; e-mail: sissengaliyevag@gmail.com, ORCID: 0000-0002-90-1704.

Khannanov, Rinat Ashatovich — master's degree, Director of "Biolife" Ltd, Stepnogorsk, 5 district, 8–80, Kazakhstan; e-mail: khanrinat@yandex.ru, ORCID ID 0000-0001-5085-7596.

Seilkhanov, Tulegen Muratovich — Candidate of chemical science, full professor, Head of the laboratory of Engineering Profile of NMR Spectroscopy, Sh. Ualikhanov Kokshetau university, Kokshetau, Abay street, 76, 020000, Kazakhstan, e-mail: tseilkhanov@mail.ru, ORCID ID 0000-0003-0079-4755.

K.M. Turdybekov^{1*}, Zh.S. Nurmaganbetov², D.M. Turdybekov³,
G.K. Mukusheva¹, Yu.V. Gatilov⁴

¹Karagandy University of the name of academician E.A. Buketov, Kazakhstan;

²Karaganda Medical University, Kazakhstan;

³Karaganda Technical University, Kazakhstan

⁴N.N. Vorozhtsov Novosibirsk Institute of Organic Chemistry, Russia

(Corresponding author's e-mail: xray-phyto@yandex.kz)

Synthesis, molecular and crystalline structure of 8-formylharmine

For the first time, synthesis of 8-formylharmine by the Vilsmeier reaction was carried out. 8-Formylharmine was obtained by treating alkaloid harmine with dichloromethoxymethane in the presence of SnCl₄. The yield of the target product was 64 %. The structure of the obtained compound was established on the basis of ¹H and ¹³C NMR spectroscopy as well as mass-spectrometry data. The crystalline structure of 8-formylharmine was determined by X-ray diffraction. It has been shown that the replacement of the hydrogen atom in the harmine molecule with a formyl group occurs at the C8 atom. It was revealed that the methoxy group at the C7 atom changes its orientation to the opposite one as compared to the orientation in the harmine molecule and its salts due to the mutual Van der Waals repulsion of the methoxy and formyl groups. A weak intramolecular hydrogen bond was found in the crystal between the O2 atom of the formyl group and the hydrogen atom of the secondary amino group. It was shown that molecules in the crystal form an intermolecular hydrogen bond between the same atoms (O2 and HN9A), as a result of which dimers are formed.

Keywords: NMR spectroscopy, mass- spectrometry, X-ray diffraction analysis, crystal structure, hydrogen bond, harmine, 8-formylharmine, harmine derivatives.

Introduction

β-Carboline fragments of heterocycles of natural origin are part of many indole alkaloids, showing valuable pharmacological properties. Known examples of compounds comprising β-carboline fragment and exhibiting antimalarial and cytotoxic effect on certain types of tumor cells, as well as of great interest as promising compounds that are leaders in the search for new physiologically active agents to treat diseases of the central nervous system and cardiovascular system [1, 2].

According to the literature, among indole alkaloids, β-carbolines are much less studied, and some of them are unknown at all. At the same time, compounds of this class have a significant potential for medical chemistry and pharmacology, since it can be assumed that they have a combination of biological properties characteristic of isomeric carbolins.

The alkaloid of the β-carboline type harmine (**1**) is contained in the plant *Peganum harmala* L., which is widespread in the Republic of Kazakhstan. Harmine has a diverse biological activity: antitumor [3], antiviral [4] and anti-inflammatory [5]. Harmine has an effect on the central nervous system, exhibiting neuroprotective activity in neurological diseases [6], and inhibits monoamine oxidase A [7].

In continuation of our studies on the conversions of the harmine alkaloid, the synthesis of a harmine derivative containing a different substituent at position C8 was carried out [8]. It should be noted that modifications at the C8 atom are of interest in connection with the valuable antitumor and antimicrobial activity of synthetic and natural 8-halogen-substituted [9] and 8-methylamino-substituted [10] β-carbolines described in the literature.

Experimental

The ¹H and ¹³C NMR spectra of compound (**2**), dissolved in CDCl₃ + CD₃OD, were recorded on a Bruker AV-600 spectrometer (operating frequencies 600.30 (¹H) and 150.96 MHz (¹³C) relative to SiMe₄. Various types of proton-proton and carbon-proton shear correlation spectroscopy (COSY, COXH, COLOC) were used for the assignment of signals in the NMR spectra. Multiplicity of signals in ¹³C NMR spectra was determined by recording the spectra in J-modulation mode. High-resolution mass spectra were recorded on a

*Corresponding author.

DFS Thermo Scientific mass spectrometer, evaporator temperature 150–240 °C, ionization of ES (70 eV). Elemental analysis was performed on the Eurovector 3000 analyzer.

Melting point was determined on an SMF-38 heating table. The reaction progress was monitored by TLC on Silufol UV-254 plates. The spots were developed by spraying the plates with a 10 % aqueous solution of H₂SO₄, followed by heating to 100 °C or by irradiation with ultraviolet radiation. The reaction product was isolated by column chromatography on silica gel ("Acros", 0.035–0.070 mm, pore diameter 6 nm), eluent: chloroform-ethyl acetate.

8-Formylharmine (2). To a solution of 1.02 g (4.8 mmol) of harmine (**1**) in 40 ml of freshly distilled CHCl₃ cooled to 0 °C, 1.21 g (10.5 mmol) of Cl₂CHOCH₃ and 0.81 g (3.1 mmol) of SnCl₄ were added with stirring. The reaction mixture was stirred for 2 hours at 0 °C, then 20 hours at room temperature, and then poured onto ice. The mixture was treated with 5 % aqueous ammonia (to pH 9) and extracted with chloroform (3×30 ml). The organic extracts were combined, washed with saturated NaCl (15 ml) and dried over MgSO₄. The desiccant is filtered off, the solvent is evaporated off under reduced pressure. The residue was chromatographed on an alumina column (eluent is chloroform — EtOAc, gradient from 100:1 to 10:1). The fraction containing the product was recrystallized from a mixture of chloroform-petroleum ether, 5:1. Yield is 312 mg (64 %), yellow fine-crystalline powder, mp. 112–115 °C.

NMR spectrum ¹H (CDCl₃+CD₃OD), δ, ppm. (*J*, Γ): 2.71 (3H, s, CH₃ at C-1); 3.95 (3H, s, OCH₃); 6.79 (1H, d, *J* = 8.7, 6-CH); 7.62 (1H, d, *J* = 5.5, 4-CH); 8.13 (1H, d, *J* = 8.7, 5-CH); 8.16 (1H, d, *J* = 5.5, 3-CH); 10.75 (1H, br.s, CHO). NMR spectrum ¹³C, (CDCl₃+CD₃OD), δ, ppm.: 19.25 (1-CH₃); 56.17 (OCH₃); 103.70 (C-6); 108.55 (C-8); 112.12 (C-4); 116.24 (C-4a); 127.42 (C-4b); 130.25 (C-5); 134.62 (C-9a); 140.06 (C-3); 141.52, 141.78 (C-1,8a); 163.50 (C-7); 190.58 (C=O). Mass spectrum, *m/z* (*I*_{OTH}, %): 241 (14), 240 (100), 239 (7), 225 (6), 194 (15), 169 (18), 18 (12). Found, *m/z*: 240.0890 [M]⁺. C₁₄H₁₂N₂O₂. Calculated, *m/z*: 240.0893. Found, %: C 69.71; H 5.12; N 11.49. C₁₄H₁₂N₂O₂. Calculated, %: C 69.99; H 5.03; N 11.66.

X-ray analysis of compound (2). The cell parameters and the intensity of 10235 reflections (2001 independent, *R*_{int}=0.0601) were measured on a diffractometer "Bruker Kappa APEX2 CCD" (MoK_α, graphite monochromator, φ, θ-scan, 1.81 ≤ θ ≤ 25.05) at 296 K. The crystals are monoclinic, *a*=11.539(2), *b*=5.0197(9), *c*=20.198(4) Å, β=103.077(8)°, *V*=1139.6(4) Å³, *Z*=4 (C₁₄H₁₂N₂O₂), The space group *P*2₁/*c*, *d*_{calc}=1.400 g/cm³, μ=0.096 mm⁻¹. The initial array of the measured intensities was processed and absorption was taken into account using the SAINT [11] and SADABS [12] programs (multi-scan, *T*_{min} = 0.9700, *T*_{max} = 0.9986).

The structure of compound (**2**) is deciphered by a direct method. The positions of non-hydrogen atoms are refined in the anisotropic approximation by the full-matrix least squares. Hydrogen atom at N9A is revealed from the difference synthesis and its position is refined in the isotropic approximation. The remaining hydrogen atoms were placed in geometrically calculated positions and positions were refined in an isotropic approximation with fixed positional and thermal parameters (the "rider" model). The structure is deciphered and refined by the complex of programs SHELXS [13] and SHELXL-2018/3 [14]. 1319 independent reflections used for calculations with *I* ≥ 2σ(*I*) (*R*_{int} = 0.0601), the number of parameters to be refined 169. The final divergence factors *R*₁=0.0428, *wR*₂=0.1100 (for reflections with *I* ≥ 2σ(*I*)), *R*₁=0.0880, *wR*₂=0.1557 (for all reflections), *Goof*=1.049. Peaks of residual density: Δρ=0.283 and -0.283 e/Å³. The CIF file containing the complete information on the structure examined is deposited in the Cambridge Center for Crystal Structural Data (CCDC), under number 1854103. The atomic coordinates are shown in Table 1.

Table 1

The coordinates of the atoms in the fractions of the cell (×10⁴, for H ×10³) and isotropic thermal parameters (Å², ×10³) in the structure (**2**)

| Atom | <i>x</i> | <i>y</i> | <i>z</i> | <i>U</i> _{эКВ.} |
|------|----------|----------|----------|--------------------------|
| 1 | 2 | 3 | 4 | 5 |
| O1 | 13413(2) | 655(4) | 4336(1) | 52(1) |
| O2 | 11107(2) | -3934(4) | 4993(1) | 48(1) |
| C1 | 7032(2) | -1004(5) | 3561(1) | 38(1) |
| N2 | 6199(2) | 286(4) | 3097(1) | 46(1) |
| C3 | 6542(3) | 2191(6) | 2713(2) | 49(1) |
| C4 | 7693(2) | 2979(5) | 2763(1) | 45(1) |

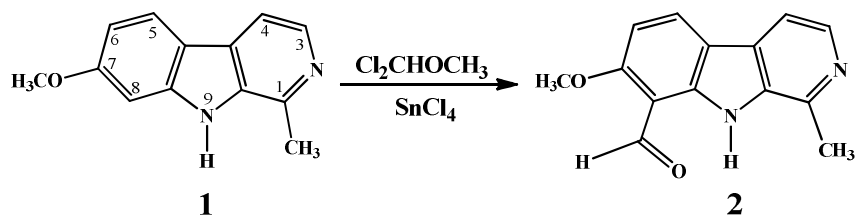
Continuation of Table 1

| 1 | 2 | 3 | 4 | 5 |
|-----|----------|----------|---------|-------|
| C4A | 8574(2) | 1681(5) | 3242(1) | 34(1) |
| C4B | 9851(2) | 1876(5) | 3447(1) | 34(1) |
| C5 | 10703(2) | 3441(5) | 3251(1) | 41(1) |
| C6 | 11894(2) | 3086(5) | 3538(1) | 41(1) |
| C7 | 12252(2) | 1134(5) | 4035(1) | 37(1) |
| C8 | 11423(2) | -494(5) | 4260(1) | 34(1) |
| C9 | 10215(2) | -94(4) | 3956(1) | 31(1) |
| N9A | 9236(2) | -1389(4) | 4064(1) | 35(1) |
| C9B | 8224(2) | -338(5) | 3632(1) | 33(1) |
| C10 | 6617(2) | -3085(6) | 3982(2) | 50(1) |
| C11 | 14304(3) | 2328(7) | 4168(2) | 68(1) |
| C12 | 11791(2) | -2498(5) | 4783(1) | 41(1) |
| H9A | 922(2) | -258(6) | 431(2) | 49(1) |

Results and Discussions

As a continuation of our research on the transformations of the harmine alkaloid (**1**) we synthesized a harmine derivative containing a different substituent in the C-8 position.

The introduction of a formyl group into the harmine (**1**) molecule by the Wilsmeier reaction leads to the formation of 8-formylharmine (**2**) with a yield of 64 %. We have proposed a method of producing 8-formylharmine when interacting with harmine dichloromethoxymethane in the presence SnCl_4 .



The structure of the obtained compound (**2**) was established on the basis of ^1H and ^{13}C NMR spectroscopy and mass-spectrometry. A peak with a molecular weight of 240.0890 Da was found in the mass-spectrum of the obtained product, corresponding to the molecular ion $\text{C}_{14}\text{H}_{12}\text{N}_2\text{O}_2^+$ (calculated: 240.0893 Da). When comparing the NMR spectra of compound (**2**) with the spectra of the original molecule (**1**), new signals were detected. The proton signal at C8 disappeared in the ^1H NMR spectrum and appeared at 10.75 ppm. (1H, br.s), corresponding to the proton of the group $\text{C}(\text{H})=\text{O}$, and in the ^{13}C NMR spectrum a signal of 190.58 ppm corresponding to the carbon of the aldehyde group ($\text{C}=\text{O}$). The full assignment of NMR signals is given in the experimental part.

In order to confirm the place of replacement of the hydrogen atom by the formyl group and to continue studying the crystal structures of alkaloids, the structure of 8-formylharmine was studied (**2**), a general view of which is shown in Figure 1.

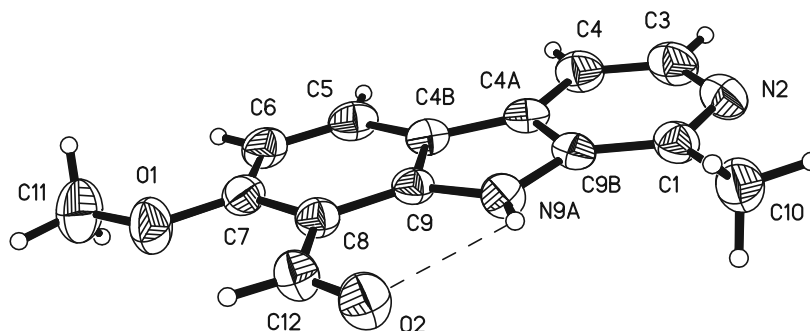


Figure 1. The structure of 8-formylharmine (thermal vibration ellipsoids shown with a probability of 50 %). The dashed line shows the hydrogen bond

From the data obtained it follows that bond lengths (Table 2) and bond angles (Table 3) in compounds (2) are close to usual [15].

Table 2

Bond lengths (d, Å) in the structure (2)

| Bond | d | Bond | d |
|---------|----------|---------|----------|
| O1-C7 | 1.362(3) | C4A-C4B | 1.441(4) |
| O1-C11 | 1.427(3) | C4B-C5 | 1.385(3) |
| O2-C12 | 1.213(3) | C4B-C9 | 1.420(3) |
| C1-N2 | 1.346(3) | C5-C6 | 1.376(4) |
| C1-C9B | 1.391(4) | C6-C7 | 1.397(4) |
| C1-C10 | 1.492(4) | C7-C8 | 1.409(3) |
| N2-C3 | 1.346(4) | C8-C9 | 1.405(3) |
| C3-C4 | 1.367(4) | C8-C12 | 1.452(4) |
| C4-C4A | 1.396(4) | C9-N9A | 1.362(3) |
| C4A-C9B | 1.399(3) | N9A-C9B | 1.394(3) |

Table 3

Valent angles (ω , deg.) in the structure (2)

| Angle | ω | Angle | ω |
|-------------|----------|-------------|----------|
| C7-O1-C11 | 118.6(2) | O1-C7-C6 | 123.1(2) |
| N2-C1-C9B | 119.3(2) | O1-C7-C8 | 115.1(2) |
| N2-C1-C10 | 117.5(2) | C6-C7-C8 | 121.8(2) |
| C9B-C1-C10 | 123.1(2) | C9-C8-C7 | 117.1(2) |
| C3-N2-C1 | 119.1(2) | C9-C8-C12 | 121.0(2) |
| N2-C3-C4 | 124.8(3) | C7-C8-C12 | 121.9(2) |
| C3-C4-C4A | 117.4(3) | N9A-C9-C8 | 129.7(2) |
| C4-C4A-C9B | 118.0(2) | N9A-C9-C4B | 109.2(2) |
| C4-C4A-C4B | 134.8(2) | C8-C9-C4B | 121.1(2) |
| C9B-C4A-C4B | 107.1(2) | C9-N9A-C9B | 109.1(2) |
| C5-C4B-C9 | 119.3(2) | C1-C9B-N9A | 130.0(2) |
| C5-C4B-C4A | 134.6(2) | C1-C9B-C4A | 121.4(2) |
| C9-C4B-C4A | 106.1(2) | N9A-C9B-C4A | 108.6(2) |
| C6-C5-C4B | 120.8(2) | O2-C12-C8 | 124.0(2) |
| C5-C6-C7 | 119.8(2) | | |

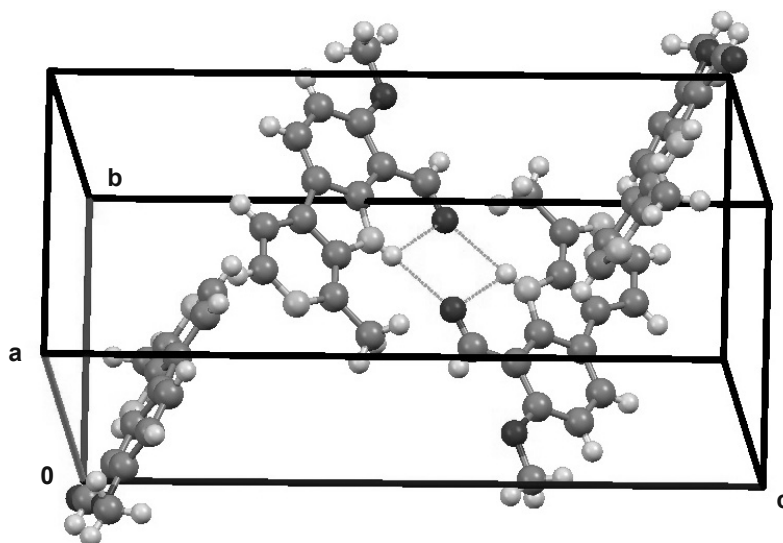


Figure 2. Packing of molecules (2) in a crystal lattice. Dotted lines show hydrogen bond

Atoms of the main frame are in the same plane with an accuracy of $\pm 0.01 \text{ \AA}$. The methoxy group is located almost in its plane (torsion angle C6C7O1C11 = 3.9°), however, it is turned in the opposite direction, and the difference from the turn in the harmine molecule [16] is in the crystal hydrate of harmine hydrochloride [17] and harmine sulfate [18] (torsion angle C6C7O1C11 = 179.9° , -178.1° and $176.4(-177.4)^\circ$ (two crystallographically independent molecules, respectively).

In the crystal, molecules (**2**) are connected by a weak intramolecular hydrogen bond N9A-H (x, y, z)... O2 (x, y, z) (distances N-H 0.78 (3) \AA , N... O 2.824 (3) \AA , H... O 2.40 (3) \AA , angle N-H... O 116 (3) $^\circ$). In addition, the intermolecular hydrogen bond N9A-H (x, y, z)... O2 (2-x, -1-y, 1-z) (distances N... O 3.105 (3) \AA , H... O 2.33 (3) \AA , angle N-H...O 172 (3) $^\circ$), as a result of which the molecules form dimers (Figure. 2).

Conclusions

As a result of synthesis and study of the spatial structure of 8-formylharmine:

- the place of substitution of the hydrogen atom in the harmine molecule with the formyl group was determined;
- it was revealed that the methoxy group at the C7 atom changes its spatial orientation to the opposite in comparison with the orientation in harmine and its salts;
- a weak hydrogen bond was detected between the O2 atom of the formyl group and the hydrogen atom of the secondary amino group;
- it was shown that in a crystal the molecules form an intermolecular hydrogen bond between the same atoms, as a result of which they form dimers.

References

- 1 Moloudizargari M. Pharmacological and Therapeutic effects of Peganum harmala and its main alkaloids / M. Moloudizargari, P. Mikaili, S. Aghajanshakeri, M.H. Asghari, J. Shayegh // *Pharmacognosy Rev.* — 2013. — Vol. 7. — P. 199–205.
- 2 Patel K. A review on medicinal importance, pharmacological activity and bioanalytical aspects of β -carboline alkaloid "Harmine" / K. Patel, M. Gadewar, R. Tripathi, S.K. Prasad, D.K. Patel // *Asian Pac. J. Trop. Biomed.* — 2012. — Vol. 2. — P. 660–665.
- 3 Ishida J. Antitumor Agents 201 Cytotoxicity of Harmine and β -Carboline Analogs / J. Ishida, H.K. Wang, K.F. Bastow, C.Q. Hu, K.H. Lee // *Bioorg. Med. Chem. Lett.* — 1999. — Vol. 9. — P. 3319–3324.
- 4 Chen D. Harmine blocks herpes simplex virus infection through downregulating cellular NF-kappaB and MAPK pathways induced by oxidative stress / D. Chen, A. Su, Y. Fu, X. Wang, X. Lu, W. Xu, S. Xu, H. Wang, Z. Wu // *Antivir. Res.* — 2015. — Vol. 123. — P. 27–38.
- 5 Zhao F. In vitro anti-inflammatory effects of β -carboline alkaloids, isolated from *Picrasma quassioides*, through inhibition of the iNOS pathway / F. Zhao, Z. Gao, W. Jiao, L. Chen, L. Chen, X. Yao // *Planta Med.* — 2012. — Vol. 78. — P. 1906–1911.
- 6 Sun P. Harmine mediated neuroprotection via evaluation of glutamate transporter 1 in a rat model of global cerebral ischemia / P. Sun, S. Zhang, Y. Li, L. Wang // *Neurosci. Lett.* — 2014. — Vol. 583. — P. 32–36.
- 7 Kim H. Inhibition of monoamine oxidase A by β -Carboline derivatives / H. Kim, S.O. Sablin, R.R. Ramsay // *Arch. Biochem. Biophys.* — 1997. — Vol. 337. — P. 137–142.
- 8 Cao R. Synthesis and structure-activity relationships of asymmetric dimeric β -carboline derivatives as potential antitumor agents / R. Cao, W. Fan, L. Guo, Q. Ma, G. Zhang, J. Li, X. Chen, Z. Ren, L. Qiu // *Eur. J. Med. Chem.* — 2013. — Vol. 60. — P. 10–22.
- 9 Zhang X.F. Synthesis and mechanisms of action of novel harmine derivatives as potential antitumor agents / X.F. Zhang, R. Sun, Y. Jia, Q. Chen, R.F. Tu, K. Li, X.D. Zhang, R.L. Du, R. Cao // *Sci. Rep.* — 2016. — Vol. 6. — P. 33204–33209.
- 10 Nurmaganbetov Zh.S. Synthesis of substituted indolizino[8,7-b]indoles from harmine and their biological activity / Zh.S. Nurmaganbetov, E.E. Shultz, S.V. Chernov, A.Zh. Turmukhambetov, R.B. Seydakhmetova, M.M. Shakirov, G.A. Tolstikov, S.M. Adekenov // *Chem. Heterocycl. Comp.* — 2011. — Vol. 46. — P. 1494–1499.
- 11 Bruker. SAINT. Bruker AXS Inc., Madison, Wisconsin, USA, 2015.
- 12 Bruker. SADABS. Bruker AXS Inc., Madison, Wisconsin, USA, 2015.
- 13 Sheldrick G.M. Crystal structure solution with SHELXS / G.M. Sheldrick // *Acta Crystollogr. Sect. A.* — 2008. — Vol. 64. — P. 112–122.
- 14 Sheldrick G.M. Crystal structure refinement with SHELXL / G.M. Sheldrick // *Acta Crystollogr. Sect. C.* — 2015. — Vol. 71. — P. 3–8.
- 15 Allen F.H. Tables of bond lengths determined by X-ray and neutron diffraction / F.H. Allen, O. Kennard, D.G. Watson, L. Brammer, A.G. Orpen, R. Taylor // *J. Chem. Soc. Perkin. Trans. 2.* — 1987. — P. 1–19.

16 Maulik P.R. Harmine (7-methoxy-1-methyl-9H-pyrido[3,4-b]indole) / P.R. Maulik, B.S. Basak // Cryst. Struct. Commun. — 1982. — Vol. 11. — P. 19–24.

17 Ferretti V. Structural features controlling the binding of beta-carbolines to the benzodiazepine receptor / V. Ferretti, P. Gilli, P.A. Borea // Acta Crystallogr. Sect. B: Struct. Sci. — 2004. — Vol. 60. — P. 481–489.

18 Turmukhambetov A.Zh. Synthesis of quaternary salts of *Peganum harmala* alkaloids / A.Zh. Turmukhambetov, M.T. Agedilova, Zh.S. Nurmaganbetov, A.V. Kazantsev, S.M. Adekenov, E.E. Shults, M.M. Shakirov, I.Yu. Bagryanskaya // Chem. Natur. Comp. — 2009. — Vol. 45. — P. 601–603.

Қ.М. Тұрдыбеков, Ж.С. Нұрмағанбетов, Д.М. Тұрдыбеков,
Г.К. Мұқышева, Ю.В. Гатилов

8-Формилгарминнің синтезі, молекулярлық және кристалдық құрылымы

Алғаш рет Вильсмайер реакциясы арқылы 8-формилгарминнің синтезі жүзеге асырылды. 8-Формилгармин туындысы гармин алкалоидын SnCl_4 қатысында дихлорметоксиметанмен өңдеу арқылы синтезделді. Мақсатты өнімнің шығымы 64 % құрайды. Синтезделген қосылыстың құрылымы ^1H , ^{13}C ЯМР спектроскопия және масс-спектрометрия әдістерімен дәлелденді. 8-Формилгарминнің кристалдық құрылымы рентген сәулелерінің дифракциясымен анықталды. Молекуладағы сутегі атомын гарминнің формил тобына алмастыру С8 атомында жүретіні көрсетілген. С7 атомындағы метокси тобы кеңістіктегі бағдарлануын, гармин мен оның тұздарындағы бағытқа қарағанда керісінше өзгертетінін байқатты. Бұл метокси- және формильді топтардың өзара ван-дер-ваальстік ығысуларынан пайда болады. Формил тобының О2 атомы мен екіншілік амин тобының сутегі атомы арасындағы кристалда ішкімолекулалық әлсіз сутектік байланысы байқалады. Кристалда молекулалар бірдей атомдар арасында молекуларалық сутектік байланысын (О2 и НН9А) құрайтыны және нәтижесінде олардың димер түзетіндігі көрсетілген.

Кілт сөздер: ЯМР-спектроскопия, масс-спектрометрия, рентгенқұрылымдық талдау, кристалдық құрылым, сутектік байланыс, гармин, 8-формилгармин, гарминнің туындысы.

К.М. Турдыбеков, Ж.С. Нурмағанбетов, Д.М. Турдыбеков,
Г.К. Мукушева, Ю.В. Гатилов

Синтез, молекулярная и кристаллическая структура 8-формилгармина

Впервые осуществлен синтез 8-формилгармина по реакции Вильсмайера. 8-Формилгармин получили обработкой алкалоида гармина дихлорметоксиметаном в присутствии SnCl_4 . Выход целевого продукта составил 64 %. Строение полученного соединения установили на основании спектров ^1H и ^{13}C ЯМР-спектроскопии, а также данных масс-спектрометрии. Кристаллическую структуру 8-формилгармина определяли с помощью дифракции рентгеновских лучей. Показано, что замещение атома водорода в молекуле гармина на формильную группу происходит при атоме С8. Выявлено, что метокси-группа при атоме С7 меняет свою ориентацию на противоположную по сравнению с ориентацией в молекуле гармина и его солях. Это происходит вследствие взаимного ван-дер-ваальсового отталкивания метокси- и формильной групп. В кристалле обнаружена слабая внутримолекулярная водородная связь между атомом О2 формильной группы и атомом водорода вторичной аминогруппы. Показано, что в кристалле молекулы образуют межмолекулярную водородную связь между теми же атомами (О2 и НН9А), в результате чего образуются димеры.

Ключевые слова: ЯМР-спектроскопия, масс-спектрометрия, рентгеноструктурный анализ, кристаллическая структура, водородная связь, гармин, 8-формилгармин, производное гармина.

References

- 1 Moloudizargari, M., Mikaili, P., Aghajanshakeri, S., Asghari, M.H., & Shayegh, J. (2013). Pharmacological and Therapeutic effects of *Peganum harmala* and its main alkaloids. *Pharmacognosy Rev.*, 7, 199–205.
- 2 Patel, K., Gadewar, M., Tripathi, R., Prasad, S.K., & Patel, D.K. (2012). A review on medicinal importance, pharmacological activity and bioanalytical aspects of β -carboline alkaloid "Harmine". *Asian Pac. J. Trop. Biomed.*, 2, 660–665.
- 3 Ishida, J., Wang, H.K., Bastow, K.F., Hu, C.Q., & Lee, K.H. (1999). Antitumor Agents 201 Cytotoxicity of Harmine and β -Carboline Analogs. *Bioorg. Med. Chem. Lett.*, 9, 3319–3324.

- 4 Chen, D., Su, A., Fu, Y., Wang, X., Lu, X., & Xu, W., et al. (2015). Harmine blocks herpes simplex virus infection through downregulating cellular NF-kappaB and MAPK pathways induced by oxidative stress. *Antivir. Res.*, *123*, 27–38.
- 5 Zhao, F., Gao, Z., Jiao, W., Chen, L., Chen, L., & Yao, X. (2012). In vitro anti-inflammatory effects of β -carboline alkaloids, isolated from *Picrasma quassioides*, through inhibition of the iNOS pathway. *Planta Med.*, *78*, 1906–1911.
- 6 Sun, P., Zhang, S., Li, Y., & Wang, L. (1997). Harmine mediated neuroprotection via evaluation of glutamate transporter 1 in a rat model of global cerebral ischemia. *Neurosci. Lett.*, *583*, 32–36.
- 7 Kim, H., Sablin, S.O., & Ramsay, R.R. (1997). Inhibition of monoamine oxidase A by β -Carboline derivatives. *Arch. Biochem. Biophys.*, *337*, 137–142.
- 8 Cao, R., Fan, W., Guo, L., Ma, Q., Zhang, G., & Li, J., et al. (2013). Synthesis and structure-activity relationships of asymmetric dimeric β -carboline derivatives as potential antitumor agents. *Eur. J. Med. Chem.*, *60*, 10–22.
- 9 Zhang, X.F., Sun, R., Jia, Y., Chen, Q., Tu, R.F., & Li, K., et al. (2016). Synthesis and mechanisms of action of novel harmine derivatives as potential antitumor agents. *Sci. Rep.*, *6*, 33204–33209.
- 10 Nurmaganbetov, Zh.S., Shultz, E.E., Chernov, S.V., Turmukhambetov, A.Zh., Seydakhmetova, R.B., & Shakirov, M.M., et al. (2011). Synthesis of substituted indolizino[8,7-*b*]indoles from harmine and their biological activity. *Chem. Heterocycl. Comp.*, *46*, 1494–1499.
- 11 Bruker (2015). *SAINTE*. Bruker AXS Inc., Madison, Wisconsin, USA.
- 12 Bruker (2015). *SADABS*. Bruker AXS Inc., Madison, Wisconsin, USA.
- 13 Sheldrick, G.M. (2008). Crystal structure solution with SHELXS. *Acta Crystallogr. Sect. A*, *64*, 112–122.
- 14 Sheldrick, G.M. (2015). Crystal structure refinement with SHELXL. *Acta Crystallogr. Sect. C*, *71*, 3–8.
- 15 Allen, F.H., Kennard, O., Watson, D.G., Brammer, L., Orpen, A.G., & Taylor, R. (1987). Tables of bond lengths determined by X-ray and neutron diffraction. *J. Chem. Soc. Perkin Trans.*, *2*, 1–19.
- 16 Maulik, P.R., & Basak, B.S. (1982). Harmine (7-methoxy-1-methyl-9H-pyrido[3,4-*b*]indole). *Cryst. Struct. Commun.*, *11*, 19–24.
- 17 Ferretti, V., Gilli, P., & Borea, P.A. (2004). Structural features controlling the binding of beta-carbolines to the benzodiazepine receptor. *Acta Crystallogr. Sect. B: Struct. Sci.*, *60*, 481–489.
- 18 Turmukhambetov, A.Zh., Agedilova, M.T., Nurmaganbetov, Zh.S., Kazantsev, A.V., Adekenov, S.M., & Shults, E.E., et al. (2009). Synthesis of quaternary salts of *Peganum harmala* alkaloids. *Chem. Natur. Comp.*, *45*, 601–603.

Information about authors

Turdybekov, Koblandy Muborykovich — Doctor of chemical sciences, Professor, Karagandy University of the name of academician E.A. Buketov, Karaganda, University street, 28, 100028, Kazakhstan; e-mail: xray-phyto@yandex.kz; <https://orcid.org/0000-0001-9625-0060>

Nurmaganbetov, Zhangel'dy Seytovich — Candidate of chemical sciences, Assistant professor, Karaganda Medical University, Karaganda, Gogol street, 40, 100000, Kazakhstan; e-mail: nzhangeldy@yandex.ru; <https://orcid.org/0000-0002-0978-5663>.

Turdybekov, Dastan Muchtarovich — Candidate of chemical sciences, Head of the Department of Physics, Karaganda Technical University, Karaganda, N. Nazarbaev street, 56, 100010, Kazakhstan; e-mail: turdas@mail.ru, <https://orcid.org/0000-0002-0245-0224>.

Mukusheva, Gulim Kenesbekovna — Candidate of chemical sciences, Professor, Karagandy University of the name of academician E.A. Buketov, Karaganda, University street, 28, 100028, Kazakhstan; e-mail: mukusheva1977@list.ru; ID Scopus 9243017000

Gatilov, Yurii Vasilevich — Doctor of chemical sciences, Leading researcher, N.N. Vorozhtsov Institute of Organic Chemistry of Siberian Branch of Russian Academy of Sciences, Novosibirsk, Lavrentiev Avenue, 9, 630090, Russia; e-mail: gatilov@nioch.ncs.ru; <https://orcid.org/0000-0001-4365-0081>.

A.S. Kishkentayeva, S.N. Mantler*, M.M. Zhakanov, S.M. Adekenov

JSC "International Research and Production Holding "Phytochemistry", Karaganda, Kazakhstan
(Corresponding author's e-mail: s.mantler@phyto.kz)

Biologically active substances from *Achillea nobilis* L.

The review summarizes data on biologically active compounds of *Achillea nobilis* L. and methods of their isolation. From *Achillea nobilis* L., collected in different places of growth, the following have been isolated: essential oil, the main components of which are monoterpene compounds; sesquiterpene lactones estafiatin, hanphyllin, anobin, chrysartemine A, canin, anolide and tanapartin- β -peroxide; the steroid acetyleucanbin; flavonoids: 3,5-dihydroxy-6,7,8-trimethoxyflavone, 5-hydroxy-3,6,7,4'-tetramethoxyflavone and 5,3'-dihydroxy-3,6,7,4'-tetramethoxyflavone. It has been determined that the component composition of the essential oil of *Achillea nobilis* L. largely depends on the soil and climatic factors in the places of its growth, the phase of the growing season and the method of its extraction from plant raw materials, and the extractant used (chloroform, ethanol, hot water, diethyl ether). Antibacterial, antimicrobial, antioxidant, antiparasitic activities are characteristic both for the sums of extractive substances from *Achillea nobilis* L. and for individual compounds isolated from them. Methods for the isolation of biologically active substances from *Achillea nobilis* L. for the development of new drug substances are described. The main aim of this work was a comparative analysis of the available research results on the phytochemical study of *Achillea nobilis* L.

Keywords: *Asteraceae*, *Achillea nobilis* L., sesquiterpene lactones, essential oil, flavonoids, isolation methods, biological activity.

Introduction

Plants of the genus *Achillea* L. of the *Asteraceae* family are considered as a promising source of biologically active substances, among which the most important are terpenoids and phenolic compounds. Other classes of natural compounds are also isolated from *Achillea* L.: carbohydrates (inulin and other polysaccharides, rhamnose, arabinose, xylose, mannose, glucose, galactose), bitter principles and tannins, microelements, acids (ascorbic, malic, aconitic, caffeic), amino acids, vitamins, alkaloids (achillein), coumarins (umbelliferone, scopoletin, isoscapoletin, scoparone and isofraxidine) [1, 2]. Essential oil of *Achillea* L. species is a source of proazulenes and azulenes [3].

Preparations based on *Achillea* L. are widely used in medical practice. They have a hemostatic, bactericidal, anti-inflammatory, wound-healing, anticonvulsant, anti-allergic effect, improve digestion, expand bile ducts, and increase bile secretion [4]. *Achillea millefolium* L. is among the top five plants containing the largest number of anthelmintic compounds, along with *Rosmarinus officinalis* L. and *Salvia officinalis* L. [5]. The results of studies of the anthelmintic efficacy of *Achillea millefolium* L. herb, carried out on experimental groups of birds (geese and ducks), showed the possibility of its use against helminthiasis of domestic waterfowl [2]. In work [6], the aqueous extract of *Achillea millefolium* L. (flowers) and a number of other plants were tested *in vitro*, and their ovicidal and larvicidal activity against nematodes in animals was confirmed.

The above-said indicates that it is promising to search among the secondary metabolites of plants of the genus *Achillea* L. for compounds responsible for their anthelmintic activity.

The main aim of this work was a comparative analysis of the available research results on the phytochemical study of *Achillea nobilis* L.

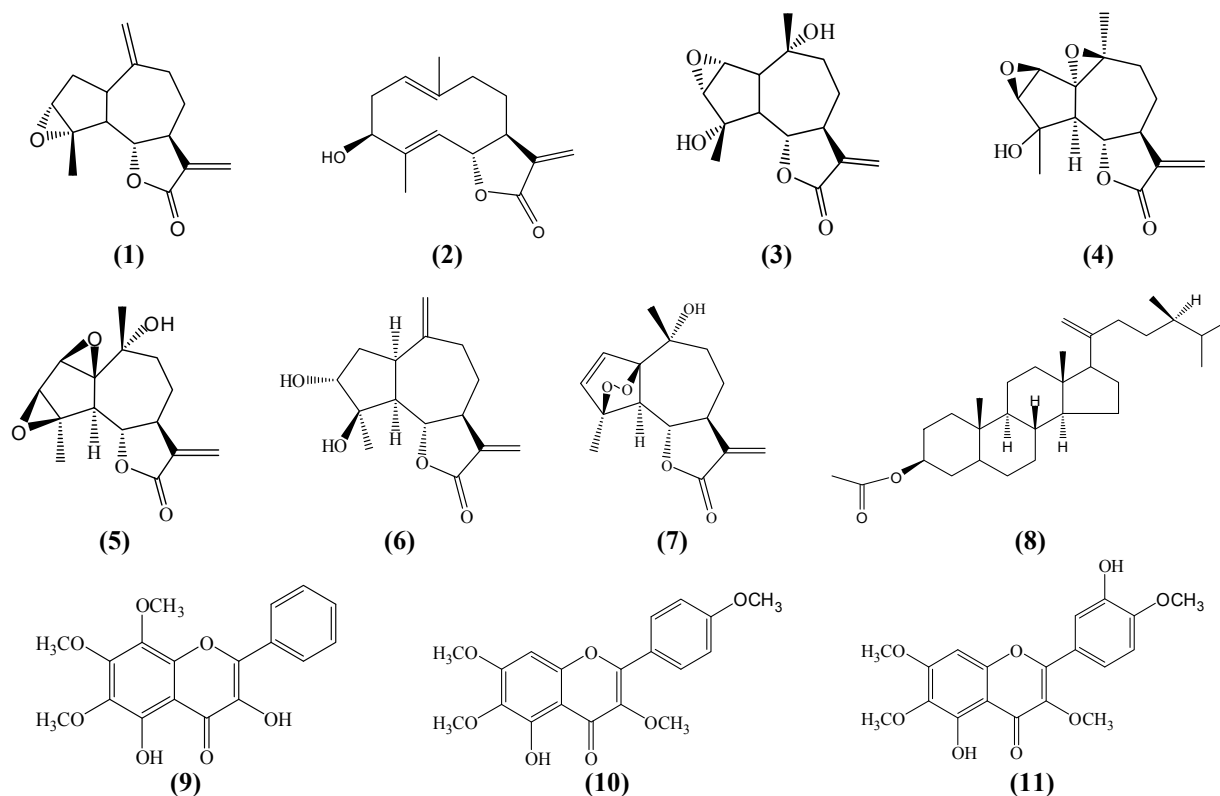
Main part

Over 10 species of plants of the genus *Achillea* L. grow on the territory of Kazakhstan. The most widespread among them are *A. asiatica* Serg., *A. setacea* Waldst. et Kit., *A. millefolium* L., *A. nobilis* L., *A. micrantha* Willd., *A. salicifolia* Bess., *A. cartilaginea* Ldb. [7]. Many taxa of this group are very similar in morphological characters and it is difficult to differentiate them without special morphological knowledge.

*Corresponding author.

There is an accessible exploitable raw material stock of *A. nobilis* L. on the territory of Central Kazakhstan, which is used in folk medicine as a phylogenetically close species to the officinal and relatively well-studied *A. millefolium* L. It is distributed over high meadow and shrub steppes, on hillsides and river valleys [7].

According to the literature data, essential oil, the main components of which are monoterpene compounds; sesquiterpene lactones: estafiatin (1), hanphyllin (2), anobin (3), chrysartemine A (4), canin (5), anolide (6) and tanapartin- β -peroxide (7); steroid acetyleucanbin (8); flavonoids: 3,5-dihydroxy-6,7,8-trimethoxyflavone (9), 5-hydroxy-3,6,7,4'-tetramethoxyflavone (10), 5,3'-dihydroxy-3,6,7,4'-tetramethoxyflavone (11) [8–12] were isolated from *A. nobilis* L., collected in different places of growth (Table).



Table

Compounds isolated from *Achillea nobilis* L.

| Name of compound | Gross formula | State of substance | Melting temperature, °C | Ref. |
|--|--|---------------------------------|-------------------------|------|
| Estafiatin (1) | C ₁₅ H ₁₈ O ₃ | Colorless acerous crystals | 102–104 | [8] |
| Hanphyllin (2) | C ₁₅ H ₂₀ O ₃ | Colorless lamellar crystals | 189 | [8] |
| Anobin (3) | C ₁₅ H ₂₀ O ₅ | Colorless rhombic crystals | 175.5–177.5 | [8] |
| Chrysartemine A (4) | C ₁₅ H ₁₈ O ₅ | Colorless crystals | 252–253 | [9] |
| Canin (5) | C ₁₅ H ₁₈ O ₅ | Colorless crystals | 241–243 | [9] |
| Anolide (6) | C ₁₅ H ₁₈ O ₅ | Colorless crystalline substance | 167–169 | [10] |
| Tanapartin- β -peroxide (7) | C ₁₅ H ₁₈ O ₅ | Colorless crystals | 117 | [12] |
| Acetyleucanbin (8) | C ₃₀ H ₅₀ O ₂ | Crystalline substance | 210–212 | [11] |
| 3,5-Dihydroxy-6,7,8-trimethoxyflavone (9) | C ₁₈ H ₁₆ O ₇ | Yellow crystalline substance | 148–150 | [8] |
| 5-Hydroxy-3,6,7,4'-tetramethoxyflavone (10) | C ₁₉ H ₁₈ O ₇ | Pale yellow crystals | 168–170 | [12] |
| 5,3'-Dihydroxy-3,6,7,4'-tetramethoxyflavone (11) | C ₁₉ H ₁₈ O ₈ | Pale yellow crystals | 182–185 | – |

The essential oil of *Achillea* L. species has antimicrobial and antibacterial action [13], its antiparasitic properties have been reported in [2].

The available literature data allow us to conclude that the component composition of *A. nobilis* L. essential oil is significantly depends on soil and climatic factors in the places of its growth, on the phase of the growing season and on the method of its extraction from plant raw materials [13]. Thus, the essential oil of *A. nobilis* L. from Yugoslavia is distinguished by a high content of α -thujone (25.7 %), artemisia ketone (14.8 %), borneol (9.9 %) and camphor (8.2 %) [14]. The Kazakhstan species of *A. nobilis* L. contain camphor (17 %), 1,8-cineole (15.6 %), terpinen-4-ol (10 %), borneol (7.1 %) and β -eudesmol (7.1 %) [15]. There are more γ -cadinene (46.7 %), α -cadinol (8.6 %) and 1,8-cineole (5.9 %) in essential oil from the Russian species of *A. nobilis* L. [16]. Italian raw materials of *A. nobilis* L. contain germacrene D (46 %), caryophyllene oxide (4.3 %), monoterpene acetate (3.9 %) and camphor (3.3 %) [17]. Essential oil of *A. nobilis* L. from Hungary is characterized by a high content of camphor, borneol and piperitone [18]. Two subspecies of *A. nobilis* subsp. *sipylea* and *A. nobilis* subsp. *neilreich* are growing on the territory of Turkey. Fragranol (19.3 %), 1,8-cineole (12–17 %), chrysanthenone (4–17 %), linalool (5–16 %) are the dominant components of the essential oil in them [19].

Extraction with chloroform, ethanol, diethyl ether, hot water is a relatively common and affordable method for isolation of terpenoids, flavonoids and other polyfunctional compounds from *Achillea* L. raw materials.

The method of sesquiterpene lactones estafiatin (**1**), hanphyllin (**2**), anobin (**3**) and flavonoid 3,5-dihydroxy-6,7,8-trimethoxyflavone (**9**) isolation from *A. nobilis* L. includes the extraction of raw materials of anthodium and leaves of *A. nobilis* L. by chloroform. Then the chloroform extract is concentrated, dissolved in 95 % ethyl alcohol and diluted with hot water in 2:1 ratio. After a day, the precipitate is filtered off; the filtrate is treated several times with chloroform. The sum of extractive substances obtained after removal of chloroform is chromatographed on macroporous silica gel (KSK grade) at a total material — sorbent ratio of 1:15. The column is eluted first with benzene, then successively with benzene-ether (4:1, 3:2, and 1:1), ether, mixture of ether-ethyl acetate (3: 2, 1: 1) and ethyl acetate [8].

The following compounds were isolated as a result of chromatographic separation of the chloroform extract of *A. nobilis* L.: anobin (**3**) was isolated from benzene fractions; estafiatin (**1**) was isolated from benzene-ether (4:1) fractions; hanphyllin (**2**) was isolated from benzene-ether (1:1) fractions; 3,5-dihydroxy-6,7,8-trimethoxyflavone (**9**) was isolated when the column was eluted with a mixture of ether-ethyl acetate (1:1) [8, 20].

Chromatography of the sum of extractive substances of the chloroform extract of *Achillea nobilis* L. (aerial part, collection in the vicinity of Karaganda, 2016) was obtained on macroporous silica gel (KSK grade) with a gradient elution with a mixture of petroleum ether – ethyl acetate (100:0 → 0:100). This solvent mixture is less toxic and less flammable than mixture of benzene-ether. As a result of chromatographic separation, compounds (**1**), (**2**), (**9**), and (**11**) were isolated. Compound (**11**) identified based on its spectral data [21] as flavonoid 5,3'-dihydroxy-3,6,7,4'-tetramethoxyflavone was isolated from *Achillea nobilis* L. for the first time. The yield of (**11**) was 0.01 % for air-dry raw materials.

Method of K.S. Rybalko [22] for the isolation from *A. nobilis* L. of sesquiterpene lactones chrysartemine A (**5**), canin (**6**) and anolide (**7**) included the extraction of *A. nobilis* L. flower heads and leaves by hot water (80–85 °C) for 1 hour, followed by treatment of the aqueous extract with chloroform. The syrup-like residue obtained after removal of chloroform was chromatographed on macroporous silica gel (KSK grade) at a total material to sorbent ratio of 1:22. Firstly the column was eluted with ether, then with a mixture of hexane-ethyl acetate (19:1) [9, 10]. As a result of chromatographic separation of an aqueous extract [10], sesquiterpene lactones anolide (**6**) from ether fractions, chrysartemine A (**4**) and canin (**5**) from hexane-ethyl acetate (19:1) fractions were isolated [9].

Isolation of the steroid acetylcucanbin (**8**) from *A. nobilis* L. was carried out by three-fold extraction of finely ground aerial parts of *A. nobilis* L, collected during the mass flowering period, with 96 % ethanol at room temperature for 3 days and by chromatographic separation of the sum of extractive substances on neutral aluminum oxide (III–IV degree of activity according to Brockmann). Firstly the column was eluted with hexane, then with a mixture of hexane-benzene, benzene, a mixture of benzene-chloroform, chloroform and a mixture of chloroform-alcohol [11, 23]. As a result of chromatographic separation of the ethanol extract, the steroid acetylcucanbin was isolated from hexane fractions (11).

Kastner et al. [12] carried out the extraction of air-dried flower heads of *A. nobilis* L. with diethyl ether. The resulting extract gave a positive reaction to the peroxides presence in it. After removal of the solvent, the

residue was extracted with 50 % methanol and further purified by column chromatography and HPLC. As a result, the guaian endoperoxide tanapartin- β -peroxide (**7**) and the flavonoid aglycone 5-hydroxy-3,6,7,4'-tetramethoxyflavone (**10**) were isolated.

Biological activity of secondary metabolites of Achillea nobilis L.

Based on the results of biological screenings, the presence of a wide spectrum of biological activity was determined both for the sums of extractive substances from *A. nobilis* L. and for individual compounds isolated from them.

Antimicrobial action of essential oils of *A. nobilis* subsp. *sipylea* and *A. nobilis* subsp. *neilreichii* collected in Turkey was studied on gram-positive and gram-negative bacterial strains as well as on the yeast *Candida albicans* [13, 19]. It was found that samples of *A. nobilis* L. essential oils significantly inhibit the growth of all tested microorganisms, except for *Pseudomonas aeruginosa*.

The authors of work [24] found that samples of essential oils from 16 species of *Achillea* L. have moderate anticholinesterase and antimicrobial effects. At the same time, the essential oil of *A. nobilis* subsp. *neilreichii* differs in composition from all others. The oils from *Achillea nobilis* L. exhibited moderate antimicrobial activities on *Fusarium verticillioides* (MIC = 0.60 mg/mL) and *Fusarium graminearum* (MIC = 0.60–1.20 mg/mL), respectively [25].

Sesquiterpene lactones of the guaian structure estafiatin (**1**) and anobin (**3**) have a pronounced antitumor activity [20]. A pronounced growth-regulating activity was found for estafiatin (**1**), while anolide (**6**) was found to have insecticidal activity [8]. Germacranolide hanphyllin (**2**) effectively inhibits the growth of Guerin's carcinoma, alveolar liver cancer and Pliss lymphosarcoma [20].

In the work [26], the antioxidant and antimicrobial activities of 15 extracts of *A. nobilis* L., obtained by 3 extraction methods (maceration, extraction in a Soxhlet apparatus and using ultrasonic radiation) with the use of 5 organic solvents (hexane, chloroform, ethyl acetate, ethanol and 50 % aqueous ethanol) were studied. Ethanol and ethyl acetate extracts showed a relatively pronounced antioxidant activity, for which a higher content of phenolic components was noted.

The antispasmodic effect of a lyophilized ethanol extract of *A. nobilis* L. subsp. *sipylea* (O. Schwarz) Bassler in rat duodenum, associated with suppression of calcium influx was established [27].

In the work [28], the antinociceptive and anti-inflammatory effects of ethanol extract of *A. nobilis* subsp. *neilreichii* (Kerner) Formanek flower heads were first studied on mice and rats; its acute toxicity was determined. The authors found that the anti-inflammatory effect of the lyophilized extract is manifested at doses much lower than $LC_{50} = 4456$ mg/kg in mice and is due to the synergistic effect of all its flavonoid components and is promising for therapeutic use.

The authors of the work [29] found that methanol extracts of six studied *Achillea* L. species demonstrate antiglycative, antioxidant and antimicrobial potential. At the same time, the *A. pachycephalla* Rech.f. and *A. nobilis* L. extracts, which are comparatively rich in polyphenolic components, showed a noticeable antiglycative ability in the bovine serum albumin (BSA)/methylglyoxal (MG) system. In work [30], a relatively high antioxidant activity of *A. nobilis* L. extracts grown under drought conditions was established, and it was noted that the total content of polyphenolic components in plant extracts growing under these conditions is significantly higher.

Conclusions

Thus, the analysis of the available literature data and the results of our own studies indicates that *Achillea nobilis* L. is a promising source of various classes of biologically active compounds, the most important of which are terpenoids of essential oil, sesquiterpene lactones and flavonoids, which determine the pharmacological action of its extracts. The component composition of the essential oil of *Achillea nobilis* L. largely depends on the soil and climatic factors in the places of its growth, the phase of the growing season, the method of its extraction from plant raw materials, and the extractant used (chloroform, ethanol, hot water, diethyl ether). Antibacterial, antimicrobial, antioxidant, antiparasitic activities are characteristic both for the sums of extractive substances from *Achillea nobilis* L. and for individual compounds isolated from them. Therefore, the search for biologically active components and the development of effective methods for their isolation from *Achillea nobilis* L. is relevant for the creation of new drugs with antibacterial, antimicrobial, antioxidant, antiparasitic action.

This research has been funded by the Science Committee of the Ministry of Education and Science of the Republic of Kazakhstan (Grant No. AP08052928).

References

- 1 Сербин А.Г. Химический состав и лечебное применение видов *Achillea* L. / А.Г. Сербин, Л.С. Кармазова, Н.М. Ткаченко // Растительные ресурсы. — 1987. — Т. 23, Вып. 2. — С. 275–286.
- 2 Мамедов Э. Применение антигельминтных растений при гельминтозах домашних водоплавающих птиц / Э. Мамедов, К. Байрамова // Sciences of Europe. — 2019. — № 38. — С. 63–65.
- 3 Коновалов Д.А. Природные азулены / Д.А. Коновалов // Растительные ресурсы. — 1995. — Т. 31, Вып. 1. — С. 101–132.
- 4 Ханин М.Л. Фитонцидные свойства экстрактов, извлеченных сжиженным углекислым газом из пряно-вкусового и лекарственно-ароматического растительного сырья / М.Л. Ханин, А.Ф. Прокопчук, Т.В. Перова, Л.А. Николаева // Фитонциды: экспериментальные исследования, вопросы теории и практики. — Киев: Наук. думка, 1975. — С. 141–143.
- 5 French K.E. Plant-Based Solutions to Global Livestock Anthelmintic Resistance / K.E. French // Ethnobiology Letters. — 2018. — Vol. 9, No. 2. — P. 110–123. DOI: 10.14237/ebi.9.2.2018.980.
- 6 Buza V. In vitro anthelmintic activity assessment of six medicinal plant aqueous extracts against donkey strongyles / V. Buza, L. Cătană, S.M. Andrei, L.C. Ștefănuț, Ș. Răileanu, M.C. Matei, I. Vlasiuc, M. Cernea // Journal of Helminthology. — 2020. — Vol. 94. — e147. DOI: 10.1017/s0022149x20000310.
- 7 Флора Казахстана / под ред. Н.В. Павлова. — Алма-Ата: Наука, 1966. — 639 с.
- 8 Adekenov S.M. A chemical investigation of *Achillea nobilis* / S.M. Adekenov, M.N. Mukhametzhonov, A.D. Kagarlitskii, A.Zh. Turmukhambetov // Chem. Nat. Compd. — 1984. — Vol. 20, No. 5. — P. 568–571. DOI: 10.1007/BF00580067.
- 9 Turmukhambetov A.Zh. Chrysartemin A and canin from *Achillea nobilis* / A.Zh. Turmukhambetov, G.K. Buketova, N.M. Gafurov, S.M. Adekenov // Chem. Nat. Compd. — 1999. — Vol. 35, No. 1. — P. 102. DOI: 10.1007/BF02238225.
- 10 Trudybekov K.M. Anolide — A new guaianolide from *Achillea nobilis* / K.M. Trudybekov, A.Zh. Turmukhambetov, S.M. Adekenov, Yu.T. Struchkov // Chem. Nat. Compd. — 1994. — Vol. 30, No. 4. — P. 460–463. DOI: 10.1007/BF00630399.
- 11 Serkerov S.V. Detection of acetylcannabin in *Achillea nobilis* / S.V. Serkerov, S.J. Mustafayeva // Chem. Nat. Compd. — 2010. — Vol. 46, No. 4. — P. 666. DOI: 10.1007/s10600-010-9709-z.
- 12 Kastner U. Guaianolide-endoperoxide and monoterpene-hydroperoxides from *Achillea nobilis* / U. Kastner, J. Breuer, S. Glasl, A. Baumann, W. Robien, J. Jurenitsch, G. Rucker, W. Kubelka // Planta medica. — 1995. — Vol. 61. — P. 83–85. DOI: 10.1055/s-2006-958010.
- 13 Ozdemir F.A. Potential Effects of Essential Oil Compositions on Antibacterial Activities of *Achillea nobilis* L. subsp. *neilreichii* / F.A. Ozdemir // Journal of Essential Oil-Bearing Plants. — 2019. — Vol. 22, No. 2. — P. 574–580. DOI: 10.1080/0972060X.2019.1623722.
- 14 Palic R. Composition and antibacterial activity of *Achillea crithmifolia* and *Achillea nobilis* essential oils / R. Palic, G. Stojanovic, T. Naskovic, N. Ranelovic // J. Essent. Oil Res. — 2003. — Vol. 15. — P. 434–437. DOI: 10.1080/10412905.2003.9698632.
- 15 Suleimenov Ye.M. Essential oil composition of three species of *Achillea* from Kazakhstan / Ye.M. Suleimenov, G.A. Atazhanova, T. Ozek, B. Demirci, A.T. Kulyyasov, S.M. Adekenov, K.H.C. Baser // Chem. Nat. Compd. — 2001. — Vol. 37, No. 5. — P. 381–384. DOI: 10.1023/A:1014471326724.
- 16 Калинкина Г.И. Химический состав эфирных масел некоторых видов тысячелистника флоры Сибири / Г.И. Калинкина, А.Д. Дембицкий, Т.П. Березовская // Химия растительного сырья. — 2000. — № 3. — С. 13–18.
- 17 Maffei M. Essential oils and chromosome numbers from Italian *Achillea* species / Maffei M., Chialva F., Codignola A. // J. Essent. Oil Res. — 1989. — Vol. 2. — P. 57–64. DOI: 10.1080/10412905.1993.9698171.
- 18 Héthelyi E. Phytochemical studies on the essential oils of species belonging to the *Achillea* genus by gas chromatography/mass spectrometry / E. Héthelyi, B. Dános, P. Tétényi // Biomedical & Environmental Mass Spectrometry. — 1989. — Vol. 18. — P. 629–636. DOI: 10.1002/bms.1200180821.
- 19 Karamenderes C. Composition and antimicrobial activity of the essential oils of *Achillea nobilis* L. subsp. *sipylea* and subsp. *neilreichii* / C. Karamenderes, N.U. Karabay-Yavasoglu, U. Zeybek // Chem. Nat. Compd. — 2007. — Vol. 43, No. 5. — P. 632–634. DOI: 10.1007/s10600-007-0213-z.
- 20 Адекенов С.М. Сесквитерпеновые лактоны растений Казахстана. Строение, свойства и применение: дис. ... д-ра хим. наук: 02.00.10 — «Биоорганическая химия» / Адекенов Сергазы Мынжасарович. — М., 1992. — 385 с.
- 21 Han X. Isolation of high-purity casticin from *Artemisia annua* L. by high-speed counter-current chromatography / X. Han, X. Ma, T. Zhang, Y. Zhang, Q. Liu, Y. Ito // Journal of chromatography. — 2007. — Vol. 1151. — P. 180–182. DOI: 10.1016/j.chroma.2007.02.105.
- 22 Рыбалко К.С. Природные сесквитерпеновые лактоны / К.С. Рыбалко. — М.: Медицина, 1978. — 320 с.
- 23 Серкеров С.В. Новый компонент *Achillea filipendulina* Lam. / С.В. Серкеров, С.Дж. Мустафаева // Химия растительного сырья. — 2009. — № 2. — С. 101–103.
- 24 Yener I. A detailed biological and chemical investigation of 16 *Achillea* species' essential oils via chemometric approach / I. Yener, M.A. Yilmaz, O.T. Olmez, M. Akdeniz, F. Tekin, N. Hasimi, ... Ertas A. // Chemistry & Biodiversity. — 2020. — Vol. 17, No. 3. — e1900484. DOI: 10.1002/cbdv.201900484.
- 25 Sampietro D.A. Chemical composition and antifungal activity of essential oils from medicinal plants of Kazakhstan / D.A. Sampietro, A. de los A. Gomez, C.M. Jimenez, E.F. Lizarraga, Z.A. Ibatayev, Y.M. Suleimen, C.A. Catalán // Natural Product Research. — 2016. — Vol. 31, No. 12. — P. 1464–1467. DOI: 10.1080/14786419.2016.1258560.

26 Taşkın D. Phenolic composition and biological properties of *Achillea nobilis* L. subsp. *neilreichii* (Kerner) Formanek, / D. Taşkın, T. Taşkın, E. Rayaman // *Industrial Crops & Products*. — 2018. — Vol. 111. — P. 555–562. DOI: 10.1016/j.indcrop.2017.11.022.

27 Karamenderes C. Antispasmodic effect of *Achillea nobilis* L. subsp. *sipylea* (O. Schwarz) Bassler on the rat isolated duodenum / C. Karamenderes, S. Apaydin // *Journal of Ethnopharmacology*. — 2003. — Vol. 84. — P. 175–179. DOI: 10.1016/s0378-8741(02)00296-9.

28 Karabay-Yavasoglu N.U. Antinociceptive and anti-inflammatory activities and acute toxicity of *Achillea nobilis* subsp. *neilreichii* extract in mice and rats / N.U. Karabay-Yavasoglu, C. Karamenderes, S. Baykan, S. Apaydin // *Pharmaceutical Biology*. — 2007. — Vol. 45, No. 2. — P. 162–168. DOI: 10.1155/2015/972827.

29 Afshari M. Variation in polyphenolic profiles, antioxidant and antimicrobial activity of different *Achillea* species as natural sources of antiglycative compounds / M. Afshari, M. Rahimmalek, M. Miroliaei // *Chemistry & Biodiversity*. — 2018. — Vol. 15, No. 8. — e1800075. DOI: 10.1002/cbdv.201800075.

30 Gharibi S. Effect of drought stress on total phenolic, lipid peroxidation, and antioxidant activity of *Achillea* species / S. Gharibi, B.E.S. Tabatabaei, G. Saeidi, S.A.H. Goli // *Applied Biochemistry and Biotechnology*. — 2015. — Vol. 178, No. 4. — P. 796–809. DOI: 10.1007/s12010-015-1909-3.

А.С. Кішкентаева, С.Н. Мантлер, М.М. Жақанов, С.М. Әдекенов

Achillea nobilis L. биологиялық белсенді заттары

Шолу мақалада кербез мыңжапырақтың (*Achillea nobilis* L.) биологиялық белсенді қосылыстары және оларды бөліп алу әдістері туралы мәліметтер жалпыланған. Әр түрлі өсу орындарында жиналған *Achillea nobilis* L. өсімдігінен негізгі компоненттері монотерпенді қосылыстар болып табылатын эфир майы; сесквитерпенді лактондар: эстафиатин, ханфиллин, анобин, хризартемин А, канин, анолид пен танапартин-β-пероксид; ацетилэуканбин стероиды; флавоноидтар: 3,5-дигидрокси-6,7,8-триметоксифлаван, 5-гидрокси-3,6,7,4'-тетраметоксифлаван, 5,3'-дигидрокси-3,6,7,4'-тетраметоксифлаван бөліп алынған. Кербез мыңжапырақ эфир майының компоненттік құрамы көбінесе оның өсу орындарындағы топырақ-климаттық факторларға, вегетациялық кезеңнің фазасына және оны өсімдік шикізатынан шығарып алу тәсіліне байланысты, ал сесквитерпенді лактондарды бөліп алуға қолданылатын экстрагент (хлороформ, этанол, ыстық су, диэтил эфирі) айтарлықтай әсер ететіні анықталды. Бактерияға, микробқа қарсы, антиоксидантты, паразитке қарсы белсенділік *Achillea nobilis* L. сығынды заттарының сомасына және олардан бөліп алынған жеке қосылыстарға да тән. Жаңа дәрілік препараттардың субстанцияларын жасау үшін кербез мыңжапырақтан биологиялық белсенді заттарды бөліп алу әдістері сипатталған. Бұл жұмыстың негізгі мақсаты — *Achillea nobilis* L. фитохимиялық зерттеу нәтижелерін салыстырмалы талдау.

Кілт сөздер: Asteraceae, *Achillea nobilis* L., сесквитерпенді лактондар, эфир майы, флавоноидтар, бөліп алу әдістері, биологиялық белсенділік.

А.С. Кишкентаева, С.Н. Мантлер, М.М. Жаканов, С.М. Адекенов

Биологически активные вещества *Achillea nobilis* L.

В обзорной статье обобщены данные о биологически активных соединениях тысячелистника благородного (*Achillea nobilis* L.) и методах их выделения. Из *Achillea nobilis* L., собранного в разных местах произрастания, выделено эфирное масло, основными компонентами которого являются монотерпеновые соединения; сесквитерпеновые лактоны: эстафиатин, ханфиллин, анобин, хризартемин А, канин, анолид и танапартин-β-пероксид; стероид ацетилэуканбин; флавоноиды: 3,5-дигидрокси-6,7,8-триметоксифлаван, 5-гидрокси-3,6,7,4'-тетраметоксифлаван, 5,3'-дигидрокси-3,6,7,4'-тетраметоксифлаван. Определено, что компонентный состав эфирного масла тысячелистника благородного во многом зависит от почвенно-климатических факторов в местах его произрастания, фазы вегетационного периода и способа его извлечения из растительного сырья, а на выделение сесквитерпеновых лактонов значительное влияние оказывает используемый экстрагент (хлороформ, этанол, горячая вода, диэтиловый эфир). Антибактериальная, противомикробная, антиоксидантная, противопаразитарная активность характерна как для сумм экстрактивных веществ из *Achillea nobilis* L., так и для выделенных из них индивидуальных соединений. Описаны методы выделения биологически активных веществ из тысячелистника благородного для разработки субстанций новых лекарственных препаратов. Основная цель данной работы — сравнительный анализ имеющихся результатов исследований по фитохимическому изучению *Achillea nobilis* L.

Ключевые слова: Asteraceae, *Achillea nobilis* L., сесквитерпеновые лактоны, эфирное масло, флавоноиды, методы выделения, биологическая активность.

References

- 1 Serbin, A.G., Karmazova, L.S., & Tkachenko, N.M. (1987). Khimicheskii sostav i lechebnoe primenenie vidov *Achillea* L. [Chemical composition and medicinal use of species *Achillea* L.]. *Rastitelnye resursy — Plant resources*, 23, 2, 275–286 [in Russian].
- 2 Mamedov, E., & Bairamova, K. (2019). Primenenie antihelmintnykh rastenii pri helmintozakh domashnikh vodoplavaiushchikh ptits [The use of anthelmintic plants for helminthiasis of domestic waterfowl]. *Sciences of Europe*, 38, 63–65 [in Russian].
- 3 Kononov, D.A. (1995). Prirodnye azuleny [Natural Azulenes]. *Rastitelnye resursy — Plant resources*, 31, 1, 101–132 [in Russian].
- 4 Khanin, M.L., Prokopchuk, A.F., Perova, T.V., & Nikolaeva, L.A. (1975). Fitontsidnye svoystva ekstraktov, izvlechennykh szhizhennym uhlekislym hazom iz priano-vkusovoho i lekarstvenno-aromaticheskoho rastitelnoho syria [Phytoncides properties of extracts isolated with liquefied carbon dioxide from spicy-flavoring and medicinal-aromatic plant raw materials]. *Fitontsidy: eksperimentalnye issledovaniia, voprosy teorii i praktiki — Phytoncides: Experimental research, theory and practice questions*. Kiev: Naukova dumka [in Russian].
- 5 French, K.E. (2018). Plant-Based Solutions to Global Livestock Anthelmintic Resistance. *Ethnobiology Letters*, 9(2), 110–123. DOI: 10.14237/ebl.9.2.2018.980.
- 6 Buza, V., Cătană, L., Andrei, S.M., Ștefănuț, L.C., Răileanu, Ș., & Matei, M.C., et al. (2020). In vitro anthelmintic activity assessment of six medicinal plant aqueous extracts against donkey strongyles. *Journal of Helminthology*, 94, e147. DOI: 10.1017/s0022149x20000310.
- 7 Pavlov, N.V. (1966). *Flora Kazakhstana [Flora of Kazakhstan]*. (Vol. 9). Alma-Ata: Nauka [in Russian].
- 8 Adekenov, S.M., Mukhametzhano, M.N., Kagarlitskii, A.D., & Turmukhambetov, A.Zh. (1984). A chemical investigation of *Achillea nobilis*. *Chem. Nat. Compd.*, 20(5), 568–571. DOI: 10.1007/BF00580067.
- 9 Turmukhambetov, A.Zh., Buketova, G.K., Gafurov, N.M., & Adekenov, S.M. (1999). Chrysertemin A and canin from *Achillea nobilis*. *Chem. Nat. Compd.*, 35(1), 102. DOI: 10.1007/BF02238225.
- 10 Trudybekov, K.M., Turmukhambetov, A.Zh., Adekenov, S.M., & Struchkov, Yu.T. (1994). Anolide — A new guaianolide from *Achillea nobilis*. *Chem. Nat. Compd.*, 30(4), 460–463. DOI: 10.1007/BF00630399.
- 11 Serkerov, S.V., Mustafaeva, S.J. (2010). Detection of acetyleucanbin in *Achillea nobilis*. *Chem. Nat. Compd.*, 46(4), 666. DOI: 10.1007/s10600-010-9709-z.
- 12 Kastner, U., Breuer, J., Glasl, S., Baumann, A., Robien, W., & Jurenitsch J., et al. (1995). Guaianolide-endoperoxide and monoterpene-hydroperoxides from *Achillea nobilis*. *Planta medica*, 61, 83–85. DOI: 10.1055/s-2006-958010.
- 13 Ozdemir, F.A. (2019). Potential effects of essential oil compositions on antibacterial activities of *Achillea nobilis* L. subsp. *neilreichii*. *Journal of Essential Oil-Bearing Plants*, 22(2), 574–580. DOI: 10.1080/0972060X.2019.1623722.
- 14 Palic, R., Stojanovic, G., Naskovic, T., & Ranelovic, N. (2003). Composition and antibacterial activity of *Achillea crithmifolia* and *Achillea nobilis* essential oils. *J. Essent. Oil Res.*, 15, 434–437. DOI: 10.1080/10412905.2003.9698632.
- 15 Suleimenov, Ye.M., Atazhanova, G.A., Ozek, T., Demirci, B., Kulyyasov, A.T., Adekenov, S.M., & Baser K.H.C. (2001). Essential oil composition of three species of *Achillea* from Kazakhstan. *Chem. Nat. Compd.*, 37(5), 381–384. DOI: 10.1023/A:1014471326724.
- 16 Kalinkina, G.I., Dembitsky, A.D., & Berezovskaya, T.P. (2000). Khimicheskii sostav efirnykh masel nekotorykh vidov tysiachelistnika flory Sibiri [Chemical composition of essential oils of some species of yarrow of the flora of Siberia]. *Khimiia rastitelnoho syria — Chemistry of plant raw materials*, 3, 13–18 [in Russian].
- 17 Maffei, M., Chialva, F., & Codignola, A. (1989). Essential oils and chromosome numbers from Italian *Achillea* species. *J. Essent. Oil Res.*, 2, 57–64. DOI: 10.1080/10412905.1993.9698171.
- 18 Héthelyi, E., Dános, B., & Tétényi, P. (1989). Phytochemical studies on the essential oils of species belonging to the *Achillea* genus by gas chromatography/mass spectrometry. *Biomedical & Environmental Mass Spectrometry*, 18, 629–636. DOI: 10.1002/bms.1200180821.
- 19 Karamenderes, C., Karabay Yavasoglu, N.U., & Zeybek, U. (2007). Composition and antimicrobial activity of the essential oils of *Achillea nobilis* L. subsp. *sipylea* and subsp. *neilreichii*. *Chem. Nat. Compd.*, 43(5), 632–634. DOI: 10.1007/s10600-007-0213-z.
- 20 Adekenov, S.M. (1992). Seskviterpenovye laktomy rastenii Kazakhstana. Stroenie, svoystva i primenenie [Sesquiterpene lactones of plants in Kazakhstan. Structure, properties and application]. *Doctor's thesis*. Moscow [in Russian].
- 21 Han, X., Ma, X., Zhang, T., Zhang, Y., Liu, Q., & Ito, Y. (2007). Isolation of high-purity casticin from *Artemisia annua* L. by high-speed counter-current chromatograph. *Journal of chromatography*, 1151, 180–182. DOI: 10.1016/j.chroma.2007.02.105.
- 22 Rybalko, K.S. (1978). *Prirodnye seskviterpenovye laktomy [Natural sesquiterpene lactones]*. Moscow: Meditsina [in Russian].
- 23 Serkerov, S.V., & Mustafaeva, S.J. (2009). Novyi komponent *Achillea filipendulina* Lam. [New ingredient *Achillea filipendulina* Lam.]. *Khimiia rastitelnoho syria — Chemistry of plant raw materials*, 2, 101–103 [in Russian].
- 24 Yener, I., Yilmaz, M.A., Olmez, O. T., Akdeniz, M., Tekin, F., & Hasimi N., et al. (2020). A detailed biological and chemical investigation of 16 *Achillea* species' essential oils via chemometric approach. *Chemistry & Biodiversity*, 17(3), e1900484. DOI: 10.1002/cbdv.201900484.

- 25 Sampietro, D.A., Gomez, A. de los A., Jimenez, C.M., Lizarraga, E.F., Ibatayev, Z.A., Suleimen, Y.M., & Catalán, C.A. (2016). Chemical composition and antifungal activity of essential oils from medicinal plants of Kazakhstan. *Natural Product Research*, 31(12), 1464–1467. DOI: 10.1080/14786419.2016.1258560.
- 26 Taşkın, D., Taşkın, T., & Rayaman, E. (2018). Phenolic composition and biological properties of *Achillea nobilis* L. subsp. *neilreichii* (Kerner) Formanek. *Industrial Crops & Products*, 111, 555–562. DOI: 10.1016/j.indcrop.2017.11.022.
- 27 Karamenderes, C., Apaydin, S. (2003). Antispasmodic effect of *Achillea nobilis* L. subsp. *sipylea* (O. Schwarz) Bassler on the rat isolated duodenum. *Journal of Ethnopharmacology*, 84, 175–179. DOI: 10.1016/s0378-8741(02)00296-9.
- 28 Karabay-Yavasoglu, N.U., Karamenderes, C., Baykan, S., & Apaydin, S. (2007). Antinociceptive and anti-inflammatory activities and acute toxicity of *Achillea nobilis* subsp. *neilreichii* extract in mice and rats. *Pharmaceutical Biology*, 45(2), 162–168. DOI: 10.1155/2015/972827.
- 29 Gharibi, S., Tabatabaei, B.E.S., Saeidi, G., & Goli, S.A.H. (2015). Effect of drought stress on total phenolic, lipid peroxidation, and antioxidant activity of *Achillea* species. *Applied Biochemistry and Biotechnology*, 178(4), 796–809. DOI: 10.1007/s12010-015-1909-3.
- 30 Afshari, M., Rahimmalek, M., & Miroliaei, M. (2018). Variation in polyphenolic profiles, antioxidant and antimicrobial activity of different *Achillea* species as natural sources of antiglycative compounds. *Chemistry & Biodiversity*, 15(8), e1800075. DOI: 10.1002/cbdv.201800075

Information about authors

- Kishkentayeva, Anarkul Serikovna** — PhD, Senior Researcher, JSC “International Research and Production Holding “Phytochemistry”, M. Gazaliev street, 4, 100009, Karaganda, Kazakhstan; e-mail: a.kishkentayeva@phyto.kz; <https://orcid.org/0000-0002-9169-3492>.
- Mantler, Svetlana Nikolaevna** — Researcher, JSC “International Research and Production Holding “Phytochemistry”, M. Gazaliev street, 4, 100009, Karaganda, Kazakhstan; e-mail: s.mantler@phyto.kz, <https://orcid.org/0000-0002-5779-3756>.
- Zhakanov, Miras Mekenovich** — Engineer, JSC “International Research and Production Holding “Phytochemistry”, M. Gazaliev street, 4, 100009, Karaganda, Kazakhstan; e-mail: m.zhakanov@phyto.kz; <https://orcid.org/0000-0001-6470-3838>.
- Adekenov, Sergazy Mynzhasarovich** — Doctor of Chemical Sciences, General Director, JSC “International Research and Production Holding “Phytochemistry”, Gazaliev str. 4, 100009, Karaganda, Kazakhstan, e-mail: arglabin@phyto.kz; <https://orcid.org/0000-0001-7588-6174>.

DOI 10.31489/2020Ch4/60-74

UDC 543.42

A.A. Bakibaev¹, M.Zh. Sadvakassova^{2*}, V.S. Malkov¹,
R.Sh. Erkasov², A.A. Sorvanov¹, O.A. Kotelnikov¹

¹National Research Tomsk State University, Tomsk, Russia;

²L.N. Gumilyov Eurasian National University, Nur-Sultan, Kazakhstan

(Corresponding author's e-mail: madinas-t@mail.ru)

Study of the biologically active acyclic ureas by nuclear magnetic resonance

A wide variety of acyclic ureas comprising alkyl, arylalkyl, acyl, and aryl functional groups are investigated by nuclear magnetic resonance spectroscopy. In general, spectral characteristics of more than 130 substances based on acyclic ureas dissolved in deuterated dimethyl sulfoxide at room temperature are studied. The results obtained based on the studies of ¹H and ¹³C NMR spectra of urea and its N-alkyl-, N-arylalkyl-, N-aryl- and 1,3-diaryl derivatives are presented, and the effect of these functional groups on the chemical shifts in carbonyl and amide moieties in acyclic urea derivatives is discussed. An introduction of any type of substituent (electron-withdrawing or electron-donating) into urea molecule is stated to result in a strong upfield shift in ¹³C NMR spectra relatively to unsubstituted urea. A strong sensitivity of NH protons to the presence of acyl and aryl groups in nuclear magnetic resonance spectra is pointed out. In some cases, qualitative dependencies between the chemical shifts in the NMR spectra and the structure of the studied acyclic ureas are revealed. A summary of the results on chemical shifts in the NMR spectra of the investigated substances allows determining the ranges of chemical shift variations of the key protons and carbon atoms in acyclic ureas. The literature describing the synthesis procedures are provided. The results obtained significantly expand the methods of reliable identification of biologically active acyclic ureas and their metabolites that makes it promising to use NMR spectroscopy both in biochemistry and in clinical practice.

Keywords: urea, alkylurea, arylurea, acylurea, diarylurea, urea fragment, amide group, NMR spectroscopy, chemical shift.

Introduction

Urea is the most important nitrogen metabolism product, the final amino acids exchange product. Urea is synthesized from ammonia, which is constantly formed in the body during the oxidative and non-oxidative amino acids deamination, in the hydrolysis of amides of glutamic and aspartic acids, as well as in the decomposition of purine and pyrimidine nucleotides [1]. It is well known that urea (carbamide) I is a product of nitrogen compounds metabolism in the mammals [2, 3], but, at the same time, there is literature evidences of an independent biological role of urea [4–6]. Targeted research in the field of urea chemistry made it possible to create many biologically active and medicinal products of the acyclic and heterocyclic structures that contain a urea fragment in their structure [7–11]. To better understand and explain some physical-chemical processes occurring with the participation of urea I, the latter is often represented in the form of Ia and Ib resonance structures.

It is believed that the given examples of resonance structures Ia and Ib plausibly explain the urea behavior features in spectral studies and in the urea interaction with a probable biological object.

Spectral methods to study the biologically active substances (including drugs) have been long and successfully used both for identification and establishing of the action mechanism. Spectral analysis methods are

*Corresponding author.

especially useful to reveal the structure and determine the metabolites composition. In the light of the foregoing, in recent years, the NMR spectroscopy is gaining strength for the biologically active compounds and drugs study.

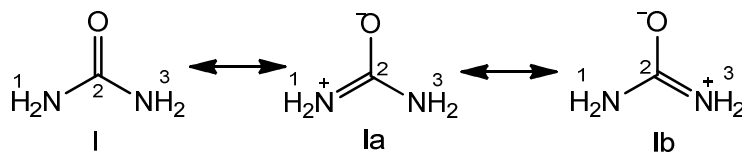


Figure 1. Urea resonance structures

The NMR studies of urea and its derivatives on ^1H , ^{13}C , ^{15}N nuclei are presented in literature [14–17]. Most published works address narrow specialized issues: the formation of intra- and intermolecular bonds, the establishment of rotation barriers, etc., or vice versa, NMR spectra are used only to confirm the synthesized compound structure. Thus, a targeted and systematic analysis of the ^1H and ^{13}C NMR spectra of acyclic urea was practically not carried out, except for the certain compounds.

In the present work, we analyzed the synthesized acyclic urea large array NMR spectral data.

Experimental

The ^1H and ^{13}C NMR spectra were recorded on a spectrometer "Bruker AVANCE III HD" (The Bruker Corporation, Germany), with 400 and 100 MHz operating frequencies, respectively, in DMSO and DMSO- d_6 solutions. Chemical shifts are given in the δ -scale relative to the tetramethylsilane (TMS) as an internal standard. The spectra were obtained in full decoupling mode from protons. The concentration of compounds was 0.5 % for ^1H NMR and 10 % for ^{13}C NMR, and the substances were synthesized and purified by known methods [18].

Results and Discussion

N-Alkyl- and N-arylalkylureas. The arylalkyl group is an independent pharmacophore fragment of many drugs and endogenous substrates [19]. On the other hand, urea is known as a well-established class of biologically active compounds [20–23]. The simultaneous presence of arylalkyl and urea groups in the compounds, as a rule, causes an increase in biological activity of the compounds studied.

To qualitatively assess the CS changes of NH protons and carbonyl carbon of N-monosubstituted urea derivatives, the ^1H and ^{13}C NMR spectra of compounds **1–35**, shown in Figure 2, were recorded and interpreted.

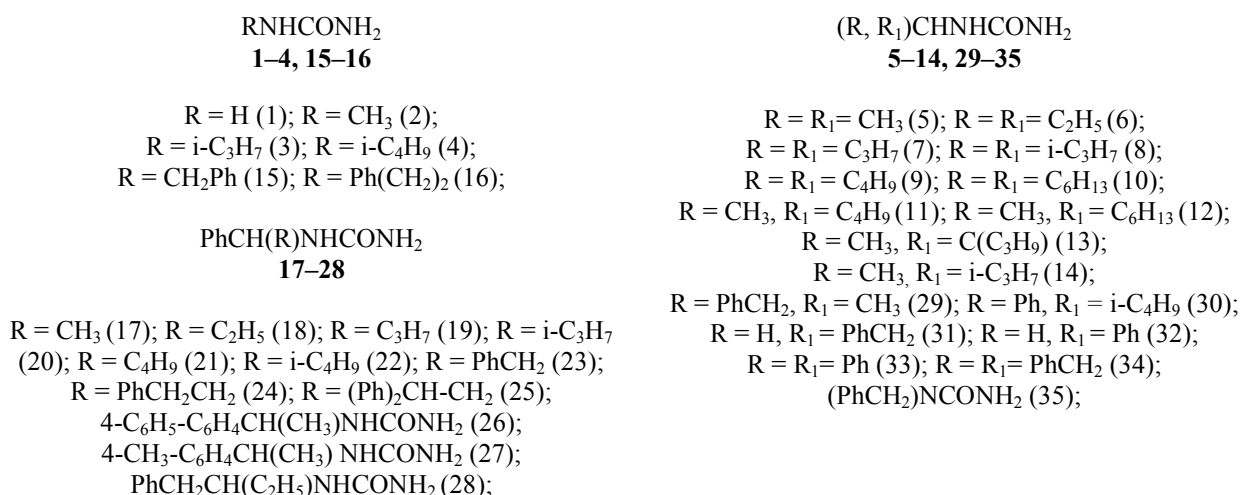


Figure 2. N-Alkyl- and N-arylalkylureas

Based on the obtained experimental data, it can be noted that, when any R and R₁ substituent is introduced into the urea **1** molecule, the carbonyl carbon atom becomes screened regardless of the substituent nature.

Given the positive alkyl substituent inductive effect on the urea nitrogen atom, one could expect screening of the nitrogen atom and the NH proton signal, and, therefore, the displacement of its CS in the strong field region. However, as it turned out, the experimental data are not simple. Thus, if in the case of a methyl group (compound **2**), the NH proton is de-screened, then the isopropyl radical (compound **3**) shields it (Table 1). Moreover, in the spectrum for compound **4** containing the isobutyl group, the amide proton is de-screened again. Therefore, the CS of NH protons is affected not only by the substituent electronic effects. The substitution of one of the NH protons in urea **1** featuring a group with a positive inductive effect leads to an increase in the bond order in the RNH–C(O) fragment compared to the unsubstituted NH₂–C(O) fragment. This is explainable in terms of the monosubstituted urea **A** resonance structure significant contribution to the molecule general hybrid due to the stabilization by the electron-donating substituent.

However, despite the fact that the alkyl group inductive effect favors the formation of structure **A**, it is unlikely to act exactly the same for the corresponding resonance structures **B** and **C**, in which the proton is cleaved from the Alk–NH fragment (Fig. 3).

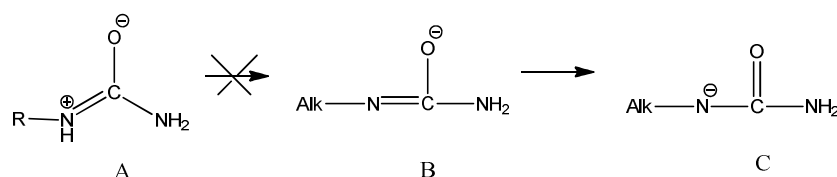


Figure 3. N-alkylurea resonance structures

Secondly, the methyl group steric effect is possible which makes the NH proton less accessible for cleavage (and substitution) with a base than the NH₂ group. Thus, the NH proton de-shielding by the methyl group can be interpreted as a result of a weak inductive effect and a small steric effect of this substituent. The isopropyl radical has a stronger inductive effect, and the branching in the form of methyl groups "shields" the amide proton from the solvent molecules. While moving from the reaction center, the electronic effect of the substituent on this center decreases. Thus, the inductive effect of the two CH₃ groups of the isobutyl radical has almost no effect on the nitrogen atom due to the large distance (through 3 bonds). This distance should also be considered by revising the steric factor. The greater distance between the methyl groups and NH protons (compared with the CH₃ groups of N-isopropylurea **3**) does not allow them to effectively "shield" the amide proton from the hydrogen bonds formation, due to which the proton signal is shifted to the low-field region.

Interestingly, the CS of NH¹ proton for N-isobutyl- and N-β-phenylethylureas (compounds **4** and **31**, respectively) coincide, which once again confirms the assumption that the electronic effects are insignificant through several bonds for the compounds studied.

Table 1

Urea **1** and its N-alkyl derivatives **2–14** ¹H and ¹³C chemical shifts

| Compound number | The ¹³ C NMR spectra, DMSO, δ, ppm | | The ¹ H NMR spectra, DMSO-d ₆ , δ, ppm | | |
|-----------------|---|--------|--|-------|---------------------|
| | CH | CO | CH | NH, d | NH ₂ , s |
| 1 | – | 161.47 | – | 5.93 | 5.93 |
| 2 | – | 160.74 | – | 6.06 | 5.75 |
| 3 | – | 158.88 | – | 5.90 | 5.46 |
| 4 | – | 159.78 | – | 6.12 | 5.67 |
| 5 | 41.18 | 158.88 | 3,61 | 5.38 | 5.90 |
| 6 | 51.48 | 158.89 | 3.54 | 6.00 | 5.56 |
| 7 | 47.97 | 158.67 | 3.69 | 5.90 | 5.47 |
| 8 | 49.46 | 158.52 | – | – | – |
| 9 | 48.49 | 158.61 | 3.70 | 5.90 | 5.47 |
| 10 | 48.50 | 158.67 | 3.70 | 5.89 | 5.45 |
| 11 | 44.61 | 158.37 | 3.76 | 5.94 | 5.56 |
| 12 | 44.69 | 158.45 | 3.81 | 6.02 | 5.52 |
| 13 | 52.73 | 159.05 | 3.74 | 5.76 | 5.34 |
| 14 | – | – | 3.70 | 6.00 | 5.52 |

Table 2

Urea 15–35 N-arylalkyl derivatives ^1H and ^{13}C chemical shifts

| Compound number | The ^{13}C NMR spectra, DMSO, δ , ppm | | The ^1H NMR spectra, DMSO- d_6 , δ , ppm | | |
|-----------------|---|--------|--|------|-----------------|
| | CH | C=O | CH | NH | NH ₂ |
| 15 | 43.04 | 159.12 | 4.41 | 6.79 | 5.86 |
| 16 | 38.13 | 158.97 | 3.19 | 6.36 | 5.87 |
| 17 | 48.57 | 158.15 | 4.94 | 6.47 | 5.68 |
| 18 | 54.62 | 158.37 | 4.72 | 6.66 | 5.65 |
| 19 | 52.75 | 158.22 | 4.82 | 6.68 | 5.68 |
| 20 | 58.58 | 158.45 | 4.67 | 6.71 | 5.71 |
| 21 | 53.12 | 158.30 | 4.79 | 6.67 | 5.66 |
| 22 | 51.33 | 158.32 | 4.89 | 6.69 | 5.70 |
| 23 | 54.77 | 158.07 | 5.12 | 6.81 | 5.71 |
| 24 | 52.83 | 158.37 | 4.88 | 6.82 | 5.72 |
| 25 | 51.56 | 158.15 | 4.55 | 6.87 | 5.63 |
| 26 | 48.04 | 157.62 | 4.99 | 6.74 | 5.69 |
| 27 | 48.27 | 158.07 | 4.90 | 6.62 | 5.70 |
| 28 | 51.70 | 158.52 | 3.84 | 6.00 | 5.55 |
| 29 | 46.69 | 158.91 | 3.79 | 5.88 | 5.42 |
| 30 | – | 158.79 | – | 6.54 | 5.55 |
| 31 | – | 159.50 | – | 6.12 | 5.68 |
| 32 | – | 159.47 | – | 6.56 | 5.72 |
| 33 | 56.45 | 157.52 | 6.12 | 7.23 | 5.84 |
| 34 | 52.39 | 158.35 | 4.12 | 6.08 | 5.58 |
| 35 | – | 158.89 | – | – | 5.83 |

The urea 1–35 NMR spectra analysis shows that significant changes in the structures of the substituted N-alkyl-2–14 and N-arylalkylureas 15–35 are reflected to a greater extent in the δ (CO) CS in the ^{13}C spectra of N-alkyl substituted ureas than N-arylalkylureas. The total range of changes in δ (CO) CS in these compounds is 3.22 ppm, and when compared with urea 1 itself, a noticeable strong field shift up to 4 ppm is observed. The carbonyl atom greatest screening can be seen in arylalkylurea 33, which is apparently due to the action of spatial factors. Despite this, the difference between the most and the least shielded carbon atoms in N-alkyl substituted ureas is δ (CO) 2.37 ppm, in arylalkyl-substituted ureas this signal is $\Delta\delta$ (CO) 1.98 ppm.

The analysis of CS values for methine carbon atom (CH) in the ^{13}C spectra of ureas 2–35 indicates its higher sensitivity to structural variations compared to the carbonyl carbon atom. As can be seen from the data given in tables 1 and 2, the difference between the most and the least shielded CH- carbon signals for alkyl ureas 5–13 is $\Delta\delta = 11.55$ ppm, and for arylalkylureas 15–35 the value is $\Delta\delta = 20.45$ ppm. In the series of compounds 5–13, there is a tendency towards a strong-field shift of δ (CH) groups as the substituent volume $R(R_1)$ increases, with the exception of compound 13 featuring the most unscreened signal. Among the N-arylalkyl-substituted compounds 15–35, the CH carbon is screened in the highest extent in the case of compound 16, which is most likely due to the spatial influence of a more branched alkyl radical and phenyl core on the methine carbon atom.

The comparison of CSs δ (NH₂) in the ^1H NMR spectra of urea 1 and its derivatives 2–35 shows that the signal of these protons in alkyl derivatives 2–14 is screened to a greater extent (up to 0.56 ppm) than in compounds 15–35 (up to 0.45 ppm). The analysis of CS values of NH- and CH-protons of compounds 2–35 shows that for alkylureas 2–14, the CS change of these protons is less pronounced ($\Delta\delta$ (NH) = 0.74 ppm, $\Delta\delta$ (CH) = 0.27 ppm), than for arylalkylureas 15–35 ($\Delta\delta$ (NH) = 1.35 ppm, $\Delta\delta$ (CH) = 2.93 ppm). At the same time, it can be observed that for N-arylalkyl compounds 15–35, the CS protons of CH and NH are shifted to weak fields by ca. 1 ppm as compared with the CS protons in CH and NH groups of N-alkylurea. This phenomenon can be explained by the anisotropic effect of the nearby phenyl ring.

N,N'-Benzhydrylureas. Benzhydrylureas are low toxic substances and are characterized by a wide physiological activity range, e.g., anticonvulsant [20, 21], antihypoxic [22], enzyme-inducing effects on cytochrome-P-450, a dependent liver monooxygenase system [21]. In this part of the article, we present the ^1H and ^{13}C NMR spectra of studied N-benzhydrylureas 36–70 showed in Figure 4. Table 3 shows the chemical shifts of N-benzhydrylureas 36–70 in the ^1H and ^{13}C NMR spectra.



R = R₁ = H (36); R = H, R₁ = 4-F (37);
 R = H, R₁ = 4-Cl (38); R = H, R₁ = 4-Br (39);
 R = H, R₁ = 4-NO₂ (40); R = H, R₁ = 4-CH₃O (41);
 R = H, R₁ = 3-F (42); R = H, R₁ = 3-Cl (43);
 R = H, R₁ = 3-Br (44); R = H, R₁ = 3-I (45);
 R = H, R₁ = 2-F (46); R = H, R₁ = 2-Cl (47);
 R = H, R₁ = 2-Br (48); R = H, R₁ = 2-I (49);
 R = H, R₁ = 2-CH₃ (50); R = 4-CH₃, R₁ = 3-F (51);
 R = 4-CH₃, R₁ = 3-CH₃ (52);
 R = 4-CH₃, R₁ = 2-CH₃ (53);
 R = 4-Cl, R₁ = 3-Cl (54); R = 4-Cl, R₁ = 2-Cl (55);
 R = R₁ = 3,8-Cl (56); R = R₁ = 2,8-Cl (57);
 R = R₁ = 3-Br (58); R = H, R₁ = 3-CH₃ (59);
 R = H, R₁ = 4-CH₃ (60); R = H, R₁ = 2,5-Cl (61);
 R = H, R₁ = 4-OH (62); R = H, R₁ = 3-F, 4-CH₃ (63);
 R = H, R₁ = 3,4-CH₃ (64); R = H, R₁ = 3-NO₂ (65);
 R = H, R₁ = 4-N (66); R = H, R₁ = α-нафтилметил (67);
 R = 4-Cl, R₁ = бензофурил (68);
 R = 4-F, R₁ = бензофурил (69);
 R = 4-Cl, R₁ = 4-Cl (70).

Figure 4. N-Benzhydrylurea

Table 3

¹H and ¹³C chemical shifts for N-benzhydrylureas 36–70

| Compound number | The ¹³ C NMR spectra, DMSO, δ, ppm | | The ¹ H NMR spectra, DMSO-d ₆ , δ, ppm | | |
|-----------------|---|--------|--|-------|---------------------|
| | CH | C=O | CH, m | NH, d | NH ₂ , s |
| 36 | 56.45 | 157.52 | 6.12 | 7.23 | 5.84 |
| 37 | 55.86 | 157.44 | 6.15 | 7.26 | 5.85 |
| 38 | 55.78 | 157.52 | 6.15 | 7.27 | 5.83 |
| 39 | 56.17 | 158.21 | 6.13 | 7.30 | 5.86 |
| 40 | 56.01 | 157.83 | 6.07 | 7.12 | 5.78 |
| 41 | 55.85 | 157.59 | 6.06 | 7.06 | 5.80 |
| 42 | 56.26 | 156.39 | 5.99 | 7.10 | 5.74 |
| 43 | 56.57 | 158.01 | 6.17 | 7.30 | 5.85 |
| 44 | 55.86 | 157.61 | 6.00 | 7.05 | 5.76 |
| 45 | 56.23 | 157.77 | 6.41 | 7.27 | 5.92 |
| 46 | 51.08 | 159.83 | 6.46 | 7.29 | 5.88 |
| 47 | 53.91 | 157.44 | 6.46 | 7.25 | 5.85 |
| 48 | 56.01 | 157.29 | 6.40 | 7.25 | 5.83 |
| 49 | 59.74 | 157.22 | 6.29 | 7.25 | 5.84 |
| 50 | 53.24 | 157.52 | 6.26 | 7.06 | 5.75 |
| 51 | 56.01 | 157.57 | 6.04 | 7.01 | 5.80 |
| 52 | 55.71 | 157.59 | 6.05 | 7.26 | 5.80 |
| 53 | 55.93 | 157.59 | 6.11 | 7.22 | 5.87 |
| 54 | 56.30 | 157.67 | 6.05 | 7.16 | 5.80 |
| 55 | 53.02 | 157.52 | 6.25 | 7.02 | 5.77 |
| 56 | 55.63 | 157.44 | 6.01 | 7.28 | 5.76 |
| 57 | 53.24 | 157.87 | 6.43 | 7.41 | 5.85 |
| 58 | 55.71 | 157.44 | 6.18 | 7.38 | 5.89 |
| 59 | 56.97 | 158.34 | 5.86 | 7.04 | 5.63 |
| 60 | 57.06 | 158.66 | 5.99 | 7.14 | 5.82 |
| 61 | 54.62 | 157.96 | 6.13 | 7.08 | 5.67 |
| 62 | 56.63 | 162.80 | 5.77 | 6.86 | 5.56 |
| 63 | 56.63 | 158.44 | 5.93 | 7.03 | 5.73 |
| 64 | 57.05 | 158.56 | 5.92 | 7.03 | 5.75 |
| 65 | 56.76 | 158.27 | 6.05 | 7.22 | 5.70 |
| 66 | 56.64 | 158.35 | 5.91 | 7.14 | 5.72 |
| 67 | 53.79 | 158.14 | 6.65 | 7.02 | 5.62 |
| 68 | 51.29 | 158.53 | 6.15 | 7.20 | 5.79 |
| 69 | 51.20 | 158.91 | 6.12 | 7.20 | 5.76 |
| 70 | 56.49 | 158.42 | 5.95 | 7.15 | 5.76 |

At first, we note the difference between the most and least shielded δCH and δCO signals in N-benzhydrylureas **36–70**: $\Delta\text{CH}=8.66$ ppm, $\Delta\text{CO}=6.41$ ppm. In this part of the work, we established the methine carbon atom screening effect relatively to the unsubstituted benzhydrylurea **36** by the substituent in the ortho-position (benzhydrylurea **46–50**, **55**, **57**). Noteworthy is the weakening of the CH groups screening effect with increasing substituent volume in the ortho position of benzhydrylureas, and for the most "bulky" substituent, i.e., iodine (compound **49**), the δCH signal is even shifted to the weak fields area. We emphasize that the chlorine atom and the methyl group characterized by the same steric constants located in the ortho position cause the same CH-carbon CS.

In the ^1H NMR spectra of the N-benzhydrylureas **36–70** (Table 3), the CS of methine protons are in the range of 5.77–6.65 ppm, and it can be seen that for ortho-halogen derivatives **46–50**, **57** (but not for ortho-methyl derivatives) and compound **67**, these protons are the most unscreened. The difference between the signals of most and the least shielded NH protons ($\Delta\text{NH} = 0.52$ ppm) and the NH_2 protons CS ($\Delta\text{NH}_2 = 0.36$ ppm) are less pronounced, despite the type of mono- or disubstitution in the aryl fragment of N-benzhydrylureas **36–70**.

Acylureas. N-Arylalkyl-N'-acylureas are known as biologically active compounds of various actions [20–22], and some representatives of these compounds have found application in clinical practice [19]. It is also important that the arylalkylureid fragment is a key component of the heterocycles of the barbituric, hydantoin, and quinazolinedione series, which are effective physiologically active substances of the most diverse actions [1–6, 24].

In this part of the work, we studied the effect on CS in the ^1H and ^{13}C NMR spectra of substituted N-alkyl(arylalkyl)-N'-acylureas **71–99** on a changes in structural parameters in the urea, amide, alkyl, and molecules acyl fragments presented in Figure 5:

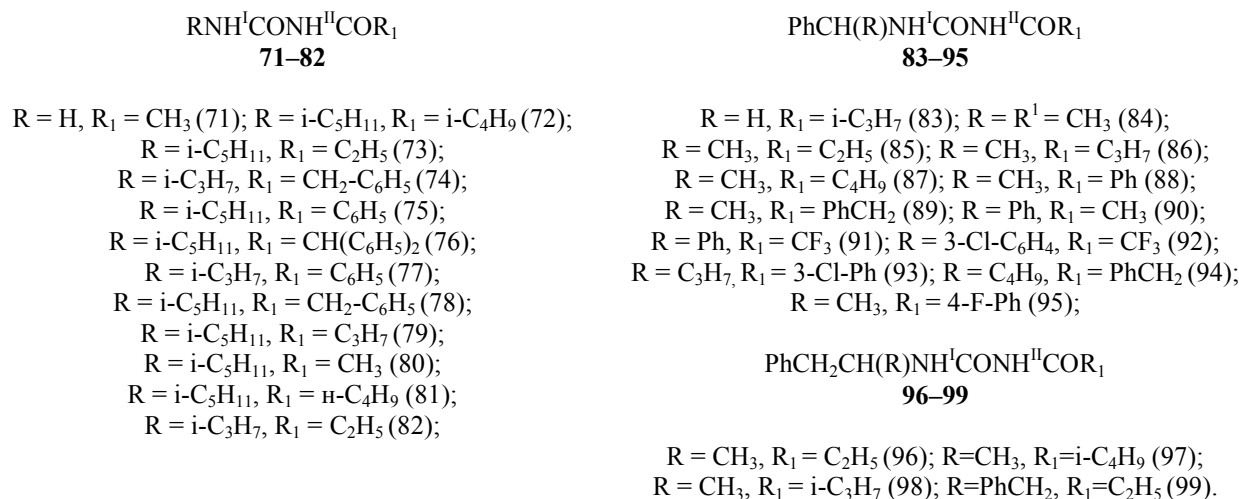


Figure 5. N-Alkyl (arylalkyl)-N'-acyl substituted urea

Chemical shifts in the ^1H and ^{13}C NMR spectra of N,N'-acylurea **71–99** are presented in Tables 4 and 5.

Table 4

^1H and ^{13}C chemical shifts for N-alkyl-N'-acylureas **71–82**

| Compound number | The ^{13}C NMR spectra, DMSO, δ , ppm | | The ^1H NMR spectra, DMSO- d_6 , δ , ppm | |
|-----------------|---|--------|--|------------------|
| | COR ₁ | C=O | NH ^I | NH ^{II} |
| 1 | 2 | 3 | 4 | 5 |
| 71 | 172.62 | 154.43 | 7.19 7.74 | 10.15 |
| 72 | 174.81 | 153.75 | 8.38 | 10.25 |
| 73 | 176.16 | 153.76 | 8.34 | 10.24 |
| 74 | 173.50 | 152.88 | 8.19 | 10.56 |
| 75 | 168.70 | 153.97 | 8.68 | 10.70 |
| 76 | 173.93 | 153.56 | 8.30 | 10.77 |
| 77 | 168.83 | 153.22 | 8.61 | 10.70 |

Continuation of Table 4

| 1 | 2 | 3 | 4 | 5 |
|----|--------|--------|------|-------|
| 78 | 173.33 | 153.73 | 8.30 | 10.59 |
| 79 | 175.38 | 153.74 | 8.34 | 10.24 |
| 80 | 172.70 | 153.67 | 8.31 | 10.28 |
| 81 | 175.53 | 153.75 | 8.34 | 10.24 |
| 82 | 176.14 | 153.00 | 8.26 | 10.19 |

Table 5

Chemical shifts in the ^1H and ^{13}C NMR spectra for N-arylalkyl-N'-acylureas **83–29**

| Compound number | The ^{13}C NMR spectra, DMSO, δ , ppm | | | The ^1H NMR spectra, DMSO- d_6 , δ , ppm | | |
|-----------------|---|-------|--------|--|----------------------|------------|
| | CONH | CH | COR | NH ^I , d | NH ^{II} , s | CH, t |
| 83 | 153.59 | – | 174.58 | 9.04 | 10.53 | - |
| 84 | 152.54 | 48.64 | 172.79 | 8.94 | 10.54 | 5.10 |
| 85 | 152.62 | 48.67 | 176.14 | 9.00 | 10.51 | 5.11 |
| 86 | 152.54 | 48.64 | 175.48 | 9.01 | 10.51 | 5.10 |
| 87 | 152.50 | 48.62 | 175.49 | 8.43 | 10.28 | 3.99–4.06 |
| 88 | 153.21 | 49.17 | 169.44 | 9.29 | 10.81 | 5.19 |
| 89 | 152.52 | 48.87 | 173.46 | 8.90 | 10.82 | 5.09 |
| 90 | 153.23 | 57.04 | 173.65 | 9.50 | 10.77 | 6.23, 6.31 |
| 91 | 151.58 | 58.16 | – | 8.73 | 11.73 | 6.10, 6.16 |
| 92 | 149.94 | 55.74 | – | 8.75 | 10.80 | 6.05, 6.12 |
| 93 | 153.21 | 55.36 | 167.75 | 9.06 | 10.92 | 4.79 k |
| 94 | 153.46 | 53.39 | 173.56 | 8.12 | 10.52 | 3.72–3.64 |
| 95 | 153.11 | 49.38 | 167.93 | 9.06 | 10.83 | 4.98 |
| 96 | 153.13 | 46.87 | 176.25 | 8.36 | 10.25 | 3.97–4.04 |
| 97 | 153.10 | 46.90 | 174.97 | 8.41 | 10.25 | 3.96–4.03 |
| 98 | 153.34 | 46.94 | 179.41 | 8.42 | 10.28 | 3.99–4.04 |
| 99 | 153.36 | 52.53 | 176.20 | 8.42 | 10.19 | 4.27 m |

We found that the introduction of additional phenyl core to the one of the reaction centers (to CH-carbon, compound **91**) compared with other compounds leads to some screening of the amide carbonyl group but at the same time causes a significant weak field shift (by 11.29 ppm) of the methine carbon atom signal (compound **90**, **91**). In our previous works [25, 26], we reported that the introduction of substituents into the ortho position of diphenylmethyl system causes progressive de-screening of CH-carbon with an increase in the substituents volume at the nitrogen atom in the diphenylmethyl fragment of the studied compounds. As can be seen from the table 5, the diphenylmethyl system formation (compounds **90–92**) leads to a sharp weak-field shift of the CH-carbon relative to CH CS of compounds **84–89**, **93–99**. A comparative analysis of the CS CH carbon atom of N-diphenylmethylamides (according to [19]), N-diphenylmethylureas (according to [25]), and N-diphenylmethylureides **90–92** established that the CH-carbon signals of compounds **90–92** are more unscreened than those of the precursors. The established fact of the highest CH-carbon of N-diphenylmethylureids **90–92** de-screening in the compared series of compounds is obviously related mainly to the spatial factor, i.e., with an increase in the substituent size in the molecules of diphenylmethyl group (the ureide group is significantly larger than the amide [19] or the urea [25] ones).

In addition, it can be noted that due to its powerful electron-withdrawing effect the N'-trifluoroacetyl group (compounds **91**, **92**) has a greater diamagnetic effect on the amide carbonyl carbon atom than the alkyl acyl and alkylaryl acyl R_1 radicals. Summing up the influence of acyl groups, it can be noted that the acyl radicals cause a strong field displacement of the amide carbonyl group of the starting N-arylalkylureas [26, 27] and N-alkyl-N'-acylureas **71–82**. The difference between the most and the least carbonyl atom screened signals in the ^{13}C spectra of acylureas **71–99** is $\delta = 4.49$ ppm. The most shielded CS of the atom in compounds **71–99** can be observed in N-diphenylmethylurea **92**.

In the ^1H NMR spectra of acylureas **71–99**, the acyl groups, being electron acceptors, cause regular weak-field shifts of the amide proton signals for compounds **71–99** and the methine proton for compounds **83–99** compared to the CS of similar protons in the initial N-arylalkylureas [26]. The difference between the most and the least shielded CH-carbon signals for compounds **83–99** is $\delta = 2.59$ ppm, and for NH^I and NH^{II}

groups (compounds **71–99**), 2.03 ppm and 1.58 ppm, respectively. The CH proton chemical shifts in the spectra of ^1H acylureas **83–99** are more screened than the signals of these protons in N-diphenylmethylureids **20–22**. We noticed that the most de-shielded NH^{II} protons group signals belong to these compounds **90–92**, which is connected, as mentioned before, with the diphenylmethyl system formation on the one hand and the trifluoroacetyl group effect on the other.

Urea aryl derivatives. It is well known that the electron-withdrawing substituent decreases the bond length in the RC-N fragment, and the substituent that is able to pair with the carbonyl group π -system increases it due to the resonance effects.

The N-phenylurea resonance structures are as follows: the carbonyl group to a large extent gathers the electron density from the unsubstituted nitrogen atom, since the lone electron pair of the N^{I} atom is delocalized in the benzene ring π system. This is also evidenced by the large de-screening of the NH_2 group. However, the anisotropic and steric influence of the aromatic fragment mainly contributes to the carbonyl carbon screening.

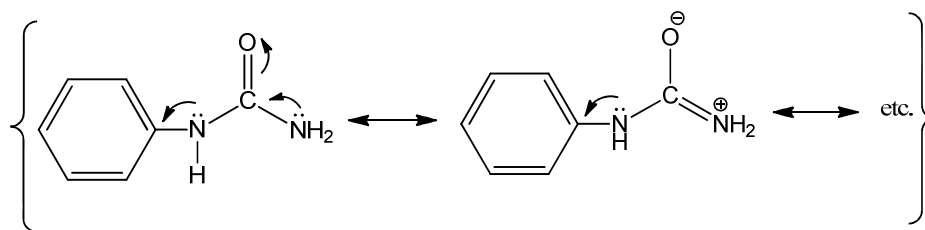


Figure 6. Electron density distribution in N-Phenylureas

The way how the direct conjugation affects the system CS can be judged by comparing the CSs in N-phenylurea with the data obtained for the remaining compounds in which the alkyl and alkylacyl radicals are present as substituents. Below we present a qualitative analysis of ^1H and ^{13}C NMR spectra of aryl derivatives of urea **100–107** (Fig. 7).



R=R₁=H (100); R=H, R₁=C₂H₅ (101); R=R₁=CH₃ (102); R=R₁=C₂H₅ (103); R=H, R₁=COCH₃ (104);
R=H, R₁=COCH₂Cl (105); R=H, R₁=COCF₃ (106); CH₃CH₂OC₆H₄NHCONH₂ (107)

Figure 7. Urea aryl derivatives

Table 6 presents the chemical shifts in the ^1H and ^{13}C NMR spectra of compounds **100–107**.

Table 6

Arylureas 1–8 chemical shifts in the ^1H and ^{13}C NMR

| Compound number | The ^{13}C NMR spectra, DMSO, δ , ppm | | The ^1H NMR spectra, DMSO- d_6 , δ , ppm | |
|-----------------|---|--|--|--------------------------------------|
| | C=O | | NH^{I} | $\text{NH}^{\text{II}}(\text{NH}_2)$ |
| 100 | 156.35 | | 8.77 | 6.15 |
| 101 | 153.59 | | 9.81 | 8.87 |
| 102 | 153.22 | | 9.75 | – |
| 103 | 153.74 | | 9.79 | – |
| 104 | 150.90 | | 10.77 | 10.89 |
| 105 | 150.38 | | 10.42 | 11.15 |
| 106 | 148.66 | | 10.04 | 12.07 |
| 107 | 156.85 | | 8.34 | 5.79 |

As can be seen from the table 6, under the influence of all substituents (except for compound **8**), the carbonyl atom CS in the ^{13}C spectrum is shifted to a strong field relative to phenylurea **100** itself. You can also notice that under the influence of the electron-donating properties of alkyl substituents, the signal is shifted to 3 ppm (101–103), and with an acetyl substituent, even more shields up to 6 ppm. But the N-tri-

fluoroacetyl group (compound **106**) has the greatest effect on the shift of the C=O group signal, the difference between the most and the least shielded atoms is 8.19 ppm compared with the unsubstituted phenylurea **100**. Probably, this is due to the fact that this substituent has a greater diamagnetic effect on the amide carbonyl carbon atom than the alkyl and alkylacyl R (R₁)-radicals.

The CS analysis of compounds **100–107** (except for the NH^{II} group of compound **107**) relatively to phenylurea **1** shows that in the ¹H spectrum, the amide protons of both groups undergo significant de-screening, moreover, the NH^{II} group protons proved to be more sensitive to the electronic influence of the substituents $\delta\text{NH}^{\text{II}} = 6.28$ ppm than the protons of NH^I ($\delta\text{NH}^{\text{I}} = 2.43$ ppm).

Urea diaryl derivatives. In a number of spectral methods to identify and establish the action mechanisms of the biologically active compounds, the NMR spectroscopy is becoming more widespread [27]. In this part of the work, we present a qualitative analysis of N,N'-diarylureas that are characterized by diverse activity [28, 29].

Previously, the effect of various substituents on the characteristics of NMR spectra in a para-substituted phenylureas series was studied [30]. Based on the analysis of ¹H and ¹³C NMR spectra, the electronic effect of the urea fragments of N-phenyl-N'-alkyl(acyl)urea on the benzene ring was estimated before.

In connection with the foregoing, it was interesting to evaluate the substituent effects in the aryl core on the CS of carbon and hydrogen atoms in urea fragment of diarylureas **108–122** (Fig. 8).

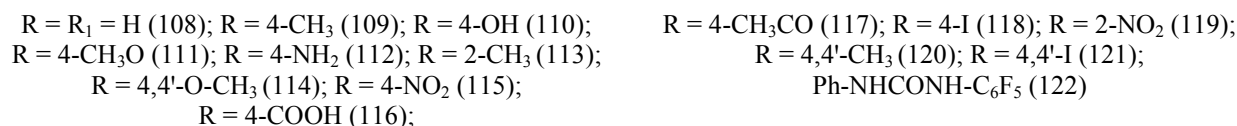


Figure 8. Urea diaryl derivatives

Table 7 represents the CS values in the ¹H and ¹³C NMR spectra of diarylureas **108–122**.

Table 7

N,N'-diarylurea 108–122 ¹H and ¹³C chemical shifts

| Compound number | The ¹³ C NMR spectra, DMSO, δ , ppm | The ¹ H NMR spectra, DMSO-d ₆ , δ , ppm | |
|-----------------|---|--|------------------|
| | C=O | NH ^I | NH ^{II} |
| 108 | 152.69 | 8.89 | 8.89 |
| 109 | 152.62 | 8.84 | 8.78 |
| 110 | 152.55 | 8.77 | 8.56 |
| 111 | 152.69 | 8.83 | 8.71 |
| 112 | 152.55 | 8.85 | 8.77 |
| 113 | 153.15 | 8.15 | 9.25 |
| 114 | 153.24 | 8.50 | 8.50 |
| 115 | 151.91 | 9.10 | 9.62 |
| 116 | 152.20 | 9.04 | 9.30 |
| 117 | 152.05 | 9.03 | 9.33 |
| 118 | 151.98 | 9.80 | 9.91 |
| 119 | 151.93 | 9.84 | 10.08 |
| 120 | 153.05 | 8.62 | 8.62 |
| 121 | 153.26 | 9.91 | 9.91 |
| 122 | 151.98 | 8.71 | 9.30 |

Judging by the carbonyl carbon atom (δCO) CS values, first of all, we note that in diphenylureas **108–122**, the CS of this carbon atom is noticeably shielded to 4.5 ppm compared to phenylurea **100** itself. Probably, this is due to the fact that the N'-arylation of phenylureas (compounds **108–122**) leads to an increase in the amide conjugation in N(I)-CO or N(II)-CO fragments due to the influence of the spatial factors, for example, due to the urea fragment effect of steric compression of molecules with N'-aryl radicals. The range of changes of δCO CS in diphenylurea **108–122** is small: $\Delta\text{CO} = 1.35$ ppm. Since the changes in the

δCO CS are not clearly connected with the electronic characteristics of R substituents, the δCO CS vibrations are apparently also caused by the urea fragment geometry deformation by aryl radicals.

The changes in the CS of urea protons ($\Delta\text{NH(I)} = 1.76$ ppm, $\Delta\text{NH(II)} = 1.52$ ppm) indicate their insignificant sensitivity to the electronic influence of variable R substituents. Thus, the electron-donating substituents (compounds **109–114**, **120**) cause NH(I) and NH(II) protons strong-field shifts, and electron-withdrawing substituents (compounds **115–119**, **121**, **122**) are a shift to weak fields, and NH(II) protons are more susceptible to the influence of the R substituents.

1,3-disubstituted ureas. By completing the assessment of qualitative changes in the CS of NH protons, carbonyl carbon, and methine atoms in the monosubstituted and disubstituted urea derivatives, we move to the final group of N,N and N,N' disubstituted ureas, amide protons and carbonyl carbon chemical shifts (Table 8), and the compounds themselves (Fig. 9).

The overall picture continues the trends observed for the N-monoprotected urea derivatives. The introduction of groups possessing donor properties shields the amide protons, and the groups capable of conjugation de-screen them. Carbonyl carbon, as expected, is shielded more strongly than in the case of monosubstitution.

It is noteworthy that in compounds **124** and **127**, the substituent enters into conjugation not only with the nitrogen atom directly bonded to it, but also with the other via the carbonyl group π system. This conclusion can be done if we consider the change in the proton of the amide linkage bound chemical shift to the tert-butyl group during the transition from compound **125** to **126**. The conjugation violation noticeably affects the signal of this NH proton, i.e., the signal is shifted towards a strong field ($\Delta = 0.62$).



R = R₁ = CH₃ (123); R = t-C₄H₉, R₁ = COC₂H₅ (124);
R = t-C₄H₉, R₁ = Ph (125); R = t-C₄H₉, R₁ = PhCH₂ (126);
R = PhCH₂, R₁ = Ph (127); R = Ph₂CH, R₁ = Ph₂CH (128);

R = Ph, R₁ = 3-Cl-C₆H₄ (129);
R = 4-CH₃Ph, R₁ = 3-CH₃Ph (130)

Figure 9. N,N'-Disubstituted ureas

Table 8

¹H and ¹³C chemical shifts for N,N'-disubstituted ureas 123–130

| Compound number | The ¹³ C NMR spectra, DMSO, δ , ppm | | The ¹ H NMR spectra, DMSO-d ₆ , δ , ppm | | |
|-----------------|---|--------|--|-------|-------|
| | CH | C=O | CH, m | NH, d | NH, d |
| 123 | – | 160.0 | – | 5.90 | 5.90 |
| 124 | – | 153.59 | – | 8.38 | 10.12 |
| 125 | – | 156.11 | – | 5.96 | 6.68 |
| 126 | – | 157.51 | – | 5.73 | 6.06 |
| 127 | – | 156.0 | – | 6.26 | 8.50 |
| 128 | 56.88 | 156.22 | 5.92 | 6.90 | 6.90 |
| 129 | 56.57 | 156.57 | 6.01 | 7.01 | 7.01 |
| 130 | 57.07 | 156.76 | 6.85 | 5.78 | 5.78 |

From the data given in Table 8 it can be seen that in contrast to N-methylation, the N,N- and N,N'-aryl-alkylation of urea causes the carbonyl carbon atom screening. For comparison, it can be noted that the N,N-dimethylation of urea de-shields the carbonyl carbon atom by 6.1 ppm, whereas N,N-dibenylation (compound **34**) shields 2.5 ppm this urea carbon atom. Given the fact that the arylalkyl groups in compounds **123–130** in relation to the urea carbonyl group exhibit at least lower electron-donating properties than the methyl group, it can be concluded that the δCO screening effect in compounds **123–130** upon urea N-aryl-alkylation is primarily due to the spatial factors. Since the steric characteristics of arylalkyl groups are significantly greater relative to methyl and due to their steric "bulkiness", it is possible that the urea arylalkyl groups **123–126** cause spatial stresses in the urea fragment of molecules simultaneously enhancing the conjugation in the amide fragment with a corresponding increase in the studied compounds amide bond order, and, as a consequence, the δCO screening in urea **123–126** relative to urea or its N-methyl derivatives. The strong field displacements of the largest carbonyl carbon atoms are observed in compound **124**, which is

caused by the presence of the most steric "bulky" radical, on the one hand, and the acyl radical effect on the other.

The CS comparison of methine carbon atoms in the ^1H spectrum of compounds **128–130** shows that this carbon atom in these compounds is significantly unscreened (relative to α -phenylethylurea **16**). As the substituent volume in the urea grows, the symbatic changes in the CS δCH occur, in other words, the larger are the steric characteristics of the substituents, the more likely the weak-field signal shift is observed.

The introduction of any substituent type (electron-donating or electron-withdrawing) causes a noticeable strong-field shift of the CS of C=O group in all the compounds studied in comparison with the pristine urea. This is especially pronounced for N-arylureas **100–107** and N-acylureas **71–99**. In the NMR ^1H spectra of the studied urea **130**, the N-arylureas **100–107** and N-acylureas **71–99** NH protons are the most sensitive to structural variations.

Conclusions

Numerous experimental data analysis for **130** N-substituted ureas cited before made it possible to determine the main intervals of chemical shifts to identify the atomic resonating groups in the NMR ^1H and ^{13}C spectra. The summarized data presented in table 9 are useful to identify urea in various studies and can be used by both chemists and biochemists or clinicians.

Table 9

Urea chemical shift intervals

| No. | The chemical compound or fragment thereof | The ^1H NMR spectra, ppm | The ^{13}C NMR spectra, ppm |
|-----|---|-----------------------------------|--------------------------------------|
| | | | C=O |
| 1 | R-NH ₂ | 5.7–6.2 | 156.4–158.2 |
| 2 | AlkNHCO | 5.8–6.06 | 158.5–158.9 |
| 3 | ArNHCO | 8.6–10.1 | 151.9–156.9 |
| 4 | ArAlkCHNHCO | 7.0–7.4 | 156.6–159.9 |
| 5 | Ar(Alk)NHCONHCOR ₁ | 8.7–9.46 | 148.7–153.6 |
| 6 | ArNHCONHCOR ₁ | 8.6–12.5 | 148.7–153.6 |

To conclude, not only do the results of ^1H and ^{13}C NMR studies of ureas facilitate the opportunities to determine the qualitative and quantitative changes of the spectral characteristics from the structural parameters in specific series of the synthesized substances, but also provide a good evidence for their structure. The chemical shifts of protons and carbon atoms in the NMR spectra of the substituted ureas can be used as initial data to correlate with the biological activity and other properties. The obtained results can be used as spectral database for chemists, biochemists and pharmacologists using similar substances in practice.

References

- 1 Brusilow S.W. Urea cycle enzymes / S.W. Brusilow, A.L. Horwich // *The Metabolic Basis of Inherited Diseases*. — 1989. — Vol. 6. — P. 629–664.
- 2 Haberle J. Suggested guidelines for the diagnosis and management of urea cycle disorders / J. Haberle, N. Boddart, A. Burlina, A. Chakrapani, M. Dixon, D. Karall et al. // *Orphanet journal of rare diseases*. — 2012. — Vol. 7, No. 1. — P. 1–30.
- 3 Andersen F.A. Final report of the safety assessment of urea / *International Journal of Toxicology*. — 2005. — Vol. 24. — P. 1–56. DOI: 10.1080/10915810500257097.
- 4 Williams A.C. Urea and Derivatives as Penetration Enhancers. Percutaneous Penetration Enhancers Chemical Methods in Penetration Enhancement / A.C. Williams, N. Dragicevic, H. Maibach (eds.) // Springer-Verlag Berlin Heidelberg. — 2015. — P. 301–308. DOI 10.1007/978-3-662-47039-8_18.
- 5 Bojic J. Spectrophotometric Determination of Urea in Dermatologic Formulations and Cosmetics / J. Bojic, B. Radovanovic, J. Dimitrijevic // *Analytical sciences*. — 2008. — Vol. 24, No. 6. — P. 769–774. DOI: 10.2116/analsci.24.769.
- 6 Decaux G. Treatment of euvoletic hyponatremia in the intensive care unit by urea / G. Decaux, C.A. Fabrice, G. Kengne, A. Soupart // *Critical Care*. — 2010. — Vol. 14, No. 5. — R184. DOI:10.1186/cc9292.
- 7 Mamidi R.N.V.S. In vitro and physiologically-based pharmacokinetic based assessment of drug–drug interaction potential of canagliflozin / R.N.V.S. Mamidi, S. Dallas, C. Sensenhauser, H.K. Lim, E. Scheers, P. Verboven et al. // *British Journal of Clinical Pharmacology*. — 2017. — Vol. 83, No. 5. — P. 1082–1096.

- 8 Citraro R. Pharmacokinetic-pharmacodynamic influence of N-palmitoylethanolamine, arachidonyl-2'-chloroethylamide and WIN 55,212-2 on the anticonvulsant activity of antiepileptic drugs against audiogenic seizures in DBA/2 mice / R. Citraro, E. Russo, A. Leo, R. Russo, C. Avagliano, M. Navarra et al. // *European Journal of Pharmacology*. — 2006. — Vol. 791. — P. 523–534.
- 9 Michael W. Anxiolytics, Anticonvulsants and Sedative-Hypnotics / W. Michael, Y. Naokata // *Annu. Rep. Med. Chem.* — 1986. — Vol. 21. — P. 11–20.
- 10 McElroy N.R. QSAR and classification of murine and human soluble epoxide hydrolase inhibition by urea-like compounds / N.R. McElroy, P.C. Jurs, C. Morisseau, B.D. Hammock // *Journal of Medicinal Chemistry*. — 2003. — Vol. 46, No. 6. — P. 1066–1080. DOI: 10.1021/jm020269o.
- 11 Librowski T. Evaluation of anticonvulsant and analgesic effects of benzyl- and benzhydryl ureides / T. Librowski, M. Kubacka, M. Meusel, S. Scolari, C.E. Mueller, M. Guetschow // *European Journal of Pharmacology*. — 2007. — Vol. 559, No. 2–3. — P. 138–149. DOI: 10.1016/j.ejphar.2006.12.002
- 12 Manimohan M. Biologically active novel N,N,O donor tridentate water soluble hydrazide based O-carboxymethyl chitosan Schiff base Cu (II) metal complexes: Synthesis and characterization / M. Manimohan, S. Pugalmani, M.A. Sithique // *Int. J. of Biological Macromol.* — 2019. — Vol. 136. — P. 738–754. DOI: 10.1016/j.ijbiomac.2019.06.115.
- 13 El Kayal W.M. Synthesis, in vivo and in silico anticonvulsant activity studies of new derivatives of 2-(2,4-dioxo-1,4-dihydroquinazolin-3(2H)-yl)acetamide / W.M. El Kayal, S.Y. Shtrygol, S.V. Zalevskiy, A. abu Shark, V.V. Tsyvunin, S.M. Kovalenko et al. // *European Journal of Medicinal Chemistry*. — 2019. — Vol. 180. — P. 134–142. DOI: 10.1016/j.ejmech.2019.06.085.
- 14 Zhao Y.R. A Proton NMR Investigation of Rotation about the C(O)-N Bonds of Urea / Y.R. Zhao, M.K. Raymond, H. Tsai, J.D. Roberts // *J. Phys. Chem.* — 1993. — Vol. 97. — P. 2910–2913.
- 15 Stilbs P. Spin-spin Couplings in Doubly ¹⁵N Labelled Urea and 1,3-Dimethylurea / P. Stilbs, S. Forsen // *Org. Magn. Reson.* — 1976. — Vol. 8. — P. 384.
- 16 Yavari I. Nitrogen-15 Nuclear Magnetic Resonance Spectroscopy. N-H Proton Exchange Reactions of Urea and Substituted Ureas / I. Yavari, J.D. Roberts // *Org. Magn. Res.* — 1980. — Vol. 13, No. 1. — P. 68–71.
- 17 Martinelli L.C. Protolysis kinetics of N-benzyl-N'-methylurea / L.C. Martinelli, C.D. Blanton, J.F. Whidby // *J. Am. Chem. Soc.* — 1971. — Vol. 93, No. 20. — P. 5111–5113.
- 18 Бакибаев А.А. Препаративные методы синтеза азотсодержащих соединений на основе мочевины / А.А. Бакибаев, Е.А. Мамаева, В.А. Яновский, А.Ю. Яговкин, Е.Л. Быстрицкий. — Томск: Аграф-Прес, 2007. — 164 с.
- 19 Патент № 2030396 РФ. Способ получения 5-хлор-2-аминозамещенных бензгидрилмочевины. Опубл. 10.03.95. Бакибаев А.А., Штрыкова В.В., Тигнибина Л.Г., Филимонов В.Д.
- 20 Бакибаев А.А. Синтетические противоэпилептические препараты: обзор и перспективы / А.А. Бакибаев, В.К. Горшкова // *Бюл. ТНЦ АМН СССР*. — 1991. — № 3. — С. 61–79.
- 21 Бакибаев А.А. Индукторы фенобарбиталового типа / А.А. Бакибаев, Т.П. Новожеева, Р.Р. Ахмеджанов, А.С. Саратиков // *Хим.-фарм. журн.* — 1995. — № 3. — С. 3–13.
- 22 Бакибаев А.А. Антигипоксические свойства органических соединений / А.А. Бакибаев, В.К. Горшкова, А.С. Саратиков // *Хим.-фарм. журн.* — 1997. — № 2. — С. 3–16.
- 23 Reynolds D.I. NMR Spectra of Ureas und Amides / D.I. Reynolds, G.A. Webb, M.L. Martin // *J. Mol. Struct.* — 1982. — Vol. 90, No. 2. — P. 379–382.
- 24 Бакибаев А.А. Мочевины в органическом синтезе. V. Реакции ароматических кетонов и 1,2-дикетонов с мочевиной в муравьиной кислоте / А.А. Бакибаев, А.Ю. Яговкин, В.Д. Филимонов // *Журн. орг. хим.* — 1991. — Т. 27, № 7. — С. 1512–1520.
- 25 Бакибаев А.А. Синтез арилметилмочевины и влияние их структуры на противосудорожную активность / А.А. Бакибаев, Л.Г. Тигнибина, В.Д. Филимонов, В.К. Горшкова, А.С. Саратиков, А.В. Пустовойтов и др. // *Хим.-фарм. журн.* — 1991. — Т. 25, № 5. — С. 31–35.
- 26 Филимонов В.Д. Количественная связь между противосудорожной активностью N-бензгидриламинов и N-бензгидрилмочевины, их структурой и спектрами ЯМР ¹³C / В.Д. Филимонов, А.А. Бакибаев, А.В. Пустовойтов и др. // *Хим.-фарм. журн.* — 1986. — № 5. — С. 540–545.
- 27 Holzgrabe U. Quantitative NMR spectroscopy — applications in drug analysis / U. Holzgrabe, R. Deubner, C. Schollmayer, B. Waibel // *J. Pharm. Biomed. Anal.* — 2005. — Vol. 38. — P. 806–812.
- 28 Wu Y.C. Research Progress of Diphenyl Urea Derivatives as Anticancer Agents and Synthetic Methodologies / Y.C. Wu, X.Y. Ren, G.W. Rao // *Mini-Reviews in Organic Chemistry*. — 2019. — Vol. 16, No. 7. — P. 617–630. DOI: 10.2174/1570193X15666181029130418.
- 29 Elmedy P. Activation of ERG2 potassium channels by the diphenylurea NS1643 / P. Elmedy, S.P. Olesen, M. Grunnet // *Neuropharmacology*. — 2007. — Vol. 53, No. 2. — P. 283–294. DOI: 10.1016/j.neuropharm.2007.05.009.
- 30 Филимонов В.Д. Спектры ЯМР фенилмочевины / В.Д. Филимонов, А.А. Бакибаев, С.В. Герасимов // *Журн. орг. хим.* — 1991. — Т. 27, № 5. — С. 1048–1052.

А.А. Бакибаев, М.Ж. Садвакасова, В.С. Мальков,
Р.Ш. Еркасов, А.А. Сорванов, О.А. Котельников

Ядролық магниттік резонанс әдісімен биологиялық белсенді ациклдік мочевиаларды зерттеу

Мочевина және оның N-ациклдік туындылары адам қызметінің түрлі салаларында әр түрлі қолдануды табатын құрамында азоты бар органикалық қосылыстардың маңызды класы болып табылады. Сонымен, олар көптеген биохимиялық процестерде маңызды рөл атқарып, ауыл шаруашылығында, косметологияда, тамақ өнеркәсібінде және т.б. салаларда кеңінен қолданылып, органикалық синтезде азоттандыру реагенті ретінде әрекет етеді. N-орынбасқан ациклдік мочевианы сәйкестендіру және талдау әдістерінің кең қатарында ЯМР-спектроскопия жетекші рөлге ие емес, ал бұл саладағы белгілі мәліметтер байланыссыз және жүйесіз сипатқа ие. Бұл жағдай алкил-, арилалкил-, ацил- және арилорынбасқан туындыларды қамтитын ациклдік мочевиалардың кең шеңберіне ядролық-магниттік резонанс әдісімен зерттеу жүргізуге түрткі болды. Жұмыста ^1H және ^{13}C ЯМР мочевина спектрлерінің және оның N-алкил-, N-арилалкил-, N-арил — және 1,3-диарил туындылары спектрлерінің негізінде алынған нәтижелері ұсынылған және осы функционалдық топтардың мочевина атомдарының карбонильді және амидті фрагменттерінің химиялық ығысуына әсері талқыланған. Жекелеген жағдайларда ЯМР спектріндегі химиялық ығысулар мен зерттелген қосылыстардың құрылымы арасында кейбір сапалық тәуелділік белгіленген. Зерттелген қосылыстардың химиялық ығысуларын өлшеу нәтижелерін қорыту ациклдік мочевиаларда протондар мен көміртегі атомының химиялық ығысуларының өзгеру аралықтарын анықтауға мүмкіндік берді. Алынған мәліметтер биологиялық белсенді ациклдік мочевиалар мен олардың метаболиттерін сенімді сәйкестендіру әдістерін едәуір кеңейтеді, ал бұл ЯМР-спектроскопияны биохимия және клиникалық практика үшін тартымды етеді.

Кілт сөздер: мочевина, N-алкилмочевина, N-арилмочевина, N-ацилмочевина, N,N-диарилмочевина, карбамид фрагменті, амидтік топ, ЯМР-спектроскопия, химиялық ығысу.

А.А. Бакибаев, М.Ж. Садвакасова, В.С. Мальков,
Р.Ш. Еркасов, А.А. Сорванов, О.А. Котельников

Исследование биологически активных ациклических мочевиин методом ядерного магнитного резонанса

Мочевина и ее N-ациклические производные представляют собой важный класс азотсодержащих органических соединений, который находит разнообразное применение в различных отраслях человеческой деятельности. Так, они играют важную роль во многих биохимических процессах, широко используются в сельском хозяйстве, косметологии, пищевой промышленности и т.д., выступают в качестве азотирующего реагента в органическом синтезе. Среди широкого арсенала методов идентификации и анализа N-замещенных ациклических мочевиин ЯМР-спектроскопия занимает далеко не лидирующую роль, а имеющиеся сведения в этой области знания носят отрывочный и несистемный характер. Данное обстоятельство послужило побудительным мотивом для проведения исследований методом ядерно-магнитного резонанса широкого круга ациклических мочевиин, охватывающих их алкил-, арилалкил-, ацил- и арилзамещенных производных. В настоящей работе представлены результаты, полученные на основании изучения ^1H и ^{13}C ЯМР-спектров мочевины и ее N-алкил-, N-арилалкил-, N-арил- и 1,3-диарилпроизводных, и определено влияние этих функциональных групп на химические сдвиги карбонильных и амидных фрагментов атомов мочевины. В отдельных случаях установлены некоторые качественные зависимости между химическими сдвигами в спектрах ЯМР и структурой исследованных соединений. Обобщение результатов измерения химических сдвигов изученных соединений позволило авторам определить интервалы изменения химических сдвигов протонов и атома углерода в ациклических мочевиинах. Полученные данные существенно расширяют методы надежной идентификации биологически активных ациклических мочевиин и их метаболитов, что делает привлекательным использование ЯМР-спектроскопии для биохимии и в клинической практике.

Ключевые слова: мочевина, N-алкилмочевины, N-арилмочевины, N-ацилмочевины, N,N-диарилмочевины, карбамидный фрагмент, амидная группа, ЯМР-спектроскопия, химический сдвиг.

References

- 1 Brusilow, S.W., & Horwich, A.L. (1989). Urea cycle enzymes. *The Metabolic Basis of Inherited Diseases*, 6, 629–664.
- 2 Haberle, J., Boddart, N., Burlina, A., Chakrapani, A., Dixon M., & Karall D., et al. (2012). Suggested guidelines for the diagnosis and management of urea cycle disorders. *Orphanet journal of rare diseases*, 7(1), 1–30.

- 3 Andersen, F.A. (2005). Final report of the safety assessment of urea. *International Journal of Toxicology*, 24, 1–56. DOI: 10.1080/10915810500257097.
- 4 Williams, A.C., Dragicevic, N., & Maibach, H. (eds.) (2015). Urea and Derivatives as Penetration Enhancers. *Percutaneous Penetration Enhancers Chemical Methods in Penetration Enhancement*. Springer-Verlag Berlin Heidelberg, 301–308. DOI 10.1007/978-3-662-47039-8_18.
- 5 Bojic, J., Radovanovic, B., & Dimitrijevic, J. (2008). Spectrophotometric Determination of Urea in Dermatologic Formulations and Cosmetics. *Analytical sciences*, 24(6), 769–774. DOI: 10.2116/analsci.24.769.
- 6 Decaux, G., Fabrice, C.A., Kengne, G., & Soupart, A. (2010). Treatment of euvoletic hyponatremia in the intensive care unit by urea. *Critical Care*, 14(5), R184. DOI:10.1186/cc9292.
- 7 Mamidi, R.N.V.S., Dallas, S., Sensenhaus, C., Lim, H.K., Scheers, E., & Verboven, P. et al. (2017). In vitro and physiologically-based pharmacokinetic based assessment of drug–drug interaction potential of canagliflozin. *British Journal of Clinical Pharmacology*, 83(5), 1082–1096.
- 8 Citraro, R., Russo, E., Leo, A., Russo, R., Avagliano, C., & Navarra, M., et al. (2006). Pharmacokinetic-pharmacodynamic influence of N-palmitoylethanolamine, arachidonyl-2'-chloroethylamide and WIN 55,212-2 on the anticonvulsant activity of antiepileptic drugs against audiogenic seizures in DBA/2 mice. *European Journal of Pharmacology*, 791, 523–534.
- 9 Michael, W., & Naokata, Y. (1986). Anxiolytics, Anticonvulsants and Sedative-Hypnotics. *Annu. Rep. Med. Chem.*, 21, 11–20.
- 10 McElroy, N.R., Jurs, P.C., Morisseau, C., & Hammock, B.D. (2003). QSAR and classification of murine and human soluble epoxide hydrolase inhibition by urea-like compounds. *Journal of Medicinal Chemistry*, 46(6), 1066–1080. DOI: 10.1021/jm020269o.
- 11 Librowski, T., Kubacka, M., Meusel, M., Scolari, S., Mueller, C.E., & Guetschow, M. (2007). Evaluation of anticonvulsant and analgesic effects of benzyl- and benzhydryl ureides. *European Journal of Pharmacology*, 559(2–3), 138–149. DOI: 10.1016/j.ejphar.2006.12.002.
- 12 Manimohan, M., Pugalmani, S., & Sithique, M.A. (2019). Biologically active novel N,N,O donor tridentate water soluble hydrazide based O-carboxymethyl chitosan Schiff base Cu (II) metal complexes: Synthesis and characterization. *Int. J. of Biological Macromol.*, 136, 738–754. DOI: 10.1016/j.ijbiomac.2019.06.115.
- 13 El Kayal, W.M., Shtrygol, S.Y., Zalevskiy, S.V., abu Shark, A., Tsyvunin, V.V., & Kovalenko, S.M., et al. (2019). Synthesis, in vivo and in silico anticonvulsant activity studies of new derivatives of 2-(2,4-dioxo-1,4-dihydroquinazolin-3(2H)-yl)acetamide. *European Journal of Medicinal Chemistry*, 180, 134–142. DOI: 10.1016/j.ejmech.2019.06.085.
- 14 Zhao, Y.R., Raymond, M.K., Tsai, H., & Roberts, J.D. (1993). A Proton NMR Investigation of Rotation about the C(O)-N Bonds of Urea. *J. Phys. Chem.*, 97, 2910–2913.
- 15 Stilbs, P., & Forsen, S. (1976). Spin–spin Couplings in Doubly ¹⁵N Labelled Urea and 1,3-Dimethylurea. *Org. Magn. Reson.*, 8, 384.
- 16 Yavari I., & Roberts J.D. (1980). Nitrogen-15 Nuclear Magnetic Resonance Spectroscopy. N-H Proton Exchange Reactions of Urea and Substituted Ureas. *Org. Magn. Res.*, 13(1), 68–71.
- 17 Martinelli, L.C., Blanton, C.D., & Whidby, J.F. (1971). Protolysis kinetics of N-benzyl-N'-methylurea. *J. Am. Chem. Soc.*, 93(20), 5111–5113.
- 18 Bakibayev, A.A., Mamaeva, E.A., Yanovskii, V.A., Yagovkin, A.Yu., & Bystrickii, E.L. (2007). *Preparativnye metody sinteza azotsoderzhashchikh soedinenii na osnove mochevin [Preparative methods of synthesis of nitrogen-containing compounds based on urea]*. Tomsk: Ahraf-Pres [in Russian].
- 19 Bakibayev, A.A., Shtrykova, V.V., Tignibidina, L.G., & Filimonov, V.D. (1995). Sposob polucheniia 5-khlor-2-aminozame-shchennykh benzhidrilmochevin [Method for producing 5-chloro-2-amino-substituted benzhydrylureas]. *Patent No. 2030396 RF*. Publ. 10.03.95 [in Russian].
- 20 Bakibaev, A.A., & Gorshkova, V.K. (1991). Sinteticheskie protivoepilepticheskie preparaty: obzor i perspektivy [Synthetic antiepileptic drugs: overview and prospects]. *Biulleten TNC AMN SSSR — Bulletin of the TNC AMN of the USSR*, 3, 61–79 [in Russian].
- 21 Bakibaev, A.A., Novozheeva, T.P., Ahmedzhanov, R.R., & Saratikov, A.S. (1995). Induktory fenobarbitalovoho tipa [Phenobarbital inductors]. *Khimiko-farmatsevticheskii zhurnal — Chemical and pharmaceutical journal*, 3, 3–13 [in Russian].
- 22 Bakibaev, A.A., Gorshkova, V.K., & Saratikov, A.S. (1997). Antihypoxicheskie svoistva orhanicheskikh soedinenii [Antihypoxic properties of organic compounds]. *Khimiko-farmatsevticheskii zhurnal — Chemical and pharmaceutical journal*, 2, 3–16 [in Russian].
- 23 Reynolds, D.I., Webb, G.A., & Martin, M.L. (1982). NMR Spectra of Ureas und Amides. *J. Mol. Struct.*, 90(2), 379–382.
- 24 Bakibayev, A.A., Yagovkin, A.Yu., & Filimonov, V.D. (1991). Mocheviny v orhanicheskom sinteze. V. Reaktsii aromaticheskikh ketonov i 1,2-diketonov s mochevinami v muravinoi kislyote [Urea in organic synthesis. V. Reactions of aromatic ketones and 1,2-diketones with urea in formic acid]. *Zhurnal orhanicheskoi khimii — Journal of organic chemistry*, 27(7), 1512–1520 [in Russian].
- 25 Bakibayev, A.A., Tignibidina, L.G., Filimonov, V.D., Gorshkova, V.K., Saratikov, A.S., & Pustovojtov, A.V. et al. (1991). Sintez arilmetilmochevin i vliianie ikh struktury na protivosudorozhnuuiu aktivnost [Synthesis of arylmethyl urea and the effect of their structure on anticonvulsant activity]. *Khimiko-farmatsevticheskii zhurnal — Chemical and pharmaceutical journal*, 5, 31–35 [in Russian].

26 Filimonov, V.D., Bakibayev, A.A., & Pustovoitov, A.V. (1986). Kolichestvennaia svyaz mezhdru protivosudorozhnoi aktivnostiu N-benzhidrilamidov i N-benzhidrilmochevin, ikh strukturoi i spektrami YaMR ^{13}C [Quantitative relationship between anticonvulsant activity of N-benzhydramides and N-benzhydramiloureas, their structure and ^{13}C NMR spectra]. *Khimiko-farmatsevticheskii zhurnal — Chemical and pharmaceutical journal*, 5, 540–545 [in Russian].

27 Holzgrabe, U., Deubner, R., Schollmayer, C., & Waibel, B. (2005). Quantitative NMR spectroscopy — applications in drug analysis. *J. Pharm. Biomed. Anal.*, 38, 806–812.

28 Wu, Y.C., Ren, X.Y., & Rao, G.W. (2019). Research Progress of Diphenyl Urea Derivatives as Anticancer Agents and Synthetic Methodologies. *Mini-Reviews in Organic Chemistry*, 16(7), 617–630. DOI: 10.2174/1570193X15666181029130418.

29 Elmedyby, P., Olesen, S.P., & Grunnet, M. (2007). Activation of ERG2 potassium channels by the diphenylurea NS1643. *Neuropharmacology*, 53(2), 283–294. DOI: 10.1016/j.neuropharm.2007.05.009.

30 Filimonov, V.D., Bakibayev, A.A., & Gerasimov, S.V. (1991). Spektry YaMR fenilmochevin [The NMR spectra of phenylacetic]. *Zhurnal orhanicheskoi khimii — Journal of organic chemistry*, 27(5), 1048–1052 [in Russian].

Information about authors

Bakibaev, Abdigali Abdimanapovich — Doctor of Chemical sciences, Engineer, Institute for Problems of Chemical and Energetic Technologies SB RAS, Socialisticheskaya street, 1, 659322, Biysk, Russia; e-mail: bakibaev@mail.ru; <https://orcid.org/0000-0002-3335-3166>.

Sadvakassova, Madina Zhumbaykyzy — 2-year PhD student of specialty chemistry, L.N. Gumilyov Eurasian National University, Nur-Sultan, K. Munaitpasov Street, 13, 010008, Kazakhstan; e-mail: madinas-t@mail.ru.

Malkov, Victor Sergeevich — Candidate of Chemical sciences, Head of laboratory of organic synthesis, National Research Tomsk State University, Lenin avenue, 36, 634050, Tomsk, Russia; e-mail: malkov.vics@gmail.com; <https://orcid.org/0000-0003-4532-2882>

Erkasov, Rakhmetulla Sharapidenovich — Doctor of Chemical Sciences, Professor of the Department of Chemistry, L.N. Gumilyov Eurasian National University, Nur-Sultan, K. Munaitpasov Street, 13, 010008, Kazakhstan; e-mail: erkass@mail.ru.

Sorvanov, Alexander Alexandrovich — 1-year postgraduate of specialty organic chemistry, National Research Tomsk State University, Tomsk, Lenin avenue, 36, 634050, Russia; e-mail: wellitson@gmail.com.

Kotelnikov, Oleg Alexeevich — Junior researcher, National Research Tomsk State University, Lenin avenue, 36, 634050, Tomsk, Russia; e-mail: kot_o_a@mail.ru; <https://orcid.org/0000-0002-1241-1312>.

I.E. Stas¹, S.S. Pavlova^{2*}¹Altai State University, Barnaul, Russia;²Yugra State University, Khanty-Mansiysk, Russia

(Corresponding author's e-mail: pavlova_ss@mail.ru)

Effect of ultrahigh-frequency electromagnetic field on the properties of associated liquids

The influence of the electromagnetic field on the refractive index, evaporation rate and surface tension of water, propanol-1 and pentanol-1 solutions have been studied. It was shown that the properties of these liquids depend on the field frequency and the time of exposure. The action of the field on the structure of water and alcohols is selective; changes in their properties are due to frequencies that are individual for each liquid. Both deceleration and acceleration of the alcohols evaporation occurs depending on the frequency of the electromagnetic field. Evaporation of the field exposed water is slowing down at all the studied frequency range. There is an increase in the surface tension for water and pentanol, and a decrease for propanol. The properties of alcohols return to their initial values, and the properties of the water remain unchanged after the termination of the field action. Thermodynamic functions of surface water and propanol-1 have been calculated on the basis of the temperature dependence of the surface tension. It has been demonstrated that the total internal energy of the surface increases for water and reduces or propanol-1. This indicates the strengthening of the structure in an aqueous solutions and a weakening of intermolecular interaction in the propanol-1 medium.

Keywords: water, propanol-1, pentanol-1, electromagnetic field, frequency, refractive index, evaporation rate, surface tension.

Introduction

Many studies demonstrate that water is able to react to any external influence. This fact is revealed in the change of its bulk and surface properties. There is an annual increase in publications devoted to the study of response of liquid water on the influence of physical fields of different nature [1–5]. Previous studies have shown that water treatment with an electromagnetic field of low-intensity of radio frequency leads to an increase in its electrical conductivity, surface tension and heat of evaporation. A decrease in the rate of evaporation and adhesion to a solid surface has been observed. These effects are revealed only at certain frequencies of the field (the range of 30–200 MHz has been studied) and rise up to a specific limit with increasing of exposure time. It has been also found that the changed properties of water do not return to their original values, and were kept for a long time; for example, the observations were carried out during the year [6–8]. The experimentally observed changes in the properties of water are associated with the rearrangement of the supramolecular organization of water due to the presence of hydrogen bonds [9–11].

However, water is not the only liquid whose molecules are hydrogen-bonded. Hydrogen bonds are also formed between alcohol molecules, carboxylic acids, esters, mercaptans, etc in a liquid state [12]. Monobasic alcohol and water differ significantly in the energy of hydrogen bonds. According to [13], the hydrogen bond energy for water is 18.8, while for methanol and ethanol is 25.9 kJ mol⁻¹. Considering that one water molecule has two hydrogen bonds, while alcohols have only one, it becomes obvious that the stability of the water structure is much higher.

Alcohol molecule is considered as a water molecule with one hydrogen atom substituted with a hydrocarbon radical [14]. The fraction of association, the composition and the form of associates depend on various factors. The association fraction of the alcohols decreases with increase of alcohols molecular weight. The so-called weighting effect is typical to them [14–16]. Its physical existence is associated with a weakening of hydrogen bonds due to steric factor and thermal vibrations of the particles. The rise in temperature and the addition of some non-polar substances act in the same direction as the weighting effect. The effect of weighting is also revealed in the fact that their structure becomes denser with an increase in the alcohols molecular weight [14].

* Corresponding author

It can be expected that the field action can change the structure of the alcohols, which should reveal in the change of their bulk and surface properties.

The aim of the work is to determine the changes in physical and chemical properties of propanol-1 and pentanol-1 and water, caused by the intermolecular interaction, as a result of exposure of electromagnetic field.

Research in this area has expanded the understanding of the nature of the interaction of electromagnetic field with the matter. Research in this area has expanded the understanding of the nature of the interaction of an electromagnetic field with matter.

Experimental

Propanol-1 (GOST 6006–78), pentanol-1 (chemically pure, TU 2632-106-4449379-07 at a concentration not less than 5 % and the water purified by using membrane distillation DME-1/B have been used. Specific conductivity of the water was 1.1 $\mu\text{s}/\text{cm}$.

Irradiation of alcohols and water was carried out in a contactless manner using a GZ-19A generator with a variable frequency in the range of 30–200 MHz. Generator power output was 1 watt. The voltage on the HF electrodes was 20–22 V. Cell of a capacitive type with a volume of 20 ml with the axially spaced electrodes has been used in the work.

The refractive index was determined using refractometer URL No. 77–2549 (accuracy ± 0.0001).

Determination of surface tension was carried out by weighing of drops (variety of stalagmometric method). Weighting of 50 drops leaked out of stalagmometry, was carried out on an analytical balance BM153M-II with an accuracy of ± 0.001 g. Deionized water has been used as the standard liquid. Thermostat TJ-TB-01 was used when studying the temperature dependence of surface tension of liquids. The temperature accuracy was ± 0.10 °C.

The evaporation of alcohol and water was performed from plastic Petri dishes (surface area of the liquid $S = 50 \text{ cm}^2$) at room temperature, (22 °C) for an hour, recording the mass loss of the dishes with the liquid every 10 minutes with the help of analytical balance BM153M-II. The experiment with irradiated and non-irradiated alcohols or water was performed simultaneously to ensure the same external conditions (atmospheric pressure, humidity and air temperature). Kinetic curves were plotted in the coordinates of the mass of evaporated liquid (m) vs time (t) based on the obtained data. The evaporation rate was determined from the slope of the kinetic curve.

Results and Discussion

Studies have shown that the refractive index (n) of propanol as a result of exposure to an electromagnetic field (EMF) practically does not change (the increase does not exceed 0.01 %). The increase in n is more signified for pentanol (0.03–0.06 %) (Table 1).

Table 1

Refractive index n of pentanol-1 exposed by electromagnetic field of different frequencies
($t_{\text{irr.}}=60 \text{ min}$, $T=295 \text{ K}$)

| f , MHz | 0 | 50 | 70 | 90 | 100 |
|----------------|---------------------|---------------------|---------------------|---------------------|---------------------|
| n | 1.4096 \pm 0.0002 | 1.4096 \pm 0.0001 | 1.4100 \pm 0.0001 | 1.4104 \pm 0.0002 | 1.4100 \pm 0.0001 |
| Δn , % | – | – | 0.03 | 0.06 | 0.04 |

The increase in refractive index is observed only at the 3 frequencies EMF: 70, 90 and 100 MHz. The effect for water is revealed at frequencies exceeding 100 MHz, and much higher — 0.10–0.15 % (Table 2).

Table 2

Refractive index of water exposed by electromagnetic field of different frequencies
($t_{\text{irr.}}=60 \text{ min}$, $T=295 \text{ K}$)

| f , MHz | 0 | 100 | 130 | 140 | 150 | 170 |
|----------------|---------------------|---------------------|---------------------|---------------------|---------------------|---------------------|
| n | 1.3330 \pm 0.0002 | 1.3338 \pm 0.0003 | 1.3345 \pm 0.0002 | 1.3344 \pm 0.0002 | 1.3343 \pm 0.0003 | 1.3350 \pm 0.0003 |
| Δn , % | - | 0.06 | 0.11 | 0.10 | 0.10 | 0.15 |

The refractive index of a liquid is related to its density by empirical relation:

$$n = 1 + a\rho, \quad (1)$$

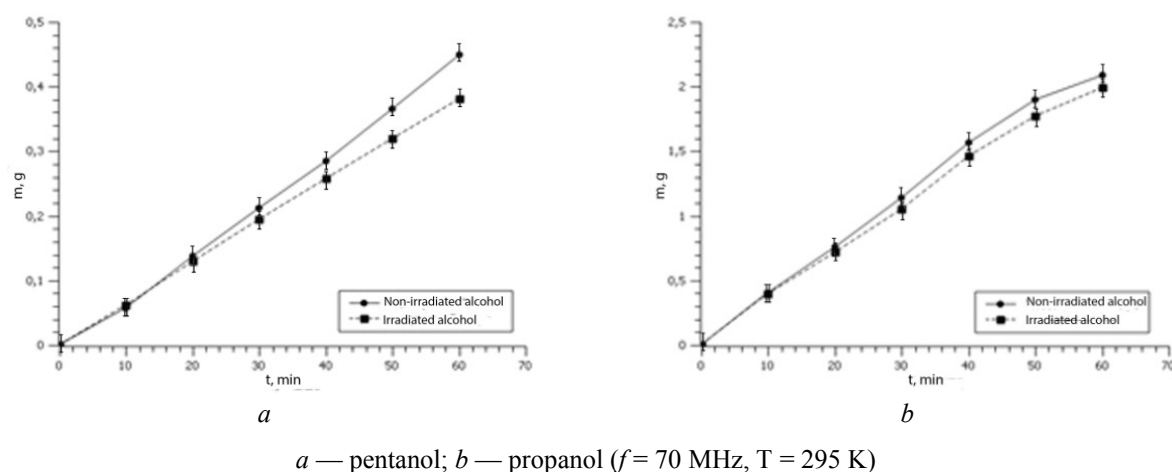
where n — is the refractive index; a — is an empirical coefficient; ρ — is the fluid density [17].

Therefore, it can be argued that the increase in n indicates a certain increase in the density of pentanol and water, which is most typical for water. And the density of a liquid is directly related to their structural organization.

The rate of evaporation is also determined by the force of intermolecular interactions in the liquid. The evaporation rate of irradiated and non-irradiated alcohols with the free surface at $T = 295$ K has been studied. The kinetic curves are presented in Figures 1 and 2. The evaporation rate was determined from the slope of the curves based on the mass of the evaporated alcohol (m) vs the time as:

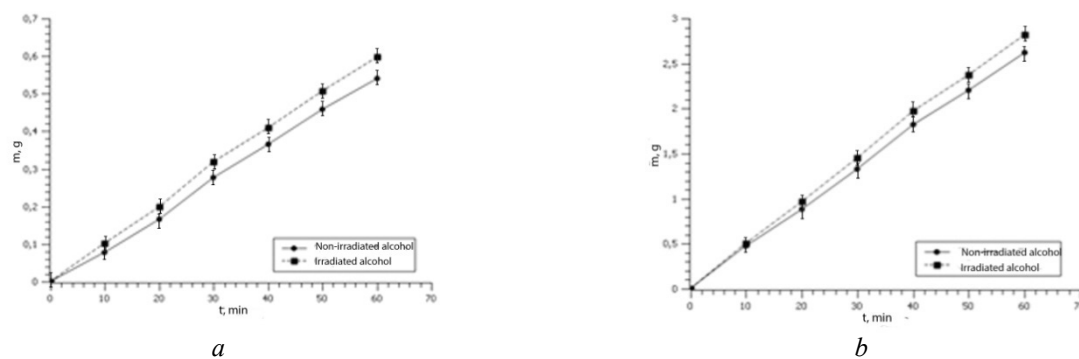
$$U = dm/dt \cdot S,$$

where dm — is the mass of the evaporated alcohol; dt — is the evaporation time; S — is the surface area of the alcohol.



a — pentanol; b — propanol ($f = 70$ MHz, $T = 295$ K)

Figure 1. Kinetic curves of evaporation



a — pentanol; b — propanol ($f = 90$ MHz, $T = 295$ K)

Figure 2. Kinetic curves of evaporation

The values of relative evaporation rate, irradiated by the field of various frequencies ($U_{rel.} = U_{irr.}/U_{non-irr.}$, where $U_{irr.}$ and $U_{non-irr.}$ — are evaporation rates of irradiated and non-irradiated alcohols, respectively) are presented in Tables 3 and 4.

Table 3

Relative evaporation rates of non-irradiated and irradiated with an electromagnetic field of different frequencies propanol ($T = 295$ K)

| Frequency f , MHz | 0 | 70 | 80 | 90 |
|---------------------------------------|-----------|-----------|-----------|-----------|
| Relative rate $U_{irr.}/U_{non-irr.}$ | 1.00±0.01 | 1.27±0.01 | 1.24±0.01 | 1.08±0.02 |

Relative evaporation rates of non-irradiated and irradiated with an electromagnetic field of different frequencies pentanol (T = 295 K)

| Frequency f , MHz | 0 | 50 | 70 | 90 |
|-------------------------------------|-----------|-----------|-----------|-----------|
| Relative rate $U_{irr}/U_{non-irr}$ | 1.00±0.02 | 1.15±0.02 | 0.85±0.01 | 1.10±0.03 |

The rate of evaporation of the irradiated alcohols differs markedly from the rate of evaporation of non-irradiated alcohol, both upward and downward. Pentanol-1 evaporates at a maximum rate after exposure to EMF with a frequency of 50 MHz, and propanol-1 — after exposure to a field with a frequency of 70–80 MHz. Reducing the rate of evaporation is observed for the pentanol at a frequency of 70 MHz.

Experiments have shown a slowdown in water evaporation as a result of exposure to EMF in the frequency range of 120 and 190 MHz. The maximum effect is achieved for EMF frequencies of 130 and 170 MHz and is approximately 20 %, as evidenced by the reduced mass of fluid evaporated in two hours (Table 5).

Mass of evaporated water irradiated with an electromagnetic field of different frequencies (T = 295 K, t_{irr} = 2 h)

| f , MHz | Mass of evaporated water, g | Δm , % |
|-----------|-----------------------------|----------------|
| 0 | 1.68±0.05 | – |
| 130 | 1.35±0.04 | 19.6 |
| 140 | 1.50±0.05 | 10.7 |
| 150 | 1.37±0.02 | 18.4 |
| 160 | 1.39±0.07 | 17.3 |
| 170 | 1.35±0.05 | 19.6 |
| 190 | 1.48±0.05 | 11.9 |

The irradiation time also influences affects the magnitude of the effect in addition to EMF frequency. Experiments on exposure of water by a field of the particular frequencies (130, 150 and 170 MHz) for different periods of time (from 30 minutes to 3 hours) were carried out.

It has been shown that 30 minutes is enough for maximum effect. When 2- and 3-hour effects of the field, evaporation slowing was exactly the same as at 30 minutes. Slower evaporation of water exposed to the electromagnetic influence, may be a consequence of strengthening of intermolecular interactions. Confirmation of this hypothesis is the previously detected increase in the boiling temperature and evaporation heat of water, which also depend on the energy of intermolecular interactions [7].

The surface tension of liquids also depends on intermolecular interactions, since it is determined by the work of the molecules coming out from the phase volume to the surface. Measurement of the surface tension of pentanol demonstrated its significant increase as a result of exposure to EMF at only three frequencies: 50, 70 and 90 MHz (Fig. 3). The maximum surface tension increases by 3.5 % at a frequency of 50 MHz (for non-irradiated alcohol $\sigma = 25.6 \pm 0.1$ MJ/m²).

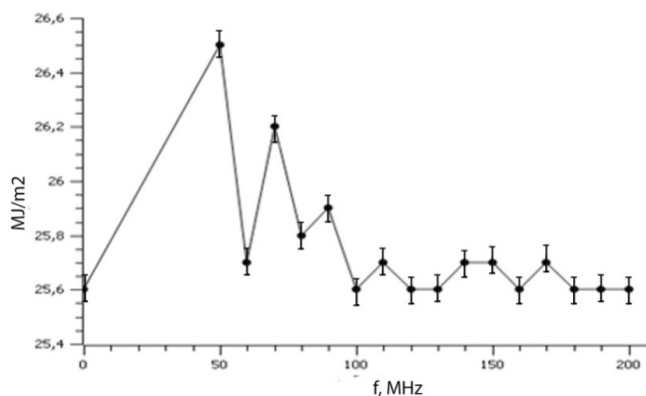


Figure 3. Dependence of surface tension of pentanol on the frequency of the electromagnetic field (T = 298 K)

Since all previous studies have shown an increase in the efficiency of field effects with an increase in the exposure time, the time dependence of the changes in surface tension during irradiation of pentanol to field of frequency 50.70 and 90 MHz was studied. Figure 4 shows the kinetic curves for two frequencies of 50 and 70 MHz.

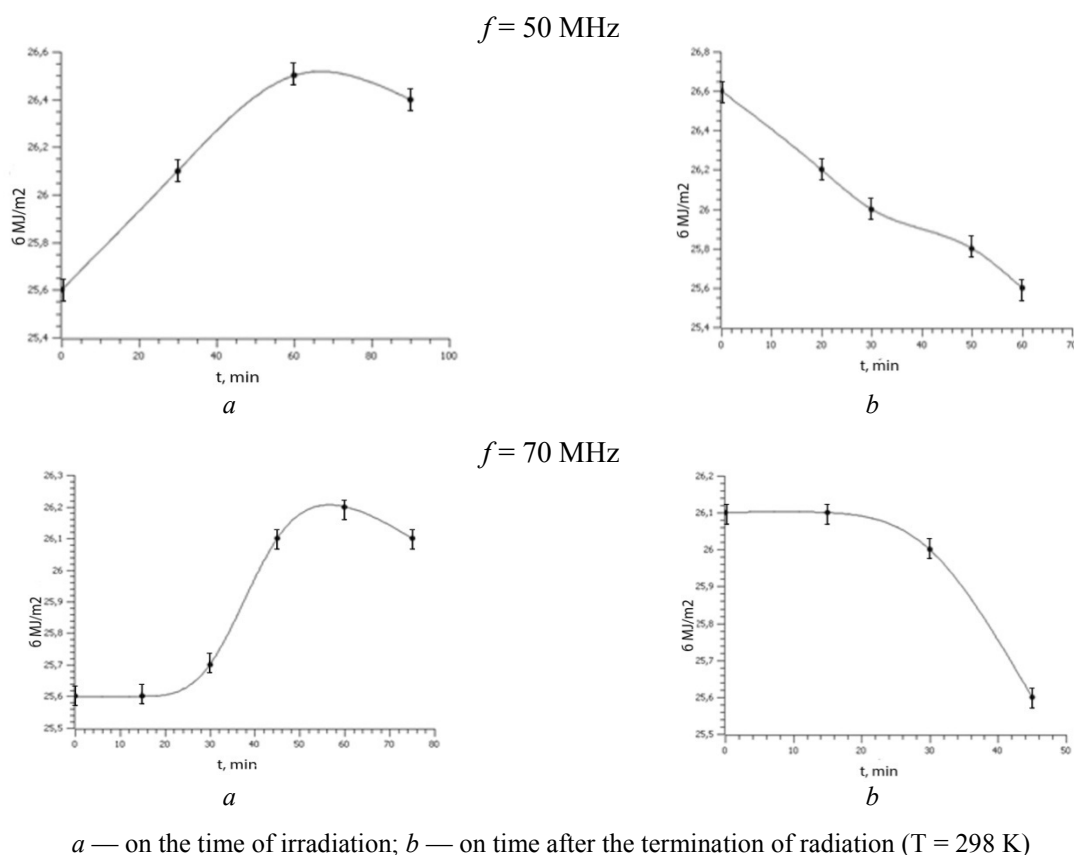


Figure 4. Dependence of surface tension of pentanol

It was detected the intensification effect by increasing the exposure time to 1 hour. Further exposure led to a slight decrease in surface tension. It is the most evident at the frequency of 90 MHz. A gradual approach of the measured value to the initial amount was observed after the termination of the EMF emission (Fig. 4b). It should be noted that the relaxation of surface tension began due to the ongoing exposure of alcohol. The relaxation time ranged from 45 minutes to 1 hour depending on the field frequency.

Strengthening of the effect and relaxation occurred simultaneously when pentanol was irradiated to a field with a frequency of 50 MHz. At the same time, the relaxation of the properties to the initial value occurred faster than the increase effect when it was exposed to fields with a frequency of 70 and 90 MHz (Table 6).

Table 6

Surface tension, increase and relaxation times for irradiated pentanol ($T = 298\text{ K}$)

| f , MHz | 50 | 70 | 90 |
|---------------------------------|----------|----------|----------|
| σ , MJ/M ² | 26.5±0.2 | 26.2±0.1 | 25.9±0.1 |
| $\Delta\sigma$, % | 3.5 | 2.6 | 1.4 |
| Increase time σ , min. | 60 | 60 | 60 |
| Relaxation time σ , min. | 60 | 45 | 45 |

Similar studies have been carried out for propanol-1. In this case, the surface tension change was well signified only for the frequencies of 70 and 80 MHz, and there was not an increase but there was a decrease by 10.9 % and 3.9 % respectively (Fig. 5).

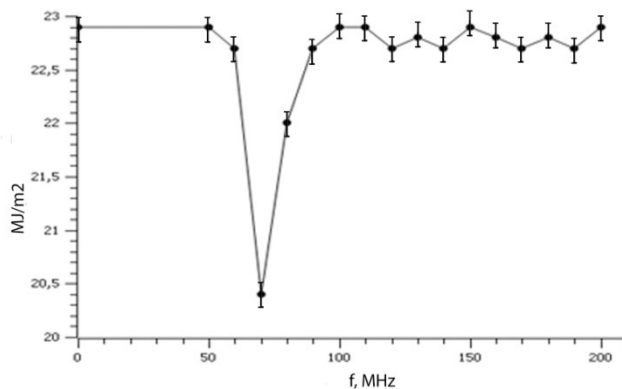
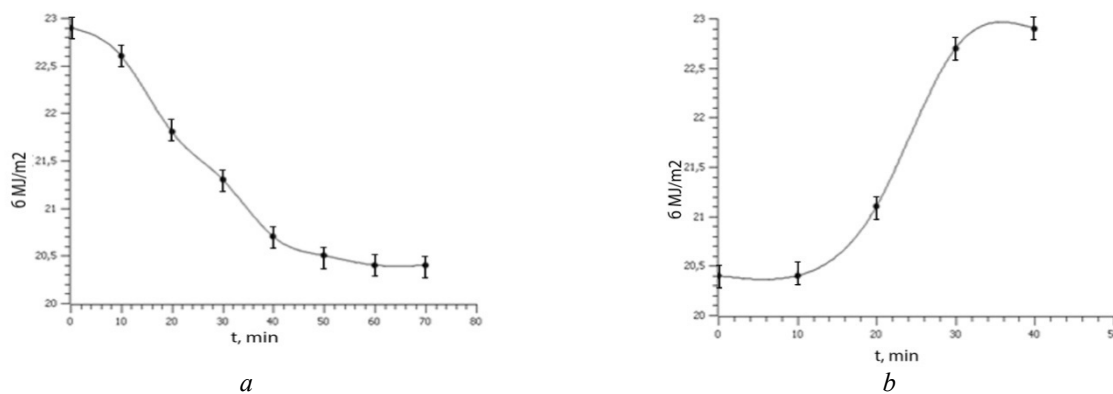


Figure 5. Dependence of surface tension of propanol on the frequency of the electromagnetic field (T = 298 K)

The maximum effect in this case was also achieved with an exposure time, of 1 hour. After the termination of the field effects the surface tension of propanol returns to its initial value in 40 minutes (Fig. 6). The presence of relaxation processes proves that the results obtained are not associated with the error in determination of the surface tension.



a — on the time of irradiation; b — on time after termination of irradiation (f = 70 MHz)

Figure 6. Dependence of surface tension of propanol

The EMF exposure on water, as well as on the pentanol led to an increase in surface tension, mainly at frequencies of 130 and 170 MHz. The maximum effect is achieved within 1 hour (Table 7). After termination of irradiation the surface tension of water decreased for 3 months, during which we conducted observations.

Table 7

Change of surface tension of water depending on the time of exposure to electromagnetic fields ($\sigma_0 = 72.8 \text{ MJ/m}^2$, T=295 K)

| t, min | 30 | 60 | 90 | 120 | 150 |
|---|----------|----------|----------|----------|----------|
| σ , MJ/m ² , f = 130 MHz | 74.7±0.7 | 82.2±1.1 | 82.3±0.9 | 82.2±0.7 | 82.2±1.0 |
| σ , MJ/m ² , f = 170 MHz | 77.4±0.8 | 82.5±1.0 | 82.5±1.0 | 82.5±0.9 | 82.5±1.1 |

It is known that the surface tension of the liquid reduces with increasing temperature. This occurs on the one hand, due to the convergence of the force fields of coexisting phases (liquid — vapor), and, on the other hand, due to the weakening of the intermolecular interactions, as a result of an increase in the intensity of the thermal motion of molecules [18]. Conducted studies have shown that the surface tension of water activated by EMF also decreases with increasing temperature, but to a greater extent compared to non-activated (Table 8). Temperature coefficient $d\sigma/dT$ for non-activated water is $(-0.154) \text{ MJ/m}^2 \cdot \text{K}$ [19]. After its electro-

magnetic treatment the linear character of the dependence of surface tension on temperature is kept, however, the temperature coefficient increases sharply $d\sigma/dT = -0.251 \text{ MJ/m}^2 \cdot \text{K}$ (130 and 170 MHz). For irradiated propanol temperature coefficient of surface tension has a lower value $d\sigma/dT = -0.05-0.06 \text{ MJ/m}^2 \cdot \text{K}$ compared to non-irradiated, for which $d\sigma/dT = -0.08 \text{ MJ/m}^2 \cdot \text{K}$ [19].

The thermodynamic functions of the surface layer (internal energy (U_s), entropy (S_s) and heat of unit of area formation (q_s)) were calculated based on the temperature dependence of the surface tension of water and propanol. The calculation was performed using the equations of Gibbs-Helmholtz [18]:

$$U_s = \sigma - T \cdot (d\sigma/dT)_p; \quad (2)$$

$$U_s = \sigma + q_s; \quad (3)$$

$$S_s = - (d\sigma/dT)_p. \quad (4)$$

The results of the calculations are presented in Tables 8 and 9.

Table 8

Thermodynamic functions of the surface layer of non-activated and activated water (170 MHz) in the temperature range 289–300 K

| T, K | 289 | 293 | 295 | 296 | 297 | 300 |
|----------------------------|------|------|------|------|------|------|
| non-activated water | | | | | | |
| σ , mJ/m^2 | 73.3 | 72.7 | 72.5 | 72.3 | 72.1 | 71.6 |
| q_s , mJ/m^2 | 43.6 | 44.3 | 44.5 | 44.7 | 44.8 | 45.3 |
| U_s , mJ/m^2 | 117 | 116 | 117 | 117 | 117 | 117 |
| activated water (170 MHz) | | | | | | |
| σ , mJ/m^2 | 82.2 | 77.1 | 76.2 | 73.2 | 72.2 | 69.2 |
| q_s , mJ/m^2 | 72.5 | 73.5 | 74.3 | 74.3 | 74.5 | 75.3 |
| U_s , mJ/m^2 | 155 | 151 | 150 | 147 | 146 | 144 |

Table 9

Thermodynamic functions of the surface layer of water activated by electromagnetic field of different frequencies

| f , MHz | 0 | 130 | 160 | 165 | 170 |
|-------------------------|-----------|-----------|-----------|-----------|-----------|
| U_s , mJ/m^2 | 117 | 153–145 | 138 | 129 | 155–144 |
| q_s , mJ/m^2 | 43.6–45.3 | 71.5–74.8 | 70.4–75.0 | 67.0–68.4 | 72.5–75.3 |
| S_s , mJ/m^2 | 0.154 | 0.251 | 0.241 | 0.160 | 0.251 |

Similar calculations have been carried out for propanol (Table 10).

Table 10

Thermodynamic functions of the surface layer of propanol

| Thermodynamic function | Unirradiated propanol | | | Irradiated propanol | | | | | |
|-----------------------------|-----------------------|------|------|------------------------|------|------|------------------------|------|------|
| | | | | $(f = 70 \text{ MHz})$ | | | $(f = 80 \text{ MHz})$ | | |
| T, K | 276 | 282 | 288 | 276 | 282 | 288 | 276 | 282 | 288 |
| σ , mJ/m^2 | 24.4 | 23.9 | 23.4 | 23.9 | 23.4 | 23.3 | 24.2 | 23.7 | 23.4 |
| U_s , J/m^2 | 46.5 | 46.5 | 46.4 | 37.7 | 37.5 | 37.7 | 40.8 | 40.6 | 40.6 |
| q_s , mJ/m^2 | 22.1 | 22.6 | 23.0 | 13.8 | 14.1 | 14.4 | 16.6 | 16.9 | 17.2 |
| $S_{s,s}$, mJ/m^2 | 0.08 | 0.08 | 0.08 | 0.05 | 0.05 | 0.05 | 0.06 | 0.06 | 0.06 |

As can be seen from Table 10, the heat of formation of the surface as an entropy component makes a significant contribution to the total surface energy. It is about half of the total surface energy for many organic substances, [18]. This is due to the fact that when molecules move from one liquid volume to its surface, bonds are broken and the substance is in a state close to the vapor phase, with higher entropy on the surface. Values U_s , q_s , and S_s of irradiated propanol-1 are significantly lower than the corresponding values for non-irradiated alcohol. Therefore, it can be concluded that the intermolecular interaction is weakened as a result of field exposure. On the contrary, the total surface energy of water increases by both enthalpy and entropy factors (Tables 8, 9). This indicates the opposite effect of the field on water, that is, on the strengthening of its structure.

Conclusions

Thus, the studies carried out have shown that alcohol, as well as water, is capable to absorb the energy of the electromagnetic field, changing its physical properties, which can be a consequence of changes in the supramolecular organization of these liquids. The absorption of electromagnetic energy is selective. Each liquid corresponds to a specific set of frequencies, where there are change in surface tension, refractive index and evaporation rate. The maximum change in properties is observed at 70 MHz for propanol-1 and at 50 MHz for pentanol-1. The extreme frequencies for water are 130 and 170 MHz and they differ significantly from those values. The magnitude of the field response at these frequencies is markedly different; the effect is much more pronounced in the water medium.

There is a common "cumulative effect" for all three liquids, which is a gradual increase in property change during irradiation. For all liquids there is a "saturation", i.e. the change in measured properties increases within 60 min. Further irradiation is ineffective. At the same time, although further action of the field on water does not lead to changes, the relaxation process begins in alcohols (the property is aimed at its initial value). With regard to the rate of evaporation of liquids, there is a correlation between its change for irradiated systems and the change in surface tension. The deceleration of evaporation corresponds to the value of the surface tension for water and pentanol-1, which increased as a result of field exposure. The acceleration of evaporation corresponds to the reduced surface tension value for propanol-1. These results suggest a greater cohesive interaction in activated water and pentanol and its weakening in propanol. The different effects of the two alcohols can probably be associated either with differences in their structural organization or with the range of studied frequencies. It is possible that different effects can be observed when exposed to a field of higher or lower frequencies.

References

- 1 Стехин А.А. Структурированная вода: нелинейные эффекты / А.А. Стехин, Г.В. Яковлева. — М.: Изд-во ЛКИ, 2008. — 320 с.
- 2 Рахманин Ю.А. Вода — космическое явление / Ю.А. Рахманин, В.К. Кондратов. — М.: РАЕН, 2002. — 402 с.
- 3 Гапочка Л.Д. Воздействие электромагнитного излучения КВЧ- и СВЧ-диапазонов на жидкую воду / Л.Д. Гапочка // Вестн. МГУ. Сер. Физика. Астрономия. — 1994. — Т. 35, № 4. — С. 71–76.
- 4 Красиков Н.Н. Действие электромагнитного поля на жидкости, осуществляемое без контакта с потенциалообразующими электродами / Н.Н. Красиков, О.В. Шуваева // Журн. физ. хим. — 2000. — Т. 74, № 6. — С. 1133–1135.
- 5 Lee S.H. et al. Changes in the electrical conductivity, infrared absorption, and surface tension of partially-degassed and magnetically-treated water / S.H. Lee // Journal of Molecular Liquids. — 2013. — Vol. 187. — P. 230–237.
- 6 Бессонова А.П. Частотная дисперсия физико-химических свойств воды, подвергшейся электромагнитному воздействию / А.П. Бессонова, И.Е. Стась // Изв. вузов. Химия и хим. технол. — 2010. — Т. 53, Вып. 4. — С. 48–50.
- 7 Чиркова В.Ю. Изменение когезионных и адгезионных характеристик воды как результат электромагнитного воздействия / В.Ю. Чиркова, Е.А. Шарлаева, И.Е. Стась // Изв. вузов. Прикл. химия и биотехнол. — 2019. — Т. 9(2). — С. 222–231.
- 8 Chirkova V.Yu. Boiling temperature and the enthalpy of water vaporization exposed to high frequency electromagnetic field / V.Yu. Chirkova, Ye.A. Sharlayeva, I.Ye. Stas // Bulletin of the university of Karaganda. Chemistry. — 2019. — Vol. 94(2). — P. 51–55.
- 9 Pang X.F. The changes of macroscopic features and microscopic structures of water under influence of magnetic field / X.F. Pang, B. Deng // Physica B: Condensed Matter. — 2008. — Vol. 403, № 19. — P. 3571–3577.
- 10 Лаптев Б.И. Структурные изменения в воде и водных растворах электролитов при различных внешних воздействиях / Б.И. Лаптев // Вестн. Томск. гос. ун-та. Сер. Химия. — 2015. — № 1. — С. 13–24.
- 11 Турсыматова О.И. Изучение влияния электромагнитного излучения на воду и водные растворы методом ядерного магнитного резонанса / О.И. Турсыматова, С.А. Турсынбай // Наука и мир. — 2015. — Т. 1, № 3. — С. 31–33.
- 12 Сойфер В.Н. Водородная связь в органической химии / В.Н. Сойфер // Соросов. обр. журн. — 1999. — № 52. — С. 58–64.
- 13 Неводные растворители / под ред. Т.М. Ваддингтона. — М.: Химия, 1971. — 372 с.
- 14 Крестов Г.А. Термодинамика процессов в растворах / Г.А. Крестов. — Л.: Химия, 1984. — 272 с.
- 15 Структурная самоорганизация в растворах и на границе раздела фаз / отв. ред. А.Ю. Цивадзе. — М.: Изд-во ЛКИ, 2008. — 544 с.
- 16 Рабинович И.Б. Влияние изотопии на физико-химические свойства жидкостей / И.Б. Рабинович. — М.: Наука, 1968. — 196 с.
- 17 Справочник химика. — Т. 1. — М.: Химия, 1966.

18 Курс коллоидной химии. Поверхностные явления и дисперсные системы / Ю.Г. Фролов. — М.: Химия, 1988. — 34 с.

19 Краткий справочник физико-химических величин. — 8-е изд. / под ред. А.А. Равделя и А.М. Пономаревой. — Л.: Химия, 1983. — С. 20, 21.

И.Е. Стась, С.С. Павлова

Ультражоғары жиіліктегі электромагниттік өрістің ассоцияланған сұйықтықтардың қасиеттеріне әсері

Электромагниттік өрістің су, пропанол-1, пентанол-1 сыну көрсеткішіне, булану жылдамдығына және беткі керілуіне әсері зерттелді. Бұл сұйықтықтардың қасиеттері өрістің жиілігіне және оның әсер ету уақытына байланысты екендігі көрсетілген. Өрістің су мен спирттердің құрылымына әсері таңдамалы; олардың қасиеттерінің өзгеруі әр сұйықтық үшін жеке жиіліктерде жүреді. Электромагниттік өрістің жиілігіне байланысты спирттердің булануының баяулауы да, үдеуі де жүреді. Өрістің әсеріне ұшыраған судың булануы барлық зерттелген жиілік диапазонында баяулайды. Пентанол мен судың беткі керілуі артып, пропанол — азаяды. Өріс әсері тоқтағаннан кейін спирттердің қасиеттері бастапқы мәндеріне оралады, ал судың қасиеттері өзгеріссіз қалады. Су мен пропанол-1 бетінің термодинамикалық функциялары беттік керілудің температуралық тәуелділігі негізінде есептеледі. Су үшін беттің жалпы ішкі энергиясы артып, пропанол-1 үшін азаятыны көрсетілді, бұл сулы ортадағы құрылымның беріктеуін және пропанол-1 ортасында молекулааралық өзара әрекеттесудің әлсіреуін көрсетеді.

Кілт сөздер: су, пропанол-1, пентанол-1, электромагниттік өріс, жиілік, сыну көрсеткіші, булану жылдамдығы, беттік керілу.

И.Е. Стась, С.С. Павлова

Влияние электромагнитного поля ультравысоких частот на свойства ассоциированных жидкостей

Изучено влияние электромагнитного поля на показатель преломления, скорость испарения и поверхностное натяжение воды, пропанола-1 и пентанола-1. Было показано, что свойства этих жидкостей зависят от частоты поля и времени его воздействия. Действие поля на структуру воды и спиртов избирательно; изменения их свойств происходят при частотах, индивидуальных для каждой жидкости. В зависимости от частоты электромагнитного поля происходит как замедление, так и ускорение испарения спиртов. Испарение воды, подвергшейся воздействию поля, замедляется во всем исследуемом диапазоне частот. Поверхностное натяжение пентанола и воды увеличивается, а пропанола — уменьшается. После прекращения действия поля свойства спиртов возвращаются к своим исходным значениям, а свойства воды остаются неизменными. Термодинамические функции поверхности воды и пропанола-1 рассчитаны на основе температурной зависимости поверхностного натяжения. Было продемонстрировано, что полная внутренняя энергия поверхности увеличивается для воды и уменьшается для пропанола-1, что указывает на упрочнение структуры в водной среде и ослабление межмолекулярного взаимодействия в среде пропанола-1.

Ключевые слова: вода, пропанол-1, пентанол-1, электромагнитное поле, частота, показатель преломления, скорость испарения, поверхностное натяжение.

References

- 1 Stekhin, A.A., & Yakovleva, G.V. (2008). *Strukturirovannaiia voda: nelineinye efekty [Structured water: Nonlinear effects]*. Moscow: Izdatelstvo LKI [in Russian].
- 2 Rakhmanin, Yu.A., & Kondratov, V.K. (2002). *Voda — kosmicheskoe yavlenie [Water — space phenomenon]*. Moscow: RAEN [in Russian].
- 3 Gapochka, L.D. (1994). Vozdeistvie elektromagnitnoho izlucheniia KVCH- i SVCH-diapazonov na zhidkuiu vodu [The influence of electromagnetic radiation of EHF and SHF-ranges on liquid water]. *Vestnik Moskovskoho gosudarstvennogo universiteta. Seriya Fizika. Astronomiia — Bulletin of Moscow State University. Ser. Physics. Astronomy*, 35, 4, 71–76 [in Russian].
- 4 Krasikov, N.N. & Shuvaeva, O.V. (2000). Deistvie elektromagnitnoho polia na zhidkosti, osushchestvliamoe bez kontakta s potentsialozadaiushchimi elektrodami [The influence of electromagnetic fields on fluid, carried out without contact with potential-assigned electrodes]. *Zhurnal fizicheskoi khimii — Journal of Physical Chemistry*, 74, 6, 1133–1135 [in Russian].

- 5 Lee, S.H., et al. (2013). Changes in the electrical conductivity, infrared absorption, and surface tension of partially-degassed and magnetically-treated water. *Journal of Molecular Liquids*, 187, 230–237.
- 6 Bessonova, A.P. & Stas', I.E. (2010). Chastotnaia dispersiia fiziko-khimicheskikh svoistv vody, podverhsheisia elektromagnitnomu vozdeistviu [Frequency dispersion of the physical and chemical properties of water exposed to the electromagnetic influence]. *Izvestiia vuzov. Khimiia i khimicheskaiia tekhnolohiia — News of Universities. Chemistry and chemical technology*, 53, 4, 48–50 [in Russian].
- 7 Chirkova, V.Yu., Sharlaeva, E.A., & Stas', I.E. (2019). Izmenenie kohezionnykh i adhezionnykh kharakteristik vody kak rezultat elektromagnitnoho vozdeistviia [Change of cohesive and adhesive characteristics of water as a result of electromagnetic influence]. *Izvestiia vuzov. Prikladnaia khimiia i biotekhnolohiia — News of universities. Applied chemistry and biotechnology*, 9(2), 222–231 [in Russian].
- 8 Chirkova, V.Yu., Sharlayeva, E.A., & Stas', I.E. (2019). Boiling temperature and the enthalpy of water vaporization exposed to high frequency electromagnetic field. *Bulletin of the university of Karaganda. Chemistry*, 94(2), 51–55.
- 9 Pang, X.F., & Deng, B. (2008). The changes of macroscopic features and microscopic structures of water under influence of magnetic field. *Physica B: Condensed Matter*, 403, 19, 3571–3577.
- 10 Laptev, B.I. (2015). Strukturnye izmeneniia v vode i vodnykh rastvorakh elektrolitov pri razlichnykh vneshnikh vozdeistviakh [Structural changes in water and aqueous electrolyte solutions under various external influences]. *Vestnik Tomskogo gosudarstvennogo universiteta. Seriia Khimiia — Bulletin of the Tomsk State University. Chemistry series*, 1, 13–24 [in Russian].
- 11 Tursymatova, O.I., & Tursynbay, S.A. (2015). Izuchenie vliianiia elektromagnitnoho izlucheniia na vodu i vodnye rastvory metodom yadernogo magnitnoho rezonansa [Study of the effect of electromagnetic radiation on water and aqueous solutions by the method of nuclear magnetic resonance]. *Nauka i mir — Science and World*, 1, 3, 31–33 [in Russian].
- 12 Soifer, V.N. (1999). Vodorodnaia sviaz v orhanicheskoi khimii [Hydrogen bond in organic chemistry]. *Sorosovskii obrazovatelnyi zhurnal — Sorosovsk educational Journal*, 52, 58–64 [in Russian].
- 13 Vaddington, T.M. (Ed.) (1971). *Nevodnye rastvoriteli [Non-aqueous solvents]*. Moscow: Khimiia [in Russian].
- 14 Krestov, G.A. (1984). *Termodinamika protsessov v rastvorakh [Thermodynamics of processes in solutions]*. Leningrad: Khimiia [in Russian].
- 15 Tsivadze, A.Yu. (Ed.) (2008). *Struktornaia samoorhanizatsiia v rastvorakh i na hranitse razdela faz [Structural self-organization in solutions and at the interface]*. Moscow: Izdatelstvo LKI [in Russian].
- 16 Rabinovich, I.B. (1968). *Vlianie izotopii na fiziko-khimicheskie svoistva zhidkostei [Effect of isotope on the physical and chemical properties of liquids]*. Moscow: Nauka [in Russian].
- 17 *Spravochnik khimika [The chemist's handbook]*. (1966). (Vol. 1). Moscow: Khimiia [in Russian].
- 18 Frolov Yu.G. (1988). *Kurs kolloidnoi khimii. Poverhnostnye yavleniia i dispersnye sistemy [Course of colloid chemistry. Surface phenomena and disperse systems]*. Moscow: Khimiia [in Russian].
- 19 Ravdel, A.A., & Ponomareva, A.M. (Eds.) (1983). *Kratkii spravochnik fiziko-khimicheskikh velichin [Quick reference of physical and chemical values]*. (8th ed.). Leningrad: Khimiia [in Russian].

Information about authors

Stas', Irina Evgen'evna — Candidate of Chemical Sciences, Associate Professor of the Department of Physical and Inorganic Chemistry, Altai State University, Lenin Ave., 61, 656049, Barnaul, Russia; e-mail: irinastas@gmail.com

Pavlova, Svetlana Stanislavovna — Candidate of Technical Sciences, Senior Lecturer at the Institute of Oil and Gas, Ugra State University, Chekhov Street 16, 628012, Khanty-Mansiysk, Russia; e-mail: pavlova_ss@mail.ru; <https://orcid.org/0000-0001-6137-3968>.

M.G. Shcherban', A.D. Solovyev, A.O. Saliakhova

*Perm State National Research University, Perm, Russia
(Corresponding author's e-mail: ma-she74@mail.ru)*

The correlation between the surface-active characteristics of SAFOL 23 – alcohol – water systems and the length of the alkyl radical of the alcohol

The effect of isobutyl and isoamyl alcohols on the surface-active characteristics of SAFOL 23 nonionic surfactant was studied. The surface tension isotherms (STI) of an aqueous solution of surfactant and its water-alcohol compositions are obtained. The structure of mixed micelles and the values of the surfactant interaction factor in the micelle, based on the STIs of SAFOL 23 – alcohol – water systems, were calculated. The dependence of surface activity on the SAFOL 23: alcohol ratio passes through a maximum, which is associated with the transition of alcohol from co-surfactant to co-solvent due to the increase in its quantity. The wetting process of high dispersed polytetrafluoroethylene (PTFE) by SAFOL 23 – alcohol – water compositions was studied, contact angle isotherms were constructed. The PTFE surface was hydrophilized by compositions at ratios which comply with surface activity maximum. SAFOL 23 is more adsorbed on the surface of the solid phase than on the liquid-gas interface. The appending of alcohol into an aqueous solution of surfactant changes the ratio between hydrophilic and lipophilic groups of the composition, which affects cloud point. It significantly expands the range of application of surfactants and allows the use of SAFOL 23 as a solubilizer, emulsifier and wetting agent.

Keywords: nonionic surfactant, micellization, mixed micelles, surface activity, adsorption, contact angle, wetting, hydrophilic-lipophilic balance.

Introduction

Surfactants are organic compounds of diphilic structure, containing in their composition the polar and non-polar parts [1]. Surfactants concentrate on the phase interface due to its structure peculiarities, cause a decrease in surface tension and significantly change the properties of the interphase surface. In this regard, they play a very significant role in such practical processes as wetting, dispersion, emulsification.

Nonionic surfactants are one of the most widely used surfactant class in industry [2]. Ethoxylated alcohols, alkyl acetylene glycols, condensation products of glucosides with fatty alcohols, carboxylic acids, and ethylene oxide are of the greatest interest among nonionic surfactants [3].

Most surfactant compositions are mixtures, which include various solvents. The components of such systems interact with each other. As a result, their physicochemical and surface-active characteristics change. The efficiency of use of the compositions depends on the influence of many factors: product uniformity, resistance to temperature effects, viscosity, etc [4].

It is necessary to study the basic physicochemical dependences to understand the behavior of such systems under various conditions and their useful for solving specific problems.

This work is devoted to the study of the isobutyl (IBA) and isoamyl (IAA) alcohols effect on the surface-active characteristics of SAFOL 23 nonionic surfactant.

Experimental

The objects of research were aqueous and water-alcohol solutions of nonionic surfactant SAFOL 23 manufactured by Sasol Olefins & Surfactants GmbH. Its general formula is $C_nH_{(2n+1)}O(C_2H_4O)_7$ where the carbon chain length $n = 10-13$. The surfactant belongs to the class of ethoxylated alcohols, which have higher biodegradability and lower toxicity compared to the widely used ethoxylated nonylphenols [5].

The studied solutions were prepared in the concentration range of the mixture $0.02-130.00 \text{ g}\cdot\text{L}^{-1}$ for the mass ratios of the system SAFOL 23 – alcohol: 1:0, 1:4, 2:3, 3:2, 4:1, 1:0. We observed areas of foliation for compositions SAFOL 23 – IBA – water with a ratio of SAFOL 23:IBA = 1:4 and SAFOL 23 – IAA – water

*Corresponding author.

with a ratio of SAFOL 23:IAA = 1:4 and 2:3 at concentrations of 40 g·L⁻¹ and higher. We couldn't include some results due to foliation of some compositions.

The surface tension of SAFOL 23 – alcohol – water, SAFOL 23 – water, alcohol – water, SAFOL 23 – alcohol systems was determined by a hanging drop method using a KRUSS DSA 25E tensiometer.

The value of the contact angle was measured by the lying drop method using the same device. It is impossible to wet powdered materials by direct methods, i.e. direct observation of a liquid drop on a particle. Therefore, we measured the contact angle by placing a liquid drop (diameter of 2 mm) on a pressed polytetrafluoroethylene (PTFE) powder, achieving reproducible values. The properties of the pressed surface were considered similar to the properties of individual particles [6, 7].

The composition of mixed micelles, according to [8, 9], was calculated by the formulas (1), (2):

$$1 = \frac{x_1^2 \ln\left(\frac{\alpha_1 C_{12}}{C_1 x_1}\right)}{(1-x_1)^2 \ln\left(\frac{\alpha_2 C_1}{C_2(1-x_1)}\right)}, \quad (1)$$

$$\beta = \frac{\ln\left(\frac{\alpha_1 C_{12}}{C_1 x_1}\right)}{(1-x_1)^2}, \quad (2)$$

where α_1 and α_2 are the mole fraction of SAFOL 23 and alcohol in mixture; x_1 and x_2 are the mole fraction of SAFOL 23 and alcohol in micelle; C_1 and C_2 is the CMC of SAFOL 23 and alcohol; C_{12} is the CMC of SAFOL 23 – alcohol system.

The adsorption at the liquid-gas interface of SAFOL 23 was determined according to the formula (3) [9]:

$$\Gamma_{LG} = -\frac{1}{RT} \frac{d\gamma}{d \ln C}, \quad (3)$$

where R is the universal gas constant; T is the temperature; γ is the surface tension at the liquid-gas interface; C is the concentration.

The adsorption isotherm at the solid-liquid interface in relative units, i.e. in comparison with the adsorption isotherm at the liquid-gas interface was determined by the formula (4) [9]:

$$\Gamma_{SL} = -\Gamma_{LG} \left(\cos \theta + \gamma_{LG} \frac{d \cos \theta}{d \gamma_{LG}} \right), \quad (4)$$

where γ_{LG} is the surface tension at the liquid-gas interface; Γ_{SL} and Γ_{LG} are the adsorption at the solid-liquid and the liquid-gas interface.

The cloud point was determined according to ISO 1065–91 [10]. The method consists in heating an aqueous solution of surfactant with a 5 g·L⁻¹ concentration to complete turbidity, cooling with continuous stirring, and determining the temperature at which the turbidity disappears.

The HLB of alcohols and a water-alcohol composition based on SAFOL 23 were calculated by using formulas (5)–(7) [11]:

$$HLB = 0.098t_c + 4.020, \quad (5)$$

where t_c is the cloud point.

$$\sum HLB = \omega_1 HLB_1 + \omega_2 HLB_2, \quad (6)$$

where $\sum HLB$ is the HLB of the mixture system; ω_1 and ω_2 are the mass fraction of the components; HLB_1 and HLB_2 are the HLB of individual components.

$$HLB = \frac{20M_h}{M}, \quad (7)$$

where M_h is the molar mass of the OH group; M is the molar mass of the alcohol.

Results and Discussion

Mixed micellization processes were studied for various SAFOL 23:alcohol ratios. We used pseudo-binary approach, which consists of considering the ternary mixture as a binary [12]. The composition SAFOL 23 – alcohol was considered as the first component of the mixture, and water as the second. The surface tension isotherms (STI) of the examined ternary mixtures based on SAFOL 23 (Fig. 1) have the typical

form for colloidal surfactants [13]: the surface tension decreases sharply at low concentrations of surfactants in the solution, but the curve reaches a horizontal plateau (the critical micelle concentration (CMC)).

A sharp reduce in surface tension at the low concentration range is associated with the formation of a monomolecular layer. The area almost parallel to the abscissa axis corresponds to the transition of surfactant molecules into the solution volume and the formation of micelles, initially spherical, then cylindrical.

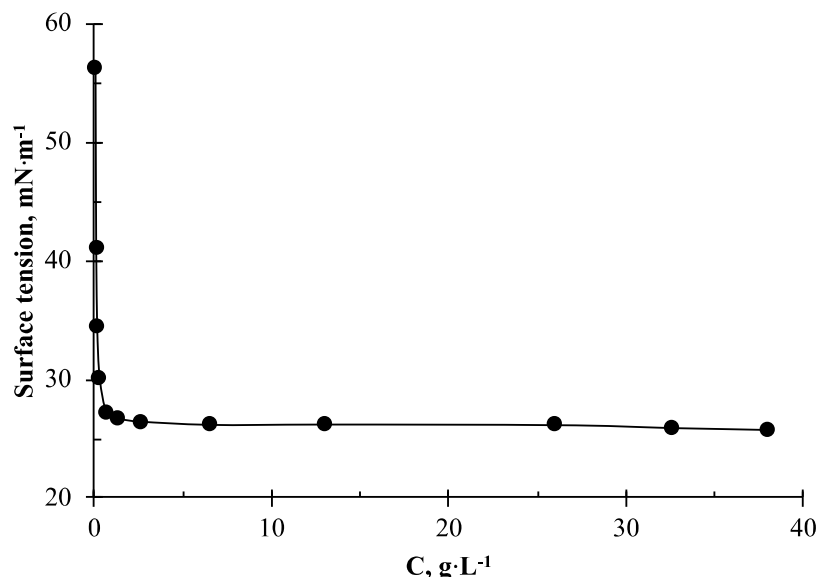


Figure 1. The surface tension isotherm of the water-alcohol composition SAFOL 23 (SAFOL 23:IBA = 3:2)

The surface-active characteristics of the individual compounds and their mixtures are presented in Table 1. The CMC were determined by the universal method for all surfactants — the concentration corresponding to the kink on the surface tension isotherm in semilogarithmic coordinates. Surface activity was calculated as the tangent of the slope of the initial portion of the STI.

Table 1

Surface-active characteristics of compositions

| Composition | γ_{\min} , mN·m ⁻¹ | CMC, g·L ⁻¹ | G, mN·m ² ·kg ⁻¹ |
|--|--------------------------------------|------------------------|--|
| SAFOL 23 – water | 26.45 | 0.27 | 169.05 |
| IBA – water | 25.81 | 8.80 | 5.32 |
| SAFOL 23 – IBA – water (SAFOL 23:IBA = 3:2) | 24.91 | 0.17 | 290.51 |
| SAFOL 23 – IAA | 27.76 | – | – |
| IAA – water | 30.12 | 3 | 14.16 |
| SAFOL 23 – IAA – water (SAFOL 23:IAA = 3:2) | 23.97 | 0.22 | 218.83 |
| SAFOL 23 – IAA | 25.16 | – | – |

Figures 2, 3 show the STI of the SAFOL 23 – alcohol – water systems (SAFOL 23:alcohol = 3:2), SAFOL 23 – water, alcohol – water, SAFOL 23 – alcohol in semilogarithmic coordinates. The curves show us, that the studied alcohols are not surface-active, however, their appending into the SAFOL 23 solution promotes an increase in the surface activity of the mixture in comparison with an individual surfactant. This phenomenon is associated with the formation of mixed micelles and a synergistic effect [14].

The compositions of mixed micelles and the values of the surfactant interaction factor β in the micelle were calculated by formulas (1) and (2) using the Rosen and Rubin method [8, 9]. The results are presented in Table 2. The interaction factor β is a quantitative characteristic of molecular interactions between surfactants in mixed micelles and, in the case of negative values, corresponds to the mutual attraction of the components in the mixture.

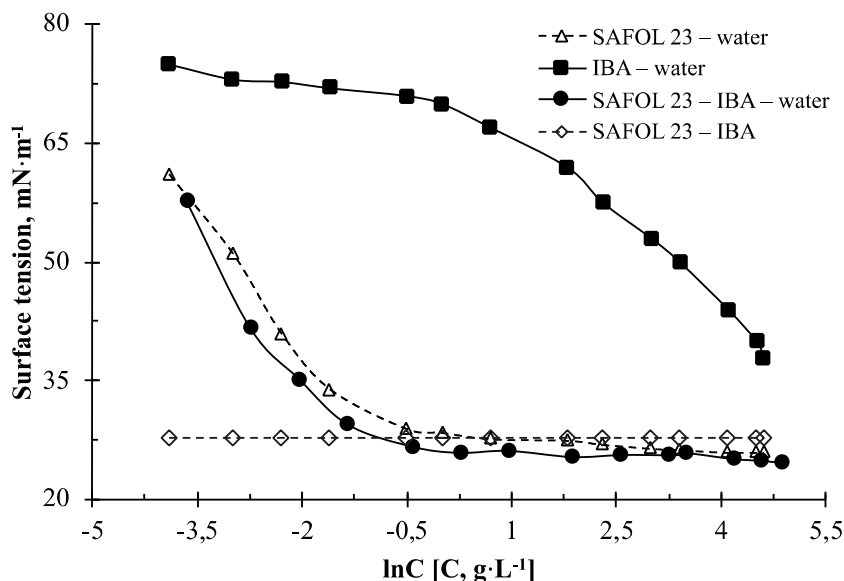


Figure 2. The surface tension isotherm of water-alcohol compositions based on SAFOL 23 and IBA

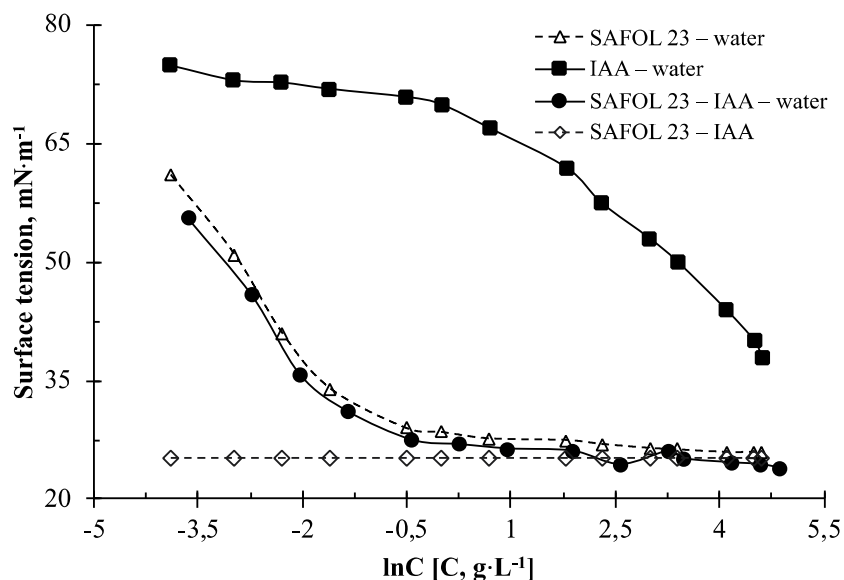


Figure 3. The surface tension isotherm of water-alcohol compositions based on SAFOL 23 and IAA

It is known that synergism during micellization in surfactant mixtures can be discussed under two conditions: $\beta < 0$, $|\ln(C_1/C_2)| < |\beta|$ — what is done in our case, i.e. alcohol behave itself as a co-surfactant and is incorporated into the micelles in this concentration range.

In all cases the dependence of surface activity on the mole fraction of surfactants is extreme (Fig. 4), while with rising radical length the surface activity of the corresponding compositions falls, and the position of the maximum shifts toward a higher surfactant content in the mixture. The force of attraction between the molecules of SAFOL 23 and the alcohol also slightly decreases with increasing length of the radical.

The similar dependence was observed by N.A. Lyapunov in the study of the surface activity of cationic surfactants in the presence of ethyl alcohol [15]. This dependence can be explained by starting from a certain concentration, the alcohol does not behave as a co-surfactant, it behaves as a co-solvent, causing the disaggregation of micelles. In addition, there is no need for the aggregation of surfactant molecules into micelles when dissolved in alcohol, because the solvent contains hydrophilic and hydrophobic groups.

The results of the study of the composition of mixed micelles SAFOL 23 – alcohol

| Mass ratio SAFOL 23:alcohol | Molar fraction of surfactant in the mixture a_j | Molar fraction of surfactant in the micelle x_1 | Interaction factor β | G , $\text{mN}\cdot\text{m}^2\cdot\text{kg}^{-1}$ |
|-----------------------------|---|---|----------------------------|---|
| IBA | | | | |
| 2:3 | 0.082 | 0.974 | -151.61 | 69.88 |
| 3:2 | 0.168 | 0.890 | -74.19 | 290.51 |
| 4:1 | 0.349 | 0.935 | -108.19 | 235.15 |
| IAA | | | | |
| 3:2 | 0.600 | 0.813 | -41.33 | 218.05 |
| 4:1 | 0.800 | 0.935 | -59.64 | 184.83 |

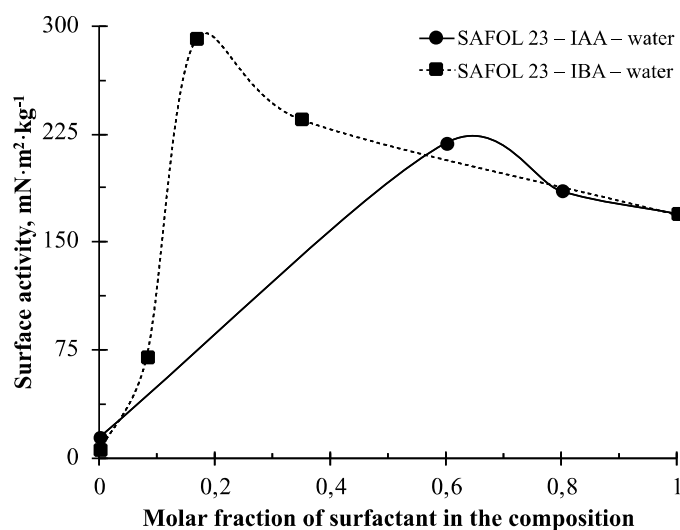


Figure 4. The influence of alkyl radical length of the alcohol on the surface activity of the composition based on SAFOL 23

The wetting characteristics of powder materials play an important role and are used to evaluate the effectiveness of processes such as wet dust collection, dust suppression, flotation, filtering, clumping of powder materials, molding of ceramic compositions, impregnation, road construction, production of gunpowder, printing [16].

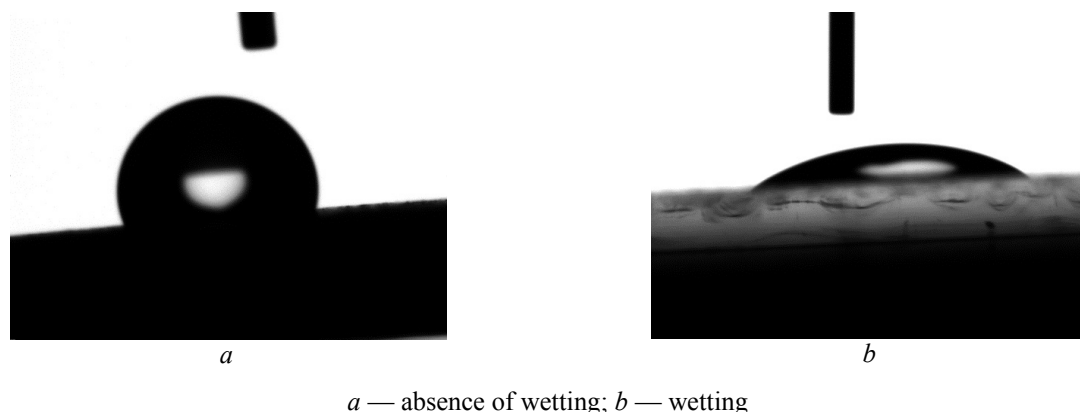
 a — absence of wetting; b — wetting

Figure 5. Studying the wetting process of highly dispersed PTFE

We were interested into studying the way surfactant molecules affect the wetting ability of powdered (PTFE). We calculated the free energy (FSE) of powdered PTFE by Zisman plot, it is $35 \text{ mN}\cdot\text{m}^{-1}$ [17] (Fig. 5). Therefore, PTFE must be wetted by liquids which surface tension is lower than the specified value.

Most of the studied solutions meet this condition. However, in practice, we were not able to achieve complete hydrophilization of the surface in both an individual surfactant and its compositions with isopropyl alcohol (IPA) [18] (the cosine values of the contact angle were negative), although the contact angle decreased with rising concentration of the mixture.

The negative influence of the roughness factor and the suboptimal HLB value, leading to the absence of wetting, can be removed with the help of compositions which contain alcohols with a longer alkyl radical length.

Indeed, the problem of hydrophilization of powder PTFE was solved by replacing IPA by IBA and IAA. Moreover, we observed the values of contact angles which are less than 90 degrees. We could observe it near the maximum of the surface activity curve. The obtained experimental dependences of the wetting isotherms (Fig. 6, 7) are symbatic: in the initial section of the isotherm, a sharp increase in the cosine of the contact angle is observed, then the character of the dependences takes on a smoother, and sometimes stepped shape. The cosine of the contact angle of the composition at the wetting inversion point reduces with rising length of the alcohol radical. So, for the composition SAFOL 23 – IBA – water, the concentration at the inversion point was $0.51 \text{ mol}\cdot\text{L}^{-1}$, for the composition SAFOL 23 – IAA – water — $0.27 \text{ mol}\cdot\text{L}^{-1}$. This phenomenon and the growth in the steepness of the wetting isotherms indicate a more intense adsorption of the composition with an increase in the length of the alkyl radical on the surface of highly dispersed PTFE.

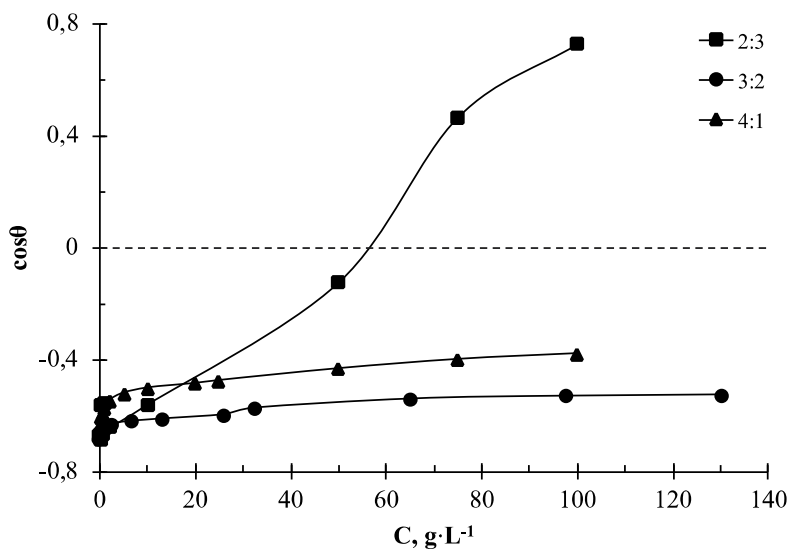


Figure 6. The contact angle isotherms of compositions at different ratios SAFOL 23:IBA

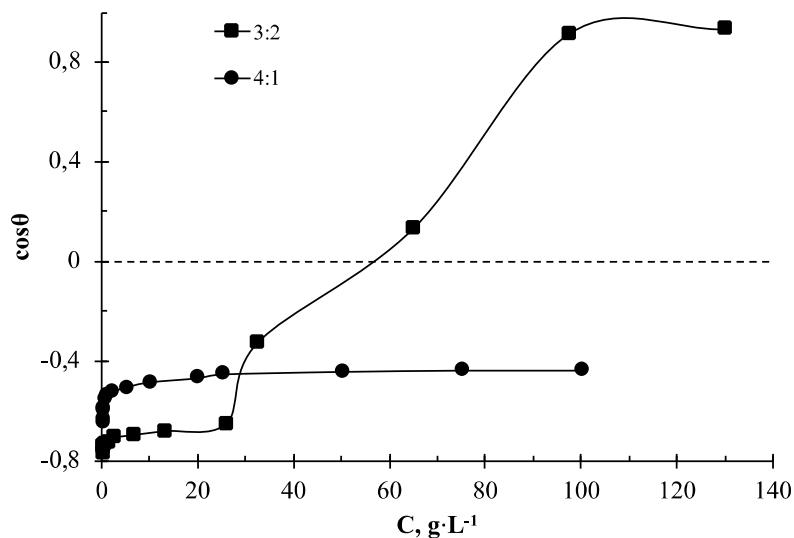


Figure 7. The contact angle isotherms of compositions at different ratios SAFOL 23:IAA

It is possible to calculate the adsorption isotherm at the liquid-gas and the solid-liquid interfaces by formulas (3), (4). This calculation was carried out for the wetting compositions SAFOL 23 – IBA – water and SAFOL 23 – IAA – water. Figures 8, 9 show the adsorption isotherms of these compositions at the liquid-gas and the solid-liquid interfaces.

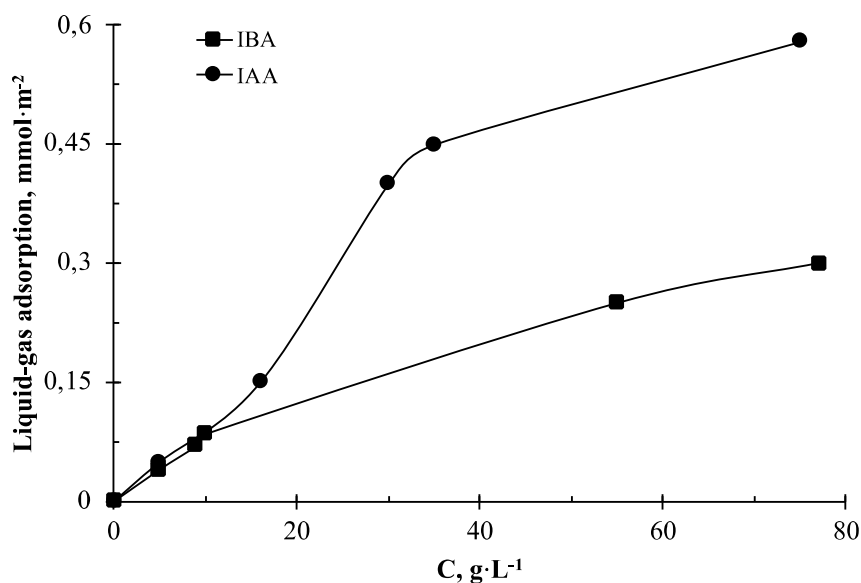


Figure 8. Liquid-gas adsorption isotherm of water-alcohol compositions based on SAFOL 23

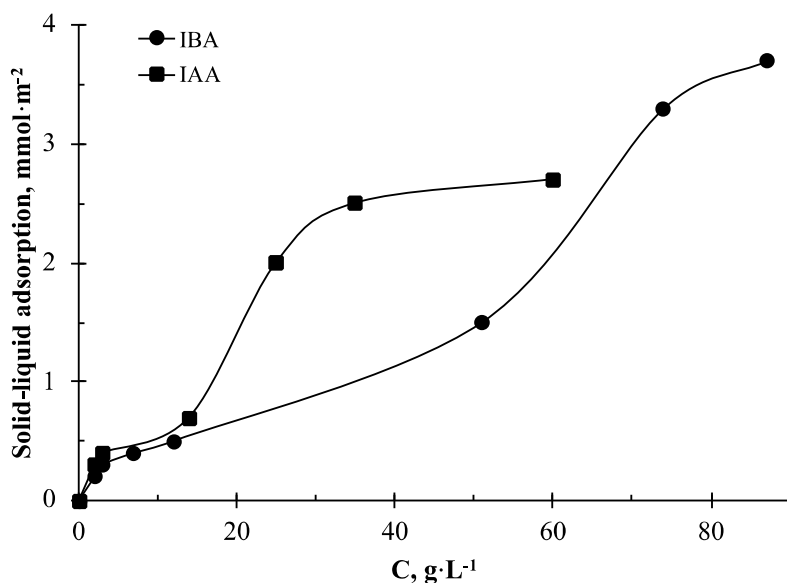


Figure 9. Solid-liquid adsorption isotherm of water-alcohol compositions based on SAFOL 23

The isotherms obtained for the solid-liquid interface are s-shaped and correspond to the scenario of weak interaction of the hydrophilic parts of surfactant molecules and the substrate [19] due to the high hydrophobicity of PTFE. As the concentration of the composition increases, the solvent composition changes. Alcohol molecules that are not included in the micelles appear in the dispersion medium. This affects the course of the further adsorption process and the organization of surfactant layers at the phase boundary.

At concentrations lower than 10 g·L⁻¹, both compositions behave in a similar way, and the quantitative adsorption values practically coincide. In the region of higher concentrations both at the liquid-gas interface and at the solid-liquid interface, SAFOL 23 compositions with IAA exhibit a significantly higher adsorption capacity compared to compositions with IBA.

From the data presented in Figures 8, 9, it follows that the studied compositions are more adsorbed at the surface of the solid phase than at the liquid-gas interface.

The appending of alcohol into an aqueous surfactant solution and the inclusion of its molecules in micelles change the ratio of hydrophilic and lipophilic groups which are reflected in the HLB value [18]. This characteristic was calculated for the mass ratio SAFOL 23:alcohol = 3:2 (Table 3). The obtained experimental results were compared with theoretical values calculated by equation (6). The HLB values of IBA and IAA were calculated according to equation (7), they amounted to 4.6 and 3.9, respectively.

Table 3

HLB determination results

| Composition | Cloud point, °C | HLB | |
|------------------------|-----------------|--------------|-------------|
| | | experimental | theoretical |
| SAFOL 23 – water | 62 | 10.1 | 10.1 |
| SAFOL 23 – IBA – water | 40 | 7.9 | 7.9 |
| SAFOL 23 – IAA – water | 32 | 7.2 | 7.6 |

Unlike the composition SAFOL 23 – water, which has an HLB value of 10 and belongs to the class of emulsifiers, the compositions SAFOL 23 – IBA – water and SAFOL 23 – IAA – water have substantially lower HLB, which allows them to be classified as lipophilic in nature wetting materials with low surface energy [3, 11], which was implemented in practice.

Thus, a growth in the length of the alcohol radical allowed us to reduce the HLB of compositions based on non-ionic surfactants SAFOL 23 and to increase their wetting ability in relation to a highly dispersed low-energy surface.

Based on the performed experiment, it can be concluded that by varying the nature of alcohol, it is possible to regulate the functional properties of surfactants, which significantly expands the scope of their application.

Conclusions

Some conclusions can be drawn from the research results. The mutual attraction of surfactant-alcohol molecules in the mixed micelle weakens with increasing length of the alkyl radical. The composition of mixed micelles weakly depends on the ratio of components in the composition and the nature of the alcohol. The wetting ability of the compositions grows with increasing length of the alkyl radical. The use of longer chain alcohols in the composition with SAFOL 23 allows one to achieve an in-version of wetting and hydrophilize the low-energy highly dispersed PTFE surface at lower surfactant concentrations. Adsorption of water – alcohol compositions at the solid phase is more intense than at the liquid-gas interface. The appending of alcohols changes the hydrophilic-lipophilic balance of SAFOL 23, which allows it to be used as a solubilizer, emulsifier or wetting agent. Varying the nature of alcohol, it is possible to regulate the functional properties of surfactants, which significantly expands their application.

References

- 1 Холмберг К. Поверхностно-активные вещества и полимеры в водных растворах / К. Холмберг, Б. Йенссон, Б. Кронберг, Б. Линдман; пер. с англ. — М.: БИНОМ. Лаборатория знаний, 2007. — 528 с.
- 2 Саутина Н.В. Адсорбционное модифицирование поверхности полимеров водными растворами оксипропилированных алкилфенолов / Н.В. Саутина, С.А. Богданова, В.П. Барабанов // Вестн. Казан. технол. ун-та. — 2009. — № 2. — С. 78–83.
- 3 Поверхностно-активные вещества: синтез, свойства, анализ, применение / К.Р. Ланге; под науч. ред. Л.П. Зайченко. — СПб.: Профессия, 2007. — 240 с.
- 4 Шилова С.В. Влияние пропанола-1 на мицеллообразование алкилсульфатов натрия в водных растворах / С.В. Шилова, Т.С. Фалалеева, А.Я. Третьякова // Химия и хим. технол. — 2014. — Т. 57, № 7. — С. 57–60.
- 5 Site of Sasol Olefins & Surfactants GmbH. Company. — URL: <https://www.sasol.com>.
- 6 Kossen N.W. The determination of the contact angle for systems with powder / N.W. Kossen, P.M. Heertjes // Chemical Engineering Science. — 1965. — Vol. 20, Iss. 6. — P. 593–599.
- 7 Drelich J. Improved Sample Preparation and Surface Analysis Methodology for Contact Angle Measurements on Coal (Heterogeneous) Surfaces / J. Drelich, J.S. Laskowski, M. Pawlik // Coal Preparation. — 2000. — Vol. 21. — P. 247–275.
- 8 Holland P.M. Nonideal multicomponent mixed micelle model / P.M. Holland, D.N. Rubingh // The Journal of Physical Chemistry. — 1983. — Vol. 87, Iss. 11. — P. 1984–1990.
- 9 Rosen J.M. Surfactants and Interfacial Phenomena / J.M. Rosen — New York, NJ: John Wiley and Sons, 2012. — 455 p.

- 10 Неионогенные поверхностно-активные вещества, полученные на основе окиси этилена и смеси неионогенных поверхностно-активных веществ. Определение температуры помутнения: ГОСТ Р 50346–92 (ISO 1065–91). — [Введен в действие от 1992–10–14]. — М.: Стандартинформ Российской Федерации, 1992. — 10 с. — (Национальный стандарт Российской Федерации).
- 11 Поверхностно-активные вещества и композиции: справ. / под ред. М.Ю. Плетнева. — М.: ООО «Фирма Клавель», 2002. — 768 с.
- 12 Szymczyk K. Behaviour of cetyltrimethylammonium bromide, Triton X-100 and Triton X-114 in mixed monolayer at the (water-air) interface / K. Szymczyk, A. Zdziennicka, J. Krawczyk, B. Janczuk // The Journal of Chemical Thermodynamics. — 2014. — Vol. 69. — P. 85–92.
- 13 Щекин А.К. Кинетика мицеллообразования при учете слияния распада сферических и цилиндрических мицелл / А.К. Щекин, М.С. Кшевецкий, О.С. Пелевин // Коллоид. журн. — 2011. — Т. 73, № 3. — С. 404–414.
- 14 Иванова Н.И. Мицеллообразование и поверхностные свойства водных растворов бинарных смесей Твин-80 и бромид-цетилтриметиламмония / Н.И. Иванова // Вестн. Моск. ун-та. Сер. 2. Химия. — 2012. — Т. 53, № 1. — С. 44–49.
- 15 Ляпунов Н.А. Поверхностно-активные, коллоидно-мицеллярные и антибактериальные свойства некоторых катионных антисептиков / Н.А. Ляпунов, А.В. Пуртов, Е.В. Дунай // Фармация. — 2013. — № 4. — С. 44–47.
- 16 Зимон А.Д. Адгезия жидкости и смачивание / А.Д. Зимон. — М.: Химия, 1974. — 416 с.
- 17 Корнилицина Е.В. Влияние степени дисперсности материала на величину свободной поверхностной энергии полимера / Е.В. Корнилицина, М.Г. Щербань, Н.В. Бабикова // Материалы Междунар. науч. конф., посвящ. 100-летию каф. орг. хим. ПГНИУ (16–18 мая 2018 г.). — Пермь: Изд-во Пермск. гос. нац. исслед. ун-та, 2018. — С. 236–238.
- 18 Щербань М.Г. Влияние изопропилового спирта на поверхностно-активные свойства SAFOL 23 / М.Г. Щербань, А.Д. Соловьев, А.О. Саляхова // Вестн. Пермск. ун-та. Сер. Химия. — 2020. — Т. 10, № 2. — С. 320–339.
- 19 Ролдугин В.И. Физикохимия поверхности: учеб.-моногр. / В.И. Ролдугин. — Долгопрудный: Изд. дом «Интеллект», 2011. — 568 с.

М.Г. Щербань, А.Д. Соловьев, А.О. Саляхова

SAFOL 23 – спирт – су жүйелерінің беттік-белсенді сипаттамаларының алкилді радикал спирттің ұзындығына тәуелділігі

Изобутил (ИБС) және изоамил (ИАС) спирттерінің SAFOL 23 ионогенді емес беттік-белсенділік сипаттамаларының әсері зерттелді. Белсенді активті заттар (БАЗ) су ерітіндісінің және оның сулы-спирттік композицияларының беттік керілу изотермалары (БКИ) алынды. Олардың негізінде SAFOL 23 сулы-спирттік жүйелері үшін аралас мицелланың құрамы және мицелледегі БАЗ өзара іс-қимыл факторының шамасы есептелген. Су-спирттік композицияның құрамы мен беттік-белсенділігі табылды және зерттелді. Беттік-белсенділіктің тәуелділігі SAFOL 23 қатынасынан: спирт монотонды сипатта болмайды және оның со-БАЗ со-еріткішке ауысуына байланысты максимум өтеді. Жоғары дисперсті политетрафторэтилен (ПТФЭ) SAFOL 23 сулы-спирттік композицияларымен жұқтыру процесі зерттелді. ПТФЭ беті гидрофизденді, тек беттік-белсенділіктің құрамына тәуелділік графигіндегі максимумға сәйкес келетін ерітінділерді пайдалану кезінде. Әр түрлі фазааралық шекараларда SAFOL 23 адсорбцияланған мөлшері мен оның концентрациясы арасындағы байланыс графигтері есептелген. SAFOL 23 ПТФЭ бетінде жақсы адсорбцияланады және ерітінді-газ шекарасында біршама әлсіз. Спиртті БАЗ су ерітіндісіне енгізу композицияның гидрофильді және липофильді топтарының саны арасындағы арақатынасты өзгертеді, бұл оның гидрофильді-липофильді балансының (ГЛБ) шамасына және лайланған температурасына әсер етеді. Бұл БАЗ қолдану ауқымын едәуір кеңейтеді және SAFOL 23 солюбилизатор, эмульгатор және гидрофизатор ретінде пайдалануға мүмкіндік береді.

Кілт сөздер: ионогенді емес БАЗ, мицеллоқұрылым аралас мицеллолар, беттік белсенділік, адсорбция, дымқылдандыру, гидрофильді-липофильді баланс.

М.Г. Щербань, А.Д. Соловьев, А.О. Саляхова

Зависимость поверхностно-активных характеристик систем SAFOL 23 – спирт – вода от длины алкильного радикала спирта

Исследовано влияние изобутилового (ИБС) и изоамилового (ИАС) спиртов на поверхностно-активные характеристики неионогенного поверхностно-активного вещества (ПАВ) SAFOL 23. Получены изотермы поверхностного натяжения (ИПН) водного раствора ПАВ и его водно-спиртовых композиций. На основе серии ИПН ряда систем SAFOL 23 – спирт – вода рассчитаны составы смешанных мицелл и величины фактора взаимодействия ПАВ в мицелле. Найдена и изучена зависимость поверхностной

активности водно-спиртовой композиции от ее состава. Зависимость поверхностной активности от соотношения SAFOL 23: спирт носит немонотонный характер и проходит через максимум, что связано с изменением функции спирта с ростом его содержания и переходу от со-ПАВА к со-растворителю. Авторами изучен процесс смачивания высокодисперсного политетрафторэтилена (ПТФЭ) композициями SAFOL 23 – спирт – вода, построены изотермы краевого угла смачивания. Поверхность гидрофилизировалась при соотношениях, которые находились в интервале максимума кривой зависимости поверхностной активности – состав композиции. Построены изотермы адсорбции на границах раздела фаз жидкость–газ, твердое тело–жидкость. SAFOL 23 в большей степени адсорбируется на поверхности твердой фазы, чем на границе жидкость–газ. Введение спирта в водный раствор ПАВ изменяет соотношение между числом гидрофильных и липофильных групп композиции, что отражается на величине ее гидрофильно-липофильного баланса (ГЛБ) и температуре помутнения. Это существенно расширяет диапазон применения ПАВ и позволяет использовать SAFOL 23 в качестве солубилизатора, эмульгатора и смачивателя.

Ключевые слова: неионогенное ПАВ, мицеллообразование, смешанные мицеллы, поверхностная активность, адсорбция, смачивание, гидрофильно-липофильный баланс.

References

- Holmberg, K., Jonsson, B., Kronberg, B., & Lindman, B. (2007). *Poverkhnostno-aktivnye veshchestva i polimery v vodnykh rastvorakh* [Surfactants and polymers in aqueous solutions]. Moscow: BINOM; Laboratoriia znanii [in Russian].
- Sautina, N.V., Bogdanova, S.A., & Barabanov, V.P. (2009). Adsorbtsionnoe modifitsirovanie poverkhnosti polimerov vodnymi rastvorami oksitilirovannykh alkilfenolov [Adsorption modification of the surface of polymers with aqueous solutions of ethoxylated alkyl phenols]. *Vestnik Kazanskogo tekhnolohicheskogo universiteta — Bulletin of Kazan Technological University*, 2, 78–83 [in Russian].
- Lange, K.R., & Zaichenko, L.P. (Eds.) (2007). *Poverkhnostno-aktivnye veshchestva: sintez, svoistva, analiz, primeneniye* [Surfactants: synthesis, properties, analysis, application]. Saint Petersburg: Professiia [in Russian].
- Shilova, S.V., Falaleeva, T.S., & Tretyakova, A.Ya. (2014). Vliianie propanola-1 na mitselloobrazovanie alkilsulfatov natriia v vodnykh rastvorakh [The effect of propanol-1 on the micelle formation of sodium alkyl sulfates in aqueous solutions]. *Khimiia i khimicheskaiia tekhnolohiia — Chemistry and chemical technology*, 57, 7, 57–60 [in Russian].
- Site of Sasol Olefins & Surfactants GmbH. Company. Retrieved from <https://www.sasol.com>.
- Kossen, N.W., & Heertjes, P.M. (1965). The determination of the contact angle for systems with powder. *Chemical Engineering Science*, 20, 6, 593–599.
- Drelich, J., Laskowski, J.S., & Pawlik, M. (2000). Improved Sample Preparation and Surface Analysis Methodology for Contact Angle Measurements on Coal (Heterogeneous) Surfaces. *Coal Preparation*, 21, 247–275.
- Holland, P.M., & Rubingh, D.N. (1983). Nonideal multicomponent mixed micelle model. *The Journal of Physical Chemistry*, 87, 11, 1984–1990.
- Rosen, J.M. (2012). *Surfactants and Interfacial Phenomena*. New York, NJ: John Wiley and Sons.
- Neionohennye poverkhnostno-aktivnye veshchestva, poluchennye na osnove okisi etilena i smesi neionohennykh poverkhnostno-aktivnykh veshchestv. Opredelenie temperatury pomutneniia [Nonionic surfactants, ethylene oxide-based substances and mixtures of nonionic surfactants. Determination of cloud point]. (1992). *HOST R 50346–92 (ISO 1065–91) from 14th October 1992*. Moscow: Standartinform Rossiiskoi Federatsii [in Russian].
- Pletnev, M.Yu. (Eds.) (2002). *Poverkhnostno-aktivnye veshchestva i kompozitsii: Spravochnik* [Surfactants and compositions. Directory]. Moscow: OOO «Firma Klavel» [in Russian].
- Szymczyk, K., Zdziennicka, A., Krawczyk, J., & Janczuk, B. (2014). Behaviour of cetyltrimethylammonium bromide, Triton X-100 and Triton X-114 in mixed monolayer at the (water-air) interface. *The Journal of Chemical Thermodynamics*, 69, 85–92.
- Shchekin, A.K., Ksheveckij, M.S., & Pelevin, O.S. (2011). Kinetika mitselloobrazovaniia pri uchete sliianiia raspada sfericheskikh i tsilindricheskikh mitsell [Kinetics of micelle formation when taking into account the merger of the decay of spherical and cylindrical micelles]. *Kolloidnyi zhurnal — Colloid journal*, 73, 3, 404–414 [in Russian].
- Ivanova, N.I. (2012). Mitselloobrazovanie i poverkhnostnye svoistva vodnykh rastvorov binarnykh smesei Tvin-80 i bromida tsetiltrimetilammonii [Micelle formation and surface properties of aqueous solutions of binary mixtures of Tween-80 and cetyltrimethylammonium bromide]. *Vestnik Moskovskogo universiteta. Serii 2. Khimiia — Bulletin of Moscow University. Series 2. Chemistry*, 53, 1, 44–49 [in Russian].
- Lyapunov, N.A., Purtov, A.V., & Dunai, E.V. (2013). Poverkhnostno-aktivnye, kolloidno-mitselliarnye i antibakterialnye svoistva nekotorykh kationnykh antiseptikov [Surface-active, colloidal micellar and antibacterial properties of certain cationic antiseptics]. *Farmatsiia — Pharmacy*, 4, 44–47 [in Russian].
- Zimon, A.D. (1974). *Adheziia zhidkosti i smachivanie* [Fluid adhesion and wetting]. Moscow: Khimiia [in Russian].
- Kornilicina, E.V., Shcherban', M.G., & Babikova, N.V. (2018). Vliianie stepeni dispersnosti materiala na velichinu svobodnoi poverkhnostnoi enerhii polimera [The effect of the degree of dispersion of the material on the amount of free surface energy of the polymer]. Proceedings from *Mezhdunarodnaia nauchnaia konferentsiia, posviashchennaia 100-letiiu kafedry orhanicheskoi*

khimii PGNIU — International scientific conference dedicated to the 100th anniversary of the Department of Organic Chemistry PSU (16–18 maia 2018 h.), (p. 236–238). Perm: PGNIU Publ. [in Russian].

18 Shcherban, M.G, Solovev, A.D., & Salyahova, A.O. (2020). Vliianie izopropilovoho spirita na poverkhnostno-aktivnye svoistva SAFOL 23 [Influence of isopropyl alcohol on the surface-active properties of SAFOL 23]. *Vestnik Permskoho universiteta. Seriya Khimiia — Bulletin of Perm University. Chemistry, 10, 2, 320–339* [in Russian].

19 Roldugin, V.I. (2011). Fizikokhimiia poverkhnosti: uchebnik-monografiia [Physical Chemistry of the Surface: Monograph Textbook]. Dolgoprudnyi: Izdatelskii dom «Intellekt» [in Russian].

Information about authors

Shcherban', Marina Grigoryevna — Candidate of chemical sciences, Assistant professor of Physical Chemistry Department, Perm State National Research University, Bukireva street, 614990, Perm, Russia; e-mail: ma-sher74@mail.ru; <https://orcid.org/0000-0002-6905-6622>.

Solovyev, Aleksandr Dmitriyevich — 2nd year student (specialist), Perm State National Research University, Bukireva street, 614990, Perm, Russia; e-mail: solovev_s92@mail.ru; <https://orcid.org/0000-0002-7852-3683>.

Saliakhova, Anna Olegovna — graduate of the Physical Chemistry Department, Perm State National Research University, Bukireva street, 614990, Perm, Russia; e-mail: sapronova1995@yandex.ru.

I.E. Stas'¹, S.S. Pavlova^{2*}¹Altai State University, Barnaul, Russia;²Yugra State University, Khanty-Mansiysk, Russia

(Corresponding author's e-mail: pavlova_ss@mail.ru)

Effect of pH and water irradiation with the electromagnetic field on the gelation of gelatin solutions

The rate of gelation was determined from the curve slope of the dependence of the gelatin solution relative viscosity on time at different pH. It was found that slow gelation of 2 % gelatin solution occurs at $T = 293$ K, and the degree of fluidity significantly depends on pH. The most stable jellies are formed at the isoelectric point ($\text{pH} = 4.7$). There are significant differences in the physical state of jellies prepared on irradiated water and control samples. Prepared on unirradiated water jellies are more mobile and retain fluidity at $T = 293$ K regardless of pH. There is a partial or full melting of the jellies with the increase in temperature at 297 K; however solid state remains for irradiated systems at $\text{pH} = 4$ and 4.7. It was shown that the viscosity of the irradiated solution and the rate of its increase are higher in comparison with the control samples at all pH values except $\text{pH} = 2$. The observed phenomenon can be caused by the weakening of the hydration of polymer macromolecules in the activated water, which facilitates their association and the formation of a structured system.

Keywords: gelatin, gelation rate, relative viscosity, electromagnetic field, frequency, medium acidity, irradiated water.

Introduction

Currently a large amount of experimental material has been accumulated, indicating significant changes in the physical and chemical properties of water [1–3] and aqueous solutions of polymers as a result of exposure to magnetic and electromagnetic fields. Thus, the effect of the electromagnetic field on glutamic acid solutions was studied by A. Ninno and A.K. Castellano using IR-spectroscopy [4].

It was shown that the solutions with a pH less than the isoelectric point (IEP) demonstrated a shift towards deprotonation of a carboxyl group as a result of field exposure. The deprotonation of residual amino groups was observed for solutions with pH above the IEP. The same authors studied the effect of weak electromagnetic fields on the structure of L-glutamine and L-phenylalanine in aqueous solution. It was assumed that the magnetic field changes the structure of water around hydrophobic molecules and their interaction, which allows the aggregation of amino acids molecules [5]. The influence of low-intensity extrahigh-frequency (EHF) radiation (27–120 GHz) on the processes of structuring of water and aqueous solutions of amino acids has been studied [6]. The strengthening of the structure of water and upgrading of hydrophobic interactions near the macromolecules of the polymer as a result of field exposure have been demonstrated. The effect of microwave electromagnetic radiation on the formation of supermolecular particles in aqueous solutions of non-hydrolyzed polyacrylamide has been studied in [7]. It was shown that the heating of the sample contributes to the emergence of large supermolecular particles. The possibility of pulse-discharge technologies using in the food industry with the aim to develop the hydration of biopolymers and improve the physical and chemical properties of the products has been discussed in [8].

The idea of relationship between the structure of water and the biological molecules dissolved in it is based on the methods of high frequency therapy used in the treatment of respiratory and blood circulation. Structural properties of water, solutions of electrolytes and non-electrolytes and their changes in the electromagnetic field have been analyzed in [9, 10]. The boundary of the first structural zone where the order is based on the original tetrahedral structure of water has been determined. It was shown that the appropriate concentrations are important for tissue cells, since they control the characteristic changes in the physical and chemical properties of aqueous systems and the possibility of jel-like structures formation. The effect of a magnetic field on the sol-gel transition of methylcellulose in water was studied by Wang K. et al. They found that the influence of the magnetic field reduced the sol-gel transition temperature by 3 °C, showing an effect

*Corresponding author.

similar to that of salt additives. There is a slight increase in jelly hardness [11]. The influence of a pulsed magnetic field on the rate of change in the mechanical strength of fibers was shown using examples of a number of fibrous polymeric materials (viscose, polyacrylonitrile, polyamide, cotton, cellulose wool) [12]. The effect of electromagnetic water treatment on the dyeing of woolen fabrics has been determined [13]. The action of an external magnetic field on the cis-trans isomerization of polybutadiene rubber has been demonstrated [14].

Previous studies have shown significant changes in physical and chemical properties of water, caused by irradiation of water with a low-intensity high-frequency (30–240 MHz) electromagnetic field (EMF) and subsequent shift in intermolecular interaction [15–17]. It was shown that the magnitude of the observed changes in the water surface tension, rate of evaporation and parameters of wetting depends on the EMF frequency and exposure time. It was also found that the degree of expansion of biopolymers such as gelatin, carboxymethylcellulose (CMC) and its sodium salt change in irradiated water, increasing the viscosity of these high molecular mass compound solutions [18–20]. The change in the energy of solvation processes in activated water can be the reason of the observed phenomena as a result of the strengthening of its supramolecular organization, which, in turn, determine the viscosity of polymer solutions, the rate and degree of polymer expansion.

The aim of this work was to study the effect of pH and preliminary irradiation of water with an electromagnetic field on the rate of gelation of gelatin solutions.

Gelatin is a polydisperse mixture of polypeptides. It is formed from collagen with prolonged alkaline treatment of cartilage, tendons, bones, dermis with subsequent extraction with water at 50–100 °C [21]. Gelatin is a very promising matrix material for in vitro cell culture and tissue engineering. When forming a medical implant of soft tissue gelatin improves the mechanical properties of hydrogels. In the pharmaceutical industry gelatine is used to manufacture hard and soft capsules, in the production of artificial plasma extenders, in the production of hemostatic agents, the hemostatic dressings.

Experimental

The high frequency generator G3–19A with an output power of 1 W and a range of variation of the frequency from 30 to 200 MHz has been used as the source of the electromagnetic field. A 200 ml capacitive cell was used to expose water with EM field.

We used deionized water purified by reverse osmosis, specific conductivity of which was 1.2 $\mu\text{S}/\text{m}$. Water samples were exposed with the field frequency of 130 MHz for 3 hours. The choice of EMFs frequency was due to previously conducted experiments, in which the exposure fields of the given frequency leads to significant changes in water properties (electrical conductivity, surface tension, heat and rate of evaporation) [15–16]. Time of exposure has been also selected on the basis of previous studies. In this case, the exposure efficiency is controlled by the value of the water specific conductivity, comparing its initial and finite value. As a result of field exposure, the electrical conductivity increased by 2.7 ± 0.2 times. To prepare gelatin solutions, we used water kept in hermetically sealed plastic vessels for a week after irradiation. During this time, no relaxation of the electrical conductivity of water to the initial value was observed.

2 % solutions of powdered food gelatin (GOST 11293–89) have been used for studies. The choice of the concentration is due to the fact that solutions of this concentration flow, gel slowly (over days) at room temperature and when the temperature drops to 15 °C gelation proceeds within 15–40 min, that allows to study the kinetics of this process. Solutions of gelatin were prepared in 2 stages. First a portion of gelatin was placed in 50.0 ml flasks. Then 20 ml of activated or non-activated water at room temperature was added and left to swell for 30–40 minutes. After that, the mixture was placed in a water bath (60–70 °C) and gelatin was dissolved with stirring until a clear solution. The resulting solutions were adjusted to the mark with water and cooled to room temperature. The required pH values were obtained by adding 0.1 M HCl or NaOH to the water used for the preparation of solutions. The acidity of the medium was controlled using the pH-meter "Anion 4100" with an accuracy of ± 0.05 pH units. Three series of parallel experiments were carried out.

Determination of kinematic viscosity was carried out using flow-through capillary viscometer VPI-2 with a capillary diameter $d = 1,31$ mm. The relative viscosity of solutions was calculated by the relative expiration time out of the viscosimeter of the solution of gelatin and water. The rate of gelation was determined from the slope of the curve of the dependence of the gelatin solution relative viscosity on time at different pH. The gelation time was determined from the time the solution stopped flowing out of the viscometer. The study of the kinetics of the solutions gelation process was carried out at a temperature of 288 K (15 °C). The

required temperature was maintained with a TJ-TB-01 thermostat (temperature measurement accuracy ± 0.1 °C).

Results and Discussion

As a result of the studies, it was found that slowly (within a day) gelation of 2 % gelatin solution proceeds at $T = 293$ K, and the degree of their fluidity depends significantly on pH. Flowage or non-flowage of the obtained systems was estimated by the presence or absence of their outflow from the tube when it was turned over. The most solid gels are formed in the IEP when $\text{pH} = 4.7$. Noticeable differences in the physical state of the jellies have been observed in those prepared from the activated water ($f = 130$ MHz), and control samples ($f = 0$). Jellies, prepared from the non-activated water were turbid and fluent. They kept the fluidity regardless pH. The only jelle, obtained at $\text{pH} = 10$ was in non-flowing state. Jellies, prepared from activated water at all pH values except $\text{pH} = 2$ showed solid properties (Table 1) and were transparent.

Table 1

State of the gelatin jellies at $T = 293$ K and 1 day after preparation

| pH | 2.0 | 4.0 | 4.7 | 6.0 | 8.0 | 10 |
|---------------------------------|---------|--------------|--------------|--------------|-------------|-------------|
| State of jelly ($f = 0$) | flowing | slow-flowing | slow-flowing | slow-flowing | flowing | non-flowing |
| State of jelly ($f = 130$ MHz) | flowing | non-flowing | non-flowing | non-flowing | non-flowing | non-flowing |

It is known that the structure is stabilized in jellies, which is appeared in the decrease of their flowage. After 4 days the non-activated systems became less fluid, and the activated kept a solid state and did not leak out of the vessels in which they were stored (Table 2).

Table 2

State of gelatin jellies at $T = 293$ K and 4 day after preparation

| pH | 2.0 | 4.0 | 4.7 | 6.0 | 8.0 | 10 |
|---------------------------------|--------------|--------------|--------------|--------------|--------------|-------------|
| State of jelly ($f = 0$) | slow-flowing | slow-flowing | slow-flowing | slow-flowing | slow-flowing | non-flowing |
| State of jelly ($f = 130$ MHz) | flowing | non-flowing | non-flowing | non-flowing | non-flowing | non-flowing |

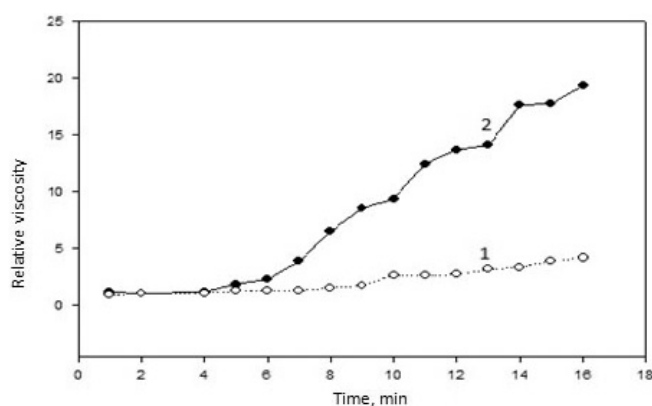
Partial or full melting of the jellies occurred with the increase in temperature to 297 K, however, solid state remained for activated systems at $\text{pH} = 4$ and 4.7 (Table 3).

Table 3

State of gelatin jellies at $T = 297$ K

| pH | 2.0 | 4.0 | 4.7 | 6.0 | 8.0 | 10 |
|---------------------------------|---------|-------------|--------------|--------------|--------------|--------------|
| State of jelly ($f = 0$) | flowing | flowing | slow-flowing | flowing | flowing | flowing |
| State of jelly ($f = 130$ MHz) | flowing | non-flowing | flowing | slow-flowing | slow-flowing | slow-flowing |

The kinetics of a 2 % solution of gelatin gelation at $T = 288$ K has been studied. The obtained jellies were melted in water bath when heated and then quickly cooled in a thermostat to specified temperature. Cooling of the gelatin solutions was carried out in the viscometer. The viscosity of solutions was measured with an interval of 1 min when reaching $T = 288$ K. It was shown that the viscosity of the activated solutions and their rate of increase is much higher compared with control samples at all pH values. Only at $\text{pH} = 2$ the viscosity of the studied and control samples increased with the same rate, and along with this no gelation was observed within 1 hour. Figure 1 shows the kinetic curves of increase in the relative viscosity of the activated and non-activated gelatin solutions at $\text{pH} = 10$.



1 — non-activated water; 2 — activated water (130 MHz)

Figure 1. Dependence of relative viscosity of 2 % solutions of gelatin on the time at $T = 288$ K and $\text{pH} = 10$

It is known that gelation process runs faster in solutions of proteins of the same concentration, provided that the protein molecules have no electrical charge and they are less hydrated, i.e. they are in isoelectric state. Therefore, the rate of gelation depends on the acidity of the medium and best of all occurs at a pH corresponding to the isoelectric point (IEP) of the protein [21], which was confirmed by our experiments. Rates and time of gelation of polymer solutions at different pH values are presented in Table 4.

Table 4

Rate ($-d\eta/dt$) and time (t) of gelation of 2 % gelatin solutions at $T=288$ K

| pH | 2.0 | 4.0 | 4.7 | 6.0 | 8.0 | 10 |
|--|---------------|---------------|---------------|---------------|---------------|---------------|
| $(d\eta/dt) \cdot 10, \text{min}^{-1}$ ($f = 0$) | 1.1 ± 0.2 | 1.3 ± 0.3 | 1.6 ± 0.1 | 1.4 ± 0.2 | 1.3 ± 0.3 | 1.2 ± 0.2 |
| $(d\eta/dt) \cdot 10, \text{min}^{-1}$ ($f = 130$ MHz) | 1.2 ± 0.1 | 1.8 ± 0.4 | 3.9 ± 0.3 | 2.5 ± 0.4 | 2.2 ± 0.2 | 2.2 ± 0.2 |
| t, min ($f = 0$) | - | 42 ± 4 | 19 ± 2 | 24 ± 3 | 36 ± 2 | 48 ± 5 |
| t, min ($f = 130$ MHz) | 58 ± 3 | 18 ± 1 | 11 ± 1 | 13 ± 3 | 18 ± 2 | 16 ± 2 |

The fluidity of the jelly is determined by the strength of the bond that occurs between the polymer macromolecules during the gelation process. The grid nodes can be caused by the hydrogen bonds, the interaction of electric charges or dipoles and chemical bonds. The strength of the bonds in the jell is small in the case if this bond is hydrogen or electrostatic (dipole), and its ability to melting and decomposition increases. Gelatin jellies are good examples of such systems [21]. The macromolecules of proteins comprising gelatin are positively charged in the acidic medium due to the suppression of dissociation of carboxylic groups and protonation of amino groups; the force of electrostatic repulsion is high, which prevents the association of molecules and the formation of a polymer three-dimensional grid in an aqueous medium. Gelling does not occur in such case. The charge of macromolecules is small (or zero in the IEP at $\text{pH} = 4.7$) in weak acid and weak-alkaline medium, which leads to weakening of the electrostatic repulsive forces. As a result, the process of formation of intermolecular bonds (dipole-dipole and hydrogen) is facilitated and the gelling of gelatin solutions occurs. The intensification of the gelling processes in water exposed to EMF may be due to the weakening of the hydration of ionogenic groups of the polymer due to increase of dipole-dipole interaction between water molecules. Strengthening the cohesive interaction in the aquatic medium was confirmed in [16]. The result is a reduction in the degree of dissociation of carboxylic groups and decrease in the total charge of the macromolecules, which contributes to their association and the formation of a structured system. The well-known fact that the addition of salts containing well-hydrated ions (sulfates, citrates) to gelatin solutions accelerates this process, indicates the influence of the hydration degree of the polymers polar groups during gelling. The greater the ability of the ion to hydrate, the more active is the dehydration of the polymer macromolecules in its presence, what facilitates their connection to each other and the formation of a structured system. Thus, it can be assumed that the effect of EMF on water is similar to the effect of elec-

trolyte additives. An increase in the viscosity of electromagnetic field solutions in activated water can also be a consequence of the enhancement of the macromolecules association due to the adhesion of their dehydrated sections.

Conclusions

The dependence of gelation of 2 % gelatin solution on pH at 293 and 297 K has been determined. It has been shown that solid systems are formed at pH = 4–6 and 10. Gelling does not occur at pH=2.

Strengthening of the gelatine structuring in water, exposed to the electromagnetic field of 130 MHz frequency was shown, that appears in the formation of solid systems at all pH values except pH=2.

The kinetics of gelation of gelatin solutions according to the changes in relative viscosity during the time has been studied. The processes acceleration in activated water has been demonstrated.

References

- 1 Fesenko E.E. Changes in the state of water, induced by radiofrequency electromagnetic fields / E.E. Fesenko, A.Y. Gluvstein // FEBS letters. — 1995. — Vol. 367, No. 1. — P. 53–55.
- 2 Vallée P. Action of pulsed low frequency electromagnetic fields on physicochemical properties of water: Incidence on its biological activity / P. Vallée // Journal Europeand'Hydrologie. — 2006. — Vol. 37(2). — P. 221–232.
- 3 Andreyev Ye.A. Dynamics of rheological parameters of water system in lowintensity millimeter wave fields / Ye.A. Andreyev, Yu.M. Barabash, M.A. Zabolotny // Proceedings of SPIE The International Society for Optical Engineering. — 1994. — Vol. 221. — P. 518–528.
- 4 De Ninno A. Influence of magnetic fields on the hydration process of amino acids: Vibrational spectroscopy study of L-phenylalanine and L-glutamine / A. De Ninno, A.C. Castellano // Bioelectromagnetics. — 2014. — Vol. 35, No. 2. — P. 129–135.
- 5 De Ninno A. Deprotonation of glutamic acid induced by weak magnetic field: An FTIR-ATR study / A. De Ninno, A.C. Castellano // Bioelectromagnetics. — 2011. — Vol. 32, No. 3. — P. 218–250.
- 6 Синицин Н.И. Структуризация воды аминокислотами разных классов / Н.И. Синицин // Бюл. мед. интернет-конф. — 2012. — Т. 2, № 6. — С. 367–374.
- 7 Нагдалян А.А. Влияние электрогидравлического эффекта на гидратацию биополимеров / А.А. Нагдалян, Н.П. Оботурова // Актуальные проблемы гуманитарных и естественных наук. — 2012. — № 12. — С. 74–78.
- 8 Стехин А.А. Влияние высокочастотного (СВЧ) облучения на биологическую ценность пищевых продуктов / А.А. Стехин, О.Н. Савостикова, М.Г. Кочеткова // Биотехнология. Вода и пищевые продукты: тр. Междунар. науч.-практ. конф. — М., 2008. — С. 280, 281.
- 9 Лященко А.К. Структура воды, миллиметровые волны и их первичная мишень в биологических объектах / А.К. Лященко // Биомедицинские технологии и радиоэлектроника. — 2007. — № 8, 9. — С. 62–77.
- 10 Девятков Н.Д. Особенности медико-биологического применения миллиметровых волн / Н.Д. Девятков, М.Б. Голант, О.В. Бецкий. — М.: ИРЭРАН, 1994. — 134 с.
- 11 Wang Q. Effects of magnetic field on the sol–gel transition of methylcellulose in water / Q. Wang // Carbohydrate polymers. — 2007. — Vol. 70, No. 3. — P. 345–349.
- 12 Персидская А.Ю. О влиянии импульсного магнитного поля на механические свойства полимерных волокон / А.Ю. Персидская, И.Р. Кузеев, В.А. Антипина // Журн. хим. физ. — 2002. — № 2. — С. 90–95.
- 13 Дерунова Г.Н. Активация процесса крашения шерстяных материалов путем электромагнитной обработки воды / Г.Н. Дерунова и др. // Изв. вузов. Технология текстильной пром-ти. — 1985. — № 2. — С. 71–73.
- 14 Френкель Р.Ш. Влияние внешнего магнитного поля на цис-транс-изомеризацию полибутадиенового каучука / Р.Ш. Френкель, В.С. Пономарев // Высокомолекул. соедин. — 1976. — Т. 18Б. — С. 505, 506.
- 15 Стась И.Е. Влияние низкоинтенсивного электромагнитного поля ультравысоких частот на свойства водных систем / И.Е. Стась, В.Ю. Чиркова // Слабые и сверхслабые поля и излучения в биологии и медицине: тр. VIII Междунар. конгр. — СПб., 2018. — С. 81.
- 16 Чиркова В.Ю. Изменение когезионных и адгезионных характеристик воды как результат электромагнитного воздействия / В.Ю. Чиркова, Е.А. Шарлаева, И.Е. Стась // Изв. вузов. Прикл. химия и биотехнол. — 2019. — Т. 9, № 2(29). — С. 222–231.
- 17 Стась И.Е. Влияние обработки воды электромагнитным полем ультравысоких частот на относительную вязкость водных растворов Na-карбоксиметилцеллюлозы / И.Е. Стась, А.В. Михайлис // Изв. Алтай. гос. ун-та. Сер. Физика. Математика. — 2018. — № 4(102). — С. 31–35.
- 18 Стась И.Е. Относительная вязкость водных растворов Na-карбоксиметилцеллюлозы и ее изменение в зависимости от кислотности среды, температуры и воздействия электромагнитного поля / И.Е. Стась, И.А. Батищева // Химия раст. сырья. — 2018. — № 3. — С. 23–31.

19 Стась И.Е. Набухание биополимеров в облученной электромагнитным полем воде / И.Е. Стась, Р.С. Тхоренко, В.Ю. Чиркова // Новые достижения в химии и химической технологии растительного сырья: тр. VI Всерос. конф. с междунар. участием. — Барнаул, 2014. — С. 109–111.

20 Стась И.Е. Вязкость растворов желатина, приготовленных на облученной электромагнитным полем воде / И.Е. Стась, В.Ю. Чиркова, М.И. Минин // Вестн. Воронеж. гос. ун-та. Сер. Химия. Биология. Фармация. — 2016. — № 2. — С. 32–36.

21 Семчиков Ю.Д. Высокомолекулярные соединения / Ю.Д. Семчиков. — М.: Изд. центр «Академия», 2003. — 368 с.

И.Е. Стась, С.С. Павлова

Желатин ерітінділерінің қатаюына рН пен суды электромагниттік өріспен өндеудің әсері

Гельдің түзілу жылдамдығы ортаның рН-ның әр түрлі мәндерінде желатин ерітіндісінің салыстырмалы тұтқырлығының уақытқа тәуелділік қисығы көлбеуімен анықталды. $T = 293$ К кезінде 2 % желатин ерітінділерінің қатуы баяулайды, ал олардың аққыштық дәрежесі рН-қа байланысты. Ең берік желе рН = 4,7 изоэлектрлік нүктеде түзіледі. Сәулелендірілген суда дайындалған желе мен бақылау үлгілерінің физикалық жағдайында айтарлықтай айырмашылықтар байқалады. Сәулеленбеген суда дайындалған желе неғұрлым жылжымалы және рН-қа қарамастан $T = 293$ К кезінде аққыштықты сактайды. Температура 297 К дейін көтерілгенде желе ішінара немесе толық балқиды, бірақ сәулелендірілген жүйелер үшін рН = 4 және 4,7 кезінде қатты күй сакталады. Бақылау үлгілерімен салыстырғанда сәулеленген ерітінділердің тұтқырлығы және оның өсу жылдамдығы рН = 2-ден басқа рН барлық мәндерінде жоғары екендігі көрсетілген. Байқалған құбылыстар сәулелендірілген судағы полимерлі макромолекулалардың гидратациясының әлсіреуіне байланысты болуы мүмкін, бұл олардың ассоциациясын және құрылымдық жүйенің қалыптасуын жеңілдетеді.

Кілт сөздер: гель, желатин, гельдің түзілу жылдамдығы, салыстырмалы тұтқырлық, электромагниттік өріс, жиілік, ортаның қышқылдығы, сәулеленген су.

И.Е. Стась, С.С. Павлова

Влияние рН и обработки воды электромагнитным полем на застудневание растворов желатина

Скорость гелеобразования определена по наклону кривой зависимости относительной вязкости раствора желатина от времени при различных значениях рН среды. Установлено, что при $T = 293$ К происходит медленное застудневание 2 % растворов желатина, а степень их текучести существенно зависит от рН. Наиболее прочные студни образуются в изоэлектрической точке при рН = 4,7. Наблюдаются заметные различия в физическом состоянии студней, приготовленных на облученной воде, и контрольных образцов. Студни, приготовленные на необлученной воде, более подвижны и сохраняют текучесть при $T = 293$ К независимо от рН. При повышении температуры до 297 К происходит частичное или полное плавление студней, однако для облученных систем при рН = 4 и 4,7 твердообразное состояние сохраняется. Показано, что вязкость облученных растворов и скорость ее нарастания выше по сравнению с контрольными образцами при всех значениях рН, кроме рН = 2. Наблюдаемые явления могут быть обусловлены ослаблением гидратации макромолекул полимера в облученной воде, что облегчает их ассоциацию и образование структурированной системы.

Ключевые слова: гель, желатин, скорость гелеобразования, относительная вязкость, электромагнитное поле, частота, кислотность среды, облученная вода.

References

- 1 Fesenko, E.E., & Gluvstein, A.Y. (1995). Changes in the state of water, induced by radiofrequency electromagnetic fields. *FEBS letters*, 367(1), 53–55.
- 2 Vallée, P. (2006). Action of pulsed low frequency electromagnetic fields on physicochemical properties of water: Incidence on its biological activity. *Journal Europeand`Hydrologie*, 37(2), 221–232.
- 3 Andreyev, Ye.A., Barabash, Yu.M., & Zabolotny, M.A. (1994). Dynamics of rheological parameters of water system in lowintensity millimeter wave fields. *Proceedings of SPIE The International Society for Optical Engineering*, 221, 518–528.

- 4 De Ninno, A., & Castellano, A.C. (2014). Influence of magnetic fields on the hydration process of amino acids: Vibrational spectroscopy study of L-phenylalanine and L-glutamine. *Bioelectromagnetics*, 35, 129–135.
- 5 De Ninno, A., & Castellano, A.C. (2011). Deprotonation of glutamic acid induced by weak magnetic field: An FTIR-ATR study. *Bioelectromagnetics*, 32, 218–250.
- 6 Sinitsin, N.I. (2012). Strukturizatsiia vody aminokislotalami raznykh klassov [Water structuring by different classes of amino acids]. *Biulleten meditsinskikh internet-konferentsii — Bulletin of Medical Internet Conferences*, 2, 367–374 [in Russian].
- 7 Naghdalyan, A.A., & Oboturova, N.P. (2012). Vliianie elektrohivdravlicheskogo effekta na hidratatsiiu biopolimerov [The influence of the electrohydraulic effect on the biopolymers hydration]. *Aktualnye problemy humanitarnykh i estestvennykh nauk — Current issues of humanitarian and natural sciences*, 12, 74–78 [in Russian].
- 8 Stekhin, A.A., Savostikova, O.N., & Kochetkova, M.G. (2008). Vliianie vysokochastotnogo (SVCH) obluchenii na biolohicheskuiu tseinnost pishchevykh produktov [Influence of high-frequency (microwave) irradiation on the biological value of food products]. Proceedings from Biotechnology. Water and food: *Mezhdunarodnaia nauchno-prakticheskaiia konferentsiia — International Scientific and Practical Conference*. (p. 280, 281). Moscow [in Russian].
- 9 Lyashchenko, A.K. (2007). Struktura vody, millimetrovye volny i ikh pervichnaia misha v biolohicheskikh obektakh [Water structure, microwaves and their initial target in biological objects]. *Biomeditsinskie tekhnologii i radioelektronika — Biomedical technologies and Radioelectronics*, 8–9, 62–77 [in Russian].
- 10 Devyatkov, N.D., Golant, M.B., & Betsky, O.V. (1994). *Osobennosti mediko-biolohicheskogo primeneniia millimetrovykh voln [Features of medical and biological application of microwaves]*. Moscow: IREAN [in Russian].
- 11 Wang, Q. (2007). Effects of magnetic field on the sol–gel transition of methylcellulose in water. *Carbohydrate polymers*, 70, 345–349.
- 12 Persidskaya, A.Yu., Kuzeev, I.R., & Antipina, V.A. (2002). O vlianii impulsnogo mahnitnogo polia na mekhanicheskie svoystva polimernykh volokon [On the influence of pulsed magnetic field on mechanical properties of polymer fibers]. *Zhurnal khimicheskoi fiziki — The Journal of Physical Chemistry*, 2, 90–95 [in Russian].
- 13 Derunova, G.N., et al. (1985). Aktivatsiia protsessa krasheniia sherstianykh materialov putem elektromahnitnoi obrabotki vody [Activation of the dyeing process of wool materials by electromagnetic water treatment]. *Izvestiia vuzov. Tekhnologiiia tekstilnoi promyshlennosti — Proceedings of higher education institutions. Textile industry technology*, 2, 71–73 [in Russian].
- 14 Frenkel, R.Sh., & Ponomaryov, V.S. (1976). Vliianie vneshnego mahnitnogo polia na tsis-trans-izomerizatsiiu polibutadienovoego kauchuka [The influence of external magnetic field on the cis-trans isomerization of polybutadiene rubber]. *Vysokomolekuliarnye soedineniia — High molecular mass compound*, 18B, 505–506 [in Russian].
- 15 Stas', I.E., & Chirkova, V.Yu. (2018). Vliianie nizkointensivnogo elektromahnitnogo polia ultravysokikh chastot na svoystva vodnykh sistem [The effect of low intensity electromagnetic field of ultrahigh frequency on the properties of aquatic systems]. Proceedings from Weak and Superweak Fields and Radiation in Biology and Medicine: *VIII Mezhdunarodnyi konhress — VIII International Congress*. (p. 81). Saint Petersburg [in Russian].
- 16 Chirkova, V.Yu., Sharlaeva, E.A., & Stas, I.E. (2019). Izmenenie koheziionnykh i adheziionnykh kharakteristik vody kak rezultat elektromahnitnogo vozdeistviia [The change in cohesive and adhesive characteristics of water as a result of electromagnetic effects]. *Izvestiia vuzov. Prikladnaia khimiia i biotekhnologiiia — Proceedings of higher education institutions. Applied chemistry and biotechnology*, 9, 222–231 [in Russian].
- 17 Stas, I.E., & Mikheyliis, A.V. (2018). Vliianie obrabotki vody elektromahnitnym polem ultravysokikh chastot na otноситelnuiu viazkost vodnykh rastvorov Na-karboksimitiltselliulozy [The influence of water treatment of the electromagnetic field of ultrahigh frequency on the relative viscosity of aqueous solutions of Na-carboxymethylcellulose]. *Izvestiia Altaiskoho gosudarstvennogo universiteta. Seriia Fizika. Matematika — News of Altai State University Journal. Physical science. Mathematics*. 4(102), 31–35 [in Russian].
- 18 Stas, I.E., & Batishcheva, I.A. (2018). Otnositelnaia viazkost vodnykh rastvorov Na-karboksimitiltselliulozy i ee izmenenie v zavisimosti ot kislotnosti sredy, temperatury i vozdeistviia elektromahnitnogo polia [The relative viscosity of aqueous solutions of Na-carboxymethylcellulose and its variation depending on the acidity, temperature and exposure to electromagnetic fields]. *Khimiia rastitel'nogo syria — Chemistry of plant raw materials*, 3, 23–31 [in Russian].
- 19 Stas, I.E., Tkhorenko, R.S., & Chirkova, V.Yu. (2014). Nabukhanie biopolimerov v obluchennoi elektromahnitnym polem vode [Swelling of biopolymers in irradiated electromagnetic field in the water]. Proceedings from New achievements in chemistry and chemical technology of plant raw materials: *VI Vserossiiskaia konferentsiia s mezhdunarodnym uchastiem — VI All-Russian conference with international involvement*. (p. 109–111). Barnaul [in Russian].
- 20 Stas, I.E., Chirkova, I.E., & Minin, M.I. (2016). Viazkost rastvorov zhelatina, prihotovlennykh na obluchennoi elektromahnitnym polem vode [The viscosity of the gelatin solutions prepared from the water activated with electromagnetic field]. *Vestnik Voronezhskogo gosudarstvennogo universiteta. Seriia Khimiia. Biologiia. Farmatsiia — Scientific Herald of the Voronezh State University. Chemistry. Biology. Pharmacy*, 2, 32–36 [in Russian].
- 21 Semchikov, Yu.D. (2003). *Vysokomolekuliarnye soedineniia [High-molecular compounds]*. Moscow: Izdatelskii tsentr «Akademiiia» [in Russian].

Information about authors

Stas', Irina Evgen'evna — Candidate of Chemical Sciences, Associate Professor of the Department of Physical and Inorganic Chemistry, Altai State University, Lenin Ave., 61, 656049, Barnaul, Russia; e-mail: irinastas@gmail.com

Pavlova, Svetlana Stanislavovna — Candidate of Technical Sciences, Senior Lecturer at the Institute of Oil and Gas, Ugra State University, Chekhov Street 16, 628012, Khanty-Mansiysk, Russia; e-mail: pavlova_ss@mail.ru; <https://orcid.org/0000-0001-6137-3968>.

A.K. Zhumabekova¹, L.K. Tastanova^{2*}, R.O. Orynbassar³, G.D. Zakumbaeva⁴

¹M. Kozybayev North Kazakhstan State University, Petropavlovsk, Kazakhstan;

²K. Zhubanov Aktobe Regional State University, Aktobe, Kazakhstan;

³Al-Farabi Kazakh National University, Almaty, Kazakhstan

⁴D.V. Sokolskii Institute of Fuel, Catalysis and Electrochemistry, Almaty, Kazakhstan

(Corresponding author's e-mail: lyazzatt@mail.ru)

Effect of modifiers on Fe-Pt/Al₂O₃ catalysts for alkanes hydrotreatment

Zeolite-containing polyfunctional catalysts Fe-Pt/Al₂O₃ (KT-17, KT-18), modified with additives of molybdenum, phosphorus and cerium, were synthesized. The developed catalytic systems were studied in treatment of C14 alkane obtaining a gasoline fraction. Reaction products contain C4-C9 iso-alkanes, C10-C14 iso-alkanes, C4-C10 alkanes, aromatic hydrocarbons and C1-C3 alkanes. In addition, 0.2–0.6 % of heavy hydrocarbons was found in reaction products. The yield of C4-C9 iso-alkanes at 380 °C reached 37.9 %. By means of physical and chemical methods it has been found that the zeolite containing catalysts Fe-Pt /Al₂O₃ modified by various additives are complex systems. Micro-diffraction and Mossbauer spectroscopy methods allowed detecting nanosized hetero clusters of Fe-Pt, Fe-Mo, Pt-Mo in catalysts structure. Depending on chemical composition of clusters, particle size varies between 20 and 80 Å. KT-18 catalyst demonstrates high activity in the process of heavy alkanes treatment; sizes of platinum (d = 200 Å) and iron (d = 30–50 Å) particles were determined by electron microscopy. Activity of KT-18 catalyst is higher than that of highly dispersed KT-17. The main feature of KT catalysts is their polyfunctionality. During alkanes processing simultaneous and consecutive reactions of hydrocracking, dehydrogenation, isomerization, dehydro-cyclization and hydro-desulfurization take place.

Keywords: hydro treatment, zeolite containing catalysts, modification, polyfunctionality, heavy alkanes, hydrocracking, hydrogenation, nanoclusters.

Introduction

The global trend in oil processing industry development is enhancing the depth of raw materials refining and to improve the quality and environmental characteristics of motor fuels through the use of catalytic systems, which allows obtaining valuable light fractions from heavy oil residues [1, 2].

Production of gasoline fractions from heavy oil is realized in several directions: thermal and catalytic cracking, hydrocracking [3, 4]. Currently, importance of hydrocracking process in oil treatment is relatively low [5]. Thermal and catalytic cracking of heavy oil is widely used in industry [6–9]. However, heavy oil cracking is characterized by obtaining great amount of olefins as a result of C-H bond breakdown [10].

According to the international regulations, content of olefins in gasoline must not exceed 15–18 % [11, 12]. In future, limitations of olefins and aromatic hydrocarbons content in gasoline, in particular benzene concentrations, will become even stricter [13]. Olefins, aromatic hydrocarbons, isoalkanes and oxygen-containing compounds in the form of methyl tert-butyl ether are octane components of gasoline. In this regard, catalytic methods of heavy alkanes hydro isomerization and hydrocracking are widely discussed in literature in recent years [14–18]. Catalysts based on various 3d metals (Ni, Mo, Co, W, Fe, etc.) are used in heavy oil feedstock treatment processes [19–22].

*Corresponding author.

Platinum-based zeolite containing catalysts [17, 23–25], which allow to rise light fraction yields are mainly used in heavy oil hydro treatment.

The aim of the present work is to develop zeolite containing modified polyfunctional catalysts for heavy paraffins hydro processing and to study their properties and performance in tetradecane treatment process.

Experimental

Modified with additives of molybdenum, phosphorus and cerium zeolite-containing polyfunctional catalysts Fe(5 %)-Pt(0,4 %)/Al₂O₃ (KT-17, KT-18) were synthesized. KT-17 contains Mo, P and Ce as modifying additives. KT-18 is modified with cerium and phosphorus.

Properties of catalysts were studied by methods of Electron Microscopy, X-ray phase analysis, BET, IRS, Mossbauer spectroscopy. Genesis of catalyst was studied by Mossbauer spectroscopy method under varying conditions (t, air, H₂). Isomeric shifts (IS) were performed according to α -Fe.

Structure and dimensionality of metal particles, which are the active phase of catalysts, were tested in catalytic transformation of C₁₄ alkanes obtaining gasoline fraction. Study was carried out in a stainless steel tubular reactor uniformly coated with electric heater. The reactor was filled first with 3 ml of quartz, then with catalyst (10 ml, d = 2–2.5 mm), pre-treated by hydrogen at 400 °C for 2 hours, and with 3 ml of quartz (particle size is 2–3 mm).

Catalysts were studied in C₁₄ treatment process at 280–400 °C temperature range, hydrogen pressure of 2 MPa, H₂:raw material ratio 200:1, and the volume rate of 5 h⁻¹.

0.83 ml / min of raw material was pumped to the reactor by drain pump. The reaction products were cooled and separated, liquid products were collected in the tank, and gas products were directed to gas meter.

The hydrocarbon content of reaction products was analyzed in γ -aluminum oxide stainless steel column of Chrom-4 chromatograph (Supelco) with argon as carrier gas.

Results and Discussion

Specific surface area of synthesized catalysts, measured by the BET method, is 192.5 m²/g for KT-17 and 222.7 m²/g for KT-18; porosity is 0.49 cm³/g and 0.48 cm³/g respectively (Fig. 1).

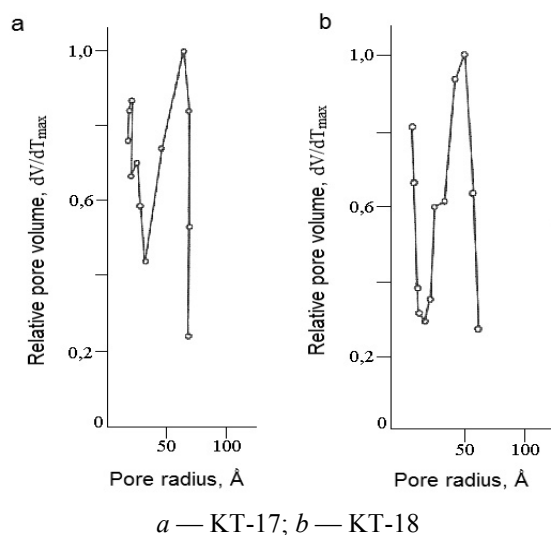


Figure 1. Porosity of catalytic systems

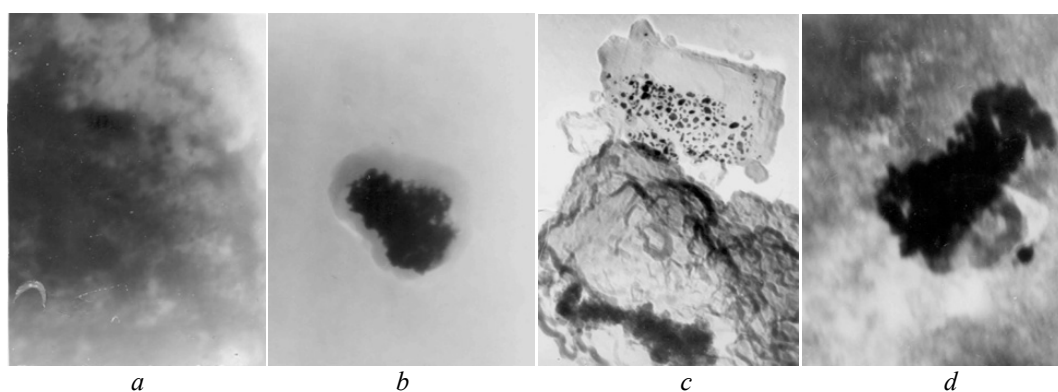
The KT-17 sample contains two types of narrow and one type of wide pores (Fig. 1, a). Narrow pores are available for formation of light hydrocarbons. Wide pores improve the adsorption capacity of catalyst in relation to hydrocarbons processing.

KT-18 catalyst has one type of narrow and wide pores available for adsorption and desorption of hydrocarbons (Fig. 1, b). Adsorption and activation of hydrogen and formation of lower alkanes molecules as result of deep hydrocracking of feedstock can occur in narrow pores.

Results of X-ray phase analysis show that catalyst KT-17 has structural elements of HZSM (reflexes 11.4; 6.7; 3.9 Å), Mo (reflex 2.30 Å) (ASTM 4–809) and γ -Al₂O₃ (reflex 1.98 Å). Structural elements of HZSM (reflexes 3.84; 3.73 Å) and Al₂O₃ (reflexes 2.26; 1.97; 1.40 Å) were found in catalyst KT-18.

By method of electron microscopy (magnification of 120000) the extensive accumulation of loose particles with size of 80–100 Å was found in catalyst KT-17, micro-diffraction of them shows the formation of phase — Pt₃Mo (ICPDS, 17–719) (Fig. 2, *a*). Small unit of dense particles with size of 50–60 Å is observed in the same catalytic system (Fig. 2, *b*). According to micro-diffraction data, particles have close sets of interplanar distances corresponding to several phases of Pt-Fe: PtFe — tetraferroplatinum (JCPDS, 26–1139); (Pt, Fe) — platinum, ferroan (JCPDS, 29–717, 29–718); Pt₃Fe — isoferroplatinum (JCPDS, 29–716).

Accumulations of large Pt crystals (200 Å) with signs of cutting on the smooth surface of zeolite component of carrier are detected in KT-18 (Fig. 2, *c*). Small rounded clusters (dark particles) composed of CeO₂ particles of 30 Å size are visible. Circular micro-diffraction data of particles with size of 30 Å can be equally attributed to Ce₆O₁₁ (JCPDS, 32–196) and ε-Fe₂O₃ (JCPDS, 16–835). Large cluster of 30–50 Å particles, which give circular diffraction of CeO₂ (JCPDS, 34–394) and unit of dense particles of 100–200 Å, microdiffraction picture of which is represented by reflexes and can be attributed to sulfur (JCPDS, 27–101), were found in KT-18 (Fig. 2, *d*).



a, b — KT-17; *c, d* — KT-18. Magnification 120000

Figure 2. Electron microscopy images of catalytic systems

Table 1 summarizes data on metal active sites of KT-17 and KT-18 catalysts nature.

Table 1

State and structure of particles in calcined (500°C, 5 h) zeolite-containing Pt(0,4 %)-Fe(5 %)/Al₂O₃ catalysts modified with cerium, molybdenum and phosphorus (KT-17) and with cerium and phosphorus (KT-18)

| Chemical composition and dispersion of KT-17 | | | |
|---|---|---|--|
| Iron | Platinum | Cerium | Molybdenum |
| Fe (d = 50–60 Å) FeFe ₂ O ₄ (d = 100–300 Å) Fe ₂ PO ₅ (d = 40–80 Å) | Pt (d = 50–60 Å) PtFe (d = 50–60 Å) Pt ₃ Fe (d = 50–60 Å) Pt ₃ Mo ₂ , β-Pt ₃ Mo (d = 80–100 Å) | CeP ₂ (d = 40–50 Å) CeP (d = ~300 Å) | MoOPO ₄ (d = ~15 Å) MoO ₂ (d = 100–300 Å) |
| Chemical composition and dispersion of KT-18 | | | |
| Iron | Platinum | Cerium | |
| ε-Fe ₂ O ₃ (30 Å) η-Fe ₂ O ₃ (d = 30–50 Å) Fe ₂ O ₃ (d = 30–50 Å) | Pt (d = 200 Å) | CeO ₂ (d = 30–50 Å) CeP (d = 100–200 Å) Ce ₆ O ₁₁ (d = 30 Å) CeAlO ₃ (d = 30–50 Å) | |

As it can be observed from Table 1, KT-17 catalyst sample contains homonuclear particles of Pt and Fe (50–60 Å), Fe₂PO₅, MoOPO₄ (15–300 Å) compounds, as well as homonuclear and heteronuclear clusters. Homonuclear clusters include FeFe₂O₄, molybdenum oxide MoO₂, the size of which varies from 100 to 300 Å. Heteronuclear clusters include PtFe, Pt₃Fe, Pt₃Mo₂, β-Pt₃Mo, CeP₂, CeP. These heteronuclear clusters have dimensions from 40 to 100 Å and 300 Å. According to electron-microscopic studies, KT-17 catalyst is nanostructured system of complex composition with particle sizes mainly from 15 to 100 Å.

KT-18 catalyst sample contains homonuclear particles of Pt, 200 Å in size, iron oxides and cerium oxides, the sizes of which range from 30 to 50 Å (Table 1). Heteronuclear cluster CeP (100–200 Å) and

CeAlO₃ compound (30–50 Å) were also found in this catalyst. The detected structures have different dimensions, mainly from 30 to 200 Å.

Catalysts were studied with Mossbauer spectroscopy method at varying conditions (t, Ar, H₂, O₂).

Spectra of initial systems (KT-17, KT-18) are superpositions of two doublets corresponding to high-spin states of Fe₁³⁺ and Fe₂³⁺ with similar values of isomeric shifts (0.30–0.31 mm/s), which are distinguished by quadruple splitting (QS): Fe₁³⁺ — 1.59 mm/s and Fe₂³⁺ — 0.95 mm/s. Fe₁³⁺/Fe₂³⁺ ratio is ~ 2/3. Since the line width corresponding to these structures is large (0.64 mm/s), it can be assumed that the forms of Fe³⁺ represent a set of close states with approximately the same isomeric shift (IS) and different quadruple splittings due to differences in the environment of iron.

The form with higher QS in KT-17 can be attributed to iron ions located on the surface of matrix. Values of isomeric shift raise with temperature growth, while the quadruple splitting practically does not change (Table 2).

Table 2

Mossbauer parameters and relative amount (S, %) of different forms of iron in KT-17 catalyst in air

| Temperature, °C | Fe ₁ ³⁺ | | | Fe ₂ ³⁺ | | |
|-----------------|-------------------------------|----------|------|-------------------------------|----------|------|
| | IS, mm/s | QS, mm/s | S, % | IS, mm/s | QS, mm/s | S, % |
| 20 | 0.31 | 1.43 | 42 | 0.31 | 0.84 | 58 |
| 100 | 0.27 | 1.40 | 42 | 0.27 | 0.85 | 58 |
| 200 | 0.21 | 1.39 | 43 | 0.20 | 0.86 | 57 |
| 300 | 0.14 | 1.43 | 42 | 0.14 | 0.85 | 58 |
| 400 | 0.07 | 1.45 | 41 | 0.07 | 0.89 | 59 |
| 500 | 0.02 | 1.39 | 45 | 0.00 | 0.94 | 55 |

Reduction of iron in catalytic system KT-17 starts in hydrogen stream at 100 °C, forming up to 3 % of Fe²⁺ (Fig. 3). At 200 °C, ~ 27 % of Fe²⁺ in two states, corresponding to two initial states of Fe³⁺, is present in system. The Fe₁²⁺ form with high QS is located on the surface as well as Fe₁³⁺. At 400 °C, one form of Fe³⁺ is more deeply located in the carrier, and two forms of Fe²⁺ remain in the system. At 500 °C, system contains only two forms of Fe²⁺.

Temperature decline from 500 to 100 °C (reverse) does not lead to new forms of iron (Table 3). However, redistribution of intensities of Fe²⁺ relative content signals takes place: the intensity of signal of iron form with higher QS increases, due to this effect's dependence on temperature. This is explained by weak interaction of Fe₁²⁺ form with carrier, since it is located on the surface. One more form of iron with Mossbauer parameters which are characteristic for Fe-Pt clusters located on the surface appears in system at 20 °C (Table 3).

Table 3

Mossbauer parameters and relative amount (S, %) of different forms of iron in KT-17 catalyst at varying temperature in hydrogen atmosphere

| t, °C | Fe ₁ ³⁺ | | | Fe ₂ ³⁺ | | | Fe ₁ ²⁺ | | | Fe ₂ ²⁺ | | | Fe-Pt phase | | |
|------------------|-------------------------------|----------|------|-------------------------------|----------|------|-------------------------------|----------|------|-------------------------------|----------|------|-------------|----------|------|
| | IS, mm/s | QS, mm/s | S, % | IS, mm/s | QS, mm/s | S, % | IS, mm/s | QS, mm/s | S, % | IS, mm/s | QS, mm/s | S, % | IS, mm/s | QS, mm/s | S, % |
| 20 | 0.31 | 1.53 | 37 | 0.30 | 0.92 | 63 | | | | | | | | | |
| 100 | 0.25 | 1.45 | 45 | 0.27 | 0.87 | 52 | 1.22 | 2.78 | 3 | | | | | | |
| 200 ¹ | 0.21 | 1.42 | 37 | 0.20 | 0.85 | 37 | 0.94 | 1.99 | 15 | 0.86 | 1.32 | 11 | | | |
| 300 | 0.14 | 1.43 | 8 | 0.14 | 0.85 | 14 | 0.86 | 1.87 | 45 | 0.81 | 1.14 | 33 | | | |
| 400 ² | | | | 0.12 | 1.03 | 11 | 0.82 | 1.66 | 47 | 0.72 | 1.10 | 42 | | | |
| 500 | | | | | | | 0.75 | 1.55 | 41 | 0.65 | 1.09 | 59 | | | |
| 400 | | | | | | | 0.80 | 1.70 | 51 | 0.71 | 1.07 | 49 | | | |
| 300 | | | | | | | 0.88 | 1.73 | 63 | 0.75 | 1.19 | 37 | | | |
| 200 | | | | | | | 0.94 | 1.95 | 64 | 0.85 | 1.21 | 36 | | | |
| 100 | | | | | | | 1.02 | 2.11 | 69 | 0.90 | 1.34 | 31 | | | |
| 20 | | | | | | | 1.08 | 2.21 | 59 | 1.00 | 1.39 | 25 | 0.33 | 1.13 | 16 |

Notes: ¹ — Fe²⁺ forms were not distinguished due to their small amounts at 200°C; ² — Fe³⁺ forms were not distinguished due to their small amounts at 400 °C.

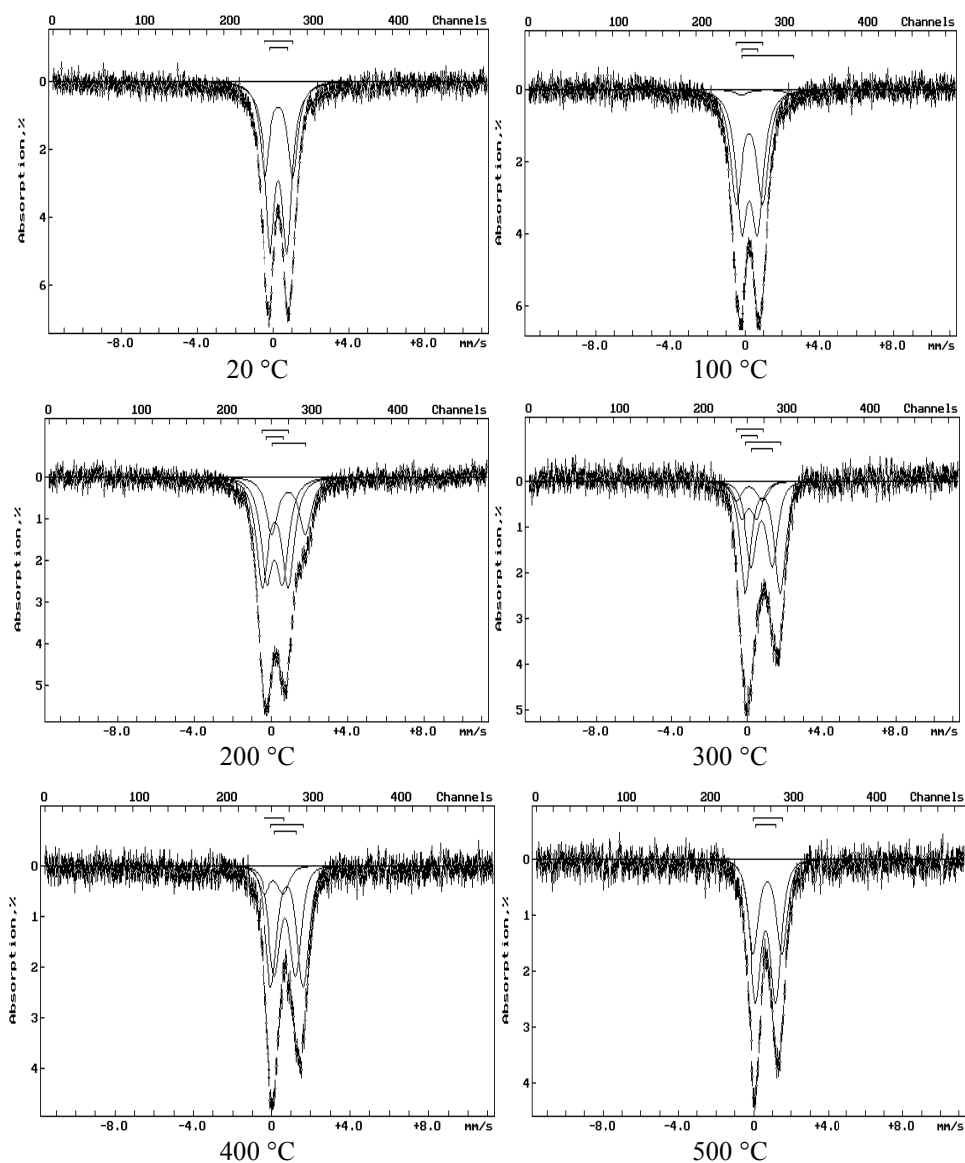


Figure 3. Mossbauer spectra of KT-17 catalytic system at varying temperature. Atmosphere — hydrogen

In air stream at 20 °C after reduction by hydrogen system contains two forms of Fe^{3+} and two forms of Fe^{2+} , Fe-Pt phase disappears (Fig. 4, *a*). More high QS value for Fe^{3+} forms than it was observed before the start of reduction cycle draws attention (Table 4). Replacing of air with hydrogen at the same temperature leads to a noticeable growth of Fe^{2+} forms amounts (Fig. 4, *b*).

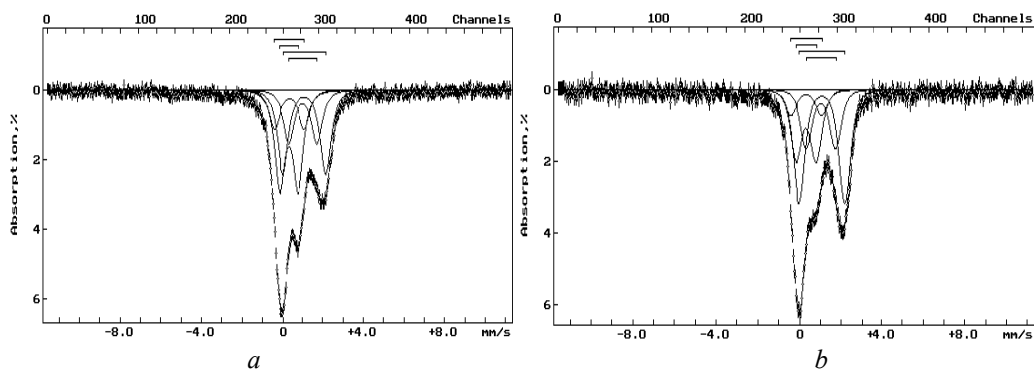
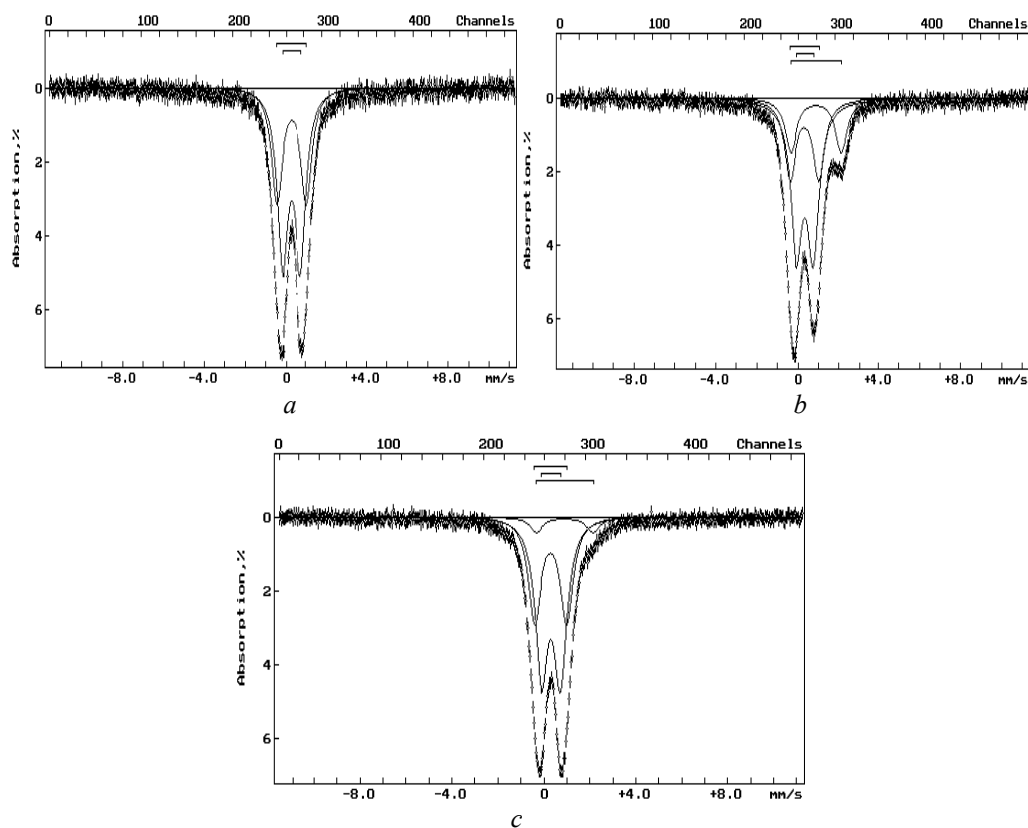


Figure 4. Mossbauer spectra of KT-17 catalytic system at 20 °C obtained after reduction and cooling in the atmosphere of: a) air, b) hydrogen

Obtained at 20 °C spectrum of system calcined at 500 °C in air is a superposition of two doublets corresponding to two states of Fe³⁺, just as it was observed for the initial state of system (Fig. 5, *a*, Table 4). However, even in this case, the observed values of quadruple splitting are much higher.



Atmosphere: *a* — air; *b* — hydrogen; *c* — air (after hydrogen)

Figure 5. Mossbauer spectra of KT-17 catalytic system at 20 °C obtained after oxidation at 500 °C

Table 4

Mossbauer parameters and relative amount (S, %) of different forms of iron in KT-17 at 20 °C

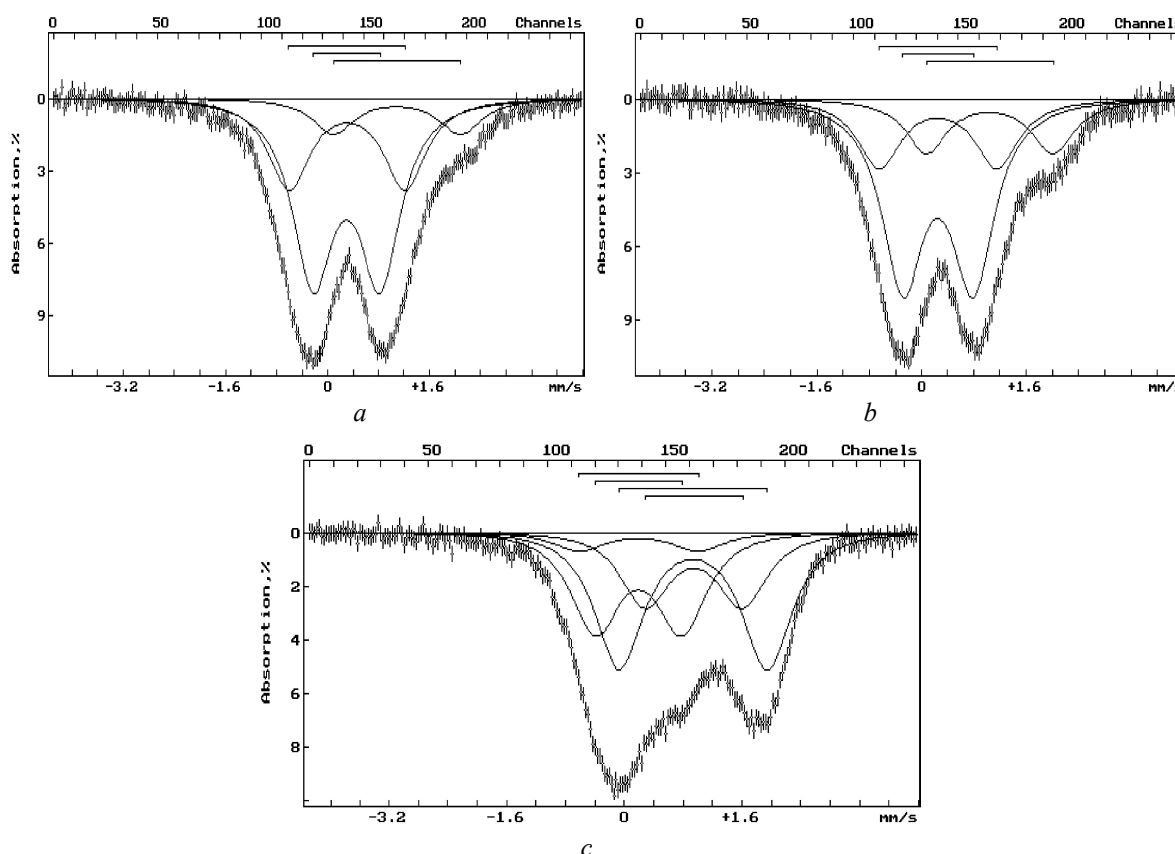
| Fe ₁ ³⁺ | | | Fe ₂ ³⁺ | | | Fe ₁ ²⁺ | | | Fe ₂ ²⁺ | | | Fe-Pt phase | | |
|--|----------|------|-------------------------------|----------|------|-------------------------------|----------|------|-------------------------------|----------|------|-------------|----------|------|
| IS, mm/s | QS, mm/s | S, % | IS, mm/s | QS, mm/s | S, % | IS, mm/s | QS, mm/s | S, % | IS, mm/s | QS, mm/s | S, % | IS, mm/s | QS, mm/s | S, % |
| In air stream after reduction by H ₂ | | | | | | | | | | | | | | |
| 0.34 | 1.52 | 14 | 0.32 | 0.95 | 36 | 1.09 | 2.17 | 31 | 1.03 | 1.43 | 19 | | | |
| In H ₂ after air | | | | | | | | | | | | | | |
| 0.33 | 1.51 | 10 | 0.33 | 0.97 | 26 | 1.09 | 2.20 | 42 | 1.04 | 1.41 | 22 | | | |
| In air (after heating in air at 500 °C) | | | | | | | | | | | | | | |
| 0.30 | 1.53 | 40 | 0.30 | 0.94 | 60 | | | | | | | | | |
| In H ₂ after calcination at 500 °C in air and cooling | | | | | | | | | | | | | | |
| 0,33 | 1.43 | 28 | 0.35 | 0.83 | 53 | | | | | | | 0.89 | 2.48 | 19 |
| In air after reduction by H ² at 20 °C | | | | | | | | | | | | | | |
| 0,30 | 1.43 | 38 | 0.32 | 0.84 | 57 | | | | | | | 0.91 | 2.48 | 5 |

After calcination at 500 °C in air and cooling, hydrogen was supplied to the system at 20 °C. In this case, partial reduction occurred and, in addition to the forms of Fe³⁺, ~ 19 % of Fe²⁺ appeared in system, however, the Mossbauer parameters of this form differed from the previously observed parameters of Fe²⁺ forms (Fig. 5, *b*, Table 4). In papers [26, 27] such behavior of systems, i.e. the ability to reduce at room temperature was considered indisputable evidence of the presence of Fe-Pt, Fe-Pd, Fe-Rh clusters. It is noteworthy that there is a very good quantitative correspondence between relative content of Fe-Pt phase at 20 °C

after fall of temperature from 500 °C in hydrogen atmosphere (Table 4) and its relative content after reduction at room temperature of system calcined in air at 500 °C (Table 3) — 19 % and 16 %, respectively.

After replacing of hydrogen by air at 20 °C, partial oxidation of Fe-Pt phase takes place, its relative content is reduced to ~ 5 % (Fig. 5, *c*. Table 4).

When calcined in air, the isomeric shift in catalytic system KT-18 decreases, and quadruple splitting raises from 1.59 to 1.70–1.74 mm/s (Fig. 6, *a*). Replacing air with hydrogen at 100 °C leads to appearance of two forms of Fe²⁺ (18 %), which are formed when the initial states of Fe³⁺ are reduced (Fig. 6, *b*). With repeated redox treatment (20–500 °C), concentration of Fe²⁺ forms increases from 18 to 60 % (*t* = 200 °C) (Fig. 6, *c*).

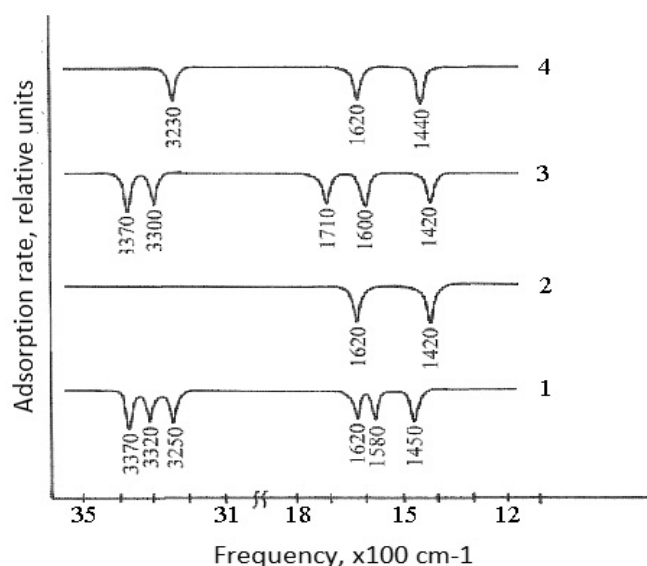


a — 20 °C — air, after oxidation at 500 °C; *b* — 100 °C — hydrogen, after oxidation at 500 °C;
c — reduction with hydrogen at 200 °C, after oxidation at 500 °C

Figure 6. Mossbauer spectra of KT-18 catalytic system at varying temperature

According to IR spectra of ammonia adsorption (10 min) on KT-17 catalyst at room temperature, the adsorption bands are fixed at 3370, 3320, 3250, 1620, 1580 and 1450 cm⁻¹ (Fig. 7, spectrum 1). The absorption bands at 3370, 3320, 1620 cm⁻¹ belong to Lewis acid centers, and at 3250, 1580, 1450 cm⁻¹ characterize Bronsted acid centers. After evacuation of sample, absorption bands are found at 1620, 1420 cm⁻¹ (Fig. 7, spectrum 2).

During ammonia adsorption at 250 °C (for 10 min), adsorption bands are detected at 3370, 3300, 1710, 1600 and 1420 cm⁻¹ (Fig. 7, spectrum 3). The absorption bands at 3370, 3300, 1600 cm⁻¹ are due to formation of coordination bond of ammonia at Lewis centers of zeolite. Surface reaction of ammonia with the Bronsted center forming NH₄⁺ gives absorption bands at 1710 and 1420 cm⁻¹. After the sample has been evacuated, absorption bands are present at 3230, 1620 and 1440 cm⁻¹ (Fig. 7, spectrum 4).

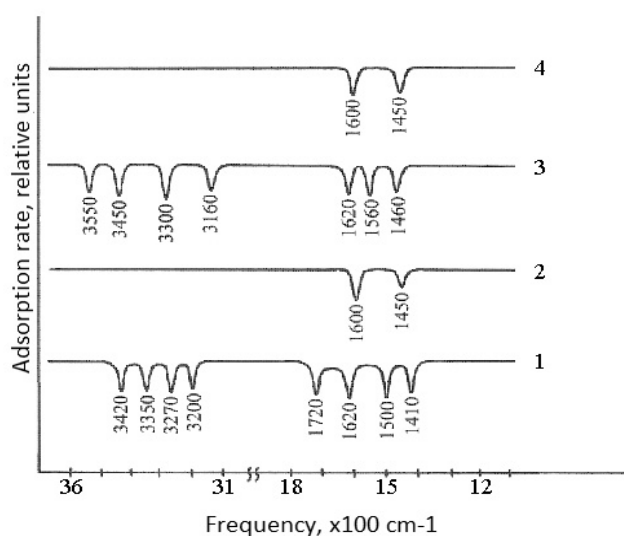


1 — NH₃ adsorption at room temperature; 2 — evacuation; 3 — NH₃ adsorption at $t = 250\text{ }^{\circ}\text{C}$; 4 — evacuation

Figure 7. IR spectra of NH₃ adsorption on KT-17 catalyst

On IR spectrum of ammonia adsorbed on KT-18 catalyst at room temperature (for 15 min), adsorption bands are fixed at 3420, 3350, 3270, 3200, 1720, 1620, 1500 and 1410 cm⁻¹ (Fig. 8, spectrum 1). Adsorption bands at 3420, 3350 and 1620 cm⁻¹ characterize Lewis acid centers, and adsorption bands at 3270, 3200, 1720, 1500 and 1410 cm⁻¹ refer to Bronsted acid centers. After the sample was evacuated, the adsorption bands were found at 1600 and 1450 cm⁻¹ (Fig. 8, spectrum 2), they belong to the most active of Lewis and Bronsted acid centers.

During the adsorption of ammonia on catalyst for 15 min at 250 °C, the adsorption bands were found at 3550, 3450, 3300, 3160, 1620, 1560 and 1460 cm⁻¹, which characterize the ammonia molecule coordination bounded with the Lewis centers (3450, 3300, 1620 cm⁻¹), and indicate formation of ammonium ions — surface reaction with the Bronsted centers (3550, 3160, 1560, 1460 cm⁻¹) (Fig. 8, spectrum 3). After evacuation, adsorption bands are observed at 1600, 1450 cm⁻¹ (Fig. 8, spectrum 4).



1 — NH₃ adsorption at room temperature; 2 — evacuation; 3 — NH₃ adsorption at $t = 250\text{ }^{\circ}\text{C}$; 4 — evacuation

Figure 8. IR spectra of NH₃ adsorption on KT-18 catalyst

Process of tetradecane hydro treatment on KT-17 and KT-18 catalysts was studied. Conversion of tetradecane on KT-17 grows from 59.1 to 94.8 % with rising temperature (Table 5). Reaction products contain C₄-C₉ iso-alkanes, C₁₀-C₁₄ iso-alkanes, C₄-C₁₀ alkanes, aromatic hydrocarbons and C₁-C₃-alkanes. In addition, 0.2–0.6 % of C₁₄₊ heavy hydrocarbons is found in reaction products. The yield of C₄-C₉ iso-alkanes at 380 °C reaches 37.9 %. It is known that gasoline fraction contains isoalkanes, n-alkanes, aromatic hydrocarbons and olefins. When tetradecane is transformed, hydrocracking of tetradecane proceeds with formation of mainly iso- and n-alkanes, content of aromatic hydrocarbons varies from 3.3 to 0.7 %.

The presence of C₄-C₉ normal and iso-alkanes, aromatic hydrocarbons, C₁-C₃ alkanes and C₁₄₊ hydrocarbons in reaction products demonstrates that KT-17 catalyst provides the parallel flow of hydrocracking, hydro-isomerization, dehydro-cyclization and alkylation reactions, thus proving its polyfunctional properties. According to the content of reaction products, tetradecane is almost totally converted. Yield of gasoline fraction is 67.9 % at 380 °C.

Table 5

Tetradecane hydro treatment over KT-17 and KT-18 catalysts. P = 2MPa, V = 5 h⁻¹, H₂:raw materials = 200:1

| Products content, % | Temperature of the process, °C | | | | | |
|---|--------------------------------|------|------|------|------|--------|
| | 280 | 300 | 320 | 350 | 380 | 400 |
| KT-17 | | | | | | |
| Conversion | 59.1 | 68.6 | 71.5 | 75.0 | 91.4 | 94.8 |
| ∑ C ₄ -C ₉ iso-alkanes | 35.3 | 31.3 | 33.4 | 32.4 | 37.9 | 36.2 |
| ∑ C ₁₀ -C ₁₄ iso-alkanes | 3.3 | 2.2 | 1.9 | 1.6 | 1 | 1.1 |
| ∑ C ₁ -C ₃ | 1.4 | 10.4 | 12.0 | 15.5 | 22.1 | 27.3 |
| ∑ C ₄ -C ₉ normal chain alkanes | 15.2 | 21.1 | 20.5 | 23.4 | 28.3 | 29.3 |
| ∑ aromatic hydrocarbons | 3.3 | 3.2 | 3.3 | 1.8 | 1.7 | 0.7 |
| C ₁₄₊ | 0.6 | 0.4 | 0.4 | 0.3 | 0.1 | 0.2 |
| Initial tetradecane | 40.9 | 31.4 | 28.5 | 25.0 | 8.6 | 5.2 |
| Yield of gasoline fraction | 53.8 | 55.6 | 57.2 | 57.6 | 67.9 | 66.2 |
| KT-18 | | | | | | |
| Conversion | 64.9 | 94.4 | 98.7 | 99.4 | 99.7 | 100 |
| ∑ C ₄ -C ₉ iso-alkanes | 33.2 | 44.4 | 42.4 | 42.6 | 36.1 | 33.0 |
| ∑ C ₁₀ -C ₁₄ iso-alkanes | 4.8 | 5.6 | 2.8 | 1.9 | 1.0 | 2.3 |
| ∑ C ₁ -C ₃ | 4.9 | 9.5 | 12.9 | 22.6 | 27.8 | 28.2 |
| ∑ C ₄ -C ₉ normal chain alkanes | 18.9 | 27.3 | 35.2 | 28.4 | 32.5 | 33.2 |
| ∑ aromatic hydrocarbons | 3.1 | 6.8 | 5.0 | 3.7 | 2.2 | 2.8 |
| Olefins | - | 0.8 | 0.4 | 0.2 | 0.1 | 0.5 |
| Initial tetradecane | 35.1 | 5.6 | 1.3 | 0.6 | 0.3 | traces |
| Yield of gasoline fraction | 55.2 | 79.3 | 83.0 | 74.9 | 70.9 | 69.5 |

Conversion of tetradecane on KT-18 raises from 64.9 to 100 % with temperature growth from 280 to 400 °C. Reaction products contain C₄-C₉ n-alkanes, C₄-C₉ and C₁₀-C₁₄ iso-alkanes, aromatic compounds (benzene, toluene, o- and p-xylenes) and olefins. Light C₁-C₃-hydrocarbons are presented with ethane, propane, ethylene and propylene; their yield rises from 4.9 to 28.2 % as temperature grows. The presence of the above mentioned organic compounds in reaction products indicates parallel sequential course of hydrocracking, dehydrogenation, isomerization, and alkylation reactions.

In liquid products content of isoalkanes C₄-C₉ prevails in the whole temperature range, the maximum yield of which (44.4 %) is observed at 300 °C. Formation of heavy isoalkanes C₁₀-C₁₄ under these conditions does not exceed 5.6 %. Quantity of C₄-C₉ n-alkanes and aromatic compounds is equal to 35.2 % (t = 320 °C) and 6.8 % (t = 300 °C) respectively. At temperature growth above 300 °C yield of liquid products reduces and deep hydrocracking of tetradecane to C₁-C₃ hydrocarbons increases; concentration of these hydrocarbons at 400 °C rises to 28.2 % (Table 5). Yield of gasoline fractions is maximal at 320 °C (83.0 %).

The temperature dependence of tetradecane conversion and isoalkanes C₄-C₉ output on KT group catalysts is presented in Figure 9.

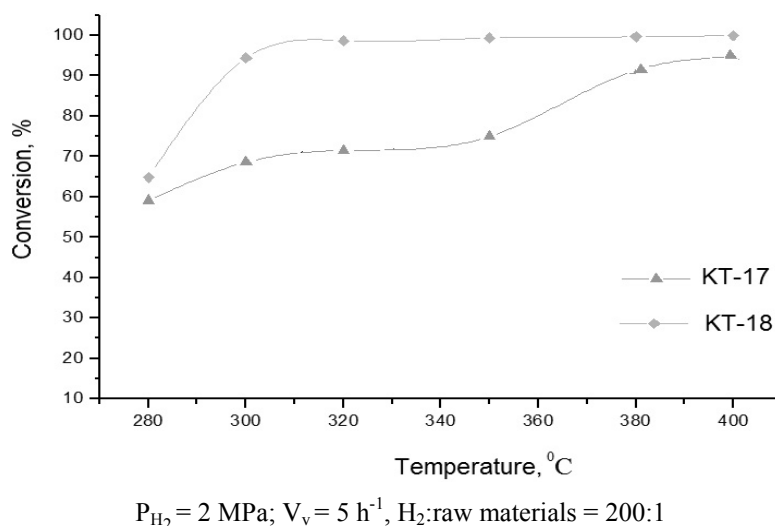


Figure 9. Influence of temperature on tetradecane conversion on zeolite-containing Pt-Fe/Al₂O₃ catalysts

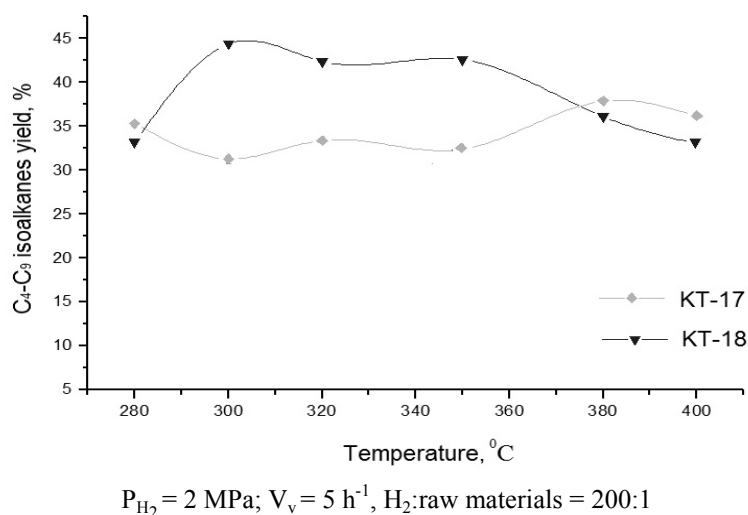


Figure 10. Influence of temperature on the output of isoalkanes C₄-C₉ at tetradecane transformation on zeolite-containing Pt-Fe/Al₂O₃ catalysts

It is clear (Fig. 9 and 10) that KT-18 catalyst is more optimal in the whole temperature range. This is probably due to a certain dispersion state of platinum ($d = 200 \text{ \AA}$), as the adsorption and activation of high molecular weight alkanes require flat orientation at active centers located on smooth surface of zeolite or near the mouths of pores. Cavities with $d = 56\text{--}53 \text{ \AA}$, typical for ZSM-5 zeolite, are inaccessible for heavy alkane molecules. Electron microscopy method shows that part of platinum in KT-18 catalyst is localized on the surface of zeolite (Fig. 2, c). At 300 °C the yield of C₄-C₉ isoalkanes is 44.4 %.

The observed direction of tetradecane transformations can be related to the combination of acid and hydro-dehydrating properties of catalysts, due to localization of platinum and Fe-Pt clusters on crystalline surface and in zeolite channels. It can be assumed that hydrocracking takes place on the active centers of Pt-zeolite, which are formed on the external crystal structure of zeolite. Smaller fragments of surface-activated decomposition particles of heavy n-alkanes can migrate into zeolite channels, where mono- and bimetallic clusters of platinum and Fe-Pt, which take part in waterproofing and hydro-isomerization with formation of isoalkanes C₄-C₉, are localized. The low yield of C₁₀-C₁₅ isoalkanes can be explained by competitive hydrocracking reaction on platinum-promoted external crystalline surface of zeolite. Deep hydrocracking of heavy alkanes on active centers of catalyst becomes prevailing at high temperatures. Narrow size of channels (0.56–0.53 nm) of ZSM-5 zeolite complicates diffusion of large molecules of n-alkanes with high molecular weight.

described reactions of tetradecane transformation. This reaction occurs mainly in high temperature area (350–400 °C). It is assumed that mononuclear particles of platinum also take part in tetradecane dehydrocyclization and dehydrogenation.

KT-18 catalyst demonstrates high activity in the process of heavy alkanes treatment; sizes of platinum ($d = 200 \text{ \AA}$) and iron ($d = 30\text{--}50 \text{ \AA}$) particles were determined by electron microscopy. Activity of KT-18 catalyst was higher than that of highly dispersed KT-17, because flat clusters have to be situated near the active sites of catalyst in order to destruct C₄-C₅ and C₉-C₁₀ bonds of C₄-C₉ normal and iso-alkanes.

Gasoline fraction with an output from 30.2 to 83.0 % containing 17.7–42.4 % of isoalkanes, 1.7–5.0 % of aromatic hydrocarbons, 0.3–0.4 % of olefins and 10.5–35.2 % of C₄-C₉ n-alkanes was received at tetradecane hydro processing on KT-18.

In general, the process is carried out relatively easily in the presence of large particles of platinum, concentrated on the outer surface or in cavities of zeolite.

Highly dispersed metal phase of HZSM zeolite cavities (53–56 Å) is not subjected to change and adsorption of long-chain alkanes under soft conditions.

The main feature of KT catalysts is their polyfunctionality. During alkanes processing simultaneous and consecutive reactions of hydrocracking, dehydrogenation, isomerization, dehydro-cyclization and hydrodesulfurization take place.

By means of physical and chemical methods it has been found that the zeolite containing catalysts Fe-Pt/Al₂O₃ modified by various additives are complex systems. Micro-diffraction and Mossbauer spectroscopy methods allowed detecting nanosized hetero clusters of Fe-Pt, Fe-Mo, Pt-Mo in catalysts structure. Depending on chemical composition of clusters, particle size varies between 20 and 80 Å. Catalysts are not exposed to carbonization, they are stable and highly active, therefore these systems can be proposed for practical testing.

References

- 1 Rana M.S. A review of recent advances on process technologies for upgrading of heavy oils and residua / M.S. Rana, V. Sarmano, J. Ancheyta, J.A.I. Diaz // *Fuel*. — 2007. Vol. 86, No. 9. — P. 1216–1231. DOI: 10.1016/j.fuel.2006.08.004
- 2 Okunev A.G. Catalytic hydroprocessing of heavy oil feedstocks / A.G. Okunev, E.V. Parkhomchuk, A.I. Lysikov, P.D. Parunin, V.S. Semykina, V.N. Parmon // *Russian Chemical Reviews*. — 2015. — Vol. 84, No. 9. — P. 981–999. DOI: 10.1070/RCR4486
- 3 Sahu R. A review of recent advances in catalytic hydrocracking of heavy residues / R. Sahu, B.J. Song, J.S. Im, Y-P. Jeon, C.W. Lee // *Journal of Industrial and Engineering Chemistry*. — 2015. — Vol. 27. — P. 12–24. DOI: 10.1016/j.jiec.2015.01.011
- 4 Fujimoto K. Hydrothermal cracking of residual oil / K. Fujimoto, J. Chang, N. Tsubaki // *Sekiyu Gakkaishi* — *Journal of the Japan Petroleum Institute*. — 2000. — Vol. 43, No. 1. — P. 25–36.
- 5 Gillis D. Upgrading Residues to Maximize Distillate Yields with UOP Uniflex (TM) Process / D. Gillis, M. VanWees, P. Zimmerman, E. Houde // *Journal of the Japan Petroleum Institute*. — 2010. — Vol. 53, No. 1. — P. 33–41. DOI: 10.1627/jpi.53.33
- 6 Corma A. Crude oil to chemicals: light olefins from crude oil / A. Corma, E. Corresa, Y. Mathieu, L. Sauvanaud, S. Al-Bogami, M.S. Al-Ghrami, A. Bourane // *Catalysis Science & Technology*. — 2017. — Vol. 7, No. 1. — P. 12–46. DOI: 10.1039/c6cy01886f
- 7 Nazarova G.Y. Effect of group composition of the vacuum distillate from heavy Kazakhstan and West Siberian oil on the yield of light fractions during the catalytic cracking / G.Y. Nazarova, E.N. Ivashkina, E.D. Ivanchina, V.I. Stebeneva, G.Z. Seytenova // *Procedia Engineering*. — 2016. — Vol. 152. — P. 18–24. DOI: 10.1016/j.proeng.2016.07.611
- 8 Kaminski T. Thermal cracking of atmospheric residue versus vacuum residue / T. Kaminski, M.M. Husein // *Fuel Processing Technology*. — 2018. — Vol. 181. — P. 331–339. DOI: 10.1016/j.fuproc.2018.10.014
- 9 Ghashghaee M. Two-Step Thermal Cracking of an Extra-Heavy Fuel Oil: Experimental Evaluation, Characterization, and Kinetics / M. Ghashghaee, S. Shirvani // *Industrial and Engineering Chemistry Research*. — 2018. — Vol. 57, No. 22. — P. 7421–7430. DOI: 10.1021/acs.iecr.8b00819
- 10 Vogt E.T.C. Fluid catalytic cracking: recent developments on the grand old lady of zeolite catalysis / E.T.C. Vogt, B.M. Weckhuysen // *Chemical Society Reviews*. — 2015. — Vol. 44, No. 20. — P. 7342–7370. DOI: 10.1039/c5cs00376h
- 11 Onoichenko S.N. Current and Promising Automotive Gasolines / S.N. Onoichenko, V.E. Emel'yanov, I.F. Krylov // *Chemistry and technology of fuels and oils*. — 2003. — Vol. 39, No. 6. — P. 303–308. DOI: 10.1023/B: CAFO.0000011901.59445.22
- 12 Hajbabaee M. Impact of olefin content on criteria and toxic emissions from modern gasoline vehicles / M. Hajbabaee, G. Karavalakis, J.W. Miller, M. Vilella, K.H. Xu, T.D. Durbin // *Fuel*. — 2013. — Vol. 107. — P. 671–679. DOI: 10.1016/j.fuel.2012.12.031

- 13 Courty P. Refining Clean Fuels for the Future / P. Courty, J.F. Gruson // *Oil & Gas Science and Technology*. — 2001. — Vol. 56, No. 5. — P. 515–524. DOI: 10.2516/ogst:2001041
- 14 Castaneda L.C. Combined process schemes for upgrading of heavy petroleum / L.C. Castaneda, J.A.D. Munoz, J. Ancheyta // *Fuel*. — 2012. — Vol. 100. — P. 110–127. DOI: 10.1016/j.fuel.2012.02.022
- 15 Bellussi G. Hydroconversion of heavy residues in slurry reactors: Developments and perspectives / G. Bellussi, G. Rispoli, A. Landoni, R. Millini, D. Molinari, E. Montanari, D. Moscotti, P. Pollesel // *Journal of Catalysis*. — 2013. — Vol. 308. — P. 189–200. DOI: 10.1016/j.jcat.2013.07.002
- 16 Zaki T. Slurry-phase catalytic hydrocracking of mazut (heavy residual fuel oil) using Ni-bentonite / T. Zaki, G.S. Mukhtarova, A.M. Al-Sabagh, F.S. Soliman, M.A. Betiha, T. Mahmoud, M. Abd El-Raouf, N.K. Afandiyeva, A. Alizade, A.B. Hasanova, V.M. Abbasov // *Petroleum Science and Technology*. — 2018. — Vol. 36, No. 19. — P. 1559–1567. DOI: 10.1080/10916466.2018.1490762
- 17 Martens J.A. Hydroisomerization and hydrocracking of linear and multibranched long model alkanes on hierarchical Pt/ZSM-22 zeolite / J.A. Martens, D. Verboekend, K. Thomas, G. Vanbutsele, J. Perez-Ramirez, J.P. Gilson // *Catalysis Today*. — 2013. — Vol. 218. — P. 135–142. DOI: 10.1016/j.cattod.2013.03.041
- 18 Batalha N. n-Hexadecane hydroisomerization over Pt-HBEA catalysts. Quantification and effect of the intimacy between metal and protonic sites / N. Batalha, L. Pinard, C. Bouchy, E. Guillon, M. Guisnet // *Journal of Catalysis*. — 2013. — Vol. 307. — P. 122–131. DOI: 10.1016/j.jcat.2013.07.014
- 19 Sosnin G.A. Catalytic steam cracking of vacuum residue in presence of dispersed catalysts based on Mo, Ni, Fe, Co, Al metals / G.A. Sosnin, O.O. Zaikina, P.M. Eletsii, V.A. Yakovlev // *Bulletin of the Tomsk Polytechnic University — Geo Assets Engineering*. — 2018. — Vol. 329, No. 12. — P. 145–154. DOI: 10.18799/24131830/2018/12/30
- 20 Mironenko O.O. Catalytic Steam Cracking of Heavy Crude Oil with Molybdenum and Nickel Nanodispersed Catalysts / O.O. Mironenko, G.A. Sosnin, P.M. Eletsii, Y.K. Gulyaeva, O.A. Bulavchenko, O.A. Stonkus, V.O. Rodina, V.A. Yakovlev // *Catalysis in Industry*. — 2017. — Vol. 9, No. 3. — P. 221–229. DOI: 10.1134/S2070050417030084
- 21 Alphazan T. Highly active nonpromoted hydrotreating catalysts through the controlled growth of a supported hexagonal WS₂ phase / T. Alphazan, A. Bonduelle-Skrzypczak, C. Legens, A.S. Gay, Z. Boudene, M. Girleanu, O. Ersen, C. Coperet, P. Raybaud // *ACS Catalysis*. — 2014. — Vol. 4, No. 12. — P. 4320–4331. DOI: 10.1021/cs501311m
- 22 Funai S. Recovery of useful lighter fuels from petroleum residual oil by oxidative cracking with steam using iron oxide catalyst / S. Funai, E. Fumoto, T. Tago, T. Masuda // *Chemical Engineering Science*. — 2010. — Vol. 65, No. 1. — P. 60–65. DOI: 10.1016/j.ces.2009.03.028
- 23 Alvarez F. Hydroisomerization and hydrocracking of alkanes — Influence of the balance between acid and hydrogenating functions on the transformation of n-decane on PTHY catalysts / F. Alvarez, F.R. Ribeiro, G. Perot, C. Thomazeau, M. Guisnet // *Journal of Catalysis*. — 1996. — Vol. 162, No. 2. — P. 179–189. DOI: 10.1006/jcat.1996.0275
- 24 Choudhury I.R. Pt/H-ZSM-22 hydroisomerization catalysts optimization guided by Single-Event MicroKinetic modeling / I.R. Choudhury, K. Hayasaka, J.W. Thybaut, C.S.L. Narasimhan, J.F. Denayer, J.A. Martens, G.B. Marin // *Journal of Catalysis*. — 2012. — Vol. 290. — P. 165–176. DOI: 10.1016/j.jcat.2012.03.015
- 25 Verboekend D. Towards more efficient monodimensional zeolite catalysts: n-alkane hydro-isomerisation on hierarchical ZSM-22 / D. Verboekend, K. Thomas, M. Milina, S. Mitchell, J. Perez-Ramirez, J.P. Gilson // *Catalysis Science & Technology*. — 2011. — Vol. 1, No. 8. — P. 1331–1335. DOI: 10.1039/c1cy00240f
- 26 Guzzi L. Structure and catalytic properties of iron-containing bimetallic catalysts / L. Guzzi // *Catalysis Reviews — Science and Engineering*. — 1981. — Vol. 23, No. 3. — P. 329–376. DOI: 10.1080/03602458108079640
- 27 Dezsi I. Characterization of silica supported Pt-Fe catalysts by Mossbauer-spectroscopy / I. Dezsi, D.L. Nagy, M. Eszterle, L. Guzzi // *Reaction Kinetics and Catalysis Letters*. — 1978. — Vol. 8, No. 3. — P. 301–307. DOI: 10.1007/BF02068170

А.К. Жұмабекова, Л.К. Тастанова, Р.О. Орынбасар, Г.Д. Закумбаева

Модификаторлардың Fe-Pt/Al₂O₃ алкандарды гидроөндеу катализаторларына әсері

Молибден, фосфор және церий қоспаларымен модификацияланған құрамында цеолиті бар Fe-Pt/Al₂O₃ (КТ-17, КТ-18) полифункционалды катализаторлары синтезделді. Модификациялық қоспалардың КТ-17 және КТ-18 каталитикалық қасиеттеріне әсері зерттелді. Өзірленген каталитикалық жүйелер бензин фракциясын алу үшін C₁₄ модельдік алканды гидроөндеу процесінде зерттелген. Реакция өнімдерінде C₄-C₉ изо-алкандар, C₁₀-C₁₄ изо-алкандар, C₄-C₁₀ алкандар, ароматты көмірсутектер және C₁-C₃ алкандар бар. Қайта өндеу өнімдеріндегі ауыр көмірсутектердің құрамы 0,2–0,6%. C₄-C₉ алкандарының 380 °C температурада шығымы 37,9% құрайды. Физика-химиялық зерттеу әдістерін қолдана отырып, әр түрлі қоспалармен модификацияланған, цеолитқұрамды Fe-Pt/Al₂O₃ катализаторлары күрделі каталитикалық жүйелер болып табылатындығы анықталды. Микродифракция және Мессбауэр спектроскопиясы әдістерімен катализаторлар құрылымындағы Fe-Pt, Fe-Mo, Pt-Mo наноөлшемді гетерокластерлері анықталды. Кластерлердің химиялық құрамына байланысты бөлшектердің мөлшері 20-дан 80 Å-ге дейін өзгереді. КТ-18 катализаторы ауыр алкандарды өндеу процесінде

жоғары белсенділік танытады. Электронды микроскопия әдісімен катализатордың құрылымы зерттелді, платина ($d = 200 \text{ \AA}$) және темір ($d = 30\text{--}50 \text{ \AA}$) бөлшектерінің өлшемдері анықталды. КТ-18 каталикалық жүйесінің белсенділігі КТ-17 катализаторына карағанда жоғары. КТ катализаторларының басты ерекшелігі — олардың полифункционалдылығы. Алкандарды өңдеу кезінде гидрокрекинг, дегидрогенизация, изомеризация, дегидроциклизация және гидрокүкіртсіздену реакциялары бір уақытта және дәйекті түрде жүреді.

Кілт сөздер: гидроөңдеу, цеолитқұрамды катализаторлар, модификация, полифункционалдык, ауыр алкандар, гидрокрекинг, гидрлеу, нанокластерлер.

А.К. Жумабекова, Л.К. Тастанова, Р.О. Орынбасар, Г.Д. Закумбаева

Влияние модификаторов на Fe-Pt/Al₂O₃ катализаторы гидропереработки алканов

Синтезированы цеолитсодержащие полифункциональные катализаторы Fe-Pt/Al₂O₃ (КТ-17, КТ-18), модифицированные добавками молибдена, фосфора и церия. Исследовано влияние модифицирующих добавок на каталитические свойства КТ-17 и КТ-18. Разработанные каталитические системы изучены в процессе гидропереработки модельного алкана С14 с получением бензиновой фракции. В продуктах реакции содержатся изо-алканы С4-С9, изо-алканы С10-С14, алканы С4-С10, ароматические углеводороды и алканы С1-С3. Содержание тяжелых углеводородов в продуктах переработки — 0,2–0,6 %. Выход изо-алканов С4-С9 при температуре 380 °С составляет 37,9 %. С помощью физико-химических методов исследования установлено, что модифицированные различными добавками цеолитсодержащие катализаторы Fe-Pt/Al₂O₃ представляют собой сложные каталитические системы. Методами микрофракции и Мессбауэровской спектроскопии в структуре катализаторов обнаружены наноразмерные гетерокластеры Fe-Pt, Fe-Mo, Pt-Mo. В зависимости от химического состава кластеров размер частиц колеблется от 20 до 80 Å. Катализатор КТ-18 проявляет высокую активность в процессе переработки тяжелых алканов. Методом электронной микроскопии исследована структура катализатора, определены размеры частиц платины ($d = 200 \text{ \AA}$) и железа ($d = 30\text{--}50 \text{ \AA}$). Активность каталитической системы КТ-18 выше, чем у высокодисперсного катализатора КТ-17. Главной особенностью катализаторов КТ является их полифункциональность. При обработке алканов одновременно и последовательно протекают реакции гидрокрекинга, дегидрогенизации, изомеризации, дегидроциклизации и гидрообессеривания.

Ключевые слова: гидропереработка, цеолитсодержащие катализаторы, модификация, полифункциональность, тяжелые алканы, гидрокрекинг, гидрирование, нанокластеры.

References

- 1 Rana, M.S., Sarmano, V., Ancheyta, J., & Diaz, J. (2007). A review of recent advances on process technologies for upgrading of heavy oils and residua. *Fuel*, 86(9), 1216–1231. DOI: 10.1016/j.fuel.2006.08.004
- 2 Okunев, A.G., Parkhomchuk, E.V., Lysikov, A.I., Parunin, P.D., Semeykina, V.S., & Parmon, V.N. (2015). Catalytic hydroprocessing of heavy oil feedstocks. *Russian Chemical Reviews*, 84(9), 981–999. DOI: 10.1070/RCR4486
- 3 Sahu, R., Song, B.J., Im, J.S., Jeon, Y-P., & Lee, C.W. (2015). A review of recent advances in catalytic hydrocracking of heavy residues. *Journal of Industrial and Engineering Chemistry*, 27, 12–24. DOI: 10.1016/j.jiec.2015.01.011
- 4 Fujimoto, K., Chang, J., & Tsubaki, N. (2000). Hydrothermal cracking of residual oil. *Sekiyu Gakkaishi — Journal of the Japan Petroleum Institute*, 43(1), 25–36.
- 5 Gillis, D., VanWees, M., Zimmerman, P., & Houde, E. (2010). Upgrading Residues to Maximize Distillate Yields with UOP Uniflex (TM) Process. *Journal of the Japan Petroleum Institute*, 53(1), 33–41. DOI: 10.1627/jpi.53.33
- 6 Corma, A., Corresa, E., Mathieu, Y., Sauvanaud, L., Al-Bogami, S., & Al-Ghrami, M. S., et al. (2017). Crude oil to chemicals: light olefins from crude oil. *Catalysis Science & Technology*, 7(1), 12–46. DOI: 10.1039/c6cy01886f
- 7 Nazarova, G.Y., Ivashkina, E.N., Ivanchina, E.D., Stebeneva, V.I., & Seytenova, G.Z. (2016). Effect of group composition of the vacuum distillate from heavy Kazakhstan and West Siberian oil on the yield of light fractions during the catalytic cracking. *Procedia Engineering*, 152, 18–24. DOI: 10.1016/j.proeng.2016.07.611
- 8 Kaminski, T., & Husein, M.M. (2018). Thermal cracking of atmospheric residue versus vacuum residue. *Fuel Processing Technology*, 181, 331–339. DOI: 10.1016/j.fuproc.2018.10.014
- 9 Ghashghaee, M., & Shirvani, S. (2018). Two-Step Thermal Cracking of an Extra-Heavy Fuel Oil: Experimental Evaluation, Characterization, and Kinetics. *Industrial and Engineering Chemistry Research*, 57(22), 7421–7430. DOI: 10.1021/acs.iecr.8b00819
- 10 Vogt, E.T.C., & Weckhuysen, B.M. (2015). Fluid catalytic cracking: recent developments on the grand old lady of zeolite catalysis. *Chemical Society Reviews*, 44(20), 7342–7370. DOI: 10.1039/c5cs00376h

- 11 Onoichenko, S.N., Emel'yanov, V.E., & Krylov, I.F. (2003). Current and Promising Automotive Gasolines. *Chemistry and technology of fuels and oils*, 39(6), 303–308. DOI: 10.1023/B: CAFO.0000011901.59445.22
- 12 Hajbabaie, M., Karavalakis, G., Miller, J.W., Villela, M., Xu, K.H., & Durbin, T.D. (2013). Impact of olefin content on criteria and toxic emissions from modern gasoline vehicles. *Fuel*, 107, 671–679. DOI: 10.1016/j.fuel.2012.12.031
- 13 Courty, P., & Gruson, J.F. (2001). Refining Clean Fuels for the Future. *Oil & Gas Science and Technology*, 56(5), 515–524. DOI: 10.2516/ogst:2001041
- 14 Castaneda, L.C., Munoz, J.A.D., & Ancheyta, J. (2012). Combined process schemes for upgrading of heavy petroleum. *Fuel*, 100, 110–127. DOI: 10.1016/j.fuel.2012.02.022
- 15 Bellussi, G., Rispoli, G., Landoni, A., Millini, R., Molinari, D., & Montanari, E., et al. (2013). Hydroconversion of heavy residues in slurry reactors: Developments and perspectives. *Journal of Catalysis*, 308, 189–200. DOI: 10.1016/j.jcat.2013.07.002
- 16 Zaki, T., Mukhtarova, G.S., Al-Sabagh, A.M., Soliman, F.S., Betiha, M.A., & Mahmoud, T., et al. (2018). Slurry-phase catalytic hydrocracking of mazut (heavy residual fuel oil) using Ni-bentonite. *Petroleum Science and Technology*, 36(19), 1559–1567. DOI: 10.1080/10916466.2018.1490762
- 17 Martens, J.A., Verboekend, D., Thomas, K., Vanbutsele, G., Perez-Ramirez, J., & Gilson, J.P. (2013). Hydroisomerization and hydrocracking of linear and multibranched long model alkanes on hierarchical Pt/ZSM-22 zeolite. *Catalysis Today*, 218, 135–142. DOI: 10.1016/j.cattod.2013.03.041
- 18 Batalha, N., Pinard, L., Bouchy, C., Guillon, E., & Guisnet, M. (2013). n-Hexadecane hydroisomerization over Pt-HBEA catalysts. Quantification and effect of the intimacy between metal and protonic sites. *Journal of Catalysis*, 307, 122–131. DOI: 10.1016/j.jcat.2013.07.014
- 19 Sosnin, G.A., Zaikina, O.O., Eletsii, P.M., & Yakovlev, V.A. (2018). Catalytic steam cracking of vacuum residue in presence of dispersed catalysts based on Mo, Ni, Fe, Co, Al metals. *Bulletin of the Tomsk Polytechnic University — Geo Assets Engineering*, 329(12), 145–154. DOI: 10.18799/24131830/2018/12/30
- 20 Mironenko, O.O., Sosnin, G.A., Eletsii, P.M., Gulyaeva, Y.K., Bulavchenko, O.A., & Stonkus, O.A., et al. (2017). Catalytic Steam Cracking of Heavy Crude Oil with Molybdenum and Nickel Nanodispersed Catalysts. *Catalysis in Industry*, 9(3), 221–229. DOI: 10.1134/S2070050417030084
- 21 Alphazan, T., Bonduelle-Skrzypczak, A., Legens, C., Gay, A.S., Boudene, Z., & Girleanu, M., et al. (2014). Highly active nonpromoted hydrotreating catalysts through the controlled growth of a supported hexagonal WS₂ phase. *ACS Catalysis*, 4(12), 4320–4331. DOI: 10.1021/cs501311m
- 22 Funai, S., Fumoto, E., Tago, T., & Masuda, T. (2010). Recovery of useful lighter fuels from petroleum residual oil by oxidative cracking with steam using iron oxide catalyst. *Chemical Engineering Science*, 65(1), 60–65. DOI: 10.1016/j.ces.2009.03.028
- 23 Alvarez, F., Ribeiro, F.R., Perot, G., Thomazeau, C., & Guisnet, M. (1996). Hydroisomerization and hydrocracking of alkanes — Influence of the balance between acid and hydrogenating functions on the transformation of n-decane on PtHY catalysts. *Journal of Catalysis*, 162(2), 179–189. DOI: 10.1006/jcat.1996.0275
- 24 Choudhury, I.R., Hayasaka, K., Thybaut, J.W., Narasimhan, C.S.L., Denayer, J.F., & Martens, J.A., et al. (2012). Pt/H-ZSM-22 hydroisomerization catalysts optimization guided by Single-Event MicroKinetic modeling. *Journal of Catalysis*, 290, 165–176. DOI: 10.1016/j.jcat.2012.03.015
- 25 Verboekend, D., Thomas, K., Milina, M., Mitchell, S., Perez-Ramirez, J., & Gilson, J.P. (2011). Towards more efficient monodimensional zeolite catalysts: n-alkane hydro-isomerisation on hierarchical ZSM-22. *Catalysis Science & Technology*, 1(8), 1331–1335. DOI: 10.1039/c1cy00240f
- 26 Guzzi, L. (1981). Structure and catalytic properties of iron-containing bimetallic catalysts. *Catalysis Reviews — Science and Engineering*, 23(3), 329–376. DOI: 10.1080/03602458108079640
- 27 Dezsi, I., Nagy, D.L., Eszterle, M., & Guzzi, L. (1978). Characterization of silica supported Pt-Fe catalysts by Mossbauer-spectroscopy. *Reaction Kinetics and Catalysis Letters*, 8(3), 301–307. DOI: 10.1007/BF02068170

Information about authors

Zhumabekova, Arai Kerimakynovna — Candidate of chemical sciences, Associate Professor, Manash Kozybayev North Kazakhstan State University, Petropavlovsk, Pushkin str., 86, 150000, Kazakhstan; e-mail: zhumabekova_ak@mail.ru; <https://orcid.org/0000-0001-6743-8953>.

Tastanova, Lyazzat Knashevna — Candidate of chemical sciences, Associate Professor, K. Zhubanov Aktobe Regional University, Aktobe, A. Moldagulova ave., 34, 030000, Kazakhstan; e-mail: lyazzatt@mail.ru; <https://orcid.org/0000-0002-9236-5909>;

Orynassar, Raigul Orynassarovna — Candidate of chemical sciences, Associate Professor, Al-Farabi Kazakh National University, Almaty, al-Farabi Ave., 71, 050040, Kazakhstan; e-mail: raihan_06_79@mail.ru; <https://orcid.org/0000-0002-6198-3018>.

Zakumbaeva, Gaukhar Daulenovna — Senior researcher, D.V. Sokolskii Institute of Fuel, Catalysis and Electrochemistry, Almaty, Kunayev Str., 142, 050010, Kazakhstan; e-mail: orynassar.raigul@gmail.com.

DOI 10.31489/2020Ch4/119-127

UDC 544.42+519.242.7

N. Mukhametgazy¹, I.Sh. Gussenov^{1,2}, A.V. Shakhvorostov², S.E. Kudaibergenov^{*1,2}

¹Satbayev University, Almaty, Kazakhstan;

²Institute of Polymer Materials and Technology, Almaty, Kazakhstan
(Corresponding author's e-mail: skudai@mail.ru)

Salt tolerant acrylamide-based quenched polyampholytes for polymer flooding

In our previous papers [1, 2] we considered the behavior of linear and crosslinked polyampholytes based on fully charged anionic monomer — 2-acrylamido-2-methyl-1-propanesulfonic acid sodium salt (AMPS) and cationic monomer — (3-acrylamidopropyl)trimethylammonium chloride (APTAC) in aqueous-salt solutions, swelling and mechanical properties. In the present paper we report the applicability of salt tolerant amphoteric terpolymers composed of AMPS, APTAC and acrylamide (AAm) in enhanced oil recovery (EOR). The amphoteric terpolymers of different compositions, particularly [AAm]:[AMPS]:[APTAC] = 50:25:25; 60:20:20; 70:15:15; 80:10:10 and 90:5:5 mol.% were prepared by free-radical polymerization, identified and their viscosifying ability with respect to reservoir saline water (salinity is 163 g·L⁻¹) at 60 °C was tested. It was found that due to polyampholytic nature, the AAm-AMPS-APTAC terpolymers exhibited improved viscosifying behavior at high salinity water. As a result, the appropriate salt tolerant sample [AAm]:[AMPS]:[APTAC] = 80:10:10 mol.% was selected for polymer flooding experiments. Polymer flooding experiments on high permeable sand pack model demonstrated that only 0.5 % oil was recovered by amphoteric terpolymer. While injection of polyampholyte solution into preliminarily water flooded core sample resulted in the increase of oil recovery up to 4.8–5 %. These results show that under certain conditions the amphoteric terpolymers have a decent oil displacement ability.

Keywords: polyampholyte terpolymers, viscosifying ability, high permeability, homogeneity, porous media, oil viscosity, incremental oil recovery (IOR), reservoir heterogeneity conditions.

Introduction

Oil and gas sector remains one of the main components of the economy of Kazakhstan, and its development will determine the prospects for the state economy. The problem of enhanced oil recovery (EOR) is especially important for Kazakhstan to enter into the world's top five oil exporters.

Nowadays many water-soluble polymers have been intensively developed and explored as viscosity-enhancing and flocculating agents, food additives, etc. [3–5]. Polyacrylamide and its derivatives have been successfully employed in wastewater treatment, papermaking and oil industry due to their thickening ability, flocculation and rheological behaviors [6–8].

The most widely used synthetic EOR polymer is polyacrylamide (PAA) and its derivatives [9–12]. This polymer is usually used in hydrolyzed polyacrylamide (HPAM) form to achieve higher viscosity within a certain range of brine salinities [13]. Unfortunately, HPAM may undergo a severe hydrolysis and precipitate at high temperature and brine salinity [14]. In this context, designing suitable polymers for EOR from high-temperature and high-salinity reservoirs is a challenging task. In fact, relatively high oil viscosity and brine salinity are common phenomena for Kazakhstani oil reservoirs. For example, the viscosity of Karazhanbas field oil may be higher than 350 cp, while brine salinity of Zhetibay and Moldabek fields may exceed 150 g·L⁻¹. In polymer flooding technology, stable oil displacement is realized through the reduction of

*Corresponding author.

oil/water viscosity ratio by using HPAM and other polymers [15]. Unfortunately, the high salinity of make-up water requires higher polymer concentrations to provide a certain viscosity value [16], which may increase the production cost of recovered oil. Moreover, high water salinity may cause polymer precipitation in the porous media of a rock, which results in permeability damage [14] and polymer waste. In order to overcome these problems, we suggest to use as viscosifying agent (or water thickeners) the tailor made amphoteric terpolymers AAm-AMPS-APTAC that possess the thermal stability and are able to swell and increase the viscosity in saline water due to specific, so called “*antipolyelectrolyte*” effect [17, 18]. Previous studies [19–21] indicated that many polymers containing AAm and ionic monomers can be used for EOR process [22–31].

In this work a series of ternary polyampholytes with different molar concentrations of AAm, AMPS, and APTAC were synthesized and tested as oil recovery agent by using sand pack model and artificial high porosity core. The obtained results are perspective for development of novel salt- and temperature tolerant amphoteric terpolymers for EOR.

Experimental

Materials

Acrylamide (AAm, purity $\geq 98.0\%$), 2-acrylamido-2-methylpropanesulfonic acid sodium salt (AMPS, 98 wt.% in water) and (3-acrylamidopropyl) trimethylammonium chloride (APTAC, 75 wt.% in water), and ammonium persulfate (APS, 99 % purity) were purchased from Sigma-Aldrich Chemical Co. and used without further purification.

To provide the sand pack flooding experiments, 250–500 μm sand grains were packed into 8.3 cm length and 4.3 cm diameter steel cylinder (Fig. 1a, b). The porosity and permeability of the sand pack were equal to 44 % and 16 Darcy, respectively. The model was saturated with 100 $\text{g}\cdot\text{L}^{-1}$ East Moldabek (well#2092 M-II) brine and East Moldabek oil (well# 2027 M-III-U-I). The viscosity and density of oil sample were equal to 138 cp and $0.8916\text{ g}\cdot\text{cm}^{-3}$ at 25 °C. Brine water solution was injected into the sand pack model at the rate of injection $0.1\text{ cm}^3\cdot\text{min}^{-1}$.

The core flooding experiments were carried out with core sample of 4.4 cm length and 2.9 cm diameter with permeability 5 Darcy (Fig. 1c). The artificial high porosity core sample with pore volume 24.12 cm^3 (porosity is 83 %) and Karazhanbas oil (well# 1913) were used. Viscosity and density of selected oils were equal to 420 cp and $0.93\text{ g}\cdot\text{cm}^{-3}$ at 30 °C and 64 cp and $0.907\text{ g}\cdot\text{cm}^{-3}$ at 60 °C. Brine solution with concentration of $163\text{ g}\cdot\text{L}^{-1}$ was used for core flooding test. 0.5 % polymer solution was injected into the core at the rate of $1\text{ cm}^3\cdot\text{min}^{-1}$.

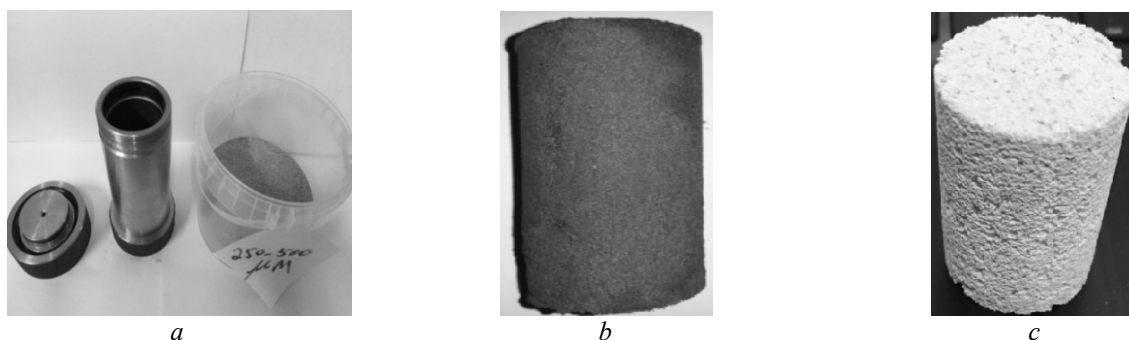


Figure 1. Sand pack (a, b) and artificial high porous core (c)

Methods

^1H NMR spectra of AMPS-APTAC-AAm terpolymers in D_2O were registered on impulse Fourier NMR spectrometer Bruker 400 MHz (Bruker, Germany).

The sand pack and core flooding experiments were conducted with the help of special core flooding set up “УИК-С(2)” (Russia).

The viscosity of polymer solutions was determined by glass capillary viscometer with diameter 1.47 mm. Oil density and viscosity were determined by Stabinger viscometer.

The following procedures for sand pack and core flooding tests were used: 1 — vacuum saturation of the porous media with brine; 2 — brine displacement by oil (drainage); 3 — oil displacement by brine (imbibition); 4 — polymer injection.

The sand pack-flooding test was conducted at room temperature and injection rate $0.1 \text{ cm}^3 \cdot \text{min}^{-1}$ while the core flooding was performed at $60 \text{ }^\circ\text{C}$ and injection rate $1 \text{ cm}^3 \cdot \text{min}^{-1}$.

Results and Discussion

Synthesis and characterization of AAm-AMPS-APTAC copolymers

Acrylamide-based quenched polyampholytes AAm-AMPS-APTAC with molecular weights $(5-6) \cdot 10^5$ Daltons were synthesized *via* conventional free radical (co)polymerization in the presence of APS at $60 \text{ }^\circ\text{C}$ during 4 h at various molar ratio of initial monomers $[\text{AAm}]:[\text{AMPS}]:[\text{APTAC}] = 50:25:25, 60:20:20, 70:15:15, 80:10:10$ and $90:5:5$ mol.% (Fig. 2).

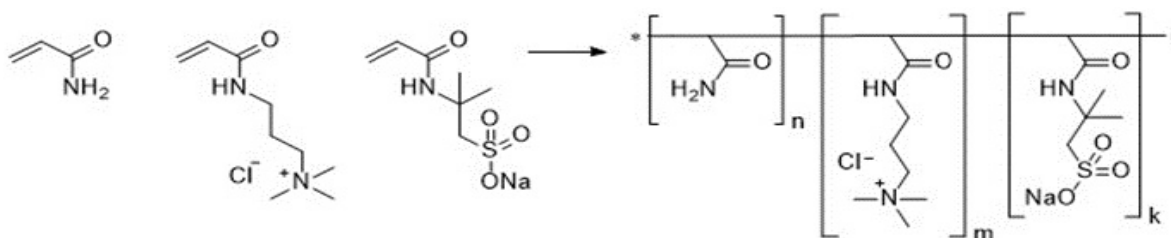


Figure 2. Preparation protocol of ternary polymers AAm-AMPS-APTAC

The results of ^1H NMR spectra of AAm-AMPS-APTAC registered in D_2O along with initial and final molar compositions of monomers are shown in Fig.3. The molar composition of AAm-AMPS-APTAC terpolymers was estimated from the integral peaks of methyl groups that belong to AMPS and APTAC monomer units. It is seen that experimentally found molar compositions of terpolymers deviate from the theoretically prescribed by 1–2 mol.% that are within the experimental error. Earlier the isoelectric points (IEP) of AMPS-APTAC copolymers were found around of $\text{pH } 6.1 \pm 0.1$ [1]. Taking into account that acrylamide is nonionic (or neutral) monomer presenting in the composition of terpolymers, one can expect that the values of the IEP will be close to AMPS-APTAC copolymers.

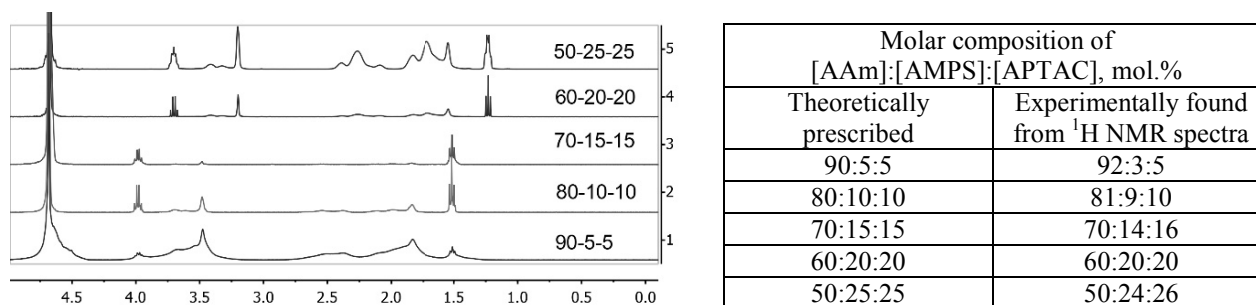


Figure 3. ^1H NMR spectra and molar composition of AAm-AMPS-APTAC terpolymers.

Sand pack flooding experiments

Figure 4 demonstrates mass of produced oil versus injected water volume and photos of effluents. The volume of each effluent sample is 10 cm^3 , whereas the pore volume (PV) of the model is 55 cm^3 . As seen from Figure 4 water breakthrough occurred before the injection of the first 10 cm^3 water ($\approx 0.18 \text{ PV}$) and oil production started to decline after 0.18 PV of injected water into the model. Water flooding oil recovery factor (ORF) demonstrates that the water flooding resulted in displacement of approximately 25.7 % of oil initially in place (OIP) (Fig. 5).

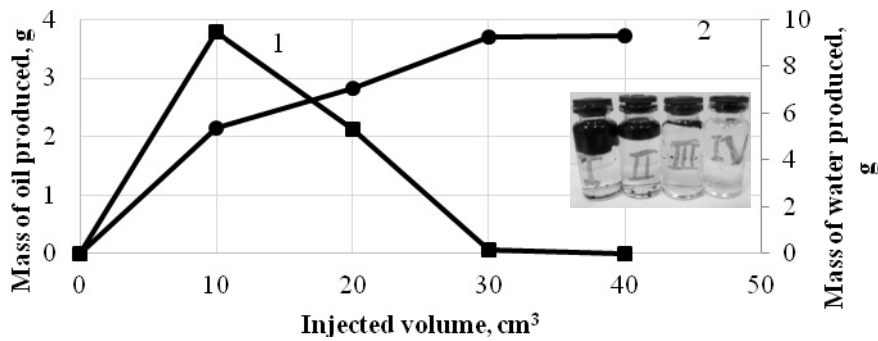


Figure 4. Dependence of mass of produced oil (curve 1) and water (curve 2) vs injected water volume. Insert is photos of each effluent containing 10 cm³ of fluid

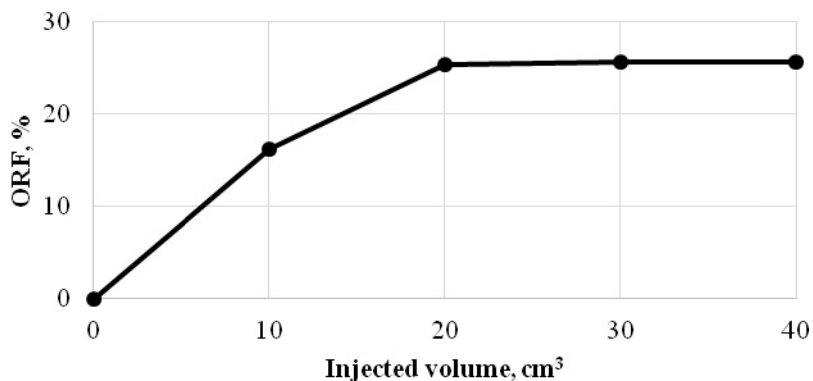
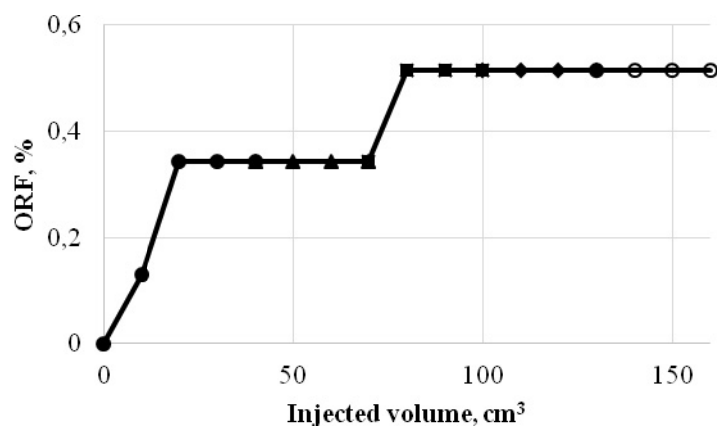


Figure 5. Dependence of ORF vs injected volume of water

Injection of 0.5 % brine solution of AAM-AMPS-APTAC terpolymers into high permeable sand pack model stepwise increases oil production (Fig.6). For instance, injection of AAM-AMPS-APTAC (50–25–25 and 60–20–20 mol.%) increases the oil recovery up to 0.35 %, while ORF is 0.51 % when terpolymers 70–15–15, 80–10–10 and 90–5–5 mol.% are injected. Thus, polymer flooding experiments on high permeable sand pack model demonstrated that only 0.51 % oil is recovered by amphoteric terpolymers in comparison with water flooding.



● — 50–25–25; ▲ — 60–20–20; ■ — 70–15–15; ◆ — 80–10–10; ○ — 90–5–5 mol. %

Figure 6. Dependence of ORF on injected volume of 0.5 % brine solution of AAm-AMPS-APTAC terpolymers

Core flooding experiments

In the next series of experiments 0.5 % solution of AAm-AMPS-APTAC (80–10–10 mol.%) in $163 \text{ g}\cdot\text{L}^{-1}$ brine was injected into preliminarily water-flooded core sample. The reason is that among the tested AAm-AMPS-APTAC terpolymers the highest viscosity in brine exhibited amphoteric terpolymer with composition of 80–10–10 mol.%. (Table 1).

Table 1

Dependence of the dynamic viscosity of AAm-AMPS-APTAC on composition of terpolymers

| Molar composition of AAm-AMPS-APTAC, mol.% | 90:5:5 | 80:10:10 | 70:15:15 | 60:20:20 | 50:25:25 |
|---|--------|----------|----------|----------|----------|
| Dynamic viscosity, $\text{mPa}\cdot\text{s}^{-1}$ | 5.5 | 10.4 | 6.7 | 8.0 | 6.6 |

The injection of 0.5 % solution of AAm-AMPS-APTAC (80–10–10 mol.%) in brine into the pre-water flooded core sample resulted in a notable oil recovery increase. Figure 7 clearly shows the increasing of the mass of produced oil in the course of polymer flooding.

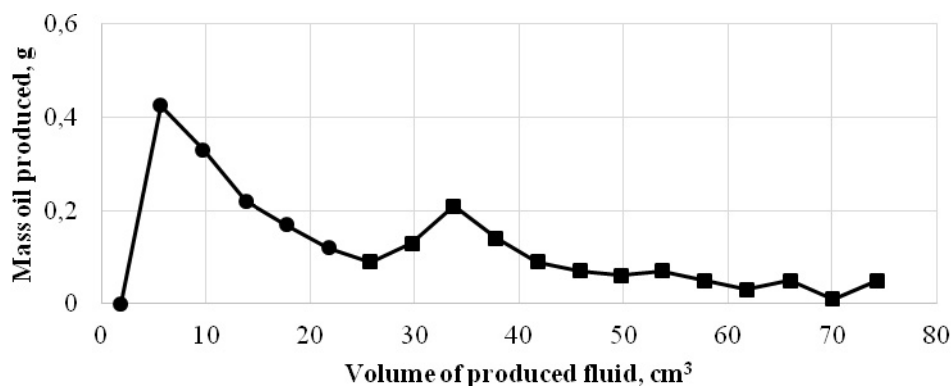


Figure 7. Mass of produced oil vs the produced volume of fluid in the course of water flood (●) and polymer flood (■). Injected polymer solution is 0.5 % AAm-AMPS-APTAC (80–10–10 mol.%) in $163 \text{ g}\cdot\text{L}^{-1}$ brine. Karazhanbas oil 64 cp at 60°C . The injection rate is $1 \text{ cm}^3\cdot\text{min}^{-1}$

The increase of the pressure drop at the beginning of polymer flooding also indicates that the *in-situ* polymer solution viscosity is higher than that of water, and the higher viscosity results in more favorable oil mobility ratio between the displacing and the displaced fluids (Fig. 8).

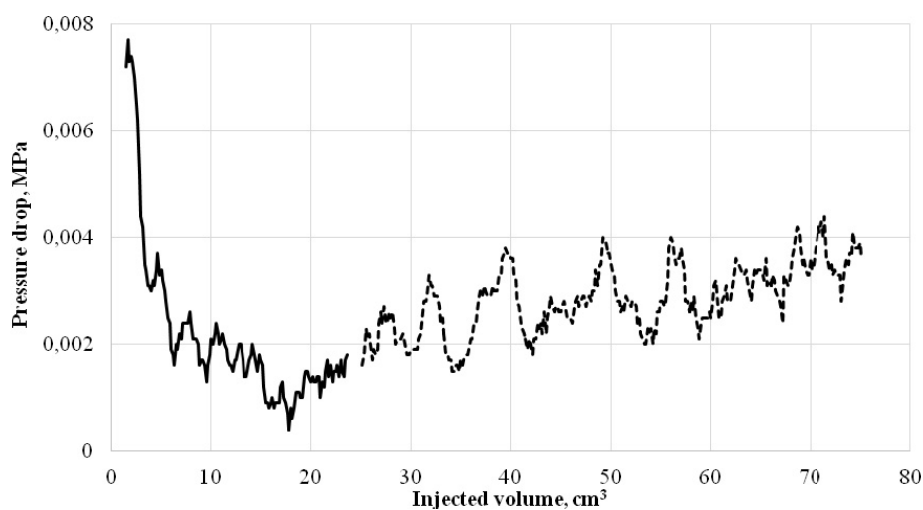


Figure 8. Change of pressure drop vs injected volume in the course of water flood (—) and polymer flood (---). Injected polymer solution is 0.5 % AAm-AMPS-APTAC (80–10–10 mol.%) in $163 \text{ g}\cdot\text{L}^{-1}$ brine. Karazhanbas oil 64 cp at 60°C . The injection rate is $1 \text{ cm}^3\cdot\text{min}^{-1}$

As seen from Figure 9 the ORF increased by 4.8–5 % due to injection of 0.5 % polymer solution. This is explained by increasing of the viscosity of brine solution (or viscosifying) due to disruption of intra- and interionic contacts between oppositely charged AMPS and APTAC moieties demonstrating *antipolyelectrolyte* effect. In pure water, the electrostatic attraction between oppositely charged macroions leads to formation of compact structure and low viscosity. In saline water the anions and cations of salts screen the electrostatic attraction between positively and negatively charged macroions and the macromolecular chain expands. This phenomenon leads to increasing of the solution viscosity and consequently to viscosifying effect. In its turn the viscosification of brine solution leads to decreasing of the mobility ratio (M_r) which is defined as ratio of displacing phase mobility (water) to displaced phase mobility (oil). It is commonly accepted that in polymer flooding, favorable M_r is achieved by increasing the viscosity of water.

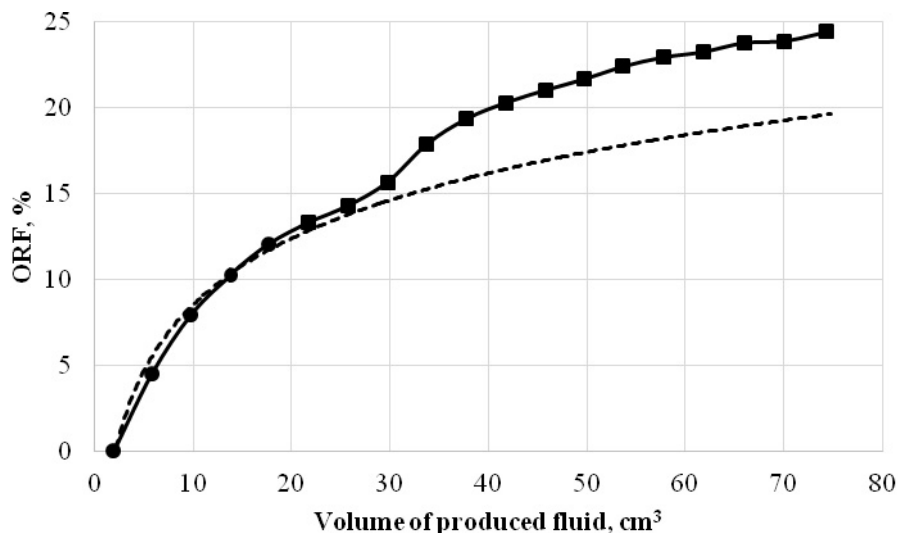


Figure 9. Dependence of ORF vs produced volume in the course of water flood (●) and polymer flood (■). Water flooding trend is shown by the dashed line (---). Injected polymer solution is 0.5 % AAm-AMPS-APTAC (80–10–10 mol.%) in 163 g·L⁻¹ brine. 0.5 % solution of AAm-AMPS-APTAC (80–10–10 mol.%) in 163 g·L⁻¹ brine. Karazhanbas oil 64 cp at 60 °C. The injection rate is 1 cm³·min⁻¹

It is interesting to evaluate the state of core samples after polymer flooding experiment. For this purpose, the sand pack model was cut into two pieces and the interior walls along with injection and outlet faces were analyzed (Fig. 10). Interior walls of core sample contain some amount of adsorbed polymer solution while the injection face of the core is less oil saturated than the outlet face. This fact confirms the oil displacement by amphoteric terpolymer in the course of injection of polymer solution.

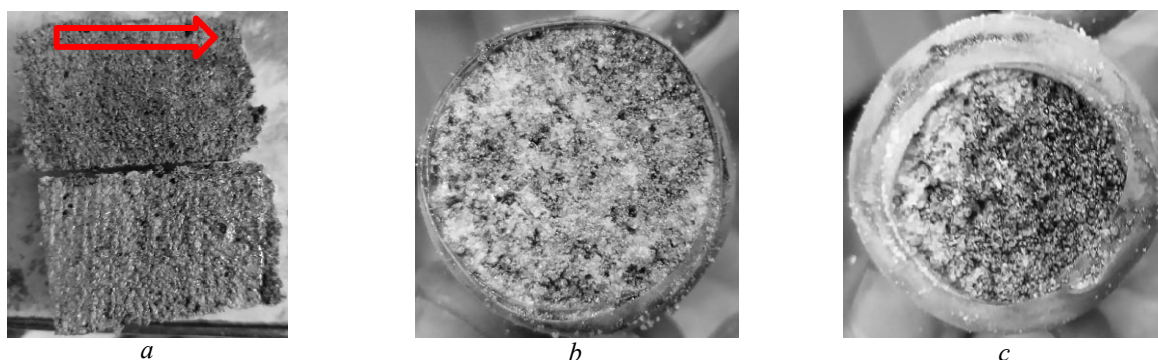


Figure 10. The view of core sample after the testing. Core cut along the axis (a), injection (b) and outlet (c) faces of core sample

Conclusions

Salt tolerant acrylamide-based quenched polyampholytes were synthesized from acrylamide (AAm), anionic (AMPS) and cationic (APTAC) monomer units by free radical polymerization. The compositions of amphoteric terpolymers were established by ¹H NMR spectroscopy. Amphoteric terpolymers showed a good solubility in oilfield water with the salinity 163 g·L⁻¹. Among the terpolymers the highest viscosity in brine exhibited amphoteric terpolymer AAm-AMPS-APTAC with composition 80–10–10 mol.%. Sand pack and core flooding experiments were carried out with 0.5 % of AAm-AMPS-APTAC (80–10–10 mol.%) solution in 163g·L⁻¹ brine for Karazhanbas oil at 60 °C. In sand pack flooding experiments, the injection of different AAm-AMPS-APTAC recipes resulted in only 0.5 % ORF increase. However, in the core flooding tests the injection of AAm-AMPS-APTAC (80–10–10 mol.%) solution resulted in 4.8–5 % ORF increase. The increase of pressure drop during polymer flood indicated improvement the mobility ratio in comparison with water flooding.

This research has been funded by the Science Committee of the Ministry of Education and Science of the Republic of Kazakhstan (Grant No. AP08855552).

References

- 1 Toleutay, G., Shakhvorostov, A., Kabdrakhmanova, S., & Kudaibergenov, S. (2019). Solution behavior of quenched or strongly charged polyampholytes in aqueous-salt solutions. *Bulletin of the University of Karaganda — Chemistry*, 2(94), 35–43.
- 2 Toleutay, G., Su, E., & Kudaibergenov, S. (2019). Swelling and mechanical properties of quenched polyampholyte hydrogels based on 2-acrylamido-2-methyl-1-propanesulfonic acid sodium salt (AMPS) and (3-acrylamidopropyl)trimethylammonium chloride (APTAC). *Bulletin of the University of Karaganda — Chemistry*, 4(96), 35–44.
- 3 Dai, C., Xu, Z., & Wu, Y. (2017). Design and Study of a Novel Thermal-Resistant and Shear-Stable Amphoteric Polyacrylamide in High-Salinity Solution. *Polymers (Basel)*, 9(7), 296.
- 4 Seright, R.S. (2016). How Much Polymer Should Be Injected During a Polymer Flood? *Society of Petroleum Engineers Journal*, 1(22). doi:10.2118/179543-MS.
- 5 Siyam, T. (2001). Development of acrylamide polymers for the treatment of waste water. *Des. Monomers Polym.*, 4, 107–168.
- 6 Bekturov, E.A., & Bakauova, Z.Kh. (1986). *Synthetic water soluble polymers in solution*. Basel, Heidelberg, New York. Huthig & Wepf Verlag.
- 7 Tha, A., Agrawal, S., Mishra, A., & Rai, J.P. (2001). Synthesis, Characterization and Flocculation Efficiency of Poly(acrylamide-co-acrylic acid) in Tannery Waste-water. *Iran. Polym. J.*, 10, 85–90.
- 8 Caulfield, M.J., Qiao, G.G., & Solomon, D.H. (2002). Some aspects of the properties and degradation of polyacrylamides. *Chem. Rev.*, 102, 3067–3084.
- 9 Jung, J.C., Zhang, K., Bo, H.C., & Choi, H.J. (2013). Rheology and polymer flooding characteristics of partially hydrolyzed polyacrylamide for enhanced heavy oil recovery. *J. Appl. Polym. Sci.*, 127, 4833–4839.
- 10 Liu, X., Liu, K., Gou, S., Liang, L., Cheng, L., & Guo, Q. (2014). Water-Soluble Acrylamide Sulfonate Copolymer for Inhibiting Shale Hydration. *Ind. Eng. Chem. Res.*, 53, 2903–2910.
- 11 Pu, W.F., Liu, R., Wang, K., Li, K., Yan, Z., Li, B., & Zhao, L. (2015). Water soluble core-shell hyperbranched polymers for enhanced oil recovery. *Ind. Eng. Chem. Res.*, 54, 798–807.
- 12 You, Q., Wang, K., Tang, Y., Zhao, G., Liu, Y., & Zhao, et al. (2015). Study of a novel self-thickening polymer for improved oil recovery. *Ind. Eng. Chem. Res.*, 54, 9667–9674.
- 13 Rabiee, A., Ebrahim Zeynali, M., & Habibollah, B. (2005). Synthesis of High Molecular Weight Partially Hydrolyzed Polyacrylamide and Investigation on its Properties. *Iranian Polymer Journal*, 14(7), 603–608.
- 14 Moradi-Araghi, A., & Doe, P.H. (1987). Hydrolysis and Precipitation of Polyacrylamides in Hard Brines at Elevated Temperatures. *Society of Petroleum Engineers*. DOI: 10.2118/13033-PA.
- 15 Firozjahi, A.M., & Saghafi, H.R. (2020). Review on chemical enhanced oil recovery using polymer flooding: Fundamentals, experimental and numerical simulation. *Petroleum*, 6(2), 115–122.
- 16 Abhijit, S., Achinta, B., Keka, O., & Ajay, M. (2010). Effects of Alkali, Salts, and Surfactant on Rheological Behavior of Partially Hydrolyzed Polyacrylamide Solutions. *Journal of Chemical & Engineering*, 55, 10, 4315–4322.
- 17 Yahaya, G.O., Ahdab, A.A., Ali, S.A., Abu-Sharkh, B.F., & Hamad, E.Z. (2001). Solution behavior of hydrophobically associating water-soluble block copolymers of acrylamide and N-benzylacrylamide. *Polymer*, 42, 3363–3372.
- 18 Ye, Z., Gou, G., Gou, S., Jiang, W., & Liu, T. (2013). Synthesis and characterization of a water-soluble sulfonates copolymer of acrylamide and N-allylbenzamide as enhanced oil recovery chemical. *J. Appl. Polym. Sci.*, 128, 2003–2011.
- 19 Zou, C., Gu, T., Xiao, P., Ge, T., Wang, M., & Wang, K. (2014). Experimental study of cucurbit[7]uril derivatives modified acrylamide polymer for enhanced oil recovery. *Ind. Eng. Chem. Res.*, 53, 7570–7578.

- 20 Bai, X., Yang, Y., Xiao, D., Pu, X., & Wang, X. (2015). Synthesis, characterization, and performance evaluation of the AM/AMPS/DMDAAC/SSS quadripolymer as a fluid loss additive for water-based drilling fluid. *J. Appl. Polym. Sci.*, 132, 27–34.
- 21 Kudaibergenov, S.E. (1999). Recent advances in the study of synthetic polyampholytes in solutions. *Adv. Polym. Sci.*, 144, 115–197.
- 22 Lowe, A.B., & McCormick, C.L. (2002). Synthesis and solution properties of zwitterionic polymers. *Chem. Rev.*, 102, 4177.
- 23 Kudaibergenov, S.E. (2002). *Polyampholytes: Synthesis, Characterization and Application*. Kluwer Academic/Plenum Publishers, New York, Boston, Dordrecht, Tokyo, Moscow.
- 24 Favero, C., & Gaillard, N. (2016). Aqueous Fracturing Fluid Composition and Fracturing Process Using the Composition. *U.S. Patent 9,249,352 B2*.
- 25 Wever, D.A.Z., Picchioni, F., & Broekhuis, A.A. (2013). Branched polyacrylamides: Synthesis and effect of molecular architecture on solution rheology. *Eur. Polym. J.*, 49, 3289–3301.
- 26 Algharaib, M., Alajmi, A., & Gharbi, R. (2014). Improving polymer flood performance in high salinity reservoirs. *J. Petrol. Sci. Eng.*, 115, 17–23.
- 27 Gussenov, I., Nuraje, N., & Kudaibergenov, S. (2019). Bulk gels for permeability reduction in fractured and matrix reservoirs. *Energy Reports*, 5, P. 733–746.
- 28 Kudaibergenov, S., Nuraje, N., Adilov, Zh., Abilkhairov, D., Ibragimov, R., Gusenov, I., & Sagindykov, A. (2015). Plugging behavior of gellan in porous saline media. *J. Appl. Polym. Sci.*, 132(2), 1–10.
- 29 Muhammad, S.K., Abdullah, S.S., Usamah, A. Al-Mubaiyedha, & Inbelwaleed, A.H. (2015). Review on Polymer Flooding: Rheology, Adsorption, Stability, and Field Applications of Various Polymer Systems. *Polymer Reviews*, 00, 1–40.
- 30 Ezell, R.G., McCormick, Ch.L. (2007). Electrolyte- and pH-responsive polyampholytes with potential as viscosity-control agents in enhanced petroleum recovery. *J. Appl. Polym. Sci.*, 104, 2812.
- 31 Mukhametgazy, N., Gussenov, I., & Shakhvorostov, A. (2019). Quenched polyampholytes for polymer flooding. *AIP Conference Proceedings*, 2167, 020236; <https://doi.org/10.1063/1.5132103>.

Н. Мұхаметғазы, И.Ш. Гусенов, А.В. Шахворостов, С.Е. Құдайбергенов

Тұзғатөзімді акриламид негізіндегі жоғары зарядталған полиамфолиттерді жер қыртысына айдау

Алдыңғы мақалаларда авторлар толығымен зарядталған анионды мономер — 2-акриламидо-2-метил-1-пропансульфон қышқылы натрий тұзы (АМПС) және катионды мономер — (3-акриламидо-пропил)триметиламмоний хлориді (АПТАХ) негізінде түзілген сызықты және айқаса байланысқан полиамфолиттердің сулы-тұзды ерітінділердегі ісінуі және механикалық қасиеттерін қарастырды. Осы мақалада мұнай өндіруді жақсартылған қалпына келтіру кезінде АМПС, АРТАХ және акриламидтен (ААм) тұратын, тұзғатөзімді амфотерлі терполимерлердің қолданылу мүмкіндігі туралы хабарланған. Әр түрлі құрамдағы амфотерлі терполимерлер, атап айтқанда [ААм]:[АМПС]:[АРТАХ] = 50:25:25; 60:20:20; 70:15:15; 80:10:10 және 90:5:5 мол.% бос радикалды полимерлеу әдісімен дайындалды, анықталды және олардың 60 °С температурада тұзды суға (тұздылығы 163 г·л⁻¹) қатысты тұтқырлық қабілеті тексерілді. Амфотерлі терполимерлер полиамфолиттік сипатта болғандықтан, ААм-АМПС-АРТАХ терполимерлері тұздылығы жоғары суларда жоғары тұтқырлық қасиеттерін көрсетті. Соның нәтижесінде, тұзғатөзімді [ААм]: [АМПС]:[АРТАХ] = 80:10:10 мол.% үлгісі полимерді айдау тәжірибесі үшін таңдап алынды. Полимер ерітіндісін айдау тәжірибесі жоғары өткізгіштігі бар құмды модельде амфотерлі терполимердің көмегімен тек 0,5 % мұнайдың алынған шығымын көрсетті. Алдын-ала сумен қаныққан керн үлгісі арқылы полиамфолит ерітіндісін айдау барысында мұнай өндірудің жоғарылауы 4,8–5,0 % дейін артты. Бұл нәтижелер амфотерлі терполимерлердің белгілі бір жағдайларда мұнайды ығыстыру қабілетіне ие екендігін көрсетеді.

Кілт сөздер: полиамфолит терполимерлері, тұтқырлық қабілеті, жоғары өткізгіштігі, біртектілігі, кеуекті орта, мұнай тұтқырлығы, мұнай өндірудің жоғарылауы, қабаттың біртектілігі.

Н. Мухаметгазы, И.Ш. Гусенов, А.В. Шахворостов, С.Е. Кудайбергенов

Солеустойчивые сильнозаряженные полиамфолиты на основе акриламида для полимерного заводнения

В предыдущих статьях авторами рассмотрены поведение линейных и сшитых полиамфолитов на основе сильнозаряженного анионного мономера — натриевой соли 2-акриламидо-2-метил-1-пропансульфоновой кислоты (АМПС) и катионного мономера — (3-акриламидопропил)триметиламмоний хлорида (АПТАХ) в водно-солевых растворах, набухание и механические свойства. В на-

стоящей статье сообщается о применимости солей амфотерных терполимеров, состоящих из АМПС, АПТАХ и акриламида (ААм) для полимерного заводнения. Амфотерные терполимеры различного состава, а именно [ААм]:[АМПС]:[АПТАХ] = 50:25:25; 60:20:20; 70:15:15; 80:10:10 и 90:5:5 мол.%, были приготовлены свободнорадикальной полимеризацией, идентифицированы и их загущающая способность протестирована применительно к пластовой (соленой) воде нефтяного резервуара (соленость 163 г·л⁻¹) при 60 °С. Найдено, что благодаря полиамфолитной природе терполимеры ААм-АМПС-АПТАХ показали улучшенный загущающий эффект при высокой солености воды. В результате этого для экспериментов по полимерному заводнению выбран солейкий образец [ААм]:[АМПС]:[АПТАХ] = 80:10:10 мол.%. Полимерное заводнение на высокопроницаемой песчаной модели показало, что только 0,5 % нефти извлекается амфотерным терполимером. Тогда как закачка раствора полиамфолита в образец керна, предварительно насыщенного водой, приводит к увеличению извлечения нефти до 4,8–5,0 %. Эти результаты показывают, что при определенных условиях амфотерные терполимеры способны в достаточной степени извлекать нефть.

Ключевые слова: терполимеры полиамфолитов, загущающая способность, высокая проницаемость, однородность, пористая среда, вязкость нефти, увеличение нефтеотдачи, условия неоднородности пласта.

Information about authors

Mukhametgazy, Nurbatyr — PhD student, Satbayev University, Almaty, Kazakhstan; Satbayev street 22a, 050013. e-mail: nurbatyr.kaz@gmail.com; <https://orcid.org/0000-0001-5957-0305>; ORCID 0000-0001-5957-0305.

Gussenov, Iskander Shakhsavanovich — PhD, Satbayev University, Senior researcher of the Institute of Polymer Materials and Technology, Almaty, Kazakhstan; Satbayev street 22a, 050013. e-mail: iskander.gussenov@mail.ru; ORCID 0000-0002-9820-7952.

Shakhvorostov, Alexey Valeryevich — M.Sc., Institute of Polymer Materials and Technology, Almaty, Kazakhstan; Atyrau-1, 3/1, 050019; e-mail: alex.hv91@gmail.com; ORCID 0000-0003-3502-6123.

Kudaibergenov, Sarkyt Elekenovich — Dr. Chem. Sci., Professor, Director, Institute of Polymer Materials and Technology, Head of the Laboratory of Engineering Profile, Satbayev University, Almaty, Kazakhstan; Atyrau-1, 3/1, 050019. e-mail: skudai@mail.ru; ORCID 0000-0002-1166-7826.

K.A. Zhaparkulova*, G.M. Gani, Z.B. Sakipova, A.A. Karaubayeva

*School of Pharmacy, Asfendiyarov Kazakh National Medical University, Almaty, Kazakhstan
(Corresponding author's e-mail: zhaparkulova.k@kaznmu.kz)*

Development of the orodispersible films based on CO₂ extract of *Ziziphora bungeana* with antimicrobial activity

The present work was intended to develop the new drug in the form of film soluble in the oral cavity: development of its composition, production technology, the study of its antimicrobial activity. The relevance of the problem is caused by the absence of drugs in the form of films on the domestic pharmaceutical market. The optimal composition of films was selected by evaluating a number of physical, chemical and technological indicators of the obtained films. The article indicates the materials used to obtain the drugs in question, presents the technology for their preparation and quality determination methods: unit measurement methods and potentiometric determination of pH, tensiometric and conductometric methods, thin-layer and gas chromatography and others. Antimicrobial activity of the resulting films has been proven in vitro. *Staphylococcus aureus* ATCC 6538-p and *Escherichia coli* ATCC 8739 have been used as the test microorganisms in order to study them by disk diffusion method in agar. The introduction of CO₂ extract of *Z. bungeana* from medicinal plant raw materials as active ingredients in medicinal films will expand the range of complex phytopreparations of the domestic pharmaceutical market for the treatment of inflammatory diseases of the oral mucosa.

Keywords: CO₂ extract of *Ziziphora bungeana*, orodispersible phytofilm, film composition, phytofilms, the parameters of the technological mode, technological process, antimicrobial activity, test microorganisms.

Introduction

Currently, the main spectrum of pharmaceutical research is aimed at finding new medications improving the existing ones and creating drug delivery systems. One of the most promising therapeutic agents are medicinal films based on biologically active compounds of plant origin and informally called "phyto films" [1]. The oral mucosa has recently become increasingly important as an alternative route of administration for individual, controlled drug delivery. Multilayer films on mucous membranes, referred to the monograph of oromucosal drugs in the European Pharmacopoeia, have the advantages of a dosage form and satisfy the requirements associated with this place of drug delivery [2].

Orally dispersible films (ODF) have recently become one of the most popular forms of drug administration due to their superior convenience and patient compliance. The main advantage of the dosage form arises from its rapid disintegration: it can be taken without water. Compared to conventional oral dosage forms, ODF generally provides a better drug bioavailability with a faster onset of action. In addition, ODFs are flexible [3].

Medicinal films (MF) are polymeric elastic plates of oval or rectangular shape with equal edges and a flat surface of various sizes and thicknesses. They are a type of transdermal therapeutic systems (TTS). The difference between Phytofilms and synthetic polymeric therapeutic systems are following: phytofilms are made in the form of a TTS (transdermal therapeutic system) matrix on carriers of natural origin (gelatin, collagen, sodium alginate, agar-agar, etc.), which makes them safer and more compatible with a living organism (1).

Despite the above advantages of films, only one of the drugs in the form of a film belonging to the ATC classification, G04BE03, is registered in the State Register of the Republic of Kazakhstan with the trade name Viniks, produced by si.L.Farm Co., LTD, Republic of Korea. In other groups of the ATC classification, there are no drugs in the form of a film [4]. The development of films is the most pressing problem in dentistry. Their use makes it possible to treat diseases associated with inflammatory periodontal diseases, such as gingivitis, periodontitis, periodontal disease, etc.

In this regard, the purpose of our activity was to develop the composition, technology and quality assessment of films with antibacterial and anti-inflammatory properties, thanks to the use of a CO₂-extract of

*Corresponding author.

the plant *Z. bungeana* Juz family *Lamiaceae* as their basis [5]. *Ziziphora* phytochemicals include monoterpene essential oils, triterpenes, and phenolic substances belonging to flavonoids. In Kazakh traditional medicine, *Ziziphora* species are used for several medicinal purposes. In particular, *Z. bungeana* Juz. and *Z. clinopodioides* Lam. are used for treating diseases associated with the cardiovascular system, or to fight various infections [6]. To emphasize the natural origin of the base of the films, we named them orodispersephyto films (hereinafter referred to as films).

Experimental

The CO₂ extract of the medicinal plant material *Z. bungeana* was used as an active substance. To select the optimal composition, we studied about 54 film-forming compositions of biodegradable polymers and plasticizers. The latter were of natural and synthetic origin and represented different ratios of film-forming agents and plasticizers.

The selection of the optimal composition of the film, providing the necessary technological and consumer properties, was carried out in 2 stages [7]. At the first stage, an experiment was carried out to select excipients (films and plasticizers) that can form a matrix film for the subsequent administration of drugs. The film-forming properties of polymer solutions at various concentrations were studied during the experiment. The polymers were of various origins (natural and synthetic) and production (domestic and foreign). The criterion for choosing film compositions at the initial stage was a satisfactory appearance: transparency, elasticity, uniformity, the absence of microcracks and tears in the film. Glycerin was added to all bases as a plasticizer. Based on a preliminary study, 6 compositions out of 54 were selected. The rest of the models did not correspond to such technological parameters as mechanical strength, solubility, elasticity, etc. The selected models are presented in Table 1.

Table 1

Selected films forming compositions

| Base | No. 1 model | No. 2 model | No. 3 model | No. 4 model | No. 5 model | No. 6 model |
|---|-------------|-------------|-------------|-------------|-------------|-------------|
| MC, g | – | – | 15 | – | – | – |
| PVA, g | – | 15 | – | – | – | – |
| PVP, g | 30 | – | – | – | – | – |
| Sodium alginate, g | – | – | – | – | – | 4.0 |
| Sodium CMC, g | – | – | – | 3.0 | – | – |
| Natrosol250G, g | – | – | – | – | 3.0 | 0 |
| CO ₂ extract of <i>Z. bungeana</i> , g | 1.5 | 1.5 | 1.5 | 1.5 | 1.5 | 1.5 |
| Glycerin, g | 1.5 | 1.5 | 1.5 | 1.5 | 1.5 | 1.5 |
| an aqueous solution of gelatin, % | 15 | 15 | 15 | 15 | 15 | 15 |
| 40 % ethanol | 15 | 15 | 15 | 15 | 15 | 15 |
| Purified water up to 50 ml | 50 ml | 50 ml | 50 ml | 50 ml | 50 ml | 50 ml |

The films were evaluated according to the following criteria: physical characteristics (color, odor, size and shape); average weight; solubility; pH of the aqueous solution; microbiological purity; weight loss on drying; authenticity. In addition, the criteria for evaluating the quality of the films included such technological parameters as vapor permeability, mechanical tensile strength, shell thickness, weight loss on drying, and dissolution time. Harrington's method of generalized preference function was used to statistically process the experimental results. Based on the results of the final activity, 3 compositions of bases No. 1, No. 3 and No. 6 were selected according to the characteristics of the films.

The second stage of the study was the selection of the optimal composition of the matrix film by the method of mathematical planning. The selection criteria were the following parameters of the film quality: the pH value of the aqueous solution, thickness and moisture content (Table 2).

According to the results of the second stage of research, the composition of samples No. 1 and No. 6 did not correspond to the main technological parameters — the indicator of dissolution and pH of the aqueous solution.

A certain contribution to the kinetics of drug release is made by the process of edema of high molecular weight substances (HMS). In the films based on natrosol 250G, Sodium CMC and Sodium alginate, small edema is observed, and in films based on PVA, PVP, moderate edema of the film based on MC is observed. At the same time, model No. 3 based on MK demonstrated the optimal composition. On the basis of this

model, an elastic, homogeneous, colorless and transparent film corresponding to the technological parameters was obtained (Table 3). The film sample contains the active pharmaceutical ingredient — CO₂-extract of the plant *Z. bungeana*, the antimicrobial properties of which are determined by the high content of pulegon.

Table 2

Technological parameters of dispersed films

| No. model | Thickness, mm | Dissolution time, min | Humidity, % | pH | Mechanical strength, kg/m ² | Average weight, g |
|-----------|---------------|-----------------------|-------------|-------------|--|-------------------|
| 1 | 0.15 ± 0.015 | 3.45 ± 0.1 | 9.81 ± 0.1 | 8.05 ± 0.07 | 8.7±0.2 | 0.049 ± 0.003 |
| 2 | 0.3 ± 0.1 | 4.30 ± 0.2 | 5.52 ± 0.1 | 5.09 ± 0.07 | 4.7±0.2 | 0.349 ± 0.002 |
| 3 | 0.25 ± 0.015 | 2.50 ± 0.1 | 9.93 ± 0.1 | 6.14 ± 0.03 | 9.2±0.1 | 0.251 ± 0.015 |
| 4 | 0.169 ± 0.016 | 6.47 ± 0.1 | 10.47 ± 0.1 | 4.2 ± 0.01 | 5.6±0.3 | 0.153 ± 0.015 |
| 5 | 0.159 ± 0.015 | 4.10 ± 0.1 | 18 ± 0.1 | 8.0 | 3.1±0.3 | 0.142 ± 0.004 |
| 6 | 0.2 ± 0.01 | 4.37 ± 0.1 | 10.12 ± 0.1 | 7.3 ± 0.5 | 9.8±0.3 | 0.047 ± 0.004 |

Table 3

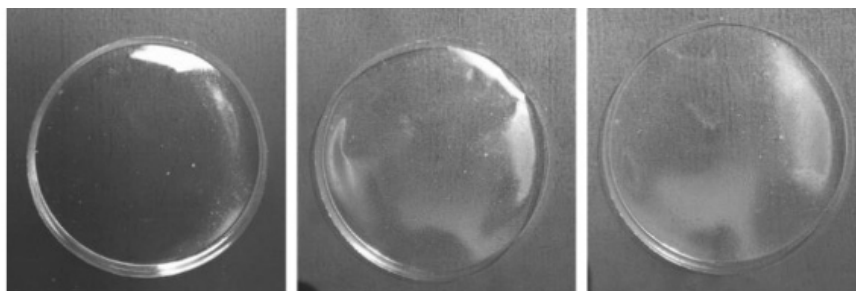
The optimal composition of the film based on CO₂ extract of *Z. bungeana*

| The name of the ingredient | ND (Normative document) | Quantity, % | Functional purpose |
|---|--|--------------|------------------------|
| Water solution of gelatin 30 % | SPRK (State pharmacopoeia of Republic of Kazakhstan) | 30 % | Film-forming |
| Water solution of MC5 % | SPRK | 30 % | The adhesive component |
| 40 % ethanol | SPRK | 30 % | Solvent |
| Glycerin | SPRK | 2 % | Plasticizer |
| CO ₂ extract of <i>Z. bungeana</i> | SPRK | 3 % | Active substance |
| Purified water | SPRK | up to 100 ml | Solvent |

The selection criterion for the films based on *Z. bungeana* CO₂ extract was a satisfactory appearance (transparency, elasticity, uniformity, absence of microcracks), sufficient, flexible and satisfactory bending strength. The films are uniform in thickness and weight.

The method of making a long-acting medicinal film consisted of 3 stages: preparation of the composition; deaeration and pouring into a special mold; drying and cutting.

Description of the technological process. Aqueous solutions of gelatin 30 % and MC5 % were mixed with the prepared components at a temperature of 40 °C, and thoroughly mixed with the addition of glycerin. The resulting mixture was heated to 40 °C and the drug substance was added there to. Then 40 % ethanol was added. By thoroughly mixing the components (exposure in a water bath at 40 °C for 30 minutes, rotation of the blades 20 ± 5 rpm), we obtained a homogeneous composition. To avoid the formation of air bubbles, centrifugation was carried out for 2 hours. The mixture was poured into a special mold, dried at a temperature of 40–45 °C to 10 % residual moisture. After drying, the films were cut into medium therapeutic doses of 1×2 cm. In practice, films dried at room temperature acquire a high-quality appearance. The films were packed with aluminum foil. The final product was placed in a box along with instructions for medical use. In appearance, the films are elastic plates of light yellow color with a specific odor, without mechanical damage and air bubbles: width (1 ± 0.2) cm, length (2 ± 0.2) cm, thickness (0.253 ± 0.015) mm (Fig. 1).

Figure 1. Orodispersible film obtained on the basis of *Z. bungeana* extract by pour method

Determination of the average mass. The average mass of a 1×2 cm film sample (an average therapeutic dose) was determined by measuring 10 films with an accuracy of 0.0002 g. The mass of an individual film was determined by a single measurement of 20 samples with an accuracy of 0.0002 g.

The permissible deviation in weight for films is up to 0.1 g and not less than $\pm 10\%$ [9].

Determination of thickness. The film thickness was measured with a MKTs-25 micrometer (GOST 6507–90).

Film disintegration time. The solubility of polymer films is the main criterion for the functional suitability of this dosage form and characterizes the ability of the film to be completely absorbed by biological body fluids. The process of dissolution of polymer films should be limited by the time required for the gradual release of the active substance and ensuring its constant concentration over a given period. The dissolution time of the films depends on the hydrophilicity of the selected polymer. A sample of 1×2 cm film was dissolved at room temperature in 2.5 ml of purified water to avoid adhesion to the wall of the glass tube, and the time of complete dissolution of the film was measured using a stopwatch [10].

The pH of the aqueous solution was determined by the method of potentiometric determination of pH (IP RK I, vol. 1, 2.2.3.). A film sample weighing 0.5 g was dissolved at room temperature in 50 ml of purified water, stirred, and the pH of an aqueous film solution was recorded.

This indicator allows predicting the irritant effect of the dosage form. The pH of the film should be closer to that of an aqueous solution of fluid from a wound, fluid of the oral mucosa, pH of an aqueous fluid, which is 6.5–7.2 [11].

Microbiological testing of film materials based on *Z. bungeana* CO₂-extract. There are a number of requirements for biomedical polymer matrices. One of them is the antimicrobial activity of the material, which is determined by its ability to slow down the growth of microorganisms. The comparative microbiological tests were carried out in order to study the bactericidal activity of the obtained films on the basis of the CO₂ extract of *Z. bungeana*. As a control model, we used CPF, which exhibits antibacterial activity against *Staphylococcus aureus* ATCC 6538-p and *Escherichia coli* ATCC 8739: these strains are sensitive to this antibiotic. The test microorganisms were investigated by the agar diffusion method using *Staphylococcus aureus* ATCC 6538-p and *Escherichia coli* ATCC 8739. Figure 2 shows the results of the microbiological tests.

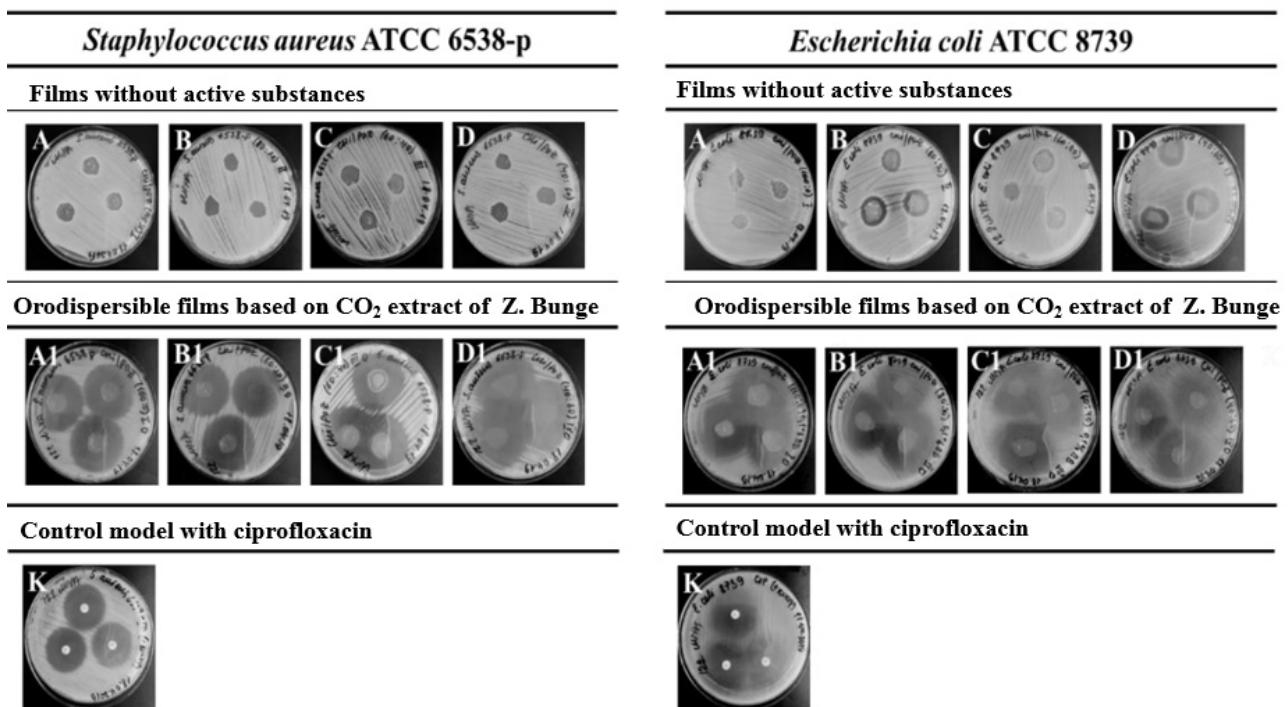


Figure 2. Zone of inhibition of the films against *Staphylococcus aureus* and *Escherichia coli* bacteria

Results and Discussion

As a result of the conducted research aimed at creating orodispersephy to films, matrices were obtained, which in appearance were films characterized by colorless or transparent, odorless, mechanical inclusions and air bubbles, good elasticity and good adhesion. The established experimental values of the indicators prove a satisfactory quality of the matrices as a rationality criterion for the composition of the developed films. An optimal composition of the films with gelatin as a polymer material has been developed and quality indicators have been determined.

Based on the transdermal therapeutic system, polymeric water-dispersible films have been obtained, which have a long-term therapeutic effect.

The results of experimental studies on the creation of medicinal films based on products of natural origin, i.e., phytofilms dispersed in water, make it possible to develop an optimal composition of medicinal preparations in the form of films with prolonged release of the active substance.

An elastic, homogeneous, colorless, transparent film corresponding to the technological parameters was obtained on the basis of model No. 3 (based on MC), which has an optimal composition with respect to edema of high molecular weight substances (HMS). In films on a different basis, either slight or moderate edema was observed.

The film compositions based on PVA, based on Sodium CMC and based on Natrosol 250G (formulations No. 2, No. 4, No. 5) did not meet the uniformity requirements due to the uneven distribution of particles and agglomerates formed in the sample based on sodium CMC. In addition, the degree of adhesion to the mucous layer was low.

Conclusions

The studies carried out during the development of new drug form and obtaining the product, as well as evaluating a number of physical, chemical and technological indicators allow making next conclusions:

- The choice of the optimal composition of the films and the assessment of the obtained orodisperse phytofilms should be done on the basis of a number of physicochemical and technological parameters. It is advisable to focus on the following indicators studied during biopharmaceutical research on the choice of the films composition and during step-by-step control during the production process: film thickness — 0.15–0.30 mm, pH of an aqueous solution — 6.0–7.2, the dissolution time is not less than 3 minutes [8], the mass loss (moisture content) is 8–10 % during drying.
- It is necessary to take into account the relationship between the kinetics of drug release and swelling of high molecular substances (HMS) during the choice of films optimal composition.
- Films based on *Z. bungeana* CO₂ extract have increased antimicrobial activity against the gram-negative strain of *Escherichia coli* and the gram-positive strain of *Staphylococcus aureus*.
- Films with MC (0.1 % w/v CPF) have a high antibacterial activity of *Staphylococcus aureus* ATCC 6538-p and *Escherichia coli* ATCC 8739.
- The high antibacterial activity of the film is explained by the presence of an active pharmaceutical ingredient in it — CO₂-extract of the *Z. bungeana* plant with a high content of pulegon.
- The developed films have the duration of action and the accuracy of the dosage of the active substance which is advantage of such dosage forms.
- The introduction of *Z. bungeana* CO₂ extract from medicinal plant materials as the active ingredient in medicinal films will expand the range of complex phytopreparations of the domestic pharmaceutical market for the treatment of inflammatory diseases of the oral mucosa.

References

- 1 Lindret, S., & Breikreutz, J. (2016). Oromucosal multilayer films for tailor-made, controlled drug delivery. *Chemistry of Natural Compounds*, 14(11), 1265–1279.
- 2 Carolina, J.V., Gabriela, E., Wouter, L.J., Raymond, R. T., Avanti, C., & Henderik, W. (2017). Development of orodispersible films with selected Indonesian medicinal plant extracts. *Journal of Herbal Medicine*, 7, 37–46.
- 3 Yeongbin, L., Kim, K., Kim, M., Hyung, C., & Seong, H. J. (2017). Orally disintegrating films focusing on formulation, manufacturing process, and characterization. *Journal of Pharmaceutical Investigation*, 47, 183–201.
- 4 State register of medicines, medical devices and medical equipment of the Republic of Kazakhstan. *ndda.kz*. Retrieved from: https://www.ndda.kz/category/search_prep

- 5 Srivedavyasari, R., Zhaparkulova, K.A., Sakipova, Z.B., Ibragimova, L., & Ross, S.A. (2018). Phytochemical and biological studies on *Ziziphora bungeana*. *Chemistry of Natural Compounds*, 54(1), January.
- 6 Šmejkal, K., Malaník, M., Zhaparkulova, K., Sakipova, Z., Ibragimova, L., & Ibadullaeva, G. (2016). Kazakh *Ziziphora* Species as Sources of Bioactive Substances. *Molecules*, 21, 826.
- 7 *European Pharmacopoeia: Edition 8. Volume 2* (2016). European Pharmacopoeia Commission. Strasbourg, France. European directorate for the quality of medicines (EDQM), 4257–4259.
- 8 Senel, S., Cansiz, M., & Rathbone, M.J. (2014). *Delivery of biopharmaceuticals: vaccines and allergens, in Mucosal delivery of biopharmaceuticals* (J. das Neves and B. Sarmiento Eds.). New York: Springer.
- 9 Silva, B.M.A., Borges, A.F., Silva, C., Coelho, J.F.J., & Simoes, S. (2015). Mucoadhesive oral films: The potential for unmet needs. *Int. J. Pharm.*, 494 (1), 537–551.
- 10 Krampe, R., Sieber, D., Pein-Hackelbusch, M. & Breitreutz, J. (2016). A new biorelevant dissolution method for orodispersible films. *Eur. J. Pharm. Biopharm.*, 98, 20–25.
- 11 Borges, A.F., Silva, C., Coelho, J.F.J., & Simoes, S. (2015). Oral films: current status and future perspectives II-Intellectual property, technologies and market needs. *J. Control Release*, 206, 108–121.

Қ.А. Жапаркулова, Г.М. Гани, З.Б. Сакипова, А.А. Караубаева

***Ziziphora bungeana* өсімдігінің сығындысы негізінде антимикробты қасиетке ие ородисперсті қабықшаларды әзірлеу**

Мақалада ауыз қуысында еритін (ородисперсті) пленка түріндегі жаңа дәрілік препараттың жасалу жолы ұсынылған: препараттың құрамын жасау, пленканы алу технологиясын әзірлеу және оның микробқа қарсы белсенділігін зерттеу. Зерттеу жұмысының өзектілігі Қазақстанның фармацевтикалық нарығында пленка түріндегі дәрілік препараттардың болмауымен түсіндіріледі. Алынған қабықша физико-химиялық және технологиялық көрсеткіштер бойынша бағаланды, олардың нәтижелері бойынша фитоқабықшаның онтайлы құрамы таңдалды. Мақалада дәрі-дәрмектерді алу үшін пайдаланылған материалдар, қабықшаны алу технологиясы және сапаны анықтау әдістері: пленканың рН-н анықтау, жеке өлшеу, потенциометриялық анықтау, тензиометриялық және кондуктометриялық әдістер, жұқа қабықты және газды хроматография және басқа әдістер ұсынылған. Алынған фитоқабықшаның микробқа қарсы белсенділігі *In vitro* жағдайында дәлелденді. Тест-микроорганизмдер ретінде *Staphylococcus aureus* ATCC 6538-р және *Escherichia coli* ATCC 8739 пайдалана отырып, агарда дискті-диффузды әдіспен зерттелді. Белсенді зат дәрілік өсімдік шикізаты *Z. bungeana* CO₂ сығындысы негізінде жасалған дәрілік қабықшаларды отандық фармацевтикалық нарыққа енгізу ауыз қуысының қабыну ауруларын емдеуге арналған кешенді фитопрепараттарын ассортиментін кеңейтеді.

Кілт сөздер: Зизифора Бунгенің CO₂-сығындысы, ауыз қуысында еритін дисперсті фитопленка, пленка құрамы, фитопленка, технологиялық режимнің параметрлері, технология, микробқа қарсы белсенділігі, тест-микроорганизмдер.

К.А. Жапаркулова, Г.М. Гани, З.Б. Сакипова, А.А. Караубаева

Разработка ородисперсных пленок на основе CO₂-экстракта *Ziziphora bungeana* с антимикробной активностью

В статье представлена разработка нового лекарственного препарата в форме растворимой в полости рта (ородисперсируемой) пленки: разработка состава, технологии получения, изучение ее антимикробной активности. Актуальность разработки данной лекарственной пленки объясняется отсутствием лекарственных препаратов в форме пленок на фармацевтическом рынке Казахстана. Полученную пленку оценивали по ряду физико-химических и технологических показателей, по результатам которых был выбран оптимальный состав фитопленок. Авторами указаны использованные материалы для получения лекарственных препаратов, представлена технология их получения и методы определения качества: методы единичного измерения и потенциометрического определения рН, тензиометрический и кондуктометрический методы, тонкослойная и газовая хроматография и др. Противомикробная активность полученных фитопленок доказана *in vitro*. Тест-микроорганизмы изучали диск-диффузионным методом в агаре. В качестве тест-микроорганизмов использовали *Staphylococcus aureus* ATCC 6538-р и *Escherichia coli* ATCC 8739. Внедрение CO₂ экстракта *Z. bungeana* из лекарственного растительного сырья в качестве активного ингредиента лекарственных пленок позволит рас-

ширить ассортимент комплексных фитопрепаратов отечественного фармацевтического рынка для лечения воспалительных заболеваний слизистой оболочки полости рта.

Ключевые слова: CO₂-экстракт зизифоры Бунге, фитопленка, диспергируемая в полости рта, состав пленки, параметры процесса технологического режима, технология, антимикробная активность, тест-микроорганизмы.

Information about authors

Zhaparkulova, Karlygash Altynbekovna — PhD, Senior teacher of School of Pharmacy Asfendiyarov Kazakh National Medical University, Tole bi street, 94, 050000, Almaty, Kazakhstan; e-mail: zhaparkulova.k@kaznmu.kz; <https://orcid.org/0000-0002-3776-2004>.

Gani, Gulfairuz Muratovna — 2nd year master's student, Technology of medicine and engineering disciplines department, Asfendiyarov Kazakh National Medical University, Tole bi street, 94, 050000, Almaty, Kazakhstan; e-mail: flower_fariza@inbox.ru.

Sakipova, Zuriyadda Bektemirovna — Professor, Doctor of pharmaceutical sciences, Dean of School of Pharmacy of Asfendiyarov Kazakh National Medical University, Tole bi street 94, 050000, Almaty, Kazakhstan; e-mail: sakipova.z@kaznmu.kz; <https://orcid.org/0000-0003-4477-4051>.

Karabayeva, Aigerim Abayevna — PhD, Doctor of pharmaceutical sciences, Dean of School of Pharmacy of Asfendiyarov Kazakh National Medical University, Tole be street, 050000, Almaty, Kazakhstan; e-mail: karabayeva.a@kaznmu.kz.

I.A. Khabarov*, V.V. Zhurov, A.N. Zhabayeva, S.M. Adekenov

*JSC "International Research and Production Holding "Phytochemistry", Karaganda, Kazakhstan
(Corresponding author's e-mail: i.khabarov@phyto.kz)*

Modeling the extraction process of medicinal raw materials

The review considers 26 mathematical models of the process of biologically active substances extraction from medicinal plant raw materials, taking into account factors affecting the extraction process: diffusion coefficient, particle size, layer porosity, extractant feed rate, raw material grinding method, pressure, temperature and duration of extraction, individual characteristics of raw materials (content of the target component) and technological equipment. In general, these models fall into four important groups: empirical models, models based on heat transfer analogies, a shrinking core model, and models based on differential mass balance. Here were described problems that occur in the selection of mathematical models, first of all, associated with the imperfect behavior of the flows of extraction liquids, and the inhomogeneous cross-section of the extraction apparatus. It was shown that first of all the extraction process modeling requires mathematical models to describe the mass transfer inside solid particles. It is also important to take into account the solubility of the target substances when simulating. It is shown that for describing the extraction processes, the optimal models are Naik and Lentz, Esquivel, diffusion, H. Sovová mass transfer, damaged and undamaged cells for calculating the main factors of extraction processes.

Keywords: mathematical modeling, mass transfer, diffusion, regression equation, criterion equation, optimization, extraction, plant raw materials

Introduction

Extraction of medicinal plant raw materials is an integral and important process in phytochemical production.

The theory and practice of the extraction process have been intensively developed in recent years due to the increase in the technical equipment of pharmaceutical production, as well as the solution of problems arising from the consideration of extraction processes in a solid-liquid system.

Analysis of the available information material and literature data indicates that three types of mathematical models can be used to calculate and optimize the process of extracting plant raw materials:

1. Model of differential equations of the process;
2. Model of criterion equations of the process;
3. Model of regression equations.

In this case, the general modeling scheme includes:

- 1) obtaining and analyzing the model;
- 2) the model check;
- 3) introduction to the model of factors that optimize the process, or optimization of the process based on the model;
- 4) obtaining of a new model;
- 5) regulation of the production process to obtain optimal yield.

Optimization of the extraction process of plant raw materials requires knowledge of the corresponding parameters of equilibrium and mass transfer, as well as the optimal operating conditions of the extraction apparatus. Mass transfer and solubility parameters can be quantified by applying an adequate mathematical model to laboratory experimental data. Each model includes several simplified assumptions about how the solute is distributed inside the solid body and the mechanisms involved in the kinetics of mass transfer: internal and external resistance to mass transfer, as well as their combination.

Over the years, mathematical models have been developed using three different approaches: (a) empirical modeling; (b) based on simulations similar to heat transfer; and (c) simulations based on differential integration of mass balance. Empirical models are suitable in the case, when there is no information about the mechanisms of mass transfer. However, the need of developing models that take into account mass transfer

*Corresponding author.

for the mathematical description of the phenomena, occurring during the extraction of plant raw materials, remains relevant.

Main part

There are several models in the available literature materials to describe the supercritical fluid extraction of plant raw materials in the extraction of oils [1, 2]. In general, these models can be divided into four important groups: empirical models, models based on heat transfer analogies, a shrinking core model, and models based on differential mass balance. The last class of models has a distinctive physical meaning and covers the coefficients of mass transfer in the liquid and solid phases or only in one phase. They take into account characteristics of the material matrix, such as particle size and layer porosity. There is necessary to determine different coefficients compared to empirical models. However, these models describe the trends and mechanisms carried out by the extraction process [3].

Criterion equations and regression equations obtained by experimental design methods are suitable to describe the extraction processes. The criterion equations interconnect a series of factors: raw material fineness, mass transfer surface, extractant velocity, other hydrodynamic process conditions (pulsations, vibrations), extraction time, concentration of substances in raw materials, coefficients of free and internal diffusion and other factors. The second important direction in modeling is the implementation of research to translate laboratory experiments into factory production conditions. Most criterion equations do not take into account the criteria of geometric similarity and are not suitable for production conditions.

To ensure maximum results by varying process conditions is an important production task in the developing a mathematical production model. Usually the maximum result (most often the yield or the lowest cost of the product) is closely related to some uncontrollable factor, such as the content of substances in the initial raw materials. Therefore, it is advisable to put this value into the model as one of the factors.

Modeling of mass transfer during continuous supercritical extraction by carbon dioxide is necessary for a deep understanding of the mechanisms of the process before it can be used for design, operation, monitoring, process control and optimization. Authors of the work [4], made a mathematical model (1) of the processes of supercritical fluid extraction of *Lupinus albus* L. seeds, which included system of integro-differential equations with a core determined by the function of the particle size distribution density:

$$f(a) = (1-r)\delta(a-1) + r\delta(a-\alpha), \quad (1)$$

where r — is the part of grains of fine fraction (dust); δ — is the Dirac delta function.

This model taking into account the polydispersity of the granular layer and the process of mass transfer of components inside the particle through the intercellular channels.

The authors of the work [5] presented the process of supercritical fluid extraction of plant raw materials as extraction with cross-flow and a constant distribution coefficient (2). They derived a dependence that has good agreement with experimental data and it is described by the equation:

$$y = k / x \{ \arcsin[\sin(mx)] \}^2, \quad (2)$$

where k — is the equilibrium concentration of biologically active substances in the extractant at the time of its saturation; m — is the time of one extraction cycle; x — is the extraction time; y — is the concentration of biologically active substances in the extractant.

Tan and Liou [6] proposed a one-parameter model describing a desorption of activated carbon loaded with toluene by supercritical fluid extraction.

In the work [7], theoretical models of diffusion of a hot ball, damaged and undamaged cells, shrinkage core and other relatively simple models are reviewed. Modeling process parameters include average particle size, solvent flow rate, pressure, temperature, and modifier concentration and their effect on mass transfer coefficients.

The mechanisms involved in the mass transfer model are described in terms of resistance to external and internal mass transfer, the interaction of a dissolved substance and a solid body, and axial dispersion. Based on the studies carried out, the model of a damaged and undamaged cell has been determined to be suitable. It can be used to simulate supercritical fluid extraction as it reflects the solid structure and kinetics of the extraction process and allows scale up of laboratory data for industrial design. This is confirmed by work [8] on the example of extraction of lupulon from *Humulus* seeds by supercritical fluid extraction.

The authors of [9] investigated the yields of essential oil components during supercritical fluid extraction ($P = 7-15$ MPa, $T = 16-50$ °C) on the example of plants of the *Apiaceae* and *Asteraceae* families. At the same time, it was determined that the resistance to mass transfer is negligible when extracting the compo-

nents of essential oils and does not depend on the degree of grinding of the raw materials. It has a significant effect only during the extraction of *Piper nigrum* L. and *Myristica*, where the extract yield directly depends on the degree of grinding of the raw materials. Based on experimental data, a mathematical model has been developed that describes the kinetics of extraction and takes into account the structure of plant raw materials.

Models of CO₂-extraction of *Ocimum basilicum* L. were studied by the authors of [10], while the factors influencing the yield of the target substances, pressure and temperature were chosen. Brunner's, Candio's and Spiro's models, Esquivel's empirical model, Gordillo's model and others were considered in the work. It was found that the process of CO₂-extraction of *Ocimum basilicum* L. for the extraction of linalool is most closely described by the Gordillo model, while its solubility is strongly dependent on pressure. At the same time the process of eugenol extraction is described by the Del Vale and Aguilera model, which characterizes the dependence of solubility on temperature.

The kinetics of the extraction process of *Satureja montana* L. with supercritical carbon dioxide for the quantitative extraction of essential oil components has been studied. Modeling was carried out using the equations of Ficks, Esquivel, Chrastil, Valle and Aguilera, Adachi and Lu, Sparks. It was established that all models have a similar deviation from the experimental data, and the Esquivel model most closely describes the extraction process of *Satureja montana* L. [11].

Researchers at the Institute of Technology (Brazil) [12] have studied the process of extracting citronella essential oil, which contains more than eighty components. It has been established that the quantitative extraction of the sum of components of the essential oil of *Cymbopogon nardus* L. is achieved at 18.0 MPa and at of 80 °C temperature. The Naik and Lentz models were used to calculate the extraction process; they showed good agreement with experimental data.

A mathematical model for the extraction of essential oil by steam distillation, based on Fick's law in a non-stationary state for a one-dimensional geometry of a rectangle, was calculated using the example of extraction of *Rosmarinus officinalis* L., *Ocimum basilicum* L. and *Lavandula dentata* L. [13].

The effective diffusion coefficient (D) is used in the model as an adjustable parameter to predict the experimental yield curves of the essential oil. It was found that the diffusion mathematical model based on mass transfer has good agreement with experimental data.

Modeling of the process of supercritical fluid extraction of *Anethum graveolens* L. seeds is given in the work [14]. Pressure, temperature and flow rate of CO₂-gas are determined as factors influencing the yield of the target substance. Two models were used for modeling. One is based on desorption, the second is based on the classical model of mass transfer proposed by H. Sovová [15]. The calculation results showed that both models are in good agreement with experimental data, but the second model requires more accurate initial calculations [14].

The process of CO₂-extraction of *Sesamum* seeds has been optimized according to the following technological parameters: pressure, temperature, CO₂-gas supply rate and raw material grinding. It was established that an increase in the pressure and flow rate of CO₂-gas increases the extract yield and shortens the extraction time, an increase in the degree of seed refinement and a decrease in diffusion resistance also increase the yield of extract. Quantitative yield (85 % with hexane extraction) is achieved under the following conditions: 35 MPa pressure, 50 °C temperature, 2 ml/min CO₂-gas supply rate and 300–600 microns particle size. Shrinking cores and undamaged cores mathematical models were used to describe the extraction process. The shrinking cores model is possessed the best convergence to experimental data [16].

Researchers from the Plapiqui University (Argentina) [17] have proposed a new two-dimensional non-stationary mathematical model for the extraction of plant oil from sunflower pellets in an industrial extractor of De Smet type. Extraction from a moving layer of oil material was modeled taking into account the different availability of oil in pellets, counter-flow of porous substance and micelle, diffusion over the entire extraction area, mass transfer between granules and micelles, micelle transfer to percolation areas, loading and drying zones, as well as transient operation of the extractor.

To describe the process of supercritical CO₂-extraction of corn oil cake, researchers at the University of Alberta (Canada) used the mathematical models of Sovová and the model of Krastil [18]. It has been established that the quantitative extraction of biologically active substances from corn oil cake is achieved at 49 MPa and at 70 °C temperature; both models have good agreement with experimental data.

The effect of drying conditions on the composition of supercritical extracts obtained from olive leaves was studied [19]. The leaves were dried on a conveyor belt and the effect of air temperature and residence time on the extraction kinetics, overall yield, antioxidant activity, total polyphenols and the chemical composition of the extracts was assessed. It was established that the drying conditions do not affect on the kinetics

of extraction. In this case, the quantitative yield was achieved at 60°C temperature and at 120 minutes as drying time. To describe the process of CO₂-extraction of olive leaves, the H. Sovová model was used, which showed good agreement with experimental data.

The H. Sovová model is widely used to optimize the process of extracting biologically active substances from plant raw materials. So its use to describe the extraction of *Salvia officinalis* L. by the method of supercritical fluid extraction made it possible to calculate the initial coefficients for multifactorial modeling of the process by an artificial neural network [20]. At the same time the model H. Sovová can also be used independently to optimize supercritical fluid extraction of plant raw materials [21–35].

A modeling approach based on thermodynamic and mass transfer phenomena confirms the Brunauer-Emmett-Teller adsorption theory, which was used in the study to correlate supercritical fluid extraction data from *Eryngium billardieri* L.

A response surface methodology based on a central composite design was used to assess the effects of operating conditions such as pressure, temperature, particle size and dynamic time. The quantitative yield of essential oil was 0.8522 % at 30 MPa pressure, 308 K temperature, 0.75 mm particle size and 130 minutes as extraction time. The predicted results showed that the response surface method is in satisfactory agreement with the experimental data. To describe the study, a quadratic model was chosen, including linear, interactive and quadratic terms [36].

First proposed by Dankwerts [37], dispersion models have come to be widely used to describe reactors with imperfect flow. The model was built on the basis of a constant linear velocity of the correspondent fluid flows. This problem creates difficulties in formulating and simulating the model when the fluid velocity changes along the flow path. This situation occurs when the reactor has a non-uniform cross-section or the void fraction changes along the flow path, which is very common in modern reactors. It has been noted that most continuous flow reactors operate at approximately constant flow rates. Given this Siripatana et al. [38] simplified the dispersion model by reformulating the model in terms of volumetric flow rate rather than linear velocity. The model was called the “volumetric dispersion model” and was used for counter-current extraction and adsorption in a fixed bed. Previous work has illustrated the simplicity of a volumetric dispersion model in describing the effect of inhomogeneous cross-section and variable steam quality along reactors [39]. Different mathematical models have been used in previous studies of supercritical fluid extraction, but most of them did not take into account the role of axial dispersion [9, 40, 41]. Nevertheless, some researchers have formulated models based on the formulation of Dankwerts [42–47]. Their models mainly focus on a situation where the fluid velocity is constant in the processing unit and it is not easy to extend them to predict the performance of non-uniform flow reactors/extractors. It is desirable to have a supercritical fluid extraction model that can be used to design and analyze non-uniform flow extractors. It is expected that volumetric variance model will simplify and expand design capabilities without unnecessary mathematical complexity [48].

Modeling of thermodynamic phase equilibrium and optimization of supercritical CO₂-extraction processes for the concentration of phytosterol and tocopherol from rapeseed oil using the Striek-Vera Peng-Robins (3) state equation made it possible to increase the yield and quality of target substances. While the average relative deviation of experimental and calculated data is about 1–12 % [49].

$$\text{objective} = \frac{1}{n} \sum_{i=1}^n \frac{\text{abs}(P_i^{\text{exp}} - P_i^{\text{EOS}})}{P_i^{\text{exp}}} + \frac{F}{n} \sum_{i=1}^n \frac{\text{abs}(y_i^{\text{exp}} - y_i^{\text{EOS}})}{y_i^{\text{exp}}}, \quad (3)$$

here n — is the number of data points; F — is a weighting parameter; P — is the pressure (MPa); y — is a gas composition (mole fraction).

The phenomenological model (4) for the supercritical extraction of alkaloids nicotine and solanesol showed that for the quantitative extraction of target substances, their solubility must be taken into account. This is in good agreement with experimental data showing that a lower pressure is required for the extraction of solanesol (15 MPa) than for nicotine (37 MPa) [50].

$$\text{K.a} = \frac{k_{SCF} * a_{SCF} * \left(\frac{F}{1 + e^{-(t-t_{c1})}}\right)}{1 + e^{-(t-t_{c2})}} + \frac{k_S * a_S}{1 + e^{-(t-t_{c2})}}, \quad (4)$$

here $k_{SCF} * a_{SCF}$ — is the external mass transfer; $k_S * a_S$ — is the internal mass transfer; factor F characterizes intermediate stage global extraction process.

Conclusions

Thus, the carried out analysis shows that for the transition from laboratory conditions to large-scale production, it is relevant to develop models that directly take into account the parameters of the extraction process, such as pressure, temperature and extraction duration, individual characteristics of raw materials and technological equipment. An empirical approach prevails or simplified differential equations of material balance are used to describe the kinetics of the plant raw materials extraction process. In this case, the H. Sovová mass transfer model and the damaged and undamaged cell model are considered to be relatively adequate models.

The work was carried out under the grant project AP08052030 "Modeling and optimization of the technology of original drugs" funded by the Science Committee of the Ministry of Education and Science of the Republic of Kazakhstan.

References

- Grosso C. Mathematical modelling of supercritical CO₂ extraction of volatile oils from aromatic plants / C. Grosso, J.P. Coelho, F.L.P. Pessoa, J.M.N.A. Fareleira, J.G. Barroso, J.S. Urieta, A.F. Palavra, H. Sovová // Chem. Eng. Sci. — 2010. — Vol. 65. — P. 3579–3590. <https://doi.org/10.1016/j.ces.2010.02.046>
- Rai A. Evaluation of models for supercritical fluid extraction / A. Rai, K.D. Punase, B. Mohanty, R. Bhargava // Int. J. Heat Mass Transf. — 2014. — Vol. 72. — P. 274–287. <https://doi.org/10.1016/j.ijheatmasstransfer.2014.01.011>
- Özkal S. Mass transfer modeling of apricot kernel oil extraction with supercritical carbon dioxide / S. Özkal, M. Yener, L. Bayındırlı // J. Supercrit. Fluids. — 2005. — Vol. 35. — P. 119–127. <https://doi.org/10.1016/j.supflu.2004.12.011>
- Максудов Р.Н. Моделирование процесса сверхкритической экстракции из полидисперсного слоя семян масличных культур / Р.Н. Максудов, А.В. Аляев, А.Г. Егоров, А.Б. Мазо // Вестн. Казан. технол. ун-та. — 2011. — № 20. — С. 200–204.
- Букин А.А. Математическая модель массопереноса при многоступенчатой экстракции из растительного сырья сжиженным диоксидом углерода / А.А. Букин, П.С. Беляев, В.Г. Однолько, Л.И. Ткач, С.А. Щербаков // Изв. высш. учеб. завед. Пищ. технол. — 2011. — Т. 320, 321, № 2, 3. — С. 69–71.
- Tan C.-S. Modeling of desorption at supercritical conditions / C.-S. Tan, D.-C. Liou // AIChE Journal. — 1989. — Vol. 35(6). — P. 1029–1031. doi:10.1002/aic.690350616
- Huang Z. Theoretical models for supercritical fluid extraction / Z. Huang, X. Shi, W. Jiang // J. Chromatogr. A. — 2012. — Vol. 1250. — P. 2–26. <https://doi.org/10.1016/j.chroma.2012.04.032>
- Kupski S.C. Mathematical modeling of supercritical CO₂-extraction of hops (*Humulus lupulus* L.) / S.C. Kupski, E.J. Klein, E.A. Silva, F. Palú, R. Guirardello, M. Gurgel, A. Vieira // J. Supercrit. Fluids. — 2017. — Vol. 130. — P. 347–356. <http://dx.doi.org/10.1016/j.supflu.2017.06.011>
- Sovová H. Modeling the supercritical fluid extraction of essential oils from plant materials / H. Sovová // J. Chromatogr. A. — 2012. — Vol. 1250. — P. 27–33. <https://doi.org/10.1016/j.chroma.2012.05.014>
- Zekovic Z. Mathematical Modeling of *Ocimum basilicum* L. Supercritical CO₂-Extraction / Z. Zeković, S. Filip, S. Vidović, S. Jokić, S. Svilović // Chem. Eng. Technol. — 2014. — Vol. 37. — P. 1–7. <https://doi.org/10.1002/ceat.201400322>
- Vladić J. Winter savory: supercritical carbon dioxide extraction and mathematical modeling of extraction process / J. Vladić, Z. Zeković, S. Jokić, S. Svilović, S. Kovačević, S. Vidović // J. Supercrit. Fluids. — 2016. — Vol. 117. — P. 89–97. <http://dx.doi.org/10.1016/j.supflu.2016.05.027>
- Silva C.F. Extraction of citronella (*Cymbopogon nardus*) essential oil using supercritical CO₂: experimental data and mathematical modeling / C.F. Silva, F.C. Moura, M.F. Mendes, F.L.P. Pessoa // Brazilian J. Chem. Eng. — 2011. — Vol. 28. — P. 343–350. <http://dx.doi.org/10.1590/S0104-66322011000200019>
- Cassel E. Steam distillation modeling for essential oil extraction process / E. Cassel, R.M.F. Vargas, N. Martinez, D. Lorenzo, E. Dellacassa // Industrial crops and products. — 2009. — Vol. 29. — P. 171–176. <https://doi.org/10.1016/j.indcrop.2008.04.017>
- Garcez J.J. Evaluation and mathematical modeling of processing variables for asupercritical fluid extraction of aromatic compounds from *Anethum graveolens* / J.J. Garcez, F. Barros, A.M. Lucas, V.B. Xavier, A.L. Fianco, E. Cassel, R.M.F. Vargas // Industrial Crops and Products. — 2017. — Vol. 95. — P. 733–741. <https://doi.org/10.1016/j.indcrop.2016.11.042>
- Sovová H. Rate of the vegetable oil extraction with supercritical CO₂-I. Modeling of extraction curves / H. Sovová // Chem. Eng. Sci. — 1994. — Vol. 49. — P. 409–414. [https://doi.org/10.1016/0009-2509\(94\)87012-8](https://doi.org/10.1016/0009-2509(94)87012-8)
- Döker O. Extraction of sesame seed oil using supercritical CO₂ and mathematical modeling / O. Döker, U. Salgin, N. Yildiz, M. Aydoğmuş, A. Çalimli // Journal of Food Engineering. — 2010. — Vol. 97. — P. 360–366. <https://doi.org/10.1016/j.jfoodeng.2009.10.030>
- Carrin M.E. Mathematical modeling of vegetable oil–solvent extraction in a multistage horizontal extractor / M.E. Carrin, G.H. Crapiste // Journal of Food Engineering. — 2008. — Vol. 85. — P. 418–425. <https://doi.org/10.1016/j.jfoodeng.2007.08.003>

- 18 Ciftci O.N. Supercritical Carbon Dioxide Extraction of Corn Distiller's Dried Grains with Solubles: Experiments and Mathematical Modeling / O.N. Ciftci, J. Calderon, F. Temelli // J. Agric. Food Chem. — 2012. — Vol. 60. — P. 12482–12490. <https://doi.org/10.1021/jf302932w>
- 19 Canabarro N.I. Drying of olive (*Olea europaea* L.) leaves on a conveyor belt for supercritical extraction of bioactive compounds: Mathematical modeling of drying/extraction operations and analysis of extracts / N.I. Canabarro, M.A. Mazutti, M.C. Ferreira // Industrial Crops & Products. — 2019. — Vol. 136. — P. 140–151. <https://doi.org/10.1016/j.indcrop.2019.05.004>
- 20 Pavlič B. Extraction kinetics and ANN simulation of supercritical fluid extraction of sage herbal dust / B. Pavlič, O. Bera, S. Vidović, L. Ilić, Z. Zeković // J. Supercrit. Fluids. — 2017. — Vol. 130. — P. 327–336. <https://doi.org/10.1016/j.supflu.2017.11.006>
- 21 Popa O. Modeling the extraction curve of *Amaranth* oil with Sovova model / O. Popa, N. Babeanu, S. Nita, D.I. Marin // Journal of Biotechnology. — 2016. — Vol. 231S. — P. S4–S109. <http://dx.doi.org/10.1016/j.jbiotec.2016.05.200>
- 22 Braga M.E.M. Mathematical modelling of turmeric compounds extraction using high pressurized solvents mixture / M.E.M. Braga, S. Quispe-Condori, P.T.V. Rosa, M. Angela, A. Meireles // J. Supercrit. Fluids. — 2018. — Vol. 140. — P. 348–355. <https://doi.org/10.1016/j.supflu.2018.07.014>
- 23 Lopes N.L. Evaluation of the effects of pressurized solvents and extraction process parameters on seed oil extraction in *Pachira aquatica* / N.L. Lopes, J.M.F. Almeida-Couto, C. Silva, M.B. Pereira, T.C. Pimentel, C.E. Barão, L. Cardozo-Filho // J. Supercrit. Fluids. — 2020. — Vol. 161. — P. 104823. <https://doi.org/10.1016/j.supflu.2020.104823>
- 24 Confortin T.C. Supercritical CO₂ extraction of compounds from different aerial parts of *Senecio brasiliensis*: Mathematical modeling and effects of parameters on extract quality / T.C. Confortin, I. Todero, N.I. Canabarro, L. Luft, G.A. Ugalde, J.R.C. Neto, et. al. // J. Supercrit. Fluids. — 2019. — Vol. 153. — P. 104589. <https://doi.org/10.1016/j.supflu.2019.104589>
- 25 Palsikowski P.A. Supercritical CO₂ oil extraction from *Bauhinia forficata* link subsp. pruinosa leaves: Composition, antioxidant activity and mathematical modeling / P.A. Palsikowski, L.M. Besen, K.A. Santos, C. Silva, E.A. Silva // J. Supercrit. Fluids. — 2019. — Vol. 153. — P. 104588. <https://doi.org/10.1016/j.supflu.2019.104588>
- 26 Santos K.A. Supercritical CO₂ extraction of favela (*Cnidocolus quercifolius*) seed oil: Yield, composition, antioxidant activity, and mathematical modeling / K.A. Santos, E.A. Silva, C. Silva // J. Supercrit. Fluids. — 2020. — Vol. 165. — P. 104981. <https://doi.org/10.1016/j.supflu.2020.104981>
- 27 Liu X. Ultrasound-assisted supercritical CO₂ extraction of cucurbitacin E from *Iberis amara* seeds / X. Liu, H. Ou, H. Gregersen // Industrial Crops and Products. — 2020. — Vol. 145. — P. 112093. <https://doi.org/10.1016/j.indcrop.2020.112093>
- 28 Mouahid A. Supercritical CO₂ extraction of oil from *Jatropha curcas*: An experimental and modelling study / A. Mouahid, H. Bouanga, C. Crampon, E. Badens // J. Supercrit. Fluids. — 2018. — Vol. 141. — P. 2–11. <https://doi.org/10.1016/j.supflu.2017.11.014>
- 29 Hassim N. Scale-up criteria and economic analysis for supercritical fluid extraction of *Phyllanthus niruri* / N. Hassim, M. Markom, M.I. Rosli, S. Harun // Chemical Engineering & Processing: Process Intensification. — 2019. — Vol. 139. — P. 14–22. <https://doi.org/10.1016/j.cep.2019.03.011>
- 30 Pavlic B. Supercritical fluid extraction of raspberry seed oil: Experiments and modeling / B. Pavlič, L. Pezo, B. Marić, L.P. Tukuljac, Z. Zeković, M.B. Solarov, N. Teslić // J. Supercrit. Fluids. — 2020. — Vol. 157. — P. 104687. <https://doi.org/10.1016/j.supflu.2019.104687>
- 31 Natolino A. Supercritical carbon dioxide extraction of pomegranate (*Punica granatum* L.) seed oil: Kinetic modelling and solubility evaluation / A. Natolino, C. Porto // J. Supercrit. Fluids. — 2019. — Vol. 151. — P. 30–39. <https://doi.org/10.1016/j.supflu.2019.05.002>
- 32 Zanqui A.B. Extraction and assessment of oil and bioactive compounds from cashew nut (*Anacardium occidentale*) using pressurized n-propane and ethanol as cosolvent / A.B. Zanqui, C.M. Silva, J.B. Ressutte, D.R. Morais, J.M. Santos, M.N. Eberlin, et. al. // J. Supercrit. Fluids. — 2020. — Vol. 157. — P. 104686. <https://doi.org/10.1016/j.supflu.2019.104686>
- 33 Kavoura D. Supercritical CO₂ extraction of *Salvia fruticosa* / D. Kavoura, K. Kyriakopoulou, G. Papaefstathiou, E. Spanidi, K. Gardikis, V. Louli, N. Aligiannis, et. al. // J. Supercrit. Fluids. — 2019. — Vol. 146. — P. 159–164. <https://doi.org/10.1016/j.supflu.2019.01.010>
- 34 Soto-Armenta L.C. Extraction yield and kinetic study of *Lippia graveolens* with supercritical CO₂ / L.C. Soto-Armenta, J.C. Sacramento-Rivero, C.A. Ruiz-Mercado, M.C. Lope-Navarrete, J.A. Rocha-Urbe // J. Supercrit. Fluids. — 2019. — Vol. 145. — P. 205–210. <https://doi.org/10.1016/j.supflu.2018.12.018>
- 35 Mouahid A. Effects of high water content and drying pre-treatment on supercritical CO₂ extraction from *Dunaliella salina* microalgae: Experiments and modeling / A. Mouahid, C. Crampon, S.-A.A. Toudji, E. Badens // J. Supercrit. Fluids. — 2016. — Vol. 116. — P. 271–280. <https://doi.org/10.1016/j.supflu.2016.06.007>
- 36 Sodeifian G. Experimental optimization and mathematical modeling of the supercritical fluid extraction of essential oil from *Eryngium billardieri*: Application of simulated annealing (SA) algorithm / G. Sodeifian, S.A. Sajadian, N.S. Ardestani // J. Supercrit. Fluids. — 2017. — Vol. 127. — P. 146–157. <https://doi.org/10.1016/j.supflu.2017.04.007>
- 37 Danckwerts P.V. Continuous flow systems: Distribution of residence times / P.V. Danckwerts // Chem. Eng. Sci. — 1953. — Vol. 2. — P. 1–13. [http://dx.doi.org/10.1016/0009-2509\(53\)80001-1](http://dx.doi.org/10.1016/0009-2509(53)80001-1)
- 38 Siripatana C. Generalized volumetric dispersion model for a class of two-phase separation/reaction: Finite difference solutions / C. Siripatana, H. Thongpan, A.A. Promraksa // J. Phys. Conf. Ser. — 2017. — Vol. 820. — P. 012015. <http://dx.doi.org/10.1088/1742-6596/820/1/012015>

- 39 Huang Z. Theoretical models for supercritical fluid extraction / Z. Huang, X. Shi, W. Jiang // J. Chromatogr. A. — 2012. — Vol. 1250. — P. 2–26. <http://dx.doi.org/10.1016/j.chroma.2012.04.032>
- 40 Salamatin A.A. Optimization of supercritical fluid extraction: Polydisperse packed beds and variable flow rates / A.A. Salamatin, A.G. Egorov // J. Supercrit. Fluids. — 2015. — Vol. 105. — P. 35–43. <http://dx.doi.org/10.1016/j.supflu.2015.01.013>
- 41 Duba K.S. Supercritical extraction of vegetable oils: Different approaches to modeling the mass transfer kinetics / K.S. Duba, L. Fiori // Chem. Eng. Trans. — 2015. — Vol. 43. — P. 1051–1056. <http://dx.doi.org/10.3303/CET1543176>
- 42 Goto M. Shrinking-core leaching model for supercritical-fluid extraction / M. Goto, B.C. Roy, T. Hirose // J. Supercrit. Fluids. — 1996. — Vol. 9. — P. 128–133. [http://dx.doi.org/10.1016/S0896-8446\(96\)90009-1](http://dx.doi.org/10.1016/S0896-8446(96)90009-1)
- 43 Honarvar B. Mathematical modeling of supercritical fluid extraction of oil from canola and sesame seeds / B. Honarvar, S.A. Sajadian, M. Khorram, A. Samimi // Braz. J. Chem. Eng. — 2013. — Vol. 30. — P. 159–166. <http://dx.doi.org/10.1590/S0104-66322013000100018>
- 44 Stamenic M. The mathematics of modelling the supercritical fluid extraction of essential oils from glandular trichomes / M. Stamenic, I. Zizovic // Comput. Chem. Eng. — 2013. — Vol. 48. — P. 89–95. <http://dx.doi.org/10.1016/j.compchemeng.2012.08.006>
- 45 Rai A. Evaluation of models for supercritical fluid extraction / A. Rai, K.D. Punase, B. Mohanty, R. Bhargava // Int. J. Heat Mass Tran. — 2014. — Vol. 72. — P. 274–287. <http://dx.doi.org/10.1016/j.ijheatmasstransfer.2014.01.011>
- 46 Pereira T.J.G. Mathematical modeling of supercritical extraction: Model of two phases with linear equilibrium / T.J.G. Pereira, L.F.G. Machado, J.L. Ferreira, E.N. Macêdo // Int. J. Model. Simul. Petrol. Ind. — 2014. — Vol. 8. — P. 9–17.
- 47 Song Y. Kinetics model for supercritical fluid extraction with variable mass transport / Y. Song, L. Zheng, X. Zhang // Int. J. Heat Mass Tran. — 2017. — Vol. 122. — P. 876–881. <http://dx.doi.org/10.1016/j.ijheatmasstransfer.2017.05.002>
- 48 Promraksa A. Modeling of Supercritical CO₂ Extraction of Palm Oil and Tocopherols Based on Volumetric Axial Dispersion / A. Promraksa, C. Siripatana, N. Rakmak, N. Chusri // J. Supercrit. Fluids. — 2020. — Vol. 166. — P. 105021. <https://doi.org/10.1016/j.supflu.2020.105021>
- 49 Jafarian A.P. Modelling and simulation of supercritical CO₂-extraction of bioactive compounds from vegetable oil waste / A.P. Jafarian, R. Niazmand // Food and Bioproducts Processing. — 2020. — Vol. 122. — P. 311–321. <https://doi.org/10.1016/j.fbp.2020.05.005>
- 50 Tita G.J. Model assisted supercritical fluid extraction and fractionation of added-value products from tobacco scrap / G.J. Tita, A. Navarrete, Á. Martín, M.J. Cocero // J. Supercrit. Fluids. — 2021. — Vol. 167. — P. 105046. <https://doi.org/10.1016/j.supflu.2020.105046>

И.А. Хабаров, В.В. Журов, А.Н. Жаббаева, С.М. Адекенов

Дәрілік шикізатты экстракциялау үдерісін модельдеу

Мақалада дәрілік өсімдік шикізатынан биологиялық белсенді компоненттерді экстракциялау үдерісінің 26 математикалық моделі қарастырылған, олар шығарып алу үдерісіне әсер ететін факторларды ескереді: диффузия коэффициенті, бөлшектердің мөлшері, қабаттың кеуектігі, экстрагент беру жылдамдығы, шикізатты ұсату тәсілі, шығарып алу қысымы, температурасы мен ұзақтығы, шикізат (мақсатты компоненттің құрамы) пен технологиялық жабдықтың жеке сипаттамасы. Жалпы алғанда, бұл модельдер төрт маңызды топқа бөлінеді: эмпирикалық модельдер, жылу беру аналогтарына негізделген модельдер, сығылатын ядро модельдері және массаның дифференциалды тепе-теңдігіне негізделген модельдер. Математикалық модельдерді таңдауда ең алдымен, экстракциялық сұйықтықтар ағындарының идеалды емес әрекетімен, экстракциялық аппараттардың біртекті емес көлденең қимасымен байланысты мәселелер сипатталған. Экстракциялау үдерісін модельдеу, ең алдымен, қатты бөлшектердің ішіндегі масса тасымалын сипаттау үшін математикалық модельдерді қажет ететіні көрсетілген. Сондай-ақ, модельдеу кезінде мақсатты заттардың ерігіштігін ескеру қажет. Жүргізілген талдау негізінде өсімдік шикізатынан биологиялық белсенді заттарды экстракциялау үдерістерінің негізгі факторларын есептеу үшін диффузиялық, H. Sovová, Naik және Lentz, Esquivel, бұзылған және зақымдалмаған ұяшық модельдері оңтайлы болып табылатыны анықталды.

Кілт сөздер: математикалық модельдеу, масса тасымалдау, диффузия, регрессия теңдеуі, критерийлік теңдеу, оңтайландыру, экстракция, дәрілік шикізат.

И.А. Хабаров, В.В. Журов, А.Н. Жаббаева, С.М. Адекенов

Моделирование процесса экстракции лекарственного сырья

В обзорной статье рассмотрены 26 математических моделей процесса экстракции биологически активных веществ из лекарственного растительного сырья, учитывающие факторы, влияющие на про-

цесс извлечения: коэффициент диффузии, размер частиц, пористость слоя, скорость подачи экстрагента, способ измельчения сырья, давление, температуру и продолжительность извлечения, индивидуальную характеристику сырья (содержание целевого компонента) и технологического оборудования. В целом, эти модели делятся на четыре важные группы: эмпирические модели; модели, основанные на аналогиях теплопередачи; модель сжимающегося ядра и модели, основанные на дифференциальном балансе массы. Описаны проблемы при подборе математических моделей, связанных, прежде всего, с неидеальным поведением потоков экстракционных жидкостей, неоднородным поперечным сечением экстракционных аппаратов. Показано, что моделирование процесса экстракции, в первую очередь, требует математических моделей для описания массопереноса внутри твердых частиц. Также при моделировании важно учитывать растворимость целевых веществ. На основании проведенного анализа определено, что для расчета основных факторов экстракционных процессов биологически активных веществ из растительного сырья оптимальными являются модели: диффузионная, H. Sovová, Naik и Lentz, Esquivel, разрушенной и неповрежденной ячейки.

Ключевые слова: математическое моделирование, массоперенос, диффузия, уравнение регрессии, критерияльное уравнение, оптимизация, экстракция, растительное сырье.

References

- Grosso, C., et al. (2010). Mathematical modelling of supercritical CO₂ extraction of volatile oils from aromatic plants. *Chem. Eng. Sci.*, 65, 3579–3590. <https://doi.org/10.1016/j.ces.2010.02.046>
- Rai, A., et al. (2014). Evaluation of models for supercritical fluid extraction. *Int. J. Heat Mass Transf.*, 72, 274–287. <https://doi.org/10.1016/j.ijheatmasstransfer.2014.01.011>
- Özkal, S., Yener, M., & Bayındırlı, L. (2005). Mass transfer modeling of apricot kernel oil extraction with supercritical carbon dioxide. *J. Supercrit. Fluids*, 35, 119–127. <https://doi.org/10.1016/j.supflu.2004.12.011>
- Maksudov, R.N., et al. (2011). Modelirovanie protsessa sverkhkriticheskoi ekstraksii iz polidispersnoho sloia semian maslichnykh kultur [Modeling the process of supercritical extraction from a polydisperse layer of oilseeds cultures]. *Vestnik Kazanskoho tekhnolohicheskoho universiteta — Bulletin of Kazan Technological University*, 20, 200–204 [in Russian].
- Bukin, A.A., et al. (2011). Matematicheskaia model massoperenosa pri mnohostupenchatoi ekstraksii iz rastitelnoho syria szhizhennym dioksidom uhleroda [Mathematical model of mass transfer during multistage extraction from plant raw materials with liquefied carbon dioxide]. *Izvestiia vysshikh uchebnykh zavedenii. Pishchevaia tekhnolohiia — News of Higher Educational Institutions. Food Technology*, 320–321, 2–3, 69–71 [in Russian].
- Tan, C.-S., & Liou, D.-C. (1989). Modeling of desorption at supercritical conditions. *AIChE Journal*, 35(6), 1029–1031. DOI: 10.1002/aic.690350616
- Huang, Z., Shi, X., & Jiang, W. (2012). Theoretical models for supercritical fluid extraction. *J. Chromatogr. A*, 1250, 2–26. <https://doi.org/10.1016/j.chroma.2012.04.032>
- Kupski, S.C., et al. (2017). Mathematical modeling of supercritical CO₂-extraction of hops (*Humulus lupulus* L.). *J. Supercrit. Fluids*, 130, 347–356. <http://dx.doi.org/10.1016/j.supflu.2017.06.011>
- Sovová, H. (2012). Modeling the supercritical fluid extraction of essential oils from plant materials. *J. Chromatogr. A*, 1250, 27–33. <https://doi.org/10.1016/j.chroma.2012.05.014>
- Zekovic, Z., et al. (2014). Mathematical Modeling of *Ocimum basilicum* L. Supercritical CO₂-Extraction. *Chem. Eng. Technol.*, 37, 1–7. <https://doi.org/10.1002/ceat.201400322>
- Vladic, J., et al. (2016). Winter savory: supercritical carbon dioxide extraction and mathematical modeling of extraction process. *J. Supercrit. Fluids*, 117, 89–97. <http://dx.doi.org/10.1016/j.supflu.2016.05.027>
- Silva, C.F., et al. (2011). Extraction of citronella (*Cymbopogon nardus*) essential oil using supercritical CO₂: experimental data and mathematical modeling. *Brazilian J. Chem. Eng.*, 28, 343–350. <http://dx.doi.org/10.1590/S0104-66322011000200019>
- Cassel, E., et al. (2009). Steam distillation modeling for essential oil extraction process. *Industrial crops and products*, 29, 171–176. <https://doi.org/10.1016/j.indcrop.2008.04.017>
- Garcez, J.J., et al. (2017). Evaluation and mathematical modeling of processing variables for asupercritical fluid extraction of aromatic compounds from *Anethum graveolens*. *Industrial Crops and Products*, 95, 733–741. <https://doi.org/10.1016/j.indcrop.2016.11.042>
- Sovová, H. (1994). Rate of the vegetable oil extraction with supercritical CO₂–I. Modeling of extraction curves. *Chem. Eng. Sci.*, 49, 409–414. [https://doi.org/10.1016/0009-2509\(94\)87012-8](https://doi.org/10.1016/0009-2509(94)87012-8)
- Döker, O., et al. (2010). Extraction of sesame seed oil using supercritical CO₂ and mathematical modeling. *Journal of Food Engineering*, 97, 360–366. <https://doi.org/10.1016/j.jfoodeng.2009.10.030>
- Carrin, M.E., & Crapiste, G.H. (2008). Mathematical modeling of vegetable oil–solvent extraction in a multistage horizontal extractor. *Journal of Food Engineering*, 85, 418–425. <https://doi.org/10.1016/j.jfoodeng.2007.08.003>
- Ciftci, O.N., Calderon, J., & Temelli, F. (2012). Supercritical Carbon Dioxide Extraction of Corn Distiller’s Dried Grains with Solubles: Experiments and Mathematical Modeling. *J. Agric. Food Chem.*, 60, 12482–12490. <https://doi.org/10.1021/jf302932w>

- 19 Canabarro, N.I., Mazutti, M.A., & Ferreira, M.C. (2019). Drying of olive (*Olea europaea* L.) leaves on a conveyor belt for supercritical extraction of bioactive compounds: Mathematical modeling of drying/extraction operations and analysis of extracts. *Industrial Crops & Products*, *136*, 140–151. <https://doi.org/10.1016/j.indcrop.2019.05.004>
- 20 Pavlič, B., et al. (2017). Extraction kinetics and ANN simulation of supercritical fluid extraction of sage herbal dust. *J. Supercrit. Fluids*, *130*, 327–336. <https://doi.org/10.1016/j.supflu.2017.11.006>
- 21 Popa, O., et al. (2016). Modeling the extraction curve of *Amaranth* oil with Sovova model. *Journal of Biotechnology*, *231S*, S4–S109. <http://dx.doi.org/10.1016/j.jbiotec.2016.05.200>
- 22 Braga, M.E.M., et al. (2018). Mathematical modelling of turmeric compounds extraction using high pressurized solvents mixture. *J. Supercrit. Fluids*, *140*, 348–355. <https://doi.org/10.1016/j.supflu.2018.07.014>
- 23 Lopes, N.L., et al. (2020). Evaluation of the effects of pressurized solvents and extraction process parameters on seed oil extraction in *Pachira aquatica*. *J. Supercrit. Fluids*, *161*, 104823. <https://doi.org/10.1016/j.supflu.2020.104823>
- 24 Confortin, T.C., et al. (2019). Supercritical CO₂ extraction of compounds from different aerial parts of *Senecio brasiliensis*: Mathematical modeling and effects of parameters on extract quality. *J. Supercrit. Fluids*, *153*, 104589. <https://doi.org/10.1016/j.supflu.2019.104589>
- 25 Palsikowski, P.A., et al. (2019). Supercritical CO₂ oil extraction from *Bauhinia forficata* link subsp. pruinosa leaves: Composition, antioxidant activity and mathematical modeling. *J. Supercrit. Fluids*, *153*, 104588. <https://doi.org/10.1016/j.supflu.2019.104588>
- 26 Santos, K.A., Silva, E.A., & Silva, C. (2020). Supercritical CO₂ extraction of favela (*Cnidioscolus quercifolius*) seed oil: Yield, composition, antioxidant activity, and mathematical modeling. *J. Supercrit. Fluids*, *165*, 104981. <https://doi.org/10.1016/j.supflu.2020.104981>
- 27 Liu, X., Ou, H., & Gregersen, H. (2020). Ultrasound-assisted supercritical CO₂ extraction of cucurbitacin E from *Iberis amara* seeds. *Industrial Crops and Products*, *145*, 112093. <https://doi.org/10.1016/j.indcrop.2020.112093>
- 28 Mouahid, A., et al. (2018). Supercritical CO₂ extraction of oil from *Jatropha curcas*: An experimental and modelling study. *J. Supercrit. Fluids*, *141*, 2–11. <https://doi.org/10.1016/j.supflu.2017.11.014>
- 29 Hassim, N., et al. (2019). Scale-up criteria and economic analysis for supercritical fluid extraction of *Phyllanthus niruri*. *Chemical Engineering & Processing: Process Intensification*, *139*, 14–22. <https://doi.org/10.1016/j.cep.2019.03.011>
- 30 Pavlic, B., et al. (2020). Supercritical fluid extraction of raspberry seed oil: Experiments and modeling. *J. Supercrit. Fluids*, *157*, 104687. <https://doi.org/10.1016/j.supflu.2019.104687>
- 31 Natolino, A., & Porto, C. (2019). Supercritical carbon dioxide extraction of pomegranate (*Punica granatum* L.) seed oil: Kinetic modelling and solubility evaluation. *J. Supercrit. Fluids*, *151*, 30–39. <https://doi.org/10.1016/j.supflu.2019.05.002>
- 32 Zanqui, A.B., et al. (2020). Extraction and assessment of oil and bioactive compounds from cashew nut (*Anacardium occidentale*) using pressurized n-propane and ethanol as cosolvent. *J. Supercrit. Fluids*, *157*, 104686. <https://doi.org/10.1016/j.supflu.2019.104686>
- 33 Kavoura, D., et al. (2019). Supercritical CO₂ extraction of *Salvia fruticosa*. *J. Supercrit. Fluids*, *146*, 159–164. <https://doi.org/10.1016/j.supflu.2019.01.010>
- 34 Soto-Armenta, L.C., et al. (2019). Extraction yield and kinetic study of *Lippia graveolens* with supercritical CO₂. *J. Supercrit. Fluids*, *145*, 205–210. <https://doi.org/10.1016/j.supflu.2018.12.018>
- 35 Mouahid, A., et al. (2016). Effects of high water content and drying pre-treatment on supercritical CO₂ extraction from *Dunaliella salina* microalgae: Experiments and modeling. *J. Supercrit. Fluids*, *116*, 271–280. <https://doi.org/10.1016/j.supflu.2016.06.007>
- 36 Sodeifian, G., Sajadian, S.A., & Ardestani, N.S. (2017). Experimental optimization and mathematical modeling of the supercritical fluid extraction of essential oil from *Eryngium billardieri*: Application of simulated annealing (SA) algorithm. *J. Supercrit. Fluids*, *127*, 146–157. <https://doi.org/10.1016/j.supflu.2017.04.007>
- 37 Danckwerts, P.V. (1953). Continuous flow systems: Distribution of residence times. *Chem. Eng. Sci.*, *2*, 1–13. [http://dx.doi.org/10.1016/0009-2509\(53\)80001-1](http://dx.doi.org/10.1016/0009-2509(53)80001-1)
- 38 Siripatana, C., Thongpan, H., & Promraksa, A.A. (2017). Generalized volumetric dispersion model for a class of two-phase separation/reaction: Finite difference solutions. *J. Phys. Conf. Ser.*, *820*, 012015. <http://dx.doi.org/10.1088/1742-6596/820/1/012015>
- 39 Huang, Z., Shi, X., & Jiang, W. (2012). Theoretical models for supercritical fluid extraction. *J. Chromatogr. A.*, *1250*, 2–26. <http://dx.doi.org/10.1016/j.chroma.2012.04.032>
- 40 Salamatin, A.A., & Egorov, A.G. (2015). Optimization of supercritical fluid extraction: Polydisperse packed beds and variable flow rates. *J. Supercrit. Fluids*, *105*, 35–43. <http://dx.doi.org/10.1016/j.supflu.2015.01.013>
- 41 Duba, K.S., & Fiori, L. (2015). Supercritical extraction of vegetable oils: Different approaches to modeling the mass transfer kinetics. *Chem. Eng. Trans.*, *43*, 1051–1056. <http://dx.doi.org/10.3303/CET1543176>
- 42 Goto, M., Roy, B.C., & Hirose, T. (1996). Shrinking-core leaching model for supercritical-fluid extraction. *J. Supercrit. Fluids*, *9*, 128–133. [http://dx.doi.org/10.1016/S0896-8446\(96\)90009-1](http://dx.doi.org/10.1016/S0896-8446(96)90009-1)
- 43 Honarvar, B., et al. (2013). Mathematical modeling of supercritical fluid extraction of oil from canola and sesame seeds. *Braz. J. Chem. Eng.*, *30*, 159–166. <http://dx.doi.org/10.1590/S0104-66322013000100018>
- 44 Stamenic, M., & Zizovic, I. (2013). The mathematics of modelling the supercritical fluid extraction of essential oils from glandular trichomes. *Comput. Chem. Eng.*, *48*, 89–95. <http://dx.doi.org/10.1016/j.compchemeng.2012.08.006>

45 Rai, A., et al. (2014). Evaluation of models for supercritical fluid extraction. *Int. J. Heat Mass Tran.*, 72, 274–287., <http://dx.doi.org/10.1016/j.ijheatmasstransfer.2014.01.011>

46 Pereira, T.J.G., et al. (2014). Mathematical modeling of supercritical extraction: Model of two phases with linear equilibrium. *Int. J. Model. Simul. Petrol. Ind.*, 8, 9–17.

47 Song, Y., Zheng, L., & Zhang, X. (2017). Kinetics model for supercritical fluid extraction with variable mass transport. *Int. J. Heat Mass Tran.*, 122, 876–881. <http://dx.doi.org/10.1016/j.ijheatmasstransfer.2017.05.002>

48 Promraksa, A., et al. (2020). Modeling of Supercritical CO₂ Extraction of Palm Oil and Tocopherols Based on Volumetric Axial Dispersion. *J. Supercrit. Fluids*, 166, 105021. <https://doi.org/10.1016/j.supflu.2020.105021>

49 Jafarian, A.P., & Niazmand, R. (2020). Modelling and simulation of supercritical CO₂-extraction of bioactive compounds from vegetable oil waste. *Food and Bioproducts Processing*, 122, 311–321. <https://doi.org/10.1016/j.fbp.2020.05.005>

50 Tita, G.J., et al. (2021). Model assisted supercritical fluid extraction and fractionation of added-value products from tobacco scrap. *J. Supercrit. Fluids*, 167, 105046. <https://doi.org/10.1016/j.supflu.2020.105046>

Information about authors

Khabarov, Iliya Anatolievich — Candidate of Pharmaceutical Sciences, Head of Laboratory, JSC “International Research and Production Holding “Phytochemistry”, Gazaliev str. 4, 100009, Karaganda, Kazakhstan, e-mail: i.khabarov@phyto.kz; <http://orcid.org/0000-0002-6727-8870>.

Zhurov, Vitaliy Vladimirovich — Candidate of Technical Sciences, Researcher, JSC “International Research and Production Holding “Phytochemistry”, Gazaliev str. 4, 100009, Karaganda, Kazakhstan, e-mail: zhurvityv@yandex.ru; <http://orcid.org/0000-0002-4413-8584>.

Zhabayeva, Anar Nikhanbaevna — Candidate of Pharmaceutical Sciences, Chief Technologist, JSC “International Research and Production Holding “Phytochemistry”, Gazaliev str. 4, 100009, Karaganda, Kazakhstan, e-mail: a.zhabaeva@phyto.kz; <https://orcid.org/0000-0002-9948-7140>.

Adekenov, Sergazy Mynzhasarovich — Doctor of Chemical Sciences, General Director, JSC “International Research and Production Holding “Phytochemistry”, Gazaliev str. 4, 100009, Karaganda, Kazakhstan, e-mail: arglabin@phyto.kz; <https://orcid.org/0000-0001-7588-6174>.

INFORMATION ABOUT AUTHORS

Adekenov, Sergazy Mynzhasarovich — Doctor of Chemical Sciences, General Director, JSC “International Research and Production Holding “Phytochemistry”, Gazaliev str. 4, 100009, Karaganda, Kazakhstan, e-mail: arglabin@phyto.kz; <https://orcid.org/0000-0001-7588-6174>.

Bakibaev, Abdigali Abdimanapovich — Doctor of Chemical sciences, Engineer, Institute for Problems of Chemical and Energetic Technologies SB RAS, Socialisticheskaya street, 1, 659322, Biysk, Russia; e-mail: bakibaev@mail.ru; <https://orcid.org/0000-0002-3335-3166>.

Balpanov, Darhan Serikovich — Candidate of chemical sciences, research associate of “Biolife” Ltd, Stepnogorsk, 5 district, 8–80, Kazakhstan; e-mail: balpan@mail.ru.

Eissa, Ibrahim Hasan — Associate professor, Pharmaceutical Medicinal Chemistry & Drug Design Department, Faculty of Pharmacy (Boys), Al-Azhar University, Cairo11884, Egypt; e-mail: ibrahimeissa@azhar.edu.eg, ORCID 0000-0002-6955-2263.

Erkasov, Rakhmetulla Sharapidenovich — Doctor of Chemical Sciences, Professor of the Department of Chemistry, L.N. Gumilyov Eurasian National University, Nur-Sultan, K. Munaitpasov Street, 13, 010008, Kazakhstan; e-mail: erkass@mail.ru.

Gani, Gulfairuz Muratovna — 2nd year master's student, Technology of medicine and engineering disciplines department, Asfendiyarov Kazakh National Medical University, Tole bi street, 94, 050000, Almaty, Kazakhstan; e-mail: flower_fariza@inbox.ru.

Gatilov, Yurii Vasilevich — Doctor of chemical sciences, Leading researcher, N.N. Vorozhtsov Institute of Organic Chemistry of Siberian Branch of Russian Academy of Sciences, Novosibirsk, Lavrentiev Avenue, 9, 630090, Russia; e-mail: gatilov@nioch.ncs.ru; <https://orcid.org/0000-0001-4365-0081>.

Gussenov, Iskander Shakhshavanovich — PhD, Satbayev University, Senior researcher of the Institute of Polymer Materials and Technology, Almaty, Kazakhstan; Satbayev street 22a, 050013. e-mail: iskander.gussenov@mail.ru; ORCID 0000-0002-9820-7952.

Iskakova, Zhanar Baktybaevna — Candidate of chemical sciences, Kazakh University of Technology and Business, Nur-Sultan, K. Mukhamedkhanov Str., 37A, Kazakhstan; e-mail: zhanariskakova@mail.ru; <https://orcid.org/0000-0002-3540-8263>.

Jalmakhanbetova, Roza Ilemisovna — Doctor of chemical sciences, Kazakh University of Technology and Business, Nur-Sultan, K. Mukhamedkhanov Str., 37A, Kazakhstan; e-mail: rozadichem@mail.ru, ORCID: 0000-0001-9937-275X.

Karabayeva, Aigerim Abayevna — PhD, Doctor of pharmaceutical sciences, Dean of School of Pharmacy of Asfendiyarov Kazakh National Medical University, Tole be street, 050000, Almaty, Kazakhstan; e-mail: karabayeva.a@kaznmu.kz.

Khabarov, Iliya Anatolievich — Candidate of Pharmaceutical Sciences, Head of Laboratory, JSC “International Research and Production Holding “Phytochemistry”, Gazaliev str. 4, 100009, Karaganda, Kazakhstan, e-mail: i.khabarov@phyto.kz; <http://orcid.org/0000-0002-6727-8870>.

Khannanov, Rinat Ashatovich — master's degree, Director of “Biolife” Ltd, Stepnogorsk, 5 district, 8–80, Kazakhstan; e-mail: khanrinat@yandex.ru, ORCID ID 0000-0001-5085-7596.

Kishkentayeva, Anarkul Serikovna — PhD, Senior Researcher, JSC “International Research and Production Holding “Phytochemistry”, M. Gazaliev street, 4, 100009, Karaganda, Kazakhstan; e-mail: a.kishkentayeva@phyto.kz; <https://orcid.org/0000-0002-9169-3492>.

Kotelnikov, Oleg Alexeevich — Junior researcher, National Research Tomsk State University, Lenin avenue, 36, 634050, Tomsk, Russia; e-mail: kot_o_a@mail.ru; <https://orcid.org/0000-0002-1241-1312>.

- Kudaibergenov, Sarkyt Elekenovich** — Dr. Chem. Sci., Professor, Director, Institute of Polymer Materials and Technology, Head of the Laboratory of Engineering Profile, Satbayev University, Almaty, Kazakhstan; Atyrau-1, 3/1, 050019. e-mail: skudai@mail.ru; ORCID 0000-0002-1166-7826.
- Kurgachev, Dmitriy Andreevich** — Engineer, Institute for Problems of Chemical and Energetic Technologies SB RAS, Socialisticheskaya street, 1, 659322, Biysk, Russia; e-mail: daemond91@mail.ru; <https://orcid.org/0000-0003-2471-7287>.
- Malkov, Victor Sergeevich** — Candidate of Chemical sciences, Head of laboratory of organic synthesis, National Research Tomsk State University, Lenin avenue, 36, 634050, Tomsk, Russia; e-mail: malkov.vics@gmail.com; <https://orcid.org/0000-0003-4532-2882>
- Mantler, Svetlana Nikolaevna** — Researcher, JSC “International Research and Production Holding “Phytochemistry”, M. Gazaliev street, 4, 100009, Karaganda, Kazakhstan; e-mail: s.mantler@phyto.kz, <https://orcid.org/0000-0002-5779-3756>.
- Metwaly, Ahmed Mohamed** — Associate professor, Pharmacognosy Department, Faculty of Pharmacy (Boys), Al-Azhar University, Cairo 11884, Egypt; e-mail: ametwaly@azhar.edu.eg, ORCID 0000-0001-8566-1980.
- Mukhametgazy, Nurbatyr** — PhD student, Satbayev University, Almaty, Kazakhstan; Satbayev street 22a, 050013. e-mail: nurbatyr.kaz@gmail.com; <https://orcid.org/0000-0001-5957-0305>; ORCID 0000-0001-5957-0305.
- Mukusheva, Gulim Kenesbekovna** — Candidate of chemical sciences, Professor, Karagandy University of the name of academician E.A. Buketov, Karaganda, University street, 28, 100028, Kazakhstan; e-mail: mukusheva1977@list.ru; ID Scopus 9243017000
- Nurmaganbetov, Zhangel'dy Seytovich** — Candidate of chemical sciences, Assistant professor, Karaganda Medical University, Karaganda, Gogol street, 40, 100000, Kazakhstan; e-mail: nzhangeldy@yandex.ru; <https://orcid.org/0000-0002-0978-5663>.
- Orynbassar, Raigul Orynbassarovna** — Candidate of chemical sciences, Associate Professor, Al-Farabi Kazakh National University, Almaty, al-Farabi Ave., 71, 050040, Kazakhstan; e-mail: raihan_06_79@mail.ru; <https://orcid.org/0000-0002-6198-3018>.
- Pavlova, Svetlana Stanislavovna** — Candidate of Technical Sciences, Senior Lecturer at the Institute of Oil and Gas, Ugra State University, Chekhov Street 16, 628012, Khanty-Mansiysk, Russia; e-mail: pavlova_ss@mail.ru; <https://orcid.org/0000-0001-6137-3968>.
- Sadvakassova, Madina Zhumabaykyzy** — 3-year PhD student of specialty chemistry, L.N. Gumilyov Eurasian National University, Nur-Sultan, K. Munaitpasov Street, 13, 010008, Kazakhstan; e-mail: madinas-t@mail.ru.
- Sakipova, Zuriyadda Bektemirovna** — Professor, Doctor of pharmaceutical sciences, Dean of School of Pharmacy of Asfendiyarov Kazakh National Medical University, Tole bi street 94, 050000, Almaty, Kazakhstan; e-mail: sakipova.z@kaznmu.kz; <https://orcid.org/0000-0003-4477-4051>.
- Saliakhova, Anna Olegovna** — graduate of the Physical Chemistry Department, Perm State National Research University, Bukireva street, 614990, Perm, Russia; e-mail: sapronova1995@yandex.ru.
- Seilkhanov, Tulegen Muratovich** — Candidate of chemical science, full professor, Head of the laboratory of Engineering Profile of NMR Spectroscopy, Sh. Ualikhanov Kokshetau university, Kokshetau, Abay street, 76, 020000, Kazakhstan, e-mail: tseilkhanov@mail.ru, ORCID ID 0000-0003-0079-4755.
- Shakhvorostov, Alexey Valeryevich** — M.Sc., Institute of Polymer Materials and Technology, Almaty, Kazakhstan; Atyrau-1, 3/1, 050019; e-mail: alex.hv91@gmail.com; ORCID 0000-0003-3502-6123.
- Shcherban', Marina Grigoryevna** — Candidate of chemical sciences, Assistant professor of Physical Chemistry Department, Perm State National Research University, Bukireva street, 614990, Perm, Russia; e-mail: ma-she74@mail.ru; <https://orcid.org/0000-0002-6905-6622>.
- Sissengaliyeva, Gulsana Galimzhankyzy** — L.N. Gumilyov Eurasian National University, Satpaev street, 2, 010000, Nur-Sultan, Kazakhstan; e-mail: sissengaliyevag@gmail.com, ORCID: 0000-0002-90-1704.
- Solovyev, Aleksandr Dmitriyevich** — 2nd year student (specialist), Perm State National Research University, Bukireva street, 614990, Perm, Russia; e-mail: solovev_s92@mail.ru; <https://orcid.org/0000-0002-7852-3683>.

- Sorvanov, Alexander Alexandrovich** — 2-year postgraduate of specialty organic chemistry, National Research Tomsk State University, Tomsk, Lenin avenue, 36, 634050, Russia; e-mail: wellitson@gmail.com.
- Stas', Irina Evgen'evna** — Candidate of Chemical Sciences, Associate Professor of the Department of Physical and Inorganic Chemistry, Altai State University, Lenin Ave., 61, 656049, Barnaul, Russia; e-mail: irinastas@gmail.com
- Suleimen, Yerlan Melsuly** — Candidate of chemical sciences, PhD, 1) Senior researcher of the laboratory of Engineering Profile of NMR Spectroscopy, Sh. Ualikhanov Kokshetau university, Kokshetau, Abay street, 76, 020000, Kazakhstan; 2) Main Scientific Secretary of Republican collection of microorganisms, Nur-Sultan, Sh. Ualikhanov 13/1, 010000, Kazakhstan; e-mail: syerlan75@yandex.kz, ORCID 0000-0002-5959-4013.
- Tastanova, Lyazzat Knashevna** — Candidate of chemical sciences, Associate Professor, K. Zhubanov Aktobe Regional University, Aktobe, A. Moldagulova ave., 34, 030000, Kazakhstan; e-mail: lyazzatt@mail.ru; <https://orcid.org/0000-0002-9236-5909>;
- Turdybekov, Dastan Muchtarovich** — Candidate of chemical sciences, Head of the Department of Physics, Karaganda Technical University, Karaganda, N. Nazarbaev street, 56, 100010, Kazakhstan; e-mail: turdas@mail.ru, <https://orcid.org/0000-0002-0245-0224>.
- Turdybekov, Koblandy Muborykovich** — Doctor of chemical sciences, Professor, Karagandy University of the name of academician E.A. Buketov, Karaganda, University street, 28, 100028, Kazakhstan; e-mail: xray-phyto@yandex.kz; <https://orcid.org/0000-0001-9625-0060>
- Zakumbaeva, Gaukhar Daulenovna** — Senior researcher, D.V. Sokolskii Institute of Fuel, Catalysis and Electrochemistry, Almaty, Kunayev Str., 142, 050010, Kazakhstan; e-mail: orynbassar.raigul@gmail.com.
- Zhabayeva, Anar Nikhanbaevna** — Candidate of Pharmaceutical Sciences, Chief Technologist, JSC “International Research and Production Holding “Phytochemistry”, Gazaliev str. 4, 100009, Karaganda, Kazakhstan, e-mail: a.zhabaeva@phyto.kz; <https://orcid.org/0000-0002-9948-7140>.
- Zhakanov, Miras Mekenovich** — Engineer, JSC “International Research and Production Holding “Phytochemistry”, M. Gazaliev street, 4, 100009, Karaganda, Kazakhstan; e-mail: m.zhakanov@phyto.kz; <https://orcid.org/0000-0001-6470-3838>.
- Zhaparkulova, Karlygash Altynbekovna** — PhD, Senior teacher of School of Pharmacy Asfendiyarov Kazakh National Medical University, Tole bi street, 94, 050000, Almaty, Kazakhstan; e-mail: zhaparkulova.k@kaznmu.kz; <https://orcid.org/0000-0002-3776-2004>.
- Zhumabekova, Arai Kerimakynovna** — Candidate of chemical sciences, Associate Professor, Manash Kozybayev North Kazakhstan State University, Petropavlovsk, Pushkin str., 86, 150000, Kazakhstan; e-mail: zhumabekova_ak@mail.ru; <https://orcid.org/0000-0001-6743-8953>.
- Zhurov, Vitaliy Vladimirovich** — Candidate of Technical Sciences, Researcher, JSC “International Research and Production Holding “Phytochemistry”, Gazaliev str. 4, 100009, Karaganda, Kazakhstan, e-mail: zhurvityv@yandex.ru; <http://orcid.org/0000-0002-4413-8584>.

**Index of articles published in
«Bulletin of the Karaganda University. Chemistry Series»
in 2020**

№ p.

ORGANIC CHEMISTRY

| | | |
|---|---|----|
| <i>Abduletip D.T., Urkimbayeva P.I., Mun G.A., Kenessova Z.A., Khavilhairat B.</i> Application of composite materials based on polyvinyl alcohol in phytoremediation soil..... | 2 | 7 |
| <i>Arinova A.E., Nurkenov O.A., Fazylov S.D., Seilkhanov T.M., Ibraev M.K., Kabieva S.K., Omarov T.S.</i> N-methyl-2-(4-styrylphenyl)-3,4-fulleropyrrolidine synthesis and structure..... | 2 | 15 |
| <i>Bakibaev A.A., Il'yasov S.G., Tatarenko O.V., Tuguldurova V.P., Zorin A.O., Malkov V.S., Kasyanova A.S.</i> Allantoin: synthesis and chemical properties | 1 | 7 |
| <i>Bakibaev A.A., Malkov V.S., Kurgachev D.A., Kotelnikov O.A.</i> Methods of analysis of glycoluril and its derivatives..... | 4 | 5 |
| <i>Burkeev M.Zh., Sarsenbekova A.Zh., Bolatbay A.N., Tazhbaev E.M., Davrenbekov S.Zh., Nasikhatuly E., Zhakupbekova E.Zh., Muratbekova A.A.</i> The use of differential calculation methods for the destruction of copolymers of polyethylene glycol fumarate with the acrylic acid..... | 3 | 4 |
| <i>Fazylov S.D., Nurkenov O.A., Mukasheva A.Zh., Seilkhanov T.M., Shulgau Z.T., Zhanzhuman A.M.</i> Supramolecular inclusion complexes of functionally substituted N-benzylidene and allylidene isonicotinohydrazides with oligosaccharides and their properties..... | 2 | 22 |
| <i>Fazylov S.D., Nurkenov O.A., Muldakhmetov Z.M., Gazaliev A.M., Arinova A.E., Ibraev M.K., Vlasova L.M., Fazylov A.S.</i> Biologically active derivatives of fullerene C60. Current state and development prospects | 3 | 11 |
| <i>Jalmakhanbetova R.I., Suleimen Ye.M., Eissa I.H., Metwaly A.M., Iskakova Zh.B., Balpanov D.S., Sissengalieva G.G., Khannanov R.A., Seilkhanov T.M.</i> Isolation and biological evaluation of roseofungin and its cyclodextrin inclusion complexes | 4 | 35 |
| <i>Karpov S.V., Dzhalumukhanova A.S., Chernyayev D.A., Lodygina V.P., Komratova V.V., Malkov G.V., Badamshina E.R.</i> Investigation of isophorone diisocyanate oligoisocyanurate effect on water dispersible polyurethane properties..... | 1 | 43 |
| <i>Kishkentayeva A.S., Mantler S.N., Zhakanov M.M., Adekenov S.M.</i> Biologically active substances from <i>Achillea nobilis</i> L..... | 4 | 52 |
| <i>Mussabayeva B.Kh., Kassymova Zh.S., Aldabergenova M.A.</i> Interpolymer complex of biopolymers as a soil structure-forming agent..... | 1 | 22 |
| <i>Nurkenov O.A., Fazylov S.D., Seilkhanov T.M., Mukasheva A.Zh., Karipova G.Zh., Takibayeva A.T., Tomabayeva A.G.</i> Production of cyclodextrin nanocomplexes based on N'-((5-nitrofuranyl)methylene)isonicotinohydrazide and research of their structure by physical and chemical methods..... | 1 | 52 |
| <i>Panshina S.Yu., Ponomarenko O.V., Bakibaev A.A., Malkov V.S., Kotelnikov O.A., Tashenov A.K.</i> Study of glycoluril and its derivatives by ¹ H and ¹³ C NMR spectroscopy..... | 3 | 21 |
| <i>Pirniyazov K.K., Rashidova S.Sh.</i> Study of the kinetics of <i>Bombyx mori</i> chitosan ascorbate formation..... | 3 | 38 |
| <i>Satpaeva Zh.B., Nurkenov O.A., Schulgau Z.T., Fazylov S.D., Burkeev M.Zh., Havlicek D.</i> Antiradical activity and bioprediction of <i>o</i> - and <i>p</i> -hydroxybenzoic acid hydrazide derivatives | 1 | 35 |
| <i>Selikhova N.Yu., Malkov V.S., Bakibaev A.A.</i> Reaction between guaiacol and glyoxalic acid under microwave irradiation | 1 | 30 |
| <i>Turdybekov K.M., Nurmaganbetov Zh.S., Turdybekov D.M., Mukusheva G.K., Gatilov Yu.V.</i> Synthesis, molecular and crystalline structure of 8-formylharmine..... | 4 | 45 |
| <i>Zhanzhaxina A.Sh., Suleimen Ye.M., Ishmuratova M.Yu., Iskakova Zh.B., Seilkhanov T.M., Birimzhanova D.A., Suleimen R.N.</i> Essential oil of <i>Pulicaria vulgaris (prostrata)</i> and its biological activity | 3 | 44 |

PHYSICAL AND ANALYTICAL CHEMISTRY

| | | |
|--|---|----|
| <i>Bakibaev A.A., Sadvakassova M.Zh., Malkov V.S., Erkasov R.Sh., Sorvanov A.A., Kotelnikov O.A.</i> Study of the biologically active acyclic ureas by nuclear magnetic resonance..... | 4 | 60 |
|--|---|----|

| | | |
|---|---|----|
| <i>Bhole R.P., Jagtap S.R., Bonde C.G., Zambare Y.B.</i> Development and validation of stability indicating HPTLC method for estimation of pifrenidone and characterization of degradation product by using mass spectroscopy | 3 | 51 |
| <i>Burkeev M.Zh., Zhumanazarova G.M., Kudaibergen G.K., Tazhbayev E.M., Turlybek G.A., Zhakupbekova E.Zh.</i> Research of the influence of external factors on copolymers based on unsaturated polyester resins | 2 | 51 |
| <i>Burkeev M.Zh., Zhumanazarova G.M., Tazhbayev E.M., Kudaibergen G.K., Aukadiyeva S.B., Zhakupbekova E.Zh.</i> Poly(propylene fumarate phthalate) and acrylic acid radical copolymerization constants and parameters | 1 | 68 |
| <i>Egorova L.S., Leites E.A.</i> Extraction-photometric determination of osmium using quaternary water-thiopyrine-trichloroacetic and orthophosphoric acid system | 3 | 61 |
| <i>Kalichkina L.E., Bakibaev A.A., Malkov V.S.</i> Spectral study of thione-thiol tautomerization of thiourea in aqueous alcohol solution..... | 3 | 66 |
| <i>Nikolskiy S.N., Abilkanova F.Zh., Golovenko A.S., Pustolaikina I.A., Masalimov A.S.</i> Investigation of intermolecular proton exchange of 3,6-di-tert-butyl-2-oxyphenoxyl with N-phenylanthranilic acid by ESR spectroscopy method | 2 | 35 |
| <i>Sarsenbekova A.Zh., Khalitova A.I., Klimova T.E., Khamitova T.O., Kudaibergen G.K., Figurinene I.V., Medeshova A.T., Sotchenko R.K.</i> Study of acid properties of new polymeric complexes of maleic acid polymethylvinyl ether cross-linked by polypropylene glycol..... | 1 | 75 |
| <i>Shcherban' M.G., Solovyev A.D., Saliakhova A.O.</i> The correlation between the surface-active characteristics of SAFOL 23 – alcohol – water systems and the length of the alkyl radical of the alcohol..... | 4 | 85 |
| <i>Shipunov B.P., Ryabykh A.V.</i> Change in the heat of D-glucose dissolution in water exposed to electromagnetic field | 1 | 83 |
| <i>Stas' I.E., Pavlova S.S.</i> Effect of pH and water irradiation with the electromagnetic field on the gelation of gelatin solutions..... | 4 | 96 |
| <i>Stas' I.E., Pavlova S.S.</i> Effect of ultrahigh-frequency electromagnetic field on the properties of associated liquids | 4 | 75 |
| <i>Totkhuskyzy B., Yskak L.K., Saparbekova I.S., Myrzakhmetova N.O., Jumadilov T.K., Gražulevicius J.V.</i> Features of the extraction of yttrium and lanthanum with an intergel system based on hydrogels of polyacrylic acid and poly-4-vinylpyridine..... | 1 | 60 |
| <i>Vissurkhanova Ya.A., Soboleva E.A., Ivanova N.M., Muldakhmetov Z.M.</i> Thermal and electrochemical reduction of nickel (II) ferrite under the influence of polymer stabilizers..... | 2 | 42 |
| <i>Zabolotnykh S.A., Shcherban M.G., Solovyev A.D.</i> Effect of the hydrochloric acid concentration on the surface-active and functional characteristics of linear alkylbenzenesulfonic acid..... | 3 | 72 |

INORGANIC CHEMISTRY

| | | |
|---|---|-----|
| <i>Bogdanova L.M., Lesnichaya V.A., Volkova N.N., Shershnev V.A., Irzhak V.I., Bukichev Yu.S., Dzhardimalieva G.I.</i> Epoxy/TiO ₂ composite materials and their mechanical properties | 3 | 80 |
| <i>Jumadilov T.K., Kondaurov R.G., Imangazy A.M.</i> Features of sorption of rare-earth metals of cerium group by intergel systems based on polyacrylic acid, polymethacrylic acid and poly-4-vinylpyridine hydrogels | 2 | 58 |
| <i>Kazhikenova A.Sh., Alibiyev D.B., Seitimbetova A.B., Smailova A.S.</i> Application of cluster-associative model for calculation of kinematic viscosity of metal melts | 2 | 68 |
| <i>Kazhikenova A.Sh., Alibiyev D.B., Seitimbetova A.B., Tentekbayeva Zh.M.</i> Relationship of associated clusters degree with metal ionization according to the cluster-associate model..... | 1 | 90 |
| <i>Sabitova A.N., Bayakhmetova B.B., Mussabayeva B.Kh., Orazhanova L.K., Ganiyeva K.G.</i> Sorption of heavy metals by humic acids of chestnut soils | 3 | 88 |
| <i>Seitmagzimov A.A., Seitmagzimova G.M., Dzhanmuldaeva Zh.K.</i> Hydrothermal grown iron oxide films on the surface of titanium and conductive glasses and their current characteristics in water photolysis.... | 1 | 97 |
| <i>Zhumabekova A.K., Tastanova L.K., Orynassar R.O., Zakumbaeva G.D.</i> Effect of modifiers on Fe-Pt/Al ₂ O ₃ catalysts for alkanes hydrotreatment..... | 4 | 104 |

CHEMICAL TECHNOLOGY

| | | |
|---|---|-----|
| <i>Abdurazova P.A., Sataev M.S., Koshkarbaeva Sh.T., Amanbaeva K.A., Raiymbekov Y.B.</i> Low temperature gas-phase technology cladding powdered silicon carbide | 2 | 76 |
| <i>Balpanova N.Zh., Gyulmaliev A.M., Pankin Yu.N., Ma F., Su K., Khalitova A.I., Aitbekova D.E., Tusipkhan A., Baikenov M.I.</i> Simulation of the kinetics of direct coal hydrogenation | 3 | 110 |
| <i>Ergozhin E.E., Chalov T.K., Kovrigina T.V., Melnikov Ye.A., Bezenova B.E.</i> Baromembrane technologies for purification of industrial wastes, using pulse water treatment | 2 | 83 |
| <i>Katkeeva G.L., Burkitseterkyzy G., Morozov Yu.P., Zhunussov E.M.</i> Thermodynamic analysis of oxidized copper minerals interaction with modified reagent | 1 | 110 |
| <i>Khabarov I.A., Zhurov V.V., Zhabayeva A.N., Adekenov S.M.</i> Modeling the extraction process of medicinal raw materials | 4 | 135 |
| <i>Mukhametgazy N., Gussenov I.Sh., Shakhvorostov A.V., Kudaibergenov S.E.</i> Salt tolerant acrylamide-based quenched polyampholytes for polymer flooding | 4 | 119 |
| <i>Mustafin E.S., Omarov Kh.B., Borsynbaev A.S., Havlichek D., Pudov A.M., Kaykenov D.A., Muratbekova A.A., Sadyrbekov D.T., Ainabaev A.A.</i> Possibility of enrichment of ore processing waste from Karagaily and Zheskazgan mining plants by dry separation method | 1 | 117 |
| <i>Raiymbekov Y.B., Besterekov U., Abdurazova P.A.</i> Review of methods for enrichment of phosphate raw materials in the world | 2 | 92 |
| <i>Tazhbayev Ye.M., Zhumagalieva T.S., Zhaparova L.Zh., Agdarbek A.A., Zhakupbekova E.Zh., Burkeeva G.K., Karimova B.N., Zhautikova S.B.</i> Synthesis and investigation of PLGA-based nanoparticles as a modern tool for the drug delivery | 2 | 97 |
| <i>Usmanova M.M., Dolgov V.V., Ashurov N.R., Rashidova S.Sh., Dadahodzhaev T.</i> Obtaining of nanocatalizers for low-temperature conversion of oxide carbon (CuO/ZnO/Al ₂ O ₃) with reduced copper content | 1 | 104 |
| <i>Yeszhanov A.B., Dosmagambetova S.S.</i> Phenol solutions treatment by using hydrophobized track-etched membranes | 3 | 99 |
| <i>Zhaparkulova K.A., Gani G.M., Sakipova Z.B., Karaubayeva A.A.</i> Development of the orodispersible films based on CO ₂ extract of <i>Ziziphora bungeana</i> with antimicrobial activity | 4 | 128 |

METHODS OF TEACHING CHEMISTRY

| | | |
|---|---|-----|
| <i>Arynova A.B., Kasymbekova D.A., Korganbayeva Zh.K.</i> Presenting lecture materials in English using CLIL technologies | 2 | 105 |
| <i>Nurdillayeva R.N., Baisalova A.Zh., Zhuman G.O.</i> Features of teaching Chemistry in English: continuity of traditional and new technologies | 2 | 113 |
| <i>Yaroshenko O.G., Blazhko O.A., Blazhko A.V., Korshevniuk T.V.</i> Group learning activities as a condition of implementing competence-based approach to students' inorganic chemistry teaching at university | 2 | 122 |